METABOLIC EFFECTS BROUGHT ABOUT BY TRICYCLIC ANTIDEPRESSANTS AND THE CONTRIBUTION OF A MEDICINAL PLANT IN ALLEVIATING HIGH FAT DIET INDUCED INSULIN RESISTANCE IN MALE WISTAR RATS

WAYNE CHADWICK

METABOLIC EFFECTS BROUGHT ABOUT BY TRICYCLIC ANTIDEPRESSANTS AND THE CONTRIBUTION OF A MEDICINAL PLANT IN ALLEVIATING HIGH FAT DIET INDUCED INSULIN RESISTANCE IN MALE WISTAR RATS

BY

WAYNE CHADWICK

Submitted in fulfillment of the requirements for the degree of Philosophiae Doctor in the Faculty of Science, at the Nelson Mandela Metropolitan University

January 2006

Promoter: Dr S Roux
Co-promoters: Dr M van de Venter &
Prof W Oelofsen

ACKNOWLEDGEMENTS

The author extends his thanks and sincere appreciation to all who helped make the present study possible and especially to:

- **My promoter Dr S Roux[1] for her invaluable guidance, patience and willing assistance throughout the duration of this study, including her advice in preparing this manuscript**
- **Dr M van de Venter[1] (co-promoter) for her expert input in the fields of cell biology and radioisotopes, also for her patience and advice throughout this study**
- **Prof W Oelofsen[1] (co-promoter) for his experienced advice and guidance**
- **Dr J Louw[2] for his advice and constant support**
- **Medical Research Council animal unit**
- **Dr P Morse Larsen[3], Dr S Fey[3], Dr A Nawrocki, Dr AR Wrzesinski[3] and Dr K Wrzesinski[3] for their hospitality and expert advice in the field of 2-D electrophoresis**
- **Dr D Winter[4] for his enthusiasm, interest and valued advice throughout my studies**
- **Funding received from the Medical Research Council, National Research Foundation (Indigenous Knowledge Systems) and Value Added Life (Pty) Ltd, Jeffreys Bay.**
- **All other staff and post-graduate students of the Department of Biochemistry and Microbiology at NMMU**
- **My friends and family for their support and encouragement**
- **Debbie for her continual inspiration, encouragement and understanding**

[1] Department of Biochemistry and Microbiology, Nelson Mandela Metropolitan University, PO Box 77000, Port Elizabeth 6031, South Africa
[2] Diabetes Research Group, Medical Research Council, PO Box 19070, Tygerberg 7505, South Africa
[3] Center for Proteome Analysis and Department of Biochemistry and Molecular Biology, University of Southern Denmark, DK-5230, Odense M, Denmark
[4] Department of Zoology Nelson Mandela Metropolitan University, PO Box 77000, Port Elizabeth 6031, South Africa

CONTENTS

CHAPTER 4
RESULTS

CHAPTER 5
DISCUSSION AND CONCLUSIONS

APPENDIX 1

LIST OF FIGURES

LIST OF TABLES

ABSTRACT

Type II diabetes is becoming a growing problem in developed countries worldwide. The median age for diagnosis was around sixty, but recent surveys have shown that the entire age distribution curve shifting left. The incidence of type II diabetes is thought to be parallel with the growing rate of obesity associated with an unhealthy western diet. Type II diabetes is an expensive disease to manage, it is for this reason that cheaper medication needs to be investigated in the form of traditional plants, such as *Sutherlandia frutescens*. Prescription medication, such as tricyclic antidepressants, may also increase body weight thereby playing a role in obesity. The cause of weight gain in such cases may go unrecognized or lead to cessation of the medication with or without the practitioner's knowledge or approval. It is therefore necessary to investigate the causative agents responsible for the excessive weight gain.

Drinking water containing extracts of *S. frutescens* or metformin was administered to two groups of eleven insulin resistant male Wistar rats. The insulin resistant control group received water without any medication. Rats were sacrificed after 8 weeks allowing for fasting blood glucose, insulin and tissue glycogen content determination. Glucose uptake was also determined using [^{3}H] deoxyglucose. The effect of the medication and the diet on muscle post receptor insulin signaling proteins was determined through Western blots. Liver proteomics was also performed using 2-D electrophoresis. In a separate experiment 26 male Wistar rats were exposed to strepotozotocin toxin, 7 of these rats received intravenous insulin treatment, 7 rats received *S. frutescens* extract and 7 rats received a combination of both medications, the remaining 5 received no treatment and served as the control. Rats were sacrificed after 6 days allowing for fasting blood glucose, insulin and tissue glycogen content determination.

Two groups of 14 male Wistar rats received amitriptyline or trimipramine (common tricyclic antidepressants) in their drinking water, the control group (30 rats) received water without any medication. The rats' weight and food consumption was monitored throughout the trial and their oxygen consumption was also determined. Rats were sacrificed after 6 weeks or 14 weeks of medicinal compliance allowing for fasting blood glucose, insulin and tissue glycogen content determination. Glucose uptake was also determined using [^{3}H] deoxyglucose.

S. frutescens treatment normalized circulating serum insulin levels and significantly increased the rate of glucose clearance. Certain post receptor insulin signaling proteins were also significantly increased relative to the insulin resistant control group. 2-D electrophoresis identified the normalization of protein levels associated with the urea cycle. *S. frutescens* was also able to, independently; maintain normoglycaemic levels in the strepotozotocin treated group. The tricyclic antidepressants significantly increased blood glucose levels while significantly reducing tissue glycogen levels for both sacrifice periods. Serum insulin remained unchanged while a significant increase in insulin degradation and insulin degrading enzyme levels were found for both antidepressants.

S. frutescens shows promise as a low cost antidiabetic medication for future use. Although the antidepressants did not promote weight gain, the increase in blood glucose levels may be cause for concern in patients with a pre-disposition toward developing diabetes.

ABBREVIATIONS

- **5HT** – 5-Hydroxytryptamine
- **ADP** – Adenosine Diphosphate
- **AMP** – Adenosine Monophosphate
- **AMPK** - AMP-Activated Protein Kinase
- **ATP** – Adenosine Triphosphate
- **BCA** - Bicinchoninic Acid
- **BMI** – Body Mass Index
- **BSA** - Bovine Serum Albumin
- **cAMP** - Cyclic AMP
- **CAP** - Cbl-Associated Protein
- **CHAPS** – 3-[(3-Cholamidopropyl) dimethylammonio]-1-Propane-Sulfonate
- **CoA** - Coenzyme A
- **CPM** – Counts per Minute
- **DMEM** - Dulbecco's Modified Eagles Medium
- **DNA** – Deoxyribonucleic Acid
- **dpm** – Disintegrations per Minute
- **DRG** - Diabetes Research Group
- **EDTA** – Ethylene Diamine Tetra-acetic Acid
- **EGTA** – Ethylene Glycol Tetra-acetic Acid
- **ERK** - Endocrine Receptor Kinase
- **EST** - Ecological Systems Theory
- **FCS** - Fetal Calf Serum
- **FFA** – Free Fatty Acids
- **FKHR** - Forkhead Family of Transcription Factors
- **FLX** – Fluoxetine
- **FNF** – Fenfluramine
- **FPG** – Free Plasma Glucose
- **g** – Grams
- **µg** - Micrograms
- **GAPs** - GTPase Activating Proteins
- **GDP** - Guanosine Nucleotide Diphosphate
- **GEP** - Guanosine Nucleotide Exchange Protein
- **GLUT** - Glucose Transporter Family
- **GSK-3** - Glycogen Synthase Kinase
- **GTP** - Guanosine Nucleotide Triphosphate
- **HEPES** – 4-(2-Hydroxyethyl)-1-Piperazineethanesulfonic Acid
- **HK** - Hexokinase
- **HRP** - Horse Radish Peroxidase
- **5-HT** - 5-Hydroxytryptamine
- **IDE** - Insulin Degrading Enzyme
- **IGF-1** - Insulin-like-Growth Factor-1
- **IGT** – Impaired Glucose Tolerance

- **IRS** - Insulin Receptor Substrate Proteins
- **IVGTT** - Intravenous Glucose Tolerance Test
- **K_{ATP}** – Potassium / Adenosine Triphosphate
- **l** – Liter
- **µl** – Microliter
- **M** – Molar
- **mg** – Milligrams
- **ml** - Milliliter
- **mM** - Millimolar
- **M_2-POPOP** - 1,4-bis-2-(Methyl-T-Phenyloxazoyl)-Benzene
- **MAPK** – Mitogen Activated Protein Kinase
- **MKKK** - Mitogen Activating Protein Kinase-Kinase-Kinase
- **MKK** - Mitogen Activating Protein Kinase-Kinase
- **MRC** - Medical Research Council
- **MW** – Molecular Weight
- **NBF** - Nucleotide Binding Folds
- **NCEP** - National Cholesterol Education Program
- **NIDDM** - Non-Insulin Dependent Diabetes Mellitus
- **NSB** - Non Specific Binding
- **OB/IR** – Obese / Insulin Resistant
- **OGTT** - Oral Glucose Tolerance Test
- **PAGE** – Polyacrylamide Gel Electrophoresis
- **PBSA** – Phosphate Buffered Saline
- **PDK-1** - Phosphatidyl Inositol Dependent Kinase
- **PEG** – Polyethylene Glycol
- **PEPCK** - Phosphoenolpyruvate Carboxykinase
- **PI-kinase** - Phosphoinositide-Kinases
- **PIP** - Phosphatidylinositol-4-Phosphate
- **PIP2** - Phosphatidylinositol-4,5-Biphosphate
- **PIP_3** – Phosphatidylinositol-3,4,5-Triphosphate
- **PKB** - Protein Kinase B
- **PKC** - Protein Kinase C
- **PMSF** – α-Toluenesulfonyl Fluoride
- **PPO** - 2,5-diphenyloxazole
- **PP1G** - Protein Phosphatase
- **R_{GL}** - Regulatory Protein
- **RNA** – Ribonucleic Acid
- **ROS** - Reactive Oxygen Species
- **SDS** - Sodium Dodecyl Sulfate
- **SH2** - Src Homology 2
- **SSRI** - Selective Serotonin Reuptake Inhibitors
- **STZ** – Streptozotocin
- **SH2** - Src Homology 2
- **SUR** - Sulphonylurea Receptor

- **TBS** – Tris Buffered Saline
- **TNF-α** - Tumor Necrosis Factor-Alpha
- **TCA** - Trichloroacetic Acid
- **UDP** - Uridine Diphosphate

FOREWORD

High fat and carbohydrate rich diets, as is customary with typical westernized foods, coupled with reduced physical activity is accelerating the morbidity rate worldwide. The resulting obesity and obesity associated complications such as hypertension, dyslipidemia, type II diabetes, coronary heart disease, stroke, gallbladder disease, osteoarthritis, sleep apnea and respiratory problems, and endometrial, breast, prostate, and colon cancers can all be attributed to this physical downfall. However, individuals who practice a healthy lifestyle by exercising regularly and following a healthy eating plan may still be susceptible to undesired weight gain as a result of prescribed medicinal side effects. Whatever the culprit of excessive weight gain, the consequences remain the same, particularly insulin resistance, the main subject of this study, which may progress to full blown diabetes and associated diabetic complications, if untreated.

The cost for managing such a complex disease and its associated complications is extremely high and may not be affordable for many individuals in the lower income bracket. Alternative remedies are therefore needed to be sought out and exploited to alleviate this economic burden. The following study focuses on a particular indigenous plant to South Africa, *Sutherlandia frutescens*, as a future potential alternative to the conventional over priced antidiabetic prescriptions.

The literature and data to follow aims at measuring the effectiveness of this plant as a potential antidiabetic agent against an already well established commercial drug, as well as attempting to determine its particular mechanisms of action.

CHAPTER 1

REVIEW OF LITERATURE

CONTENTS

1.1. OBESITY: A RISK FACTOR FOR LATE ONSET TYPE II DIABETES MELLITUS

1.1.1. Introduction

Obesity is a complex multifactorial chronic disease that develops from an interaction of genotype and the environment. Our understanding of how and why obesity occurs is unclear, but is undoubtedly interlinked with social, behavioral, cultural, physiological, metabolic and genetic factors (Pi-Sunyer, 1998).

The enormous economic and health cost associated with obesity places it among the most pressing health care problems facing the westernised world to date. The United States and many other countries are facing an epidemic of insulin resistance, an evolving cardiovascular disease risk factor. This arises in the setting of a marked increase in the number of individuals diagnosed with type II diabetes and a dramatic increase in obesity. These trends are expected to increase throughout the next half century if serious actions are not undertaken (Case *et al*., 2002; JAMA, 2004).

1.1.2. Criteria for Obesity

Body mass index (BMI) is the cornerstone of the current classification system for obesity and its advantages are widely exploited across disciplines ranging from international surveillance to individual patient assessment, (Prentice and Jebb, 2001). Body mass index is a measure to correlate an individual's body weight with his/her height (kg/m^2). Health risks associated with obesity begin in the range of 25 to 30kg/m^2 (table 1.1). Values above 40kg/m^2 indicate severe obesity (Williams, 1997).

Body mass index is, however, only a surrogate measurement of body fatness while obesity is defined as an excess accumulation of body fat, and it is the amount of this excess fat that correlates with ill health. A wide range of conditions supporting this argument have been put forward which may provide misleading information about body fat content. These include infancy and childhood, ageing, racial differences, athletes,

military and civil forces personnel, weight loss with or without exercise, physical training and special clinical circumstances (Prentice and Jebb, 2001).

Table 1.1: BMI classification of overweight and obesity, waist circumference and associated disease risks (Pi-Sunyer, 1998).

			Disease Risk* Relative to Normal Weight and Waist Circumference	
	BMI (kg/m²)	Obesity Class	Men ≤ 102 cm (≤ 40 In) Women ≤ 88 cm (≤ 35 In)	> 102 cm (> 40 In) > 88 cm (> 35 In)
Underweight	<18.5		—	—
Normal+	18.5 –24.9		—	—
Overweight	25.0 – 29.9		Increased	High
Obesity	30.0 – 34.9	I	High	Very High
	35.0 – 39.9	II	Very High	Very High
Extreme Obesity	≥40	III	Extremely High	Extremely High

* Disease risk for type 2 diabetes, hypertension, and cardiovascular disease.
\+ Increased waist circumference can also be a marker for increased risk even in persons of normal weight.

A more practical way of identifying obesity is through the use of the metabolic syndrome. The metabolic syndrome is a clustering of risk factors such as increased plasma triglycerides, low density lipoprotein cholesterol, blood pressure and abdominal obesity defined by the National Cholesterol Education Program (NCEP). These are serious cardiovascular risk factors and are closely associated with insulin resistance. Epidemiological studies have shown that individuals with the metabolic syndrome and insulin resistance have a threefold increase in cardiovascular disease and a significant increase in cardiovascular mortality (Case *et al*., 2002).

Case *et al.* (2002) showed that individuals tend to be more obese as the number of metabolic syndrome components increased. They also showed that obesity and weight loss were statistically and significantly related to the baseline changes in components of the metabolic syndrome. The study suggested that a very low calorie diet induced weight loss in individuals with the metabolic syndrome resulted in substantial reductions of systolic and diastolic blood pressure, plasma glucose, triglycerides and total cholesterol

after four weeks. These results occurred despite the persistence of a significantly elevated body mass index. The weight loss continued along with further significant reductions in blood pressure and triglycerides until the individuals no longer met the criteria for the metabolic syndrome (Case *et al*., 2002). This study displayed that a very low calorie diet is associated with a greater initial weight loss and active weight maintenance programme.

Calculating BMI is simple, rapid and inexpensive, making this procedure of excessive weight gain determination the more favoured. BMI has also been correlated with both morbidity and mortality; the relative risk for cardiovascular disease and cardiovascular disease incidence increases in a graded fashion with increasing BMI in all population groups (Pi-Sunyer, 1998).

1.1.3. Who is to Blame?

The factors that contribute to excessive weight gain in humans are widespread and mostly unknown, this accounts for the fact that present treatments intended to produce a long-term reduction in body weight are largely ineffective (Clement, 1999). Obesity is not considered to be the result of a single genetic anomaly, but instead, is thought to depend on interactions between the following:

- **Environmental and physiological factors**

  This includes physical activity, eating habits, social and cultural habits. Increases in the rate of childhood overweight are of particular concern due to the negative health and physiological effects noted among overweight children. The development of childhood overweight involves a complex set of factors from multiple contexts that interact with each other to place a child at risk of obesity. This multifaceted system can be conceptualised using Ecological Systems Theory (EST). This system highlights the importance of considering the context, or ecological niche, in which a person is located in order to understand the emergence of a particular characteristic. In the case of a child this ecological niche includes the family and the school, which in turn are embedded in larger social contexts including the community and society at large (Davison and Birch, 2001).

  Specific characteristics which place an individual at risk for the development of obesity include: dietary intake, lack of physical activity and sedentary behaviour

(James, 1995). Increases in cases of obesity are also a reflection in lifestyle changes brought about by the mechanisation of modern life (Vass, 2002). Hanely *et al*. (2000) showed that increased television viewing was associated with a significant higher risk of becoming overweight.

It is evident that the fast pace of today's society favours an unhealthy lifestyle which includes high stress jobs, increased fast foods consumption and reduced exercise, due to time constraints. Increased demand for punctuality and greater distances to commute favour modern transport over conventional cycling or walking to destinations.

- **Genetic and hormonal factors**

Although overeating and a decreased physical activity all contribute to obesity, recent research strongly indicates that hereditary factors could be of equal importance for the development of both obesity and obesity complications. During the last decade, a continuously increasing interest has been focused on identifying genes that contribute to obesity and type II diabetes in humans, and the mode of action of these genes (Lonnqvist *et al*., 1999).

It has long been postulated that secondary to overeating, the storage of additional fat will give signals to the brain that the body is obese, which in turn makes the subject eat less and burn more fuel. The discovery of such a determinator, leptin, and its receptor has therefore opened new avenues for obesity research. Both are parts of a complex lipostatic hormonal feedback loop regulating body fat stores through effects on both satiety and energy expenditure (Lonnqvist *et al*., 1999).

Leptin is encoded by the *ob* gene, which is expressed exclusively in white and brown adipose tissue. Under normal conditions leptin mRNA levels correlate with the amount of body fat. The *ob* gene contains three exons; the coding sequence spans the last two exons and is interrupted by a 2kb intronic sequence. The major transcription of the human *ob* gene is a 4.5kb mRNA containing a long 3'-untranslated region. The 167 amino acid protein leptin is well conserved between species. The leptin receptor is, in turn encoded by the *db* gene (Clement, 1999).

Except in very rare monogenic cases leading to disruption of the leptin axis in humans, genetic studies have shown that *ob* and *db* loci do not have a major role in common forms of human obesity for a large proportion of the population. However, the results of linkage and association studies with the *ob* and *db* genes do not exclude a minor role for these genes in the development of obesity. The polygenic nature of human obesity means that the presence of susceptibility alleles of numerous genes could increase the probability that the bearer develops obesity. The presence of the genetic variation is not enough to explain the expression of the disorder, but rather interacts with other genetic, metabolic or environmental factors. Mutations associated with the peroxisome proliferator activated receptor (PPAR) family could also play a role in the development of human obesity (Clement, 1999), refer to section 1.4.7.

1.1.4. Treatment of Obesity and Maintenance of a Desirable Weight

Prevention of overweight and obesity is as important as treatment. This prevention can be categorized into primary prevention; which includes the prevention of overweight or obesity itself, and secondary prevention which prevents weight regain following weight loss, and preventing further weight increases in obese individuals unable to lose weight (Thomas, 1995).

The first goal of a patient with excess weight should be to prevent further weight increase, then to lose a modest amount on a twelve week structured programme which includes diets, physical activity, and behavioural modification followed by a further twelve week programme for weight maintenance to allow for stabilisation of the energy balance (MIMS, 2000). Weight management programs make use of one or more of the following criteria:

Diet:

Very low calorie diets, providing 400 to 800 kcal/day, have become less popular as many patients seem to regain all the weight they have lost shortly after the diet. The energy profile of any diet should obtain less than 35% of the energy from fat, and 10-15% from protein; however a protein intake of 70g/day in elderly individuals is desirable. When calorie intake exceeds that expended, excess fat intake is stored as fat, whereas excess carbohydrate is mainly oxidised in the short term but can lead to substantial gain in fat stores because of the reduced fat oxidation and considerable new fat formation in the long term (MIMS, 2000; CDC/NCHS 2004).

Exercise:

Evidence suggests that aerobic exercise in obese adults results in modest weight loss and that physical activity in overweight and obese adults increases cardiorespiratory fitness, independent of weight loss. Increased physical activity in obese and overweight adults reduces abdominal fat only modestly or not at all, while regular physical activity reduces the risk of cardiovascular disease (Pi-Sunyer, 1998). A more

active life-style should therefore be adopted, including a daily cumulative thirty minutes or more of moderate-intensity activity (MIMS, 2000).

Pharmacotherapy:

This treatment is only recommended to patients with high risk obesity and who have not managed to reduce their body weight by adaptations to their lifestyle alone. If such drugs are required then their use should be considered for long-term administration, similar to the current practice with drugs used for other chronic diseases. Over the counter drugs are generally harmless, questionably ineffective, and best avoided (MIMS, 2000).

Surgical options:

Vertical banded gastroplast is recommended for the morbidly obese individuals (BMI>40) with high co-morbid risk factors (MIMS, 2000).

1.1.5. Motivation

Obesity is the gateway to many metabolic disorders including cardiovascular disease, type II diabetes, hypertension, gallbladder disease and stroke. This alone makes obesity an extremely expensive disorder, an economic burden many individuals cannot cope with.

The rapid onset of obesity in South Africa is associated with a swift increase in insulin resistance and cardiovascular disease brought about by the westernised way of living in rural areas. Although the adoption of a westernised culture is the main instigator, certain genetic factors may be to blame in some cases, and certain prescription medication may also cause excessive weight gain. The fact remains that insulin resistance associated with type II diabetes is a fast growing pandemic in Southern Africa, placing a large economic burden on the government for overpriced medication. It is for this reason that new avenues need to be investigated, including the potential use of traditional medicine. This may relieve the economic burden and open opportunities for export of an indigenous medication against type II diabetes.

1.2. DEPRESSION AND TRICYCLIC ANTIDEPRESSANTS: THE IMPORTANCE OF BIOGENIC AMINES AND THEORIES OF EXCESS WEIGHT GAIN ASSOCIATED WITH TRICYCLIC ANTIDEPRESSANTS COMPLIANCE

1.2.1. Introduction

Many drugs, including tricyclic antidepressants, may be the cause of undesired increases in body weight (Rigler *et al*., 2001; Deshmukh and Franco, 2003). Common symptoms of depression include anorexia and weight loss, and yet some patients receiving antidepressant therapy complain of an excess of unwanted weight gain, leading ultimately to obesity, associated with these drugs. This unwanted side effect is described with tricyclic antidepressants. Undesirable weight gain may jeopardize patient compliance with antidepressant therapy (Garland *et al*., 1988; Hinze-Selch *et al*., 2000; Fava, 2000). Both dose and therapy duration are related to the degree of weight gain in the individual.

The average weight gain reported for the tricyclic antidepressants is in the range of 0.57 to 1.37kg/month, with an average dose of 100-150mg/day, of the drug, over a time period of three months (Garland *et al*., 1988). Investigators also reported that patients that were withdrawn from taking any form of the tricyclic antidepressant ceased to gain weight, after three months. A follow up study of these individuals was then made six months later, and it was found that they had lost almost all of the weight gained during the treatment. This evidence can therefore confirm the suspicions that tricyclic antidepressants cause an unwanted weight increase. In fact the tricyclic antidepressant, amitriptyline, has been used in the past to treat anorexia nervosa (Gottfries, 1981).

1.2.2. Reason for Depression States

The drug reserpine (which inhibits the storage of norepinephrine and serotonin thereby lowering the level of both neurotransmitters) has been shown to deplete intracellular norepinephrine levels and induce vital depressive states, including suicidal tendencies. It

was therefore concluded that a decrease in the amine neurotransmitter levels can be directly related to depression (Becker, 1974).

The aim of antidepressants is to increase the amine neurotransmitter levels in the brain. The effects of antidepressants, however, are not exclusive to the brain, and their influence on other organs in the body may contribute to undesired side effects.

1.2.3. Tricyclic Antidepressants and How these Drugs Work

These drugs gain their name from their characteristic three ring nuclear structure. Tricyclic antidepressants are very lipophilic substances and are highly bound to plasma proteins especially to albumin, α_1-acid glycoproteins, and lipoproteins. Since only free drug is diffusible, variations in plasma protein binding may affect tricyclic antidepressant distribution and their concentration at receptor sites, thus conditioning the antidepressant response. They bind to extravascular tissues, which accounts for their generally large distribution volumes and low rates of elimination. They follow two main routes of metabolism in the liver, namely N-demethylation, whereby tertiary amines are converted to secondary amines and ring hydroxylation (Rang and Dale, 1991).

Tricyclic antidepressants are useful in the treatment of acute depression, maintenance of remission once it is established, and prophylaxis against recurrence (Griest and Griest, 1979). The classic tricyclic antidepressants increase the synaptic availability of catecholamines and of 5-hydroxytryptamine (5HT) by blocking neuronal reuptake, thereby prolonging their physiological action at corresponding receptor sites (Hieble *et al*., 1995).

Some tricyclic antidepressants appear to increase transmitter release indirectly by blocking presynaptic α-2 adrenoreceptors (Gram, 1983; Rang and Dale, 1991). The α-2 receptor is overactive in depressed patients in that this inhibitory receptor closes down the noradrenergic pathway by its continuous blocking of the function of the presynaptic cell (Kwok and Mitchelson, 1981; Ransford, 1982; Gram, 1983; Shaw, 1984). Therefore

specific tricyclic antidepressant drugs block this hypersensitive or overactive α-2 receptor, thereby allowing the neuron to work again (blocking a receptor whose function is to stop the neuron working, allows it to start up again) (Ransford, 1982; Gram *et al*., 1983; Shaw, 1984).

Even though blockade of amine uptake is established promptly, the appearance of antidepressant effects typically requires administration of the drugs for several weeks. Thus, it is clear that potentiation of monoaminergic neurotransmission may be only an early event in a potentially complex cascade of events that is linked to a down regulation of β-adrenoreceptors (Hieble *et al*., 1995).

It was then proposed that these drugs enhance the receptivity of depressives to their environment, which in turn has an effect with the drugs on improving mood (Becker, 1974). However endogenous depressives tend to be unresponsive to this.

1.2.4. Tricyclic Antidepressants are they Necessary?

With the emergence of selective serotonin reuptake inhibitors (SSRI) the use of tricyclic antidepressants is not as common as it once was. Many physicians prefer to prescribe SSRI to their patients, as they seem to be more effective. Individuals taking the SSRI generally suffer fewer side effects in comparison to individuals taking tricyclic antidepressants (Gallo, 1999; Tan, 1999).

Despite the popular use of SSRI, tricyclic antidepressants are still used as an effective medication in certain cases. SSRI are often associated with increased anxiety, this is either remedied by lowering the dose or changing to a tricyclic antidepressant instead. Tricyclic antidepressants may also be used in the case of treatment failure or adverse side effects associated with SSRI (Gallo, 1999).

The cost of tricyclic antidepressants is somewhat lower in comparison to SSRI (Gallo, 1999); this appeals to the lower income class and the elderly. Tricyclic antidepressants

are also effective in controlling the pain arising in post therapeutic neuralgia and peripheral nerve injuries (Nowak and Handford, 1999). Long term, chronic amitriptyline treatment produces a number of actions that are uniquely expressed following chronic administration paradigms, and many of these could also influence the neuroplastic changes that occur with neuropathic pain. These include downregulation of β-adrenoceptors and $GABA_B$ receptors, upregulation of α_1-adrenoceptors, decreased activity of α_2-adrenoceptors and 2 dopamine autoreceptors, alterations in 5-hydroxytryptamine (5-HT) mechanisms, downregulation of NMDA receptors and enhancement of cyclic AMP, protein kinase A, cyclic AMP response element binding protein and brain-derived neurotrophic factor (BDNF). A number of these actions are potentially relevant to neuropathic pain mechanisms which involve multiple changes at central synapses reviewed (Esser *et al*., 2003). Although tricyclic antidepressants are not as commonly prescribed, as they were in the past, many individuals still rely on them.

1.2.5. Epidemiology of depression in diabetes mellitus

Data from the Baltimore site of the Epidemiologic Catchment area program found the risk of developing type II diabetes over a period of twelve years to be twice as high in patients already suffering from depression (Eaton *et al*., 1996; Kawakami *et al*., 1999). A series of case reports have confirmed this; three patients, suffering from depression, showed a decreased glucose tolerance with an increased insulin secretion, accompanied with increased insulin resistance, after receiving an oral glucose tolerance test. The circulating serum insulin levels fell, significantly, from 324μU/ml to 182μU/ml, 570μU/ml to 306μU/ml and 389μU/ml to 240μU/ml in these three patients after another oral glucose tolerance test was taken, prior to this however they received serotonin reuptake inhibitor therapy (Okamura *et al*., 1999).

Insulin sensitivity can be related to the catecholamine and serotonin pathways, both of which are affected in clinically depressed patients. Catecholamines, such as dopamine and norepinephrine, have been shown to decrease insulin release and promote insulin resistance leading to hyperglycaemia (Goodnick, 2001). Studies have confirmed that 1-

dopa and dopamine cause hyperglycaemia at the same time that norepinephrine, which is enzymatically converted from dopamine, promotes insulin resistance (Hakanson *et al*., 1967; Aleyassine and Lee, 1972). When catecholamine release is blocked, insulin release and glucose uptake is normalized (Feldman, 1976; Lekas *et al*., 1999). These results imply that a prolonged tricyclic antidepressant therapy could ultimately lead to an insulin resistant type II diabetic state in the patient.

Increased serotonin levels have been found to be associated with increasing insulin sensitivity and in so doing promoting glucose disposal. Reductions in HbA1c and free fatty acids have also been reported with SSRI (Greco *et al*., 1995; Willey *et al*., 1994). Table 1.2 summarizes these effects.

Alterations in the biochemistry of norepinephrine and serotonin lead to reduced and elevated efficiency of glucose utilization respectively. The tricyclic antidepressants that effect both serotonin and norepinephrine have proven to be most effective in alleviating diabetic neuropathy (Goodnick, 2001).

In a reverse scenario, long term diabetes can also lead to clinical depression. Three hypotheses exist as to why this may occur:

- The intensity and scope of repetitive treatment regimes burden the patients and intrude on their everyday lives (Fisher *et al*., 2001).
- The disease brings about chronic ongoing stress and the complications brought about with the disease affects the quality of life over time (Fisher *et al*., 2001).
- Diabetes and depression are parts of a common or linked set of metabolic disorders (Fisher *et al*., 2001).

These three hypotheses incorporate the results of a large number of studies that show wide variations in the rate of depression among patients with diabetes due to differences in patient demographics, disease characteristics and other factors that contribute to general psychological distress (Fisher *et al*., 2001).

Table 1.2: Biochemical effects of depression and treatment thereof related to type II diabetes (taken from Goodnick, 2001)

Parameter	Results
Catecholamines	
Animal studies	
Dopa, dopamine	Acute increase blood glucose in mice 75–80 mg/100 ml
Norepinephrine	100% blockade of glucose-mediated insulin release
Phentolamine	Increase glucose-mediated insulin release by a-antagonist
Adrenergic blockade	In dogs, glucose uptake induced by intracerebroventricular injection augmented by a, B-catcholamine effects
Human studies	
Norepinephrine	Reduction in glucose disposal vs. saline: 0.73 vs. 0.61 [10^{-2} min^{-1}]
B3 adrenergic gene polymorphism	Development of resistance to insulin
Norepinephrine	Physiologic elevation reduce insulin sensitivity without effecting secretion
Norepinephrine	Infusions: Insulin secretion reduced vs. saline (2.13 vs. 1.82 pmol/kg/min, $p < .05$); no change in acute insulin sensitivity
Serotonin	
Animal studies	
5HTP	Pretreatment reduces glibenclamide-induced plasma insulin from 150 to 100 uU/ml
	Reduces plasma glucose [in presence of nialamide] from 100 to 30 mg/100 ml, plasma insuline from 25 to 10 uU/ml
	At 60 mg/kg, reduces plasma glucose [in presence of nialamide] from 120 to 70 mg/100 ml without change in plasma insuline
	At 400 mg/kg, reducces plasma glucose with elevated plasma insulin
Cyproheptadine	Serotonin antagonist blocks 5HTP from reducing plasma glucose & plasma insuline in presence of nialamide
Fluoxetine, clomipramine	In presence of 5HTP or nialamide produces dose-dependent reduction in plasma glucose with change in plasma insulin
Fluoxetine, fenfluramine	In presence of 5HTP, reduces plasma glucose from 6.89 to 2.67 mmol/L (FLX), from 6.61 to 4.56 mmol/L (FNF)
Serotonin	5 uM in explanted rat langerhan's islets increases insulin release
Serotonin	0.01–10 ugm/ml/stimulates insulin-like growth factor I (IGF-1) release
Serotonin	Causes rapid increase of 50% in glucose uptake in L6 myotubes & isolated rat skeletal muscle
5HT2c receptor gene	Mutation leads to chronic hyperphagia in NIDDM model
Human studies	
FNF	(d,l): 30 mg bid for 4 weeks reduced FPG 35%, no change in plasma insulin
	(dex): 15 mg bid for 1 week reduced FPG 15%, FFA 30%
	15 mg bid for 10 days: 11 obese NIDDM females—FPG fell from 120.3 to 89.8 mg/dl
	(dex): 12-week study: 20 obese NIDDM: HbA1c fell from 8.5% to 71%

1.2.6. Mechanisms of Tricyclic Antidepressant Weight Gain

There are many theories as to why these drugs cause such a fluctuation in body weight, but it is still not clear which of these theories are correct. Some hypotheses are listed below:

- Hypoglycaemia-induced hunger was proposed, however contradictory results have been reported. Specific experiments to test this hypothesis in healthy

volunteers and depressed patients have shown that neither hyperinsulinaemia nor hypoglycaemia occurs during tricyclic antidepressant treatment (Garland *et al*., 1988). However other studies have shown an increase in plasma insulin levels in rats and humans, after administering a course of tricyclic antidepressants (Hurr, 1996).

- It was also proposed that amitriptyline, a tricyclic antidepressant, might alter the hypothalamic sensitivity to a given level of glucose, thereby causing an excessive craving for sweets, leading to weight gain (Garland *et al*., 1988; Fava, 2000).

- The increased appetite could be the result of the antidepressant action on neurotransmitter systems at the hypothalamic level. A relative increase in α-noradrenergic activity could, for example, inhibit satiety and promote carbohydrate craving. This hypothesis has also been proved false (Garland *et al*., 1988; Rigler *et al*., 2001).

- The antihistaminic effects of tricyclics, which they share with the structurally related phenothiazines, which also promote weight gain, have been proposed as responsible for increased appetite (Garland *et al*., 1988). However this hypothesis remains to be proven.

- Evidence has been provided that tricyclic antidepressants may cause a decrease in energy expenditure, thereby contributing to induced weight gain. It was observed that a 17% to 24% decrease in basal metabolic rate occurred in three female patients after the drug was administered to them. The net effect of a decrease of this magnitude could account for a weight gain of up to 1.3kg/month, an increase of this magnitude ranges within the documented average gains with tricyclic antidepressants (Garland *et al*., 1988).

None of the above mentioned theories fully explain the weight gain of 1.3kg/month as found by Garland (1988). Walker (2000) proposed that tricyclic antidepressants may bind to the sulphonylurea receptors, stimulating the pancreas to secrete more insulin. The hypoglycaemia following may increase carbohydrate craving which may lead to an increased weight gain. This still, however, needs to be tested. This hypothesis is supported by the fact that heart muscle has SUR2 receptors and tricyclic antidepressants cause arrhythmia in some patients.

Many of these hypotheses have already been proven false or are yet to be proved true. In the proposed research project, the hypothesis that antidepressants can cause hyperinsulinaemia will be tested, specifically by decreasing insulin degradation or by

stimulating the pancreas to produce and secrete more insulin. For this study the tricyclic antidepressants amitriptyline and trimipramine were used. These are some of the oldest and most prescribed drugs and have been shown to be significantly associated with weight gain (Holister 1995).

1.3. HIGH FAT DIET ASSOCIATED WITH WEIGHT GAIN

High fat diet feeding, whether it be short term or prolonged, necessitates an increased rate of fat oxidation to maintain body composition (Flatt, 1995). The rate of adaptation to a high fat diet depends on the level of physical activity and aerobic fitness, sustained by an individual. Accelerated fat oxidation during exercise, following a high fat meal, may be advantageous for physical endurance, as the high fat diet may spare muscle and liver glycogen (Zderic *et al*., 2004). Prolonged high fat feeding associated with a decreased physical activity results in severe weight gain and obesity due to the inability of sufficient fat oxidation to compensate for the excess fat intake (Tremblay, 2004).

The resulting excess adipose tissue can play an important role in the development of cardiovascular risk factors such as hypertension, hyperglycaemia, hyperinsulinaemia, dyslipidaemia and insulin resistance, all these traits are collectively referred to as the metabolic syndrome (Kahn and Flier, 2000; Spiegelman and Flier, 2001). Elevated free fatty acids, derived from β-oxidation, contribute to insulin resistance by inhibiting glucose uptake, glycogen synthesis, and glycolysis and by increasing hepatic glucose production (Reaven *et al*., 1998; McGarry, 1992; Boden *et al*., 1994). Insulin receptor substrate-1 (IRS-1) phosphorylation and PI-3-kinase activation, both of which are associated with post receptor insulin signalling in peripheral tissue, are impaired by elevated circulating free fatty acids. Gluconeogenic enzymes, in particular, glucose-6-phosphatase expression are significantly increased in the presence of elevated circulating free fatty acids (Zhou and Zhang, 2002).

Increased circulating concentrations of diacylglycerol and other lipid derived metabolites has been shown to be associated with the activation of a number of protein kinases, in particular protein kinase C, as well as promote serine or threonine phosphorylation of insulin receptor and IRS proteins, again associated with post receptor insulin signalling. This serine phosphorylation is favoured over the tyrosine phosphorylation, which would otherwise promote the activation of these proteins. These serine phosphorylations function as negative feedback loops for insulin signal transduction and provide a basis for

cross talk with other pathways that may mediate insulin resistance (Zhou and Zhang, 2002).

Adipose tissue is recognized as an active endocrine organ as it is able to produce and secrete metabolically active hormones. Elevated serum levels of tumour necrosis factor-α (TNF-α) have been identified in obese animal models and human subjects. These elevated levels are a result of significant increases in TNF-α expression in adipose tissue (Zhou and Zhang, 2002). Various experiments, utilizing a variety of cell lines treated with TNF-α, displayed impaired insulin signalling through IRS-1 serine phosphorylation or through reduced expression of IRS-1 and GLUT4 (Hotamisligil *et al*., 1996; Feinstein *et al*., 1993; Stephens *et al*., 1997; Bays *et al*., 2004). TNF-α has also been linked with decreased adipocyte differentiation (Zhang *et al*., 1996).

Leptin is another hormone produced and secreted by the adipose tissue. This hormone targets receptors in the central nervous system and periphery. Severe leptin deficiency or leptin signalling deficiency is associated with insulin resistance (Zhou and Zhang, 2002). This hormone has also been shown to mediate insulin action in muscle and liver tissues, while controlling body weight and satiety (Shimomura *et al*., 1999; Minokoshi *et al*., 2002).

Another controversial hormone produced and secreted by adipocytes is resistin, this hormone has recently been the topic of many debates as to whether it significantly contributes to the metabolic syndrome and the progression of full blown diabetes. Correlation of increased resistin expression with obesity and insulin resistance has been observed in some human subjects, but not others (McTernan *et al*., 2002; Nagaev and Smith, 2001; Savage *et al*., 2001; Janke *et al*., 2002; Bays *et al*., 2004). Further investigation is required to put this debate to rest.

Adiponectin, another protein produced and secreted by adipocytes, has been shown to slow the process of insulin resistance associated with type II diabetes and obesity by enhancing insulin action, reverse insulin resistance and promote β-oxidation and weight

loss (Yamauchi *et al*., 2001; Fruebis *et al*., 2001; Bays *et al*., 2004). The above stated facts provide sufficient evidence that prolonged high fat feeding, such as is common with typical westernised diets, in conjunction with a significant decrease in physical activity can lead to metabolic changes implied by diabetes and diabetic associated complications.

1.4. DIABETES MELLITUS: CLASSIFICATION, SYMPTOMS, PREVENTION, AND TREATMENT OF THIS FAST GROWING PANDEMIC

1.4.1. Introduction

Diabetes mellitus usually falls into one of two classes, which have been known for many years as juvenile onset and maturity onset diabetes, or the more commonly termed, type I and type II diabetes, respectively. The disease is characteristic of a state of extreme hyperglycaemia within the body, resulting from internal or external events which may take place in the life of an individual.

Diabetes, particularly type II diabetes, is becoming a serious problem in developed countries worldwide. Traditionally the median age at diagnosis for type II diabetes was around about sixty, but recent surveys have shown that the entire age distribution curve has shifted to the left. The United States boasts the worst statistics in which type II diabetes is now being reported in children under the age of ten. At such a young age the disease often goes undiagnosed for long periods of time, which allows considerable damage to occur to the pancreas. It is also expected that the earlier the onset of the disease the higher the rate of complications could potentially result from it (Dyer, 2002). The incidence of type II diabetes is thought to be parallel with the growing rate of childhood obesity, a sad statistic considering the disease is easily preventable by following a healthy diet and by exercising regularly.

The graph, in figure 1.1, illustrates the strain obesity and insulin resistance place on the pancreas. The figure displays the hypothetical blood insulin levels for an obese, insulin resistant individual after a 75g slow intravenous glucose tolerance test. It is clear that there is a progressive disappearance of the first peak of plasma insulin levels (green line), in comparison to the normal glucose response. In order for the body to maintain accurate plasma glucose levels, the pancreas compensates by over producing insulin in the second peak/phase (green line). This procedure will however eventually exhaust the pancreas and

over a period of time the second peak will also disappear, leading ultimately to a state of hyperglycaemia (red line) and severe diabetes (Servier, 2001).

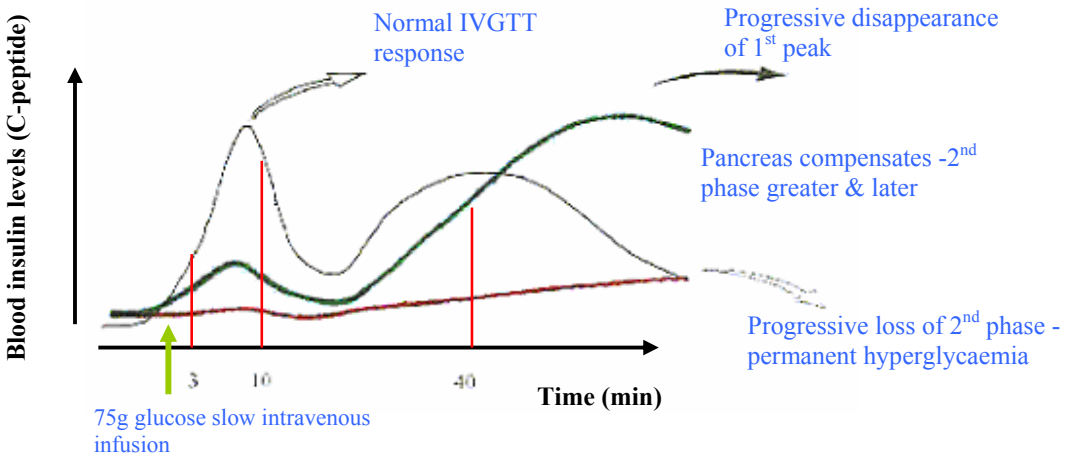

Figure 1.1: A representation of the progression of hyperglycaemia (IVGTT= Intravenous Glucose Tolerance Test) (taken from Servier, 2001)

1.4.2. Diagnosis for Diabetes Mellitus

The cardinal clinical feature of diabetes mellitus is glucose intolerance, therefore clinical diagnosis depends upon tests to demonstrate such intolerance (Tortora and Grabowski, 2003). An elevated blood glucose concentration together with an elevated blood ketone body concentration and ketonuria may be sufficient to diagnose diabetes mellitus. In addition, the oral glucose tolerance test (oral GTT), which is designed to test the ability of the patient's β-cells to secrete insulin, may also be used (Newsholme and Leech, 1994).

Table 1.3: Blood glucose concentration criteria for diabetes mellitus (taken from Newsholme and Leech, 1994)

	Glucose concentration (mM)		
Condition	**Venous whole blood**	**Capillary whole blood**	**Venous plasma**
Patient fasted overnight	**7.0**	**7.0**	**8.0**
120 min after oral glucose	**10.0**	**11.0**	**11.0**
Any intervening time after glucose ingestion	**10.0**	**11.0**	**11.0**

Table 1.3 shows concentrations of glucose, put forward by The European Association for the Study of Diabetes, at or above which diabetes is indicated. Diabetes mellitus will be diagnosed if the fasting blood glucose concentration, at 120 minutes and one other concentration at an earlier time interval are at or above those given in the table. However if only one or two are at, or above, the given concentration, impaired glucose tolerance is indicated and further tests are carried out to investigate the cause (Newsholme and Leech, 1994).

Most of the patients who suffer from non-insulin dependent diabetes mellitus (NIDDM) are obese and suffer from insulin resistance. The disease may also stem from a genetic background, however negligence to follow a healthy diet and exercise regularly are often the most common causative agents for insulin resistance, which in time can lead to type II diabetes as displayed in figure 1.2.

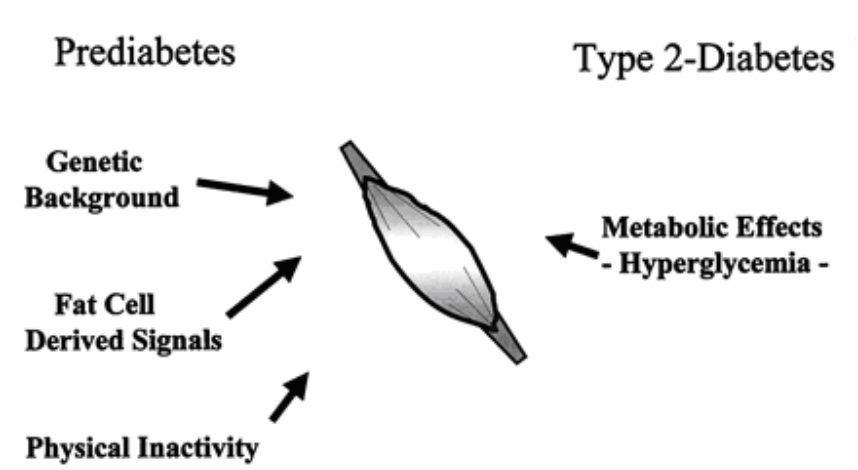

Figure 1.2: Pathogenesis of skeletal muscle insulin resistance. Schematic presentation of factors involved in the pathogenesis of skeletal muscle insulin resistance in pre-diabetes and type 2 diabetes (taken from Matthaei *et al*., 2000)

The monocytes and adipocytes isolated from patients suffering from type II diabetes mellitus have fewer insulin receptors having the same affinity as those isolated from healthy individuals. Non-insulin dependent diabetes is basically a further pathological development of obesity. In obese individuals the changes in glucose concentration are within the normal range whereas the changes of plasma insulin are greatly in excess of the normal, as can be seen in figure 1.3.

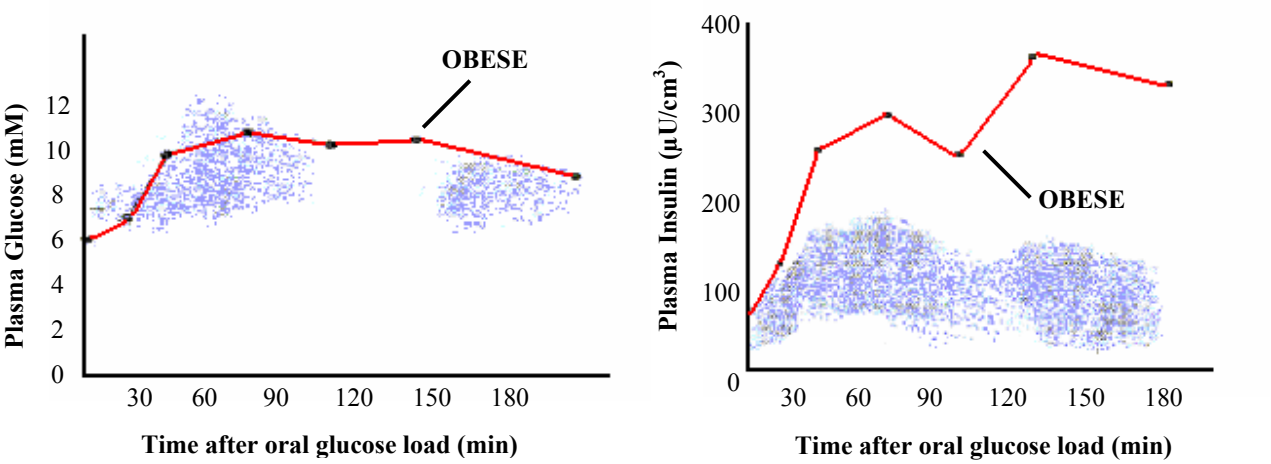

Figure 1.3: A representation of insulin secretion in response to an increased blood glucose concentration in non diabetic obese patients. Shaded areas represent the normal ranges for insulin and glucose levels (taken from Newsholme and Leech, 1994)

It is clear from the figure 1.3, that the β-cells of the pancreas can secrete sufficient insulin to improve glucose uptake by moderate insulin resistant cells and thereby maintain the blood glucose concentration within the normal range. However, if the resistance is too severe and the pancreas is unable to secrete sufficient insulin to overcome the resistance, the blood glucose concentration will not be maintained within the normal limits, despite the high levels of circulating insulin, and diabetes results (Newsholme and Leech, 1994). Proinsulin concentrations are increased relative to insulin concentrations in individuals with type II diabetes (Mykkanen, *et al*., 1999). It can therefore be summarised that if there is a sufficient insulin secretory reserve in the β-cells, the individual will remain obese, while with a small reserve the patient will usually becomes diabetic at a later stage.

Several theories exist as to why insulin resistance is present:

- Increased levels of free fatty acids in the blood which coats the insulin receptor and leads to decreased insulin binding (Servier, 2001). Increased intracellular levels of fatty acyl-CoAs leads to hyperinsulinaemia in β-cells and post receptor insulin signalling complications in muscle and liver tissues (Bays *et al*., 2004).

- Overweight causes a relative reduction in the number of insulin receptors (Servier, 2001).

- Poor quality of insulin being produced, i.e. immature or pre-proinsulin (Servier, 2001).

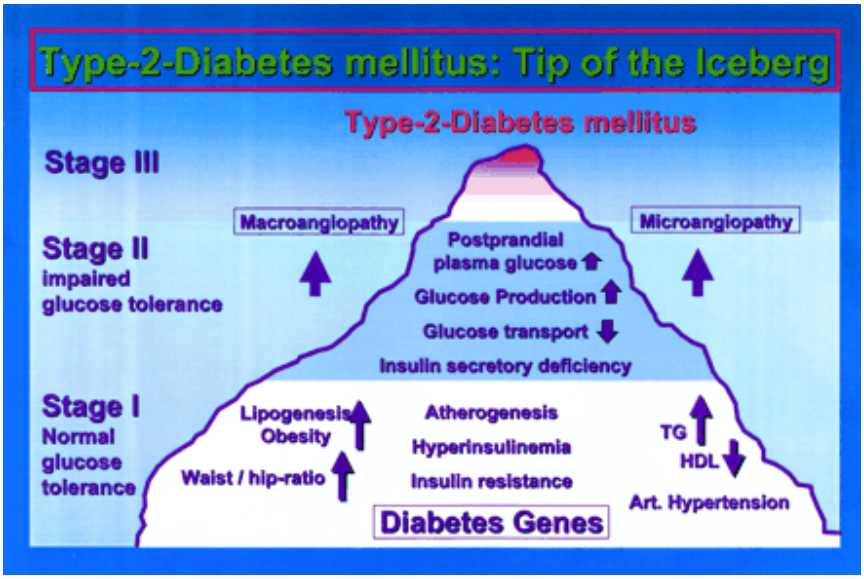

Figure 1.4: Pathogenesis of type II diabetes mellitus: the tip of the iceberg (taken from Matthaei *et al.*, 2000)

The simplified schematic presentation in figure 1.4 illustrates the evolution of type II diabetes mellitus. Type II diabetes mellitus represents the end stage of long lasting metabolic disturbances caused by insulin resistance associated with hyperinsulinaemia, obesity, dyslipoproteinaemia, arterial hypertension, and consequently premature atherosclerosis. Since this detrimental metabolic milieu is present for many years before plasma glucose levels (as our diagnostic indicator) are elevated, it is not surprising that type II diabetic patients have already micro- and/or macrovascular complications at the time of the initial diagnosis. Subjects in stage I have normal glucose tolerance due to the ability of their β-cells to compensate for the insulin-resistant state. At this stage elevated triglyceride levels and reduced HDL levels as well as an increased waist to hip ratio may indicate insulin resistance and should lead to therapeutic action. In stage II, glucose tolerance after an oral glucose load (75 g) is impaired due to developing insulin-secretory deficiency. To avoid progression to clinically overt type II diabetes (stage III), these IGT subjects must receive treatment options to reduce insulin resistance, such as dietary

advice and increase of physical activity. The stage model of the pathophysiology of type II diabetes is adopted from Matthaei *et al*., (2000).

1.4.3. Cellular mechanisms of insulin resistance

Insulin receptor binding, activation thereof and the subsequent downstream post receptor cascade signaling is discussed in great detail in section 1.5.8.1. As each kinase, in the respective pathway, relies on the phosphorylation of the kinase, situated immediately upstream from it, any defect along the pathway will render the initial signal, brought about by insulin binding, useless.

A significant decrease in insulin receptor number has been observed on monocytes and adipocytes isolated from type II diabetic subjects, leading to a 20-30% reduction in insulin binding (Freidenberg *et al.*, 1987; Caro *et al.*, 1987; Caro *et al*., 1986; Molina *et al*., 1989; Trichitta *et al*., 1989; Comi *et al*., 1987). However many studies have shown the insulin receptors isolated from the muscle and liver tissues of type II diabetic individuals to be equivalent to those of healthy individuals, when expressed per milligram of protein (Trichitta *et al*., 1989; Comi *et al*., 1987; Klein *et al*., 1995; Obermaier-Kusser *et al.,* 1989). No significant consistent trend could be observed in genetic mutations of the insulin receptor in type II diabetic patients either, indicating that generally the number and affinity of the receptor is not the cause of insulin resistance in most cases of type II diabetes (Moller *et al*., 1989; Kusari *et al*., 1991).

A significant decrease in insulin receptor tyrosine kinase activity has been reported in several tissues, including skeletal muscle, adipocytes, hepatocytes, and erythrocytes, of obese and type II diabetic patients by a number of investigators (Bak *et al*., 1992; Klein *et al*., 1995; Bays *et al*., 2004). This decrease cannot be explained by receptor number or even receptor binding affinity. However the normalization of plasma glucose concentration corrects the decreased kinase activity, suggesting that a combination of hyperglycaemia, hyperinsulinaemia and defective intracellular glucose metabolism all play a part in affecting the tyrosine kinase activity (Freidenberg *et al*., 1988; Kellerer *et al*., 1994).

Studies have also shown an 80% reduction in IRS-1 and IRS-2 phosphorylation as well as a 90% decrease in p85 PI-3-kinase activity in the muscle of obese and type II diabetic subjects when compared to those of healthy individuals. Several groups (Imai *et al*., 1997; Hitman *et al.,* 1995) have reported that a common mutation in the IRS-1 gene (Gly 972 Arg) is associated with type 2 diabetes, insulin resistance, and obesity, but the physiologic significance of this mutation remains to be established (Pratley *et al*., 1998).

Insulin resistance has been shown to have no effect on the MAPK pathway of insulin signalling (Krook *et al*., 2000; Cusi *et al.,* 2000). Possible reasons for this may lie in the fact that both MAPK and PI-3-kinase have independent insulin signalling pathways and they have differential signal amplification. In the case of signal amplification, the MAPK pathway can be activated by either Grb2/Sos interaction with IRS-1/IRS-2 or with Shc. As already discussed IRS-1 tyrosine phosphorylation is dramatically reduced in diabetic subjects leaving insulin activation of the MAPK pathway to Shc activation. Past studies have shown Shc phosphorylation as well as ERK and MEK activity to be unchanged during insulin stimulation in obese and type II diabetic subjects when compared to that of healthy volunteers (Cusi *et al.,* 2000). The latter statement implies that even in the case of insulin resistance insulin stimulation provides enough phosphorylation of the tyrosine kinase receptor to significantly phosphorylate the Shc residue.

ERK has been shown to phosphorylate the serine residues of IRS-1, and serine phosphorylation of IRS-1 and the insulin receptor itself has been reported to be involved in desensitization of the insulin receptor signalling (De Fea and Roth, 1997; Dunaif *et al*., 1995; Gual *et al*., 2005). Continued ERK activity could lead to an increase in insulin resistance if the IRS-1 functioning is already impaired. Insulin resistance in the PI-3-kinase pathway, with its compensatory increase in β-cell function and hyperinsulinaemia, leads to excessive stimulation of the MAPK pathway in vascular tissue (Cusi *et al*., 2000; Hsueh and Law, 1999), leading to the proliferation of vascular smooth muscle cells, increased collagen formation, and increased production of growth factors and inflammatory cytokines, possibly explaining the accelerated rate of atherosclerosis in type II diabetic individuals (DeFronzo and Mandarino, 2003).

Investigations have also showed a decrease in GLUT4 mRNA expression as well as a decrease in insulin stimulated GLUT4 translocation in both adipose and muscle tissue of diabetic and obese subjects in comparison to healthy controls (Shepherd and Kahn, 1999; Garvey 1998; Zierath *et al*., 1996; Krook *et al*., 2000; Andreasson *et al*., 1991).

Hexokinase (HK) is responsible for converting glucose, taken up by the cell, into glucose-6-phosphate for cellular metabolism. Several isoforms of this enzyme exist, HKI-HKIV, all of which perform the same function but vary in glucose specificity and tissue distribution (Colowick, 1973; Printz *et al*., 1993; Rogers *et al*., 1975; Magnuson *et al*., 1989). HKII is found in the skeletal muscle of humans and rats, has a high specificity for glucose and transcription of this enzyme is regulated by insulin (Mandarino *et al*., 1995). Decreased basal HKII activity and mRNA levels as well as reduced insulin stimulated HKII activity has been found in type II diabetic individuals (Kruszynska *et al*., 1998; Vogt *et al*., 2000; Vestergaard *et al*., 1995; Ducluzeau *et al*., 2001). The question still remains whether the decreased glucose transport into the cell or the reduced HKII activity is responsible for the low levels of glucose-6-phosphate formed (Pendergrass *et al*., 1995; Rothman *et al*., 1992; Cline *et al*., 1999). Although several nucleotide substitutions have been found in the gene encoding HKII none have been located close enough to the ATP binding sites and none have been associated with insulin resistance (Lehto *et al*., 1995; Laakso *et al*., 1995; Echwald *et al*., 1995).

The alternative to oxidation of glucose-6-phosphate is glycogen synthesis, which is discussed in section 1.5.6. Investigators have uncovered that glycogen levels are severely reduced in individuals suffering from type II diabetes, which is related to a decrease in mRNA expression as well as the activity of both glycogen synthase and its activator, phosphoprotein phosphatase (Vestergaard *et al*., 1991; Browner *et al*., 1989; Bays *et al*., 2004). This defect cannot, however, be explained by mutations in the genes encoding for glycogen synthase or those of other proteins responsible for its activation (Schalin-Jantti *et al*., 1992). Enzyme activities along the glycolytic pathway of insulin resistant individuals do not seem to differ from those of healthy volunteers, however some contradictions do occur particularly with the pyruvate dehydrogenase complex (Mandarino *et al*., 1986; Kelley *et al*., 1992).

In summary it seems clear that insulin resistance is attributed to post receptor binding defects; including diminished insulin receptor tyrosine kinase activity, insulin signal transduction abnormalities, decreased glucose transport, reduced glucose phosphorylation and impaired glycogen synthase activity.

1.4.4. 'Misguided' Genes

It is of common knowledge that even the most basic forms of life are dependent on some form of genetic material for survival from generation to generation. Genes differentiate between individuals and code different sequences for important hormones, proteins and enzymes within the body which are essential for life. However errors may exist in the genetic code of some individuals, leading to the formation of certain constituents with some form of functional error. This can be detrimental to the individual's health and could even lead to death. Many genetic disorders have been linked with type II diabetes, but at the same time genetic manipulation is being used as a cure in some cases.

Mutations of several genes encoding transcriptional regulators (HNF-α-, HNF-β-, HNF4-α-, IDX1, and NEUROD/β-2) cause autosomal dominant diabetes. The most prevalent form results from defective HNF1-α-. Although HNF1-α- is known to regulate the transcription of liver, kidney, and intestinal genes, the human phenotype is essentially insulin secretory dysfunction, suggesting that this factor must be critically involved in β-cell specific transcription (Parrizas *et al*., 2000).

Genome wide screening procedures have identified several susceptibility loci for non-insulin dependent diabetes within the human genome. The human proto-oncogene PBX1 codes for a homeodomain containing protein that modulates expression of several genes, including those contributing to regulation of insulin action and glucose metabolism. PBX1 is located on chromosome Iq22, a region linked with type II diabetes, and is composed of nine exons spanning approximately 117kb and is located within 300kb of microsatellite DIS1677, which marks the peak linkage to diabetes susceptibility. Sixteen single nucleotide polymorphisms were also located in PBX1 including one which causes a glycine to serine substitution at position 21 (Thameem *et al*., 2001).

Another two regions were found to be linked to type II diabetes and insulin resistance, namely a location on chromosome 2q, near marker D2S141, and another location on chromosome 6q, near marker D6S264. A positional candidate gene for insulin resistance in this chromosomal region is the plasma cell membrane glycoprotein PC-1 (6q22-q23) (Duggirala *et al*., 2001).

A gene conferring susceptibility to type II diabetes has also been located on chromosome 18p11. There is also evidence for linkage of chromosome I, near marker D1S3462; chromosome 4; near marker D4S2361; chromosome 5, near marker D5S1505; and chromosome 17, near marker D17S1301 (Parker *et al*., 2001).

A putative sugar transporter has been localized to human chromosome 20q12-q13.1, one of the genomic loci associated with type II diabetes. This protein has a strong resemblance to members of the mammalian facilitative glucose transporter family (GLUT), and this protein is therefore known as GLUT10. GLUT10 contains 541 amino acids with several glucose transporter sequence motifs and amino acids essential for glucose transport function (McVie-Wylie *et al*., 2001).

Genetic susceptibility also exists for type I diabetes. For Asians, the human major histocompatibility complex (MHC) locus (HLA region), especially the class two region, is the major susceptibility interval. The role of insulin dependent diabetes locus has been questioned in Asia, because in contrast to Caucasians, Asian populations have a very low incidence of type I diabetes. This may be due to the population frequency distribution of susceptible type I genes, especially of HLA. The overall risk for type I diabetes from HLA DR and DQ is determined by alleles and particular combinations of alleles in a given individual. In Asians it is very common that a protective DR4 allele is associated with susceptible DQ alleles while neutral/protective DQ alleles are associated with DR4 alleles. The theory therefore stands that the counterbalance between susceptible DRB1 and protective DQB1, and visa versa, is a factor that may contribute to the low incidence of diabetes in Asians (Park and Eisenbarth, 2001).

1.4.5. Sub Groups of Type II Diabetes

Several forms of type II diabetes may exist which may not necessarily be permanent, and may be alleviated once the individual is removed from that environment or situation.

- Malnutrition related diabetes mellitus or tropical diabetes is divided into fibrocalculous or protein deficient pancreatic diabetes. In both cases the patients are usually inhabitants of poor tropical countries, are underweight, and have clinical signs of present or past malnutrition and other dietary deficiency states (Benn and Sonksen, 1993).

- Gestational diabetes is restricted to women in whom the onset of diabetes occurs first during pregnancy, and is only associated with approximately 3% of pregnancies. Women who show impaired glucose tolerance during pregnancy are included in this class, but it excludes diabetic women who become pregnant. The clinical recognition of gestational diabetes mellitus is important because the baby is at increased risk of macrosomia, though rates of perinatal mortality and congenital anomalies are no greater than in pregnant women who have normal glucose tolerance. The glucose tolerance often becomes normal after the birth of the child, however there remains a lifetime risk of developing non insulin dependent diabetes later in life (Benn and Sonksen, 1993).

- Diabetes may be associated with various other conditions and syndromes. This group is usually very small and diverse and may be secondary to certain specific endocrine diseases or certain genetic syndromes (Benn and Sonksen, 1993).

- Impaired glucose tolerance is not always associated with diabetes. Some individuals may suffer from glucose intolerance and still show no signs of microangiopathic renal and retinal complications associated with the classical diabetes diagnosis. Individuals suffering from impaired glucose tolerance have shown an increased prevalence to atherosclerotic disease and associations with other known cardiovascular disease risk factors including hypertension, dyslipidemia, and central obesity. Individuals who suffer from impaired glucose tolerance do of course stand a higher chance of developing diabetes than normal individuals. It has been estimated that approximately 33% of individuals diagnosed with impaired glucose tolerance will develop diabetes, while a similar percentage will return to a normal glucose tolerance, and the others will remain in the impaired glucose tolerance group, after approximately 5-10 years (Benn and Sonksen, 1993).

1.4.6. Current Treatment for Diabetes Mellitus

Type II diabetes is best treated by a change in lifestyle combined with medication. Lifestyle changes include weight loss, exercise and dietary changes. Medications include sulphonylureas, thiazolidinediones, biguanides and insulin.

(a) Weight Loss

Many type II diabetic patients need to lose weight. A reduction in energy intake reduces blood glucose concentrations as well as reducing the risk factors associated with obesity. Even modest weight loss is usually associated with a reduction of insulin resistance and a fall in the accelerated rate of glucose production in the liver. Weight loss can produce a decrease in low density lipoprotein and very low density lipoprotein levels, an increase in high density lipoprotein levels and a reduction in blood pressure. Thus, the overall cardiovascular risk profile can be improved (Benn and Sonksen, 1993).

(b) Exercise

Exercise is beneficial in many aspects to the body, and has been shown to be effective in the treatment of diabetes mellitus. Glucose, ketone bodies, and fatty acids in the blood are used up at a faster rate due to exercise. The glycogen content of the liver and muscle will also be reduced, thereby increasing the activity of glycogen synthase and reducing the requirement for insulin in the stimulation of glycogen synthesis after a meal. It has also been shown that endurance training in healthy individuals increases insulin sensitivity so that lower insulin concentrations are required to control the blood glucose concentration after an oral glucose load (Newsholme and Leech, 1994).

(c) Dietary Fiber

The faster the rate of digestion and absorption of food the greater the change in the blood fuel concentrations and therefore the greater the requirement for insulin. It is therefore important that the diabetic patient realises that the ingestion of glucose and sucrose should be avoided and only slow digesting carbohydrates should be ingested, such as starchy foods. A natural agent such as fiber should be taken in with each meal to further increase the time of digestion. Fiber has been shown to reduce the rate of absorption of

glucose thereby lowering the peak concentrations of this sugar in the blood in both normal and diabetic patients, and reduce urinary excretion of glucose and ketone bodies in diabetic patients. Dietary fiber has also proven to improve the control of the blood glucose concentration and reduce the peak concentration of insulin in non insulin dependant diabetics (Newsholme and Leech, 1994).

(d) Sulphonylurea Drugs

Sulphonylurea drugs are hypoglycaemic drugs used to lower the blood glucose concentration in non-insulin dependent diabetics. It was initially thought that they caused an increase in the secretion of insulin from the pancreas, thereby lowering the circulating glucose concentration, this however was later found not to be their sole mode of action. The way in which these drugs function is through some way increasing the number of insulin receptors, which has proven to be a safe and long lasting effective process of lowering the concentration of circulating insulin (Newsholme and Leech, 1994).

The main action of these drugs is however by the inactivation of the sulphonylurea receptor causing the subsequent opening of the voltage dependent calcium channels, thereby promoting insulin secretion. More information about these channels can be found in section 1.6.

(e) Thiazolidinediones

The thiazolidinediones are an exciting and relatively new class of insulin sensitising drugs used in the treatment of type II diabetes. The molecular target for these compounds is the nuclear hormone receptor, peroxisome proliferator-activated receptor γ (PPARγ), which is predominantly expressed in the adipose tissue (Reginato and Lazar, 1999; Akiyama *et al*., 2005).

The thiazolidinediones, which include troglitazone, pioglitazone, and rosiglitazone, are thought to sensitise tissues to the action of insulin and are effective in lowering serum glucose levels in the absence of insulin (Reginato and Lazar, 1999). These drugs act as high affinity ligands for the PPARγ. The PPARγ plays a role in adipocyte differentiation and therefore brings about an induction of small adipocytes through the subsequent

conversion of larger adipocytes. This process is then able to lower insulin resistance because large adipocytes produce such insulin resistant related substances as tumour necrosis factor and non-esterfied fatty acids whereas small ones do not (Suzuki *et al*., 2002).

Thiazolidinediones have also been shown to increase the expression of the lipoprotein lipase gene via the PPARγ or to enhance lipoprotein lipase activity, thereby causing triglyceride levels to decrease. These drugs are also associated with a decrease in plasma ketone body levels, however a side effect is weight gain in accordance with the adipocyte differentiation (Suzuki *et al*., 2002).

Recent literature has found that heterozygous PPARγ knockout mice, fed a high fat diet, displayed increased insulin sensitivity and decreased adipocyte hypertrophy in comparison to a wild type model fed a high fat diet. An explanation for this may be due to elevated levels of serum leptin in the PPARγ deficient strain, despite a significant decrease in fat mass. It seems as if removal or activation of the PPARγ receptor both seem to alleviate insulin resistance associated with high fat feeding. Reasons for this lie in alternative pathways. As already mentioned PPARγ antagonists stimulate adipogenesis which promotes the flux of free fatty acids from muscle and liver into white adipose tissue, thereby decreasing the content of triglycerides in these tissues and improvement of insulin sensitivity at the expense of increased white adipose tissue mass. PPARγ deficiency causes a decrease in muscle, liver and white adipose tissue triglyceride content, a result of increased leptin expression and activation of enzymes involved in β-oxidation, through the PPARα pathway (Tsuchida *et al*., 2005). It is however important to state that fat or muscle, specific, PPARγ knockout leads to insulin resistance, increased serum triglycerides and free fatty acids content, typical of the metabolic syndrome (Freedman *et al*., 2005).

(f) Biguanides

Biguanides are guanide derivatives in which two molecules of guanidine are linked together with the elimination of an amino group. Guanidine itself has been shown to

lower plasma glucose levels in animals, but its toxicity prevents its clinical use. In the 1950s, three major biguanides became available for clinical use, phenformin (phenethylbiguanide), metformin (*N*,*N*-dimethylbiguanide), and buformin (*N*-butylbiguanide). Phenformin was used successfully in the United States but was withdrawn because of associated cases of lactic acidosis, metformin does not have this problem and is widely used as a hypoglycaemic agent (Vigneri and Goldfine, 1987). Figure 1.5 displays a diagrammatic summary of some of the above mentioned medications.

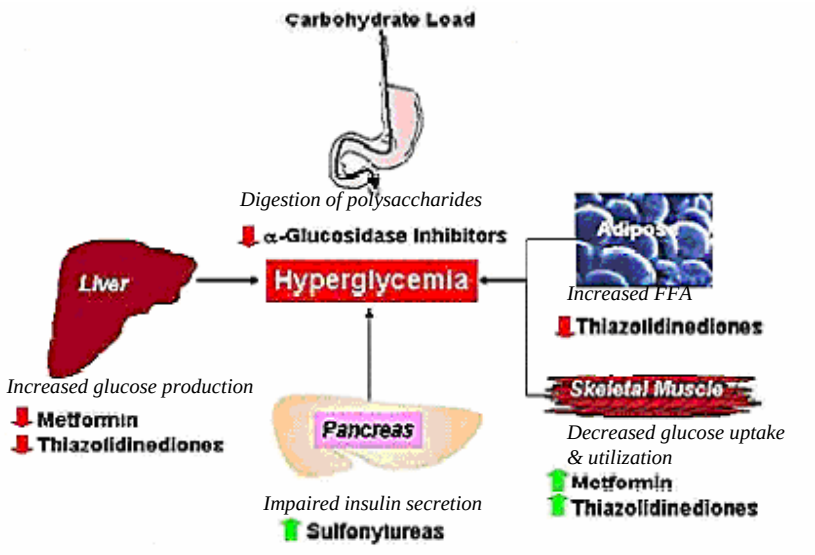

Figure 1.5: Sites of action of the current pharmacological therapies for the treatment of type 2 diabetes (taken from Evans and Rushakoff, 2002)

(g) Insulin Administration

This is the most common form of treatment for insulin dependent and sometimes non insulin dependent diabetic patients. The insulin is usually administered in the form of injections consisting of either a mixture of long and short lasting insulin twice a day, or short acting insulin before each main meal plus an injection of long lasting insulin in the evening to provide basal insulin levels throughout the night. The maximum concentration of insulin in the blood occurs 30-60 minutes after a meal, in normal individuals, which coincides with the period of rapid glucose absorption (Newsholme and Leech, 1994).

However, subcutaneous injections of short acting insulin results in the maximum blood insulin concentration only 2-3 hours after injection, which does not coincide with the maximum blood glucose concentration, which as a result will be much higher than normal. Hypoglycaemia may also be experienced 2-3 hours after a main meal (Newsholme and Leech, 1994). It is therefore concluded that this form of treatment may inhibit extreme variations in the blood glucose concentration, but it does not maintain it within the narrow limits found in healthy individuals.

In an attempt to eliminate this problem biomedical researchers have been trying to develop an artificial pancreas, but have failed to produce one small enough to be inserted inside the patient. Transplanting islets and the tail of a healthy pancreas is another alternative which researchers are looking into, however there is always the problem of adequate sources of islet tissues and rejection of the tissue (Newsholme and Leech, 1994).

(h) Alternative Medicines

Despite the impressive technical advances made in the diagnosis and therapy of diabetes many individuals still use alternative forms of therapy due to cost, religious or traditional reasons. Plants such as garlic and onion bulbs, karela (bitter melon) and Indian cluster bean (guar galactomannan), aloe and fenugreek seeds have all been studied and shown some benefit in lowering plasma glucose levels, but overall, there is little information about herbal remedies (Ryan *et al*., 2001).

Some trace elements may improve glycaemic control, such as chromium, zinc, magnesium, manganese, molybdenum and vanadium, which could prove beneficial in certain circumstances such as parental nutrition therapy (Mooradian *et al*., 1994). Certain minerals may, however, be present in excess in diabetes causing more harm than good, such as copper and iron (Walter *et al*., 1991; Cutler, 1989). Certain vitamins and micronutrients have been proposed as nutraceutical interventions in diabetes and these may be present in medicinal plants. Fish oil supplementation has been suggested for diabetes complications and L-carnitine in type II diabetes, folic acid and vitamin B6

improve homocystein levels and may reduce the risk of cardiovascular complications (Ryan *et al*., 2001).

Many plants are used by traditional healers around South Africa as a substitute for western medication. The fact that local tradition as well as lack of sufficient funding encourages many individuals to turn to their traditional healers for treatment is suspected by many health care professionals to result in many premature deaths or increased advanced diabetic associated complications. Not enough information is available for these alternative forms of diabetic medication, and one should not substitute any of the above mentioned alternative medicines for that which is prescribed by a health care professional. It is also important to remember that toxicity studies are essential before taking any form of medicinal plant or herb.

(i) Islet Transplants

This is a relatively new procedure in which islets are taken from a donor pancreas (currently, deceased donors) and transplanted into the recipient during a short, minimally invasive procedure. The islets are extremely fragile and must immediately be separated from the remaining pancreatic tissue. The procedure takes approximately an hour and entails the use of ultrasound to guide a small catheter through the upper abdomen into the portal vein of the liver (see adjacent figure). The islets are then injected through the catheter and, once implanted, begin to produce insulin in response to the bodies needs (Hering, 2005).

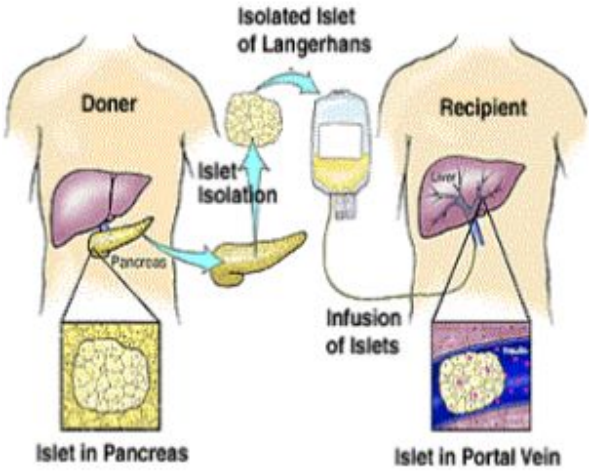

Figure 1.6: Schematic diagram illustrating islet transplants (Taken from Hering, 2005)

1.4.7. Review of Hypoglycaemic Medication to be used Throughout the Project

As two hypoglycaemic agents were used throughout the duration of the project it was important to understand the mechanism of action of these drugs and any side effects that they may have. The drugs which were used are the biguanide, metformin, and a traditional medicinal plant *Sutherlandia frutescens*, subspecies *Microfilla* (kankerbos).

(a) Metformin

Despite the fact that this drug has been around since the 1950s, for the treatment of type II diabetes, its mechanism of action still remains unclear and controversial. Biguanides are not truly hypoglycaemic agents as they lower the blood glucose levels in non-insulin dependent diabetic patients but do not lower the glucose values in nondiabetics, unless there has been prolonged fasting. Metformin is not metabolised in the liver, is not bound to serum proteins, and has a mean plasma half-life of 1.5-2.8 hours (Vigneri and Goldfine, 1987).

The blood glucose lowering effect of metformin is not caused by increased insulin secretion, although the presence of some insulin is a prerequisite for a therapeutic response, but is postulated to be due to a multifactorial mode of actions involving decreased intestinal glucose absorption, decreased gluconeogenesis, and increased glucose uptake by muscle (Klip and Leiter, 1990). Nosadini *et al*. (1987) demonstrated that it is not possible for metformin to act as effectively independently of insulin. In an *in vivo* glucose disposal experiment, using the euglycaemic clamp technique, it was demonstrated that metformin increased glucose utilization of peripheral tissues by 50% at a high insulin infusion rate and by 25% at a low infusion rate.

In the past it was believed that metformin's main site of action was adipose tissue, however it seems that the muscle and liver are the more favoured tissues (Zou *et al*., 2004). The cellular mechanism of action could involve any of the rate limiting steps in glucose metabolism, either basal (insulin independent) and/or insulin stimulated. These include insulin receptor binding and signals derived from it, glucose transport across the

cell membrane, glucose oxidation at the level of pyruvate dehydrogenase, and glycogen synthesis at the level of the glycogen synthase complex (Klip and Leiter, 1990).

Early studies undertaken by Lord *et al.* (1983) showed convincing evidence that metformin increased the number of insulin receptor binding sites on erythrocytes in type II diabetes. However many others have followed this path, using different cell models, and have shown conflicting results; even in instances when metformin was shown to increase insulin binding to cells, this effect did not appear to be directly related to the subsequent metabolic and clinical effects of the drug (Klip and Leiter, 1990). Therefore the ability of metformin to increase insulin receptors and insulin binding cannot be consistently demonstrated. It was therefore suggested that metformin may be acting at a post insulin binding level (Vigneri and Goldfine, 1987; Klip and Leiter, 1990).

One way in which metformin acts on post receptor insulin binding is through the insulin receptor kinase activity and receptor internalisation. Circulating cells and cultured fibroblasts from insulin resistant patients have abnormal insulin receptor kinase activity, as do muscle cells from diverse diabetic animal models (Klip and Leiter, 1990). The insulin receptor kinase forms an important part of the insulin signalling process, including stimulation of glucose transport. It has been demonstrated in the past that a decrease in kinase activity associated with streptozotocin induced diabetic rat muscle is increased to supranormal levels in response to metformin treatment (Rossetti *et al*., 1990). Benzi *et al.* (1988) also found that insulin receptor internalisation, after ligand binding, is diminished in monocytes from obese non-insulin dependent diabetics in comparison to control subjects. This reduction was however corrected for after *in vivo* metformin treatment. These responses to metformin treatment may however not be a direct result of the medication but may be a consequence of improved glycaemic control or a lower body mass index. It has been shown that improving glycaemia and insulin receptor kinase activity is possible through weight loss alone in obese individuals (Klip and Leiter, 1990).

Metformin also has the ability to decrease excess weight in obese individuals, which is advantageous as this helps in the lowering of insulin resistance (Faghanel *et al*., 1996). The drug is thought to decrease the desire for food intake through one of the following three hypotheses:

- The concentration of the hypothalamic neuropeptide Y is thought to be directly associated with food intake. Acute and chronic injection of neuropeptide Y into paraventricular nucleus elicits a long lasting hyperphagic effect. An anorectic effect of metformin has been shown to be associated with an increase in neuropeptide Y content of the paraventricular nuclei and arcuate nuclei without affecting preproneuropeptide Y mRNA expression in the arcuate nuclei, in obese rats. Similar findings were found in food deprived lean rats (Paolisso *et al*., 1998).

- Another hypothesis states that the insulin action in the brain participates in body weight regulation. Various studies have shown that chronic intracerebroventricular administration of insulin in different animals led to a dose dependent reduction in food intake. The possible relationship between the insulin action and the anorectic effect is thought to be through the plasma insulin like growth factor, a proxy of insulin action. This suspicion was confirmed when the results of the experiment showed that before starting and after metformin treatment plasma insulin like growth factor was significantly associated with food intake (Paolisso *et al*., 1998).

- A further mechanism by which metformin may affect food intake is through the improvement in energy production. It has been proposed that a decline in ATP synthesis is a metabolic stimulus that triggers feeding behavior. Because ATP is a final end product of the oxidation of both glucose and fatty acids, changes in the amount of ATP in hepatocytes could provide an integrated signal for feeding behavior. It is therefore assumed that overeating is a result of fuels that would be otherwise oxidized to produce ATP in a detectable manner being redirected into fat stores. It therefore seems that overeating appears to be an appropriate response to a need for energy created not by the lack of food inside the body but rather by the sequestration of energy stores within the body (Paolisso *et al*., 1998).

Metformin has also been shown to have an effect on lipid metabolism, significantly reducing hepatic triglyceride synthesis (Vigneri and Goldfine, 1987). However these results prove to be controversial according to a paper published by Suzuki *et al.* (2002). Metformin has been shown to affect glucose metabolism through action on glycogen synthase *a* and glycogen phosphorylase *a*. It seems that the drug stimulates both glycogen phosphorylase *a* and synthase *a* in the liver, thereby increasing the turnover of hepatic glycogen metabolism resulting in no net accumulation of glycogen. The muscle, on the

other hand shows an increase in glycogen synthase *a* only, associated with metformin treatment. This allows for an accumulation of glycogen in the muscle (Reddi and Jyothirmayi, 1992). The increase of these enzymes allows for glucose to rather be converted into glycogen than into lipids, this alteration in glucose metabolism may also play a role in the reduction of body fat in obese individuals (Suzuki *et al*., 2002).

Another way by which metformin improves glucose metabolism is by increasing the glucose transporters in the plasma membrane, namely GLUT4 (Klip and Leiter, 1990). The number of transporters have been shown to be diminished in streptozotocin diabetic rats. Metformin has, however, been shown to enhance basal 2-deoxyglucose and 3-*O*-methylglucose uptake by muscle cells in culture through stimulation of GLUT4 glucose transporters (Reddi and Jyothirmayi, 1992). It has been established that metformin inhibits the enzymatic activity of comlex I of the respiratory chain and thereby impairs both mitochondrial function and cell respiration. Mitochondrial disruption on the level of complex I immediately reduces the ratios of ATP to AMP, ATP to ADP and phosphocreatine to creatine which activates AMP-activated protein kinases which causes catabolic responses on the short term and insulin sensitization on the long term (Brunmair *et al*., 2004, Tiikkainen *et al*., 2004).

There are not many side effects to report with metformin therapy. DeFronzo *et al*. (1995) did however report nausea, diarrhea, and a decreased vitamin B_{12} in patients receiving metformin treatment. The dosage was however extremely high, 2550mg per day, and these symptoms subsided when the dosage was lowered. The normal dosage is in the range of 500mg every 8 hours, 850mg twice daily, or 3g daily if needed (Cooper and Gerlis, 1997; Nisbet *et al*., 2004). It is also evident that metformin does not cause lactic acidosis, as phenformin does, due to a difference in lactate metabolism. Metformin has been found to reduce lactate use for gluconeogenesis without altering the plasma lactate concentration or the plasma lactate turnover, but by increasing lactate oxidation (Stumvoll *et al*., 1995).

All in all metformin seems to be an extremely effective drug for non-insulin dependent diabetic therapy, displaying few side effects, and producing normoglycaemic levels effectively. However to increase the effectiveness of this drug combination therapies are being used with sulphonylurea receptor drugs (Hermann *et al*., 1994) and with thiazolidinediones (Suzuki *et al*., 2002).

(b) *Sutherlandia frutescens*

The genus *Sutherlandia*, commonly known as the cancer bush or kankerbos comprises of six species, all of which are endemic to Southern Africa. These six species can be reduced to two, namely *S. frutescens* and *S. tomentosa*, the former is further divided into three subspecies, namely subsp. *frutescens*, subsp. *microphylla*, and subsp. *speciosa*. The species are distinguished from one another from their habitat, the shape of the pods, and the shape and pubescence of the leaflets (Moshe, 1998). The genus has been renamed to *Lessertia* but is still referred to by its more favoured name of *Sutherlandia* (Müller, 2002). A typical *S. frutescens* flower is shown in figure 1.7.

Figure 1.7: Example of a typical *S. frutescens* flower (taken from Seier *et al*., 2002)

This plant has been used for medicinal purposes for many years. It is thought that the Khoi and Nama people were the first to use it against fevers and a variety of other ailments including cleansing of open wounds (van Wyk *et al*., 1997). The plant has been used as a remedy for stomach problems and even internal cancers. The virtues of the

plant, however, extend beyond this as it has also been used for colds, influenza, chicken pox, diabetes, varicose veins, piles, inflammation, liver problems, backache and rheumatism. The leaves are the main portion of the plant used for medicinal purposes, however the stems are often also included (van Wyk *et al*., 1997). The plant is currently being investigated for any anti-cancer or anti-HIV activities which it may have (Tai *et al*., 2004; Kundua *et al*., 2005; Chinkwo, 2005; Harnett *et al*., 2005). *Sutherlandia* is available in tablet form, for which the recommended dosage is 300mg twice daily. Patients on antihypertensive or diabetic medication may need the doses reduced while taking *Sutherlandia* (Gericke, 2001).

In 2002 the South African Medical Research Council released a 3 month toxicity study of oral *Sutherlandia* leaf powder in vervet monkeys. The report showed that *Sutherlandia* leaf powder consumption was safe and not associated with biochemical or haematological abnormalities at the dose used for this study as well as 3x and 9x this dose (Medical Research Council and National Research Foundation of South Africa, 2002).

Three important compounds, which are of medicinal value, are associated with the *Sutherlandia* species:

1. **Triterpenoids**

Triterpenoids are compounds which are biologically active against various diseases and even display anticancer activity. These compounds inhibit cancer cell proliferation by acting as spindle poisons, for example lymphocytic leukaemia cells P-388 and L-1210 and human lung carcinoma cells A-549 displayed a decreased rate of proliferation in the presence of ursolic acid. Some examples of medicinally important triterpenoids include oleanic acid putranoside, swartziasaponin, asiaticoside, soyasapogenol, and medicagenic acid (Moshe, 1998).

Moshe was able to isolate two triterpenoids from *Sutherlandia*, however identification and purification proved to be difficult and was therefore not undertaken.

2. Amino acids

Canavanine: L-canavanine, 2-amino-4 (guanidinooxy) butyric acid is a structural analogue of arginine and is a common seed metabolite of most legumes but is also stored in vegetative organs and vacuoles in leaves where it acts as a nitrogen store and an insecticide (Moshe, 1998). Canavanine has been used effectively against cancer, colds, and flu viruses (Tai *et al*., 2004; Kundua *et al*., 2005; Chinkwo, 2005). The anti-cancer activities of this amino acid have been demonstrated when mice bearing L-1210 leukemic cells were treated with canavanine, and lived longer than mice that were not treated. Canavanine also inhibited rat colon carcinoma and pancreatic cancer cell proliferation (Moshe, 1998). Various hypotheses have been put forward as to the biochemical nature of the anticancer and medicinal effects associated with canavanine.

- Canavanine is substituted for arginine in most metabolic reactions, as canavanine is a structural analogue of arginine, resulting in structural and functional protein aberrations occurring in canavanine sensitive organisms (Moshe, 1998). This process can cause the inhibition of tumour growth resulting from the incorporation of canavanine into tumour proteins, causing the production of aberrant macromolecules which exhibit impaired function. These proteins are then degraded more rapidly than their normal counterparts (Moshe, 1998; Kundua *et al*., 2005).

- Canavanine also interferes with RNA synthesis and disrupts DNA replication and transcription. This has been demonstrated when canavanine prevented RNA polymerase synthesis in Semilik Forest virus, and reduced DNA synthesis in the herpes simplex virus (Moshe, 1998; Kundua *et al*., 2005).

Arginine and nitric oxide: Nitric oxide is formed from arginine by nitric oxide synthase, and is a messenger molecule in living organisms. Other functions of this compound include smooth muscle relaxation, platelet aggregation, neurotransmission, immune cell activation, tumour cell killing, protection against damage to cardiac myocytes, protection of endothelial cells and maintainance of vascular wall integrity, prevent intestinal ischaemia and induction of intestinal fluid secretion into the jejunum (Moshe, 1998).

L-Arginine is a common substrate in many metabolic reactions and is essential in the regulation of cell growth and differentiation. Arginine has also displayed anticancer activities by shortening tumour regression and retarding tumour growth (Moshe, 1998).

GABA: Glutamate decarboxylation gives rise to γ-aminobutyrate (GABA), an inhibitory neurotransmitter. Its underproduction is associated with epileptic seizures, and is used pharmacologically in the treatment of epilepsy and hypertension (Nelson and Cox, 2000). GABAA and GABAB are the two GABA receptors which mediate messages to the brain via ion channels (Moshe, 1998). The smoking of *Sutherlandia* seeds has been recorded to be associated with high levels of GABA, which could prove beneficial to the treatment of epilepsy (Moshe, 1998).

3. Pinitol

Pinitol, derivatives, and metabolites thereof are useful in nutritional and medicinal compositions for lowering plasma free fatty acid levels, for treating conditions associated with insulin resistance, such as diabetes mellitus and its chronic complications (hyperlipidaemias, dyslipidaemias, atherosclerosis, hypertension, and cardiovascular disease), AIDS, cancer, wasting/cachexia, sepsis, burn wounds, malnutrition, stress, lupus, endocrine diseases, hyperuricemia, polycystic ovary syndrome and complications arising from athletic activity (Ostlund and Sherman, 1998). Pinitol is very effective in lowering blood glucose levels, and is claimed to have insulin like effects (Ostlund and Sherman, 1998; Bates *et al*., 2000; Davis *et al*., 2000). Bates *et al*. (2000) reported that pinitol can exert an insulin like effect to improve glycaemic control in hypoinsulinaemic streptozotocin diabetic mice, and it is proposed that it acts via a post receptor pathway. The structure of D-Pinitol (3-O-methyl-D-chiro-inositol) is shown in figure 1.8 (taken from http://www.irl.cri.nz/carbo/products/inositols.html).

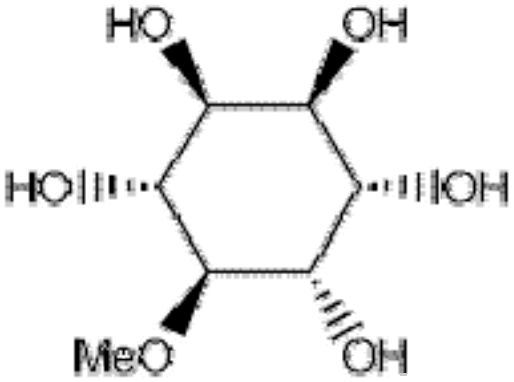

Figure 1.8: The chemical structure of D-Pinitol

The dosage of pinitol, metabolite or derivative thereof, ranges from 0.1 to 1mg per day, per kilogram body weight of a mammal. This can be administered orally, enterally, or intravenously (Ostlund and Sherman, 1998). The exact biochemical action associated with the hypoglycaemic effects of pinitol is still not clearly understood and further investigation into this compound is necessary. The concentration of pinitol, in *Sutherlandia*, has been calculated through HPLC analysis to be approximately 14mg/g of dry leaves. This concentration may however differ between seasons and varying geographical locations of the plant (Moshe, 1998).

1.5. INSULIN: A CLOSER LOOK INTO THE FORMATION, STRUCTURE, FUNCTION, AND DEGRADATION OF THIS MULTIFUNCTIONAL HORMONE

1.5.1. Structural Detail of Insulin

Insulin is a 51 amino acid polypeptide hormone produced in the pancreatic β-cells in the islets of Langerhans. It is a small protein with a molecular weight of 5700, which is released in response to increased glucose levels in the blood. It consists of two polypeptide chains, namely A and B which are joined by two disulfide bonds (Nelson and Cox, 2000), see figure 1.9.

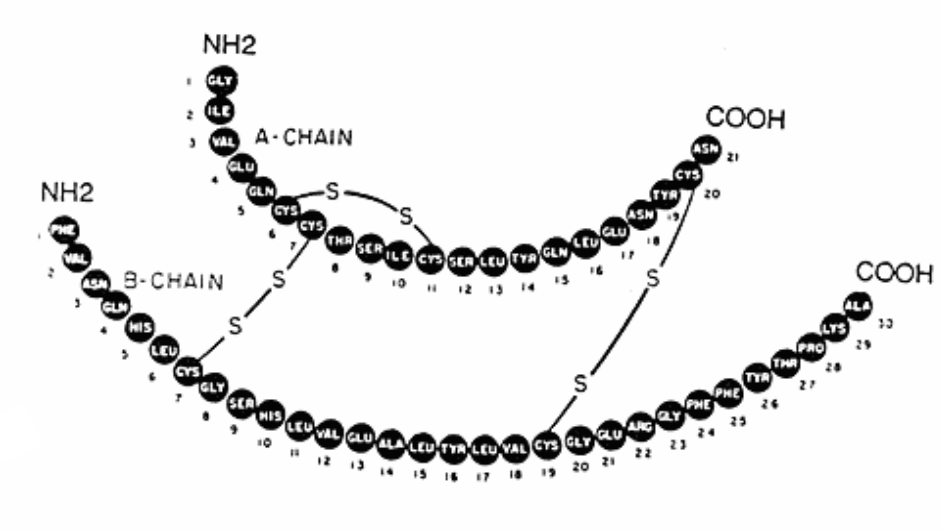

Figure 1.9: The amino acid sequence of the two chains of porcine insulin, joined by disulfide bridges (taken from Pittman *et al*., 2004)

Porcine insulin is identical to that found in humans except for the change of alanine to threonine at position 30 on the B chain in human insulin. The structures of mouse and rat insulin are also identical to that of humans, except for a slight divergence in comparison to the A and B chains of the human insulin structure. On the A chain it has been found that glutamate has been replaced by aspartate at position 4, for mouse insulin, while three changes are apparent on the B chain of human insulin at positions 3, 9, and 30, which are lysine replacing asparagine, phenylalanine replacing serine, and serine replacing threonine respectively (Beintema and Campagne, 1987). Despite these four changes

setting these two almost identical hormones apart, their role and function within the body appears to be exactly the same.

The three dimensional X-ray structure of insulin has allowed for specific residue positions and side chain orientations to be determined and related to synthetic, as well as, genetic mutants of insulin in order to obtain a clearer understanding of which residues and positions are necessary for receptor binding (Blundell *et al*., 1972). Three regions located on or near the surface of insulin are thought to interact with the insulin receptor; they are the NH_2-terminal A-chain (GlyA1-IleA2-ValA3-GluA4 or AspA4), COOH-terminal A-chain (TyrA19-CysA20-AsnA21), and the COOH-terminal B-chain (GlyB23-PheB24-PheB25-TyrB26) residues (Pullen *et al*., 1976).

GlyA1 deletion or N-acetylation of the NH_2 terminus on the A-chain decreases insulin-receptor binding between 15-30% (Wollmer *et al.*, 1987). A LeuA3 for ValA3 substitution can decrease the insulin-receptor binding by 95% (Kwok *et al*., 1983, Shoelson *et al*., 1983, Kobayashi *et al*., 1982, Nanjo *et al.,* 1986). Substitutions of GlyA1 with L-Ala, L-Val, L-Leu, L-Pro, L-Trp, L-Lys, or L-Glu result in a 2-20% decrease in insulin-receptor binding, however if GlyA1 is substituted with D-Phe, D-Leu, D-Trp, D-Ala, D-Lys, or D-Glu no alteration in binding occurs (Cosmatos *et al*., 1978, Geiger *et al*. 1975, Geiger *et al*., 1980, Geiger *et al*., 1982, Nakagawa *et al*., 1989). These results suggest that it is not necessarily the nature of the terminal amino acid that determines the insulin-receptor specificity but the chirality of the amino acid in that position.

Mono or di-iodination of TyrA19 on the COOH A-chain terminus results in 20-50% reduced binding affinity (Wieneke *et al*., 1983; Ohta *et al*., 1988), while the deletion of AsnA21 leaves the hormone with only a 4% binding specificity (Slobin *et al.*, 1963). Substitutions in the B-chain COOH terminus has also been extensively studied; a LeuB25 for PheB25 substitution or a SerB24 for PheB24 substitution decreases insulin-receptor binding by nearly 100% (Kwok *et al.*, 1983, Shoelson *et al.*, 1983, Kobayashi *et al*., 1982, Nanjo *et al.*, 1986). Removal of residues PheB25 and PheB24 results in analogs with 6% and 0.2% binding, respectively; and the subsequent removal of GlyB23 produces an analog with a 0.1% binding affinity (Nakagawa *et al*., 1986).

The NH_2 B-chain terminus has also been extensively studied, and evidence suggests that any deletions or substitutions of this terminus (PheB1-ValB2-AsnB3-GlnB4) results in a minimal alteration in insulin-receptor binding affinity (Cao *et al*., 1986; Schwartz and Katsoyannis, 1978).

1.5.2. Insulin, the Initiation of its Being

In adult mammals the insulin gene is expressed solely in the pancreatic β-cells. The β-cells' specific expression is controlled by transcriptional enhancer and promoter sequence elements in the 5' flanking DNA of the gene (Flatt, 1992).

The initial translational product of this gene is pre-proinsulin, which consists of an N-terminal signal peptide linked to proinsulin. Like most nascent secretory proteins, translocation of pre-proinsulin across the rough endoplasmic reticulum membrane commences by interaction of the signal sequence with the 54kDa polypeptide component of the signal recognition particle, an event which retards further elongation of the peptide chain (Flatt, 1992).

The association of this complex with the rough endoplasmic reticulum membrane is mediated by the affinity of the signal recognition particle for the signal recognition receptor, also known as the docking protein. This interaction then promotes the release of the signal recognition particle from both the ribosome and the signal sequence, which is then transferred to the signal sequence receptor, a glycosylated, integral membrane protein (Flatt, 1992).

1.5.3. Formation and Packaging of Insulin

Proteolytic cleavage of the 23 amino acid signal sequence, at the amino terminus, of pre-proinsulin and the formation of three disulfide bonds produces pro-insulin, see figure 1.10.

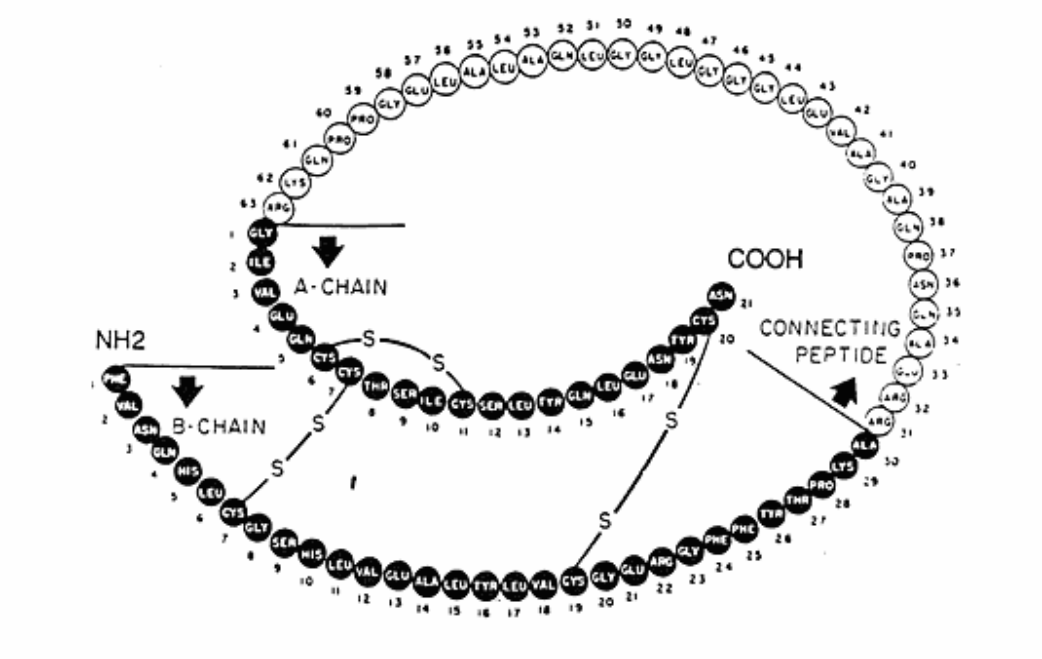

Figure 1.10: Primary structure of porcine pro-insulin (taken from Pittman *et al*., 2004)

Proinsulin is then transported through the cisternae of the endoplasmic reticulum to the Golgi complex for packaging into secretory granules. The proinsulin is then converted into insulin, through the proteolytic cleavage of the C-peptide, all of which takes place in the secretory granule.

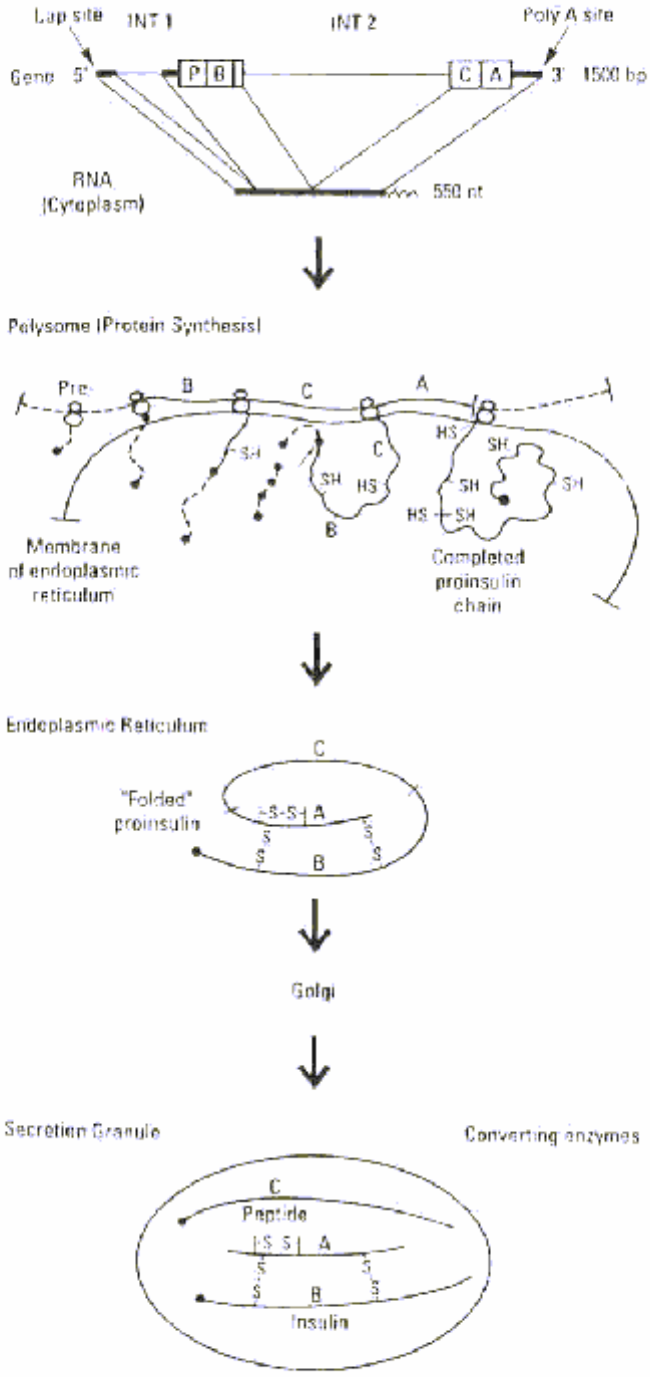

Figure 1.11: A schematic representation of insulin formation (bp, base pairs; nt, nucleotides and INT, intron) (taken from Ganong, 1993)

The three exons, in figure 1.11, of the insulin gene are separated by two introns (INT 1 and INT 2). Exons 1 and 2 code for an untranslated part of the mRNA, exon 2 codes for the signal peptide (P) and the B chain (B), exons 2 and 3 code for the C peptide (C), and exon 3 codes for the A chain (A) plus an untranslated part of the mRNA. The signal peptide guides the polypeptide chain into the endoplasmic reticulum and is then removed. The molecule is next folded, with formation of the disulfide bonds. The C peptide is separated by one or more converting enzymes in the secretory granules. The insulin is then stored as a hexamer which is stabilized by two zinc ions, as seen in figure 1.12. The hexameric units are formed when three insulin dimers and two zinc ions associate through the imidazole groups of HisB10 and in a particular instance to HisB5. This hexameric form of insulin does however not occur at any significant concentration in the blood, as electrostatic repulsion and a decreased insulin concentration favour the typical monomer formation following insulin secretion from the vesicles (Blundell *et al*., 1972; Cutfield *et al*., 1981; Bentley *et al*., 1976).

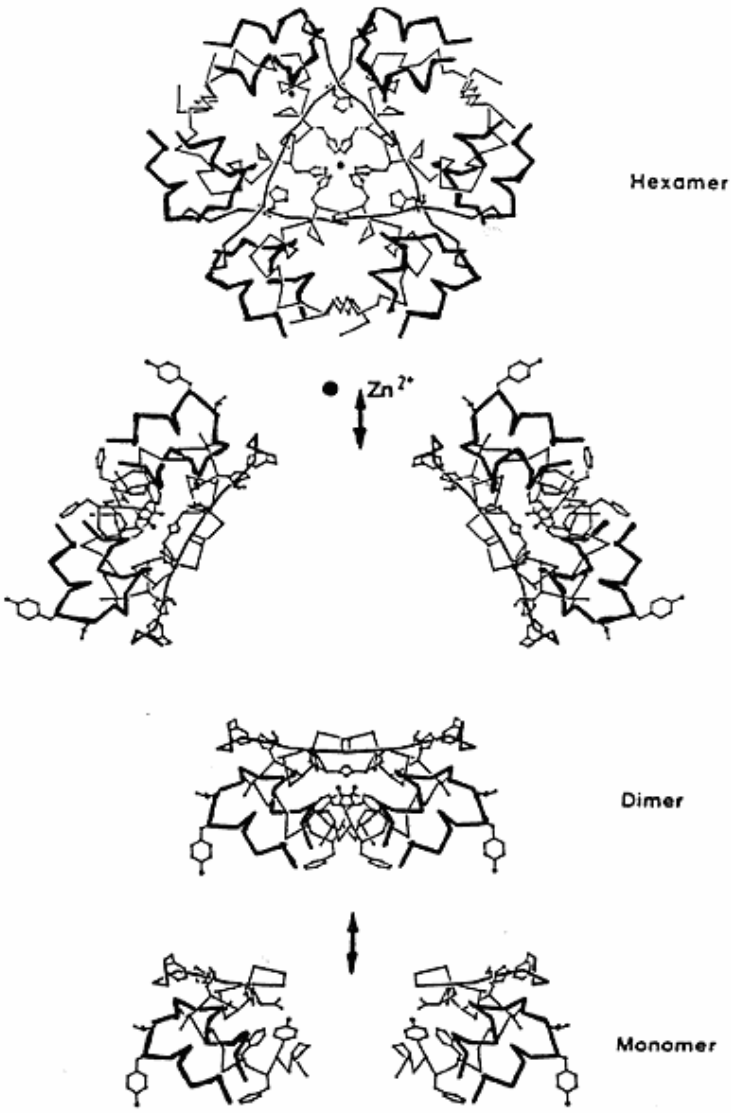

Figure 1.12: Assembly of the Zn^{2+} insulin hexamer starting from the insulin monomer and including the, intermediate, insulin dimmer. The A-chain of insulin is illustrated as a thickened black line, and the B-chain as a thinner line (taken from Pittman *et al*., 2004)

The intact insulin, C-peptide, and some basic amino acids are all released into the extracellular fluid during insulin secretion. This allows an assessment of endogenous insulin, released from diabetic patients, receiving insulin to be determined through measuring the concentration of C-peptide released in conjunction with the endogenous insulin (Newsholme and Leech, 1994).

1.5.4. Factors which Govern Insulin Secretion

The biosynthesis and secretion of insulin by the islets of Langerhans are regulated by many circulating factors including glucose, neurotransmitters and hormones.

(a) As controlled through insulin gene transcription

It has been demonstrated that in isolated islets there is an increase in the synthesis of insulin mRNA relative to other cellular mRNA, when the islets are induced with glucose. An experiment confirmed this by demonstrating that the insulin mRNA content of islets was reduced by culture in low glucose (0-3.3mM) compared with islets cultured in high glucose (17-20mM). In addition, the rate of insulin gene transcription was approximately 3-fold higher in islets cultured in 17mM glucose compared with 3.3mM glucose. The experiment was also able to show that the half-life of insulin mRNA was 2.6 fold greater in islets cultured in 17mM glucose compared to those cultured in 3.3mM glucose (Flatt, 1992).

(b) As controlled through glucose concentrations

Insulin is released from their granules, in the β-cells of the pancreas, through exocytosis in response to an elevated blood glucose level, usually above 5mM (Tortora and Grabowski, 2003). The movement of the granules to the cell membrane in response to stimulation is due to microfilaments and microtubules which are organized in a subcytosolic web with individual microfilaments inserting in the cell membrane and the microtubules. Insulin secretion can therefore be inhibited through the depolymerization of tubulin, which results in the breakdown of the microtubules (Newsholme and Leech, 1994).

It is thought that there is a link between a glycolytic intermediate and insulin secretion, which together is known as the coupling factor and is thought to involve calcium ions. Phosphoenolpyruvate is thought to be the intermediate involved. The intracellular protein that detects the change in concentration of calcium ions is probably calmodulin, a heat stable protein with a molecular mass of about 17 000. This protein is able to bind up to four calcium ions at a time, thereby changing the three dimensional structure of the protein which in turn somehow controls the contractile activity of the microtubules (Newsholme and Leech, 1994).

The entire process is then thought to interact with one another to bring about insulin secretion as follows: when the glucose concentration increases to about 5mM, the rate of glycolysis increases proportionally, thereby raising the concentration of phosphoenolpyruvate. The increased activity of the glycolytic pathway generates signals that close ATP-sensitive K^+channels in the plasma membrane. The resulting decrease in K^+ conductance leads to depolarization with subsequent opening of voltage dependent calcium channels. The calcium influx through these channels increases, causing a rise in free cytoplasmic calcium which serves as the triggering signal (Shepard and Henquin, 1995).

The triggering signal then functions via calmodulin which causes contraction of the microfilaments or microtubules, which may contain actin or myosin and hence contract in a similar way to skeletal muscles. This contraction then results in an increased rate of exocytosis and insulin secretion (Newsholme and Leech, 1994).

(c) As controlled through hormonal regulation

It has also been demonstrated that endogenous insulin itself is able to stimulate insulin secretion in pancreatic β-cells. Functional insulin receptors have been found on β-cells, and the insulin concentration necessary to activate these receptors to bring about insulin secretion is in the nanomolar range (Aspinwall *et al*., 1998).

The insulin-stimulated insulin secretion is not controlled by glucose or increased glucose utilization as the effect occurs even at 0mM glucose. Insulin does however cause a rise in the intracellular calcium concentration which subsequently initiates insulin secretion as described earlier, through the binding of the calcium to the calmodulin protein. The β-cell insulin system is a rare example of positive feedback on secretion as most auto receptors mediate negative feedback on secretion (Aspinwall *et al*., 1998).

This positive feedback mechanism would cause augmented secretion during the initial stages of elevated glucose levels giving rise to a greater bolus of insulin release, however, other mechanisms must eventually take over to suppress the release. This could therefore be the reason that a rapid increase is observed in the first phase of insulin secretion and the sustained, lower secretion is observed during the second phase of secretion. It has also been discovered that type II diabetics have a reduction in first phase insulin secretion, which could be a result involving a lack of positive feedback from the β-cell insulin receptor (Aspinwall *et al*., 1998).

Figure 1.13 illustrates the way in which insulin is secreted in its two peaks. The first peak is released approximately 3-10 minutes after the ingestion of glucose. This insulin has already been produced by the β-cells of the pancreas, and is in storage. Its main function is to stop the blood glucose from rising too high, as this could over stimulate, and thereby damage the pancreas. The second phase of insulin secretion occurs approximately 30 minutes later from the β-cells. This insulin is not from a stored reserve but has been produced for this specific task. The size of this phase is directly proportional to the elevation of glycaemia (Servier, 2001).

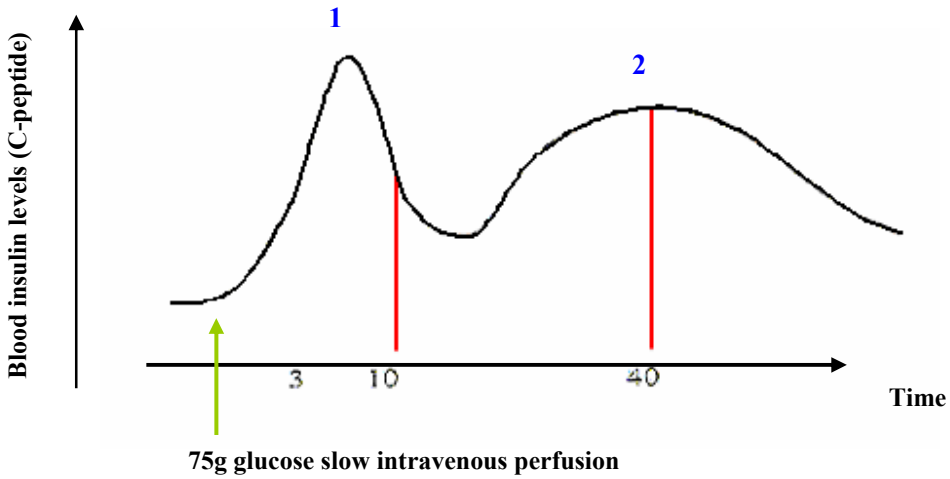

Figure 1.13: A representation of the two insulin peaks experienced during a typical insulin secretion (taken from Servier, 2001)

(d) As controlled through a secondary messenger

Cyclic AMP (cAMP) is also thought to be related to insulin secretion, not directly but rather by increasing the magnitude of the secretory response to glucose or other sugars which can enter the glycolytic pathway. It is likely that this effect is achieved by activation of cyclic AMP dependent protein kinase and phosphorylation of a protein involved in control of calcium transport, so that for a given concentration of glucose more calcium enters the cytosolic compartment of the cell, or phosphorylation of microtubules could increase their responsiveness to a given change in the calcium ion concentration (Newsholme and Leech, 1994).

1.5.5. Insulin: Hard at Work

This polypeptide hormone is invaluable through its actions within the human body, as are many other hormones. Insulin's sole function, however, is not only to decrease the concentration of circulating glucose in the blood through the promotion of glycolysis or its conversion into glycogen, but it has many other important tasks:

(a) Effects of insulin on carbohydrate metabolism

1. Insulin increases transport of glucose across the cell membrane into adipose tissue and muscle, for storage when excess glucose is present and for the breakdown of glucose into ATP respectively (Montgomery *et al*., 1996).

2. Insulin stimulates glycogen synthesis (to be discussed later in more detail) in a number of tissues including adipose tissue, liver, and muscle (Nelson and Cox, 2000).

3. Insulin increases glycolysis, indirectly, by stimulating other processes (triacylglycerol, glycogen, and protein synthesis) requiring increased rates of ATP formation (Montgomery *et al*., 1996).

4. Insulin inhibits the rates of glycogenolysis, by inhibiting the glucagon hormone which promotes the breakdown of glycogen into glucose, and gluconeogenesis in the liver. Gluconeogenesis is inhibited due to the fact that the cellular uptake of glucose is promoted by insulin, thereby initiating the breakdown of the carbohydrate to produce energy for the body. If insulin is not present in a sufficient amount to promote the cellular uptake of glucose then there is no energy being produced and the body assumes that it is being starved. In such a case acetyl-CoA and oxaloacetate, from the citric acid cycle, are converted through the process of gluconeogenesis into glucose in an attempt to increase the blood glucose concentration so that the body may be able to once again produce sufficient energy for survival of important organs, including the most important of all the brain, which is only able to obtain its energy from glycolysis (Nelson and Cox, 2000).

5. Insulin increases the activity of the glucokinase enzyme in the liver. This enzyme is responsible for converting glucose into glucose-6-phosphate during glycogen synthesis. This may play an important part in decreasing the rate of glucose release and facilitating an increase in glucose uptake, by the liver, after a meal (Nelson and Cox, 2000).

6. Insulin increases the rate of glucose oxidation by the pentose phosphate pathway in liver and adipose tissue, this is however secondary to the stimulation of fatty acid synthesis by this hormone (Newsholme and Leech, 1994).

Certain tissues, such as the kidney, brain, and intestine, are totally insensitive to the action of insulin on carbohydrate metabolism. During starvation tissues which rely on glucose as their sole source of energy, such as the brain and other neurons, are allowed preference of circulating glucose, while other tissues utilize ketone bodies as an energy source. Ketoneogenesis occurs in the liver from fatty acid oxidation, producing three

ketone bodies, namely, acetone, acetoacetate, β-hydroxybutyrate (Newsholme and Leech, 1994).

(b) Effects of insulin on lipid metabolism

1. Insulin inhibits lipolysis in adipose tissue because it is involved in the activation of the pyruvate dehydrogenase complex and citrate lyase, both of which supply acetyl-CoA, thereby promoting fatty acid synthesis. If fatty acid synthesis and β-oxidation were to occur simultaneously, the two processes would constitute a futile cycle, wasting energy. Thus during fatty acid synthesis, the production of the first intermediate, malonyl-CoA, shuts down β-oxidation at the level of the transport system in the mitochondrial inner membrane (Nelson and Cox, 2000).

2. Insulin inhibits ketone body synthesis in the liver, by ensuring sufficient glucose is taken up by cells in the body. If insulin is not present in sufficient amounts, to promote the cellular uptake of glucose, then the citric acid cycle intermediates are used for glucose synthesis via gluconeogenesis. This causes the subsequent slowing of the oxidation of the citric acid cycle intermediates as well as the oxidation of acetyl-CoA. Moreover, the liver contains only a limited amount of coenzyme A, and when most of it is tied up in acetyl-CoA, β-oxidation of fatty acids slows for lack of the free coenzyme. However the production and export of the ketone bodies frees the coenzyme A, thereby allowing continued fatty acid oxidation (Nelson and Cox, 2000).

3. Insulin also stimulates fatty acid and triacylglycerol synthesis in adipose tissue and liver (Newsholme and Leech, 1994). Insulin promotes the conversion of carbohydrates into triacylglycerols. The pyruvate dehydrogenase complex and citrate lyase, both of which supply acetyl-CoA, are activated by insulin. The acetyl-CoA then goes on to form malonyl-CoA which participates in the biosynthesis of fatty acids (Nelson and Cox, 2000).

(c) Effects of insulin on protein metabolism

1. Insulin increases the rate of amino acid transport into the muscle, adipose tissue, and liver cells, so that amino acids may be used for protein synthesis rather than gluconeogenesis (MacSween and Whaley, 1992).

2. Insulin increases the rate of protein synthesis in muscle, adipose tissue, liver and other tissues (MacSween and Whaley, 1992).

3. Protein degradation in muscles is also decreased through the action of insulin (Newsholme and Leech, 1994).

(d) Effects of insulin and glucagon on metabolism in the liver

Glucagon is responsible for increasing the rate of both glycogenolysis and gluconeogenesis, which thereby increases the rate of glucose release by the liver. This effect may however be reduced or abolished if the concentration of insulin is increased (Newsholme and Leech, 1994).

1.5.6. Main Action of Insulin

As mentioned earlier insulin stimulates glucose uptake, and more importantly, glycogen synthesis, which is the main function of this polypeptide hormone, and will therefore be discussed in more detail in the section to follow.

In all animals excess glucose from carbohydrates in the diet or from gluconeogenesis is stored as glycogen mainly in muscle or liver tissue. The balance between glycogen synthesis and degradation in the liver is controlled by the hormones glucagon and insulin. The starting point for glycogen synthesis is glucose-6-phosphate, which is derived from free glucose by the hexokinase reaction:

$$\text{D-glucose} + \text{ATP} \xrightarrow{\text{hexokinase}} \text{D-glucose-6-phosphate} + \text{ADP}$$

To initiate glycogen synthesis the glucose-6-phosphate is first reversibly converted into glucose-1-phosphate by phosphoglucomutase:

$$\text{Glucose-6-phosphate} \xrightarrow{\text{phosphoglucomutase}} \text{glucose-1-phosphate}$$

This reaction is followed by the formation of uridine diphosphate-glucose (UDP-glucose), a key reaction in glycogen biosynthesis, which is catalyzed by the enzyme, UDP-glucose pyrophosphorylase:

$$\text{Glucose-1-phosphate} + \text{UTP} \xrightarrow{\text{UDP-glucose pyrophosphorylase}} \text{UDP-glucose} + \text{PPi}$$

The energy produced in this reaction is -25kJ/mol, because the pyrophosphate is rapidly hydrolyzed to orthophosphate by the inorganic pyrophosphatase (Nelson and Cox, 2000).

UDP-glucose is the intermediate donor of glucose residues in the enzymatic formation of glycogen by the action of glycogen synthase, which promotes the transfer of the glucosyl residue from UDP-glucose to a nonreducing end of the branched glycogen (Nelson and Cox, 2000). Glycogen synthesis is regulated by both covalent and allosteric modulation of glycogen synthase which occurs in two forms, the active, dephosphorylated form, glycogen synthase *a*; and the inactive, phosphorylated form, glycogen synthase *b*. Conversion of the active form of enzyme to the inactive form occurs through the phosphorylation of two serine hydroxyl groups by a protein kinase. Phosphoprotein phosphatase removes these phosphate groups thereby activating the enzyme once again (Montgomery *et al*., 1996).

Glycogen phosphorylase is the enzyme responsible for glycogen breakdown and also occurs in a phosphorylated and dephosphorylated form but is regulated in a reciprocal manner, opposite to that of glycogen synthase. Phosphorylase *a*, the active form, which contains active phosphorylated serine residues, is dephosphorylated by phosphorylase *a* phosphatase to yield to yield phosphorylase *b*, the inactive form, which can also be stimulated by AMP, its allosteric modulator. Phosphorylase *b* kinase can convert phosphorylase *b* back into the active phosphorylase *a* by phosphorylating the essential serine residues (Nelson and Cox, 2000).

Glycogen phosphorylase catalysis the catabolism of glycogen into its building blocks, glucose-1-phosphate, and this intermediate is then converted into glucose-6-phosphate by the previously mentioned enzyme phosphoglucomutase. These reactions occur in both the liver as well as the muscle tissue. The formation of glucose from the glucose-6-phospate intermediate is in turn catalysed by glucose-6-phosphatase, a key enzyme in gluconeogenesis.

$$\text{Glucose-6-phosphate} + H_2O \xrightarrow{\text{Glucose-6-phosphatase}} \text{glucose} + P_i$$

This enzyme is limited, with regards to its distribution, to the liver, making it the only organ able to actively produce free glucose for secretion into the circulatory system.

Glycogen synthesis and break down is meticulously controlled by insulin and glucagon, through the regulation of cAMP levels in the target tissues which in turn determine the ratio of active to inactive forms of glycogen phosphorylase and glycogen synthase.

1.5.7. Insulin Receptor

The insulin receptor is a protein kinase, which transfers a phosphate group from ATP to the hydroxyl group of tyrosine residues. The receptor consists of two identical α-chains protruding from the outer face of the plasma membrane, and two transmembrane β-subunits, with their carboxyl termini on the cytosolic face (Nelson and Cox, 2000; Bjornholm and Zierath, 2005).

The receptor is able to phosphorylate and autophosphorylate substrates which are essential for the mediation of the complex cellular responses to insulin (Kasuga *et al*., 1982; Rosen *et al*., 1983; Yu and Czech 1984; Ellis *et al*., 1987). Structural studies have revealed that the two α-subunits jointly participate in insulin binding, while the β-chains containing the kinase domains are in a juxtaposition allowing autophosphorylation of the tyrosine kinase domain, this being the first step in the insulin signalling cascade (Luo *et al*., 1999, Ottensmeyer *et al*., 2000). A conformational change is brought about on the kinase domain due to the autophosphorylation of its tyrosine residue, and in so doing provides the active form of the enzyme bringing about binding of downstream signalling molecules (Hubbard 1997; Hubbard *et al*., 1994). Figure 1.14 shows the structure of the insulin receptor complexed with insulin and provides a better understanding of the functional complexities associated with this receptor as well as the downstream signalling brought about as a result of insulin binding.

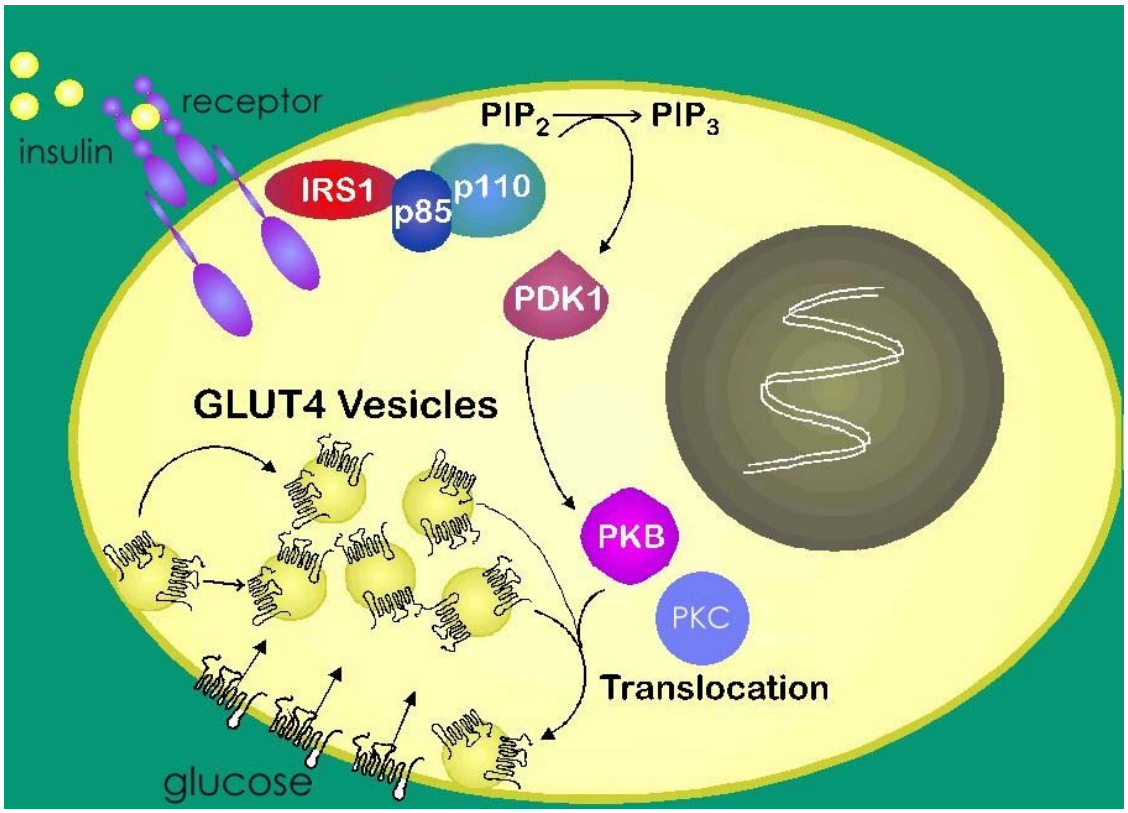

Figure 1.14: A schematic representation depicting the functional characteristics of the insulin receptor. PIP2, phosphatidylinositol-4,5-biphosphate; PIP_3, phosphatidylinositol-3,4,5-triphosphate; PDK, phosphatidylinositol-3,4,5-phosphate-dependent kinase; IRS, insulin receptor substrate; PKB, Protein kinase B; PKC, Protein kinase C (taken from Nelson and Cox, 2000)

1.5.7.1. Activation of insulin receptor signaling cascade

As mentioned previously, activation of the signaling cascade occurs once insulin has bound to the α-subunits of the insulin receptor stimulating the tyrosine kinase, situated intrinsic to the insulin receptor's β-subunit, which in turn initiates a cascade of phosphorylation leading ultimately to GLUT4 translocation and glucose uptake. These post-receptor signaling cascades will be discussed in more detail in the literature to follow.

The autophosphorylation of the insulin receptor β-subunit initiates the phosphorylation of other tyrosine residues located on the insulin receptor substrate proteins (IRS) 1-6, three isoforms of Shc, Gab-1, Cbl, APS, and $p62^{dok}$, respectively. Each of these proteins serves as docking sites for other signalling proteins containing Src homology 2 (SH2) domains (White and Yenush, 1998; Bjornholm and Zierath, 2005).

Genetic deletions in mouse models and cell lines show that the four insulin receptor substrate proteins are highly homologous with overlapping and differential tissue distribution. IRS-1-knockout mice displayed growth retardation, due to insulin resistance and insulin-like-growth factor-1 (IGF-1), β-cell hyperplasia, impaired glucose tolerance and type II diabetes (Tamemoto *et al*., 1994; Araki *et al*., 1994; Tamemoto *et al*., 1997). IRS-2-knockout mice exhibit increased insulin resistance in the liver and developed overt type 2 diabetes as a result of severe insulin resistance combined with impaired β-cell function (Withers *et al*., 1998). Combined heterozygous deletions of insulin receptor, IRS-1, and IRS-2 in different tissues develop severe insulin resistance in skeletal muscle and liver and marked β-cell hyperplasia. The above data provide evidence that IRS proteins are tissue specific, each with a different and specific function, IRS-1 playing a prominent role in skeletal muscle and IRS-2 is more specific to the liver (Kido *et al*., 2000; Taniguchi *et al*., 2005).

1.5.7.2. The Insulin Signaling Pathway

The insulin receptor is able to initiate two independent post receptor signalling pathways, the PI-3-K (phosphatidyl inositol-3-kinase) and the MAPK (mitogen activating protein kinase) pathway, as seen in figure 1.15. The pathway on the left is the PI-3-K pathway and the pathway on the right is designated MAPK pathway. It has recently been proposed that the MAPK pathway of liver and adipose tissue terminates in the nucleus with the induction or repression (transcription) of a set of genes encoding key enzymes involved in insulin-glucagon sensitive (long term) control of metabolic pathways. The PI-3-K pathway signals an increase in protein synthesis through the promotion of translation and may also be responsible for the net dephosphorylation of key enzymes in the liver, adipose, and muscle which promote the formation of glycogen and triglycerides (Gibson and Harris, 2002; Jiang and Zhang, 2005).

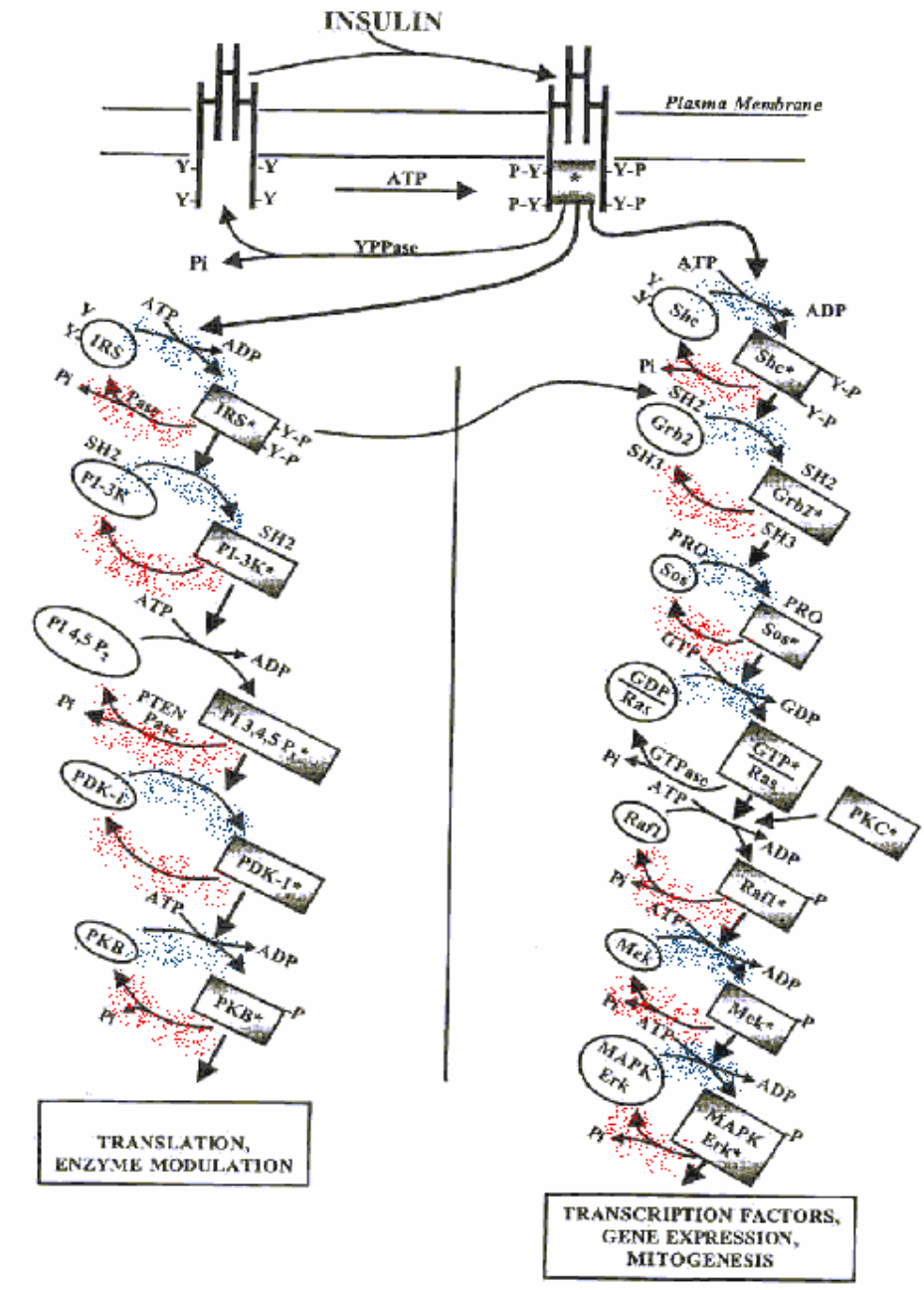

Figure 1.15: A schematic diagram displaying the two routes of insulin signalling (taken from Gibson and Harris, 2002). For abbreviations refer to text.

- **The PI-3-Kinase Pathway**

IRS binds reversibly to the activated insulin receptor β-domains to initiate this pathway. Once the insulin receptor tyrosine kinase is phosphorylated the bound IRS undergoes a conformational change and attracts a specific recognition site, the SH2,

on the PI-3-K through its p85 regulatory subunit (figure 1.16). The specificity of the protein-protein interactions depends not only on the SH2 domains, but also on adjacent amino acid sequences (Gibson and Harris, 2002).

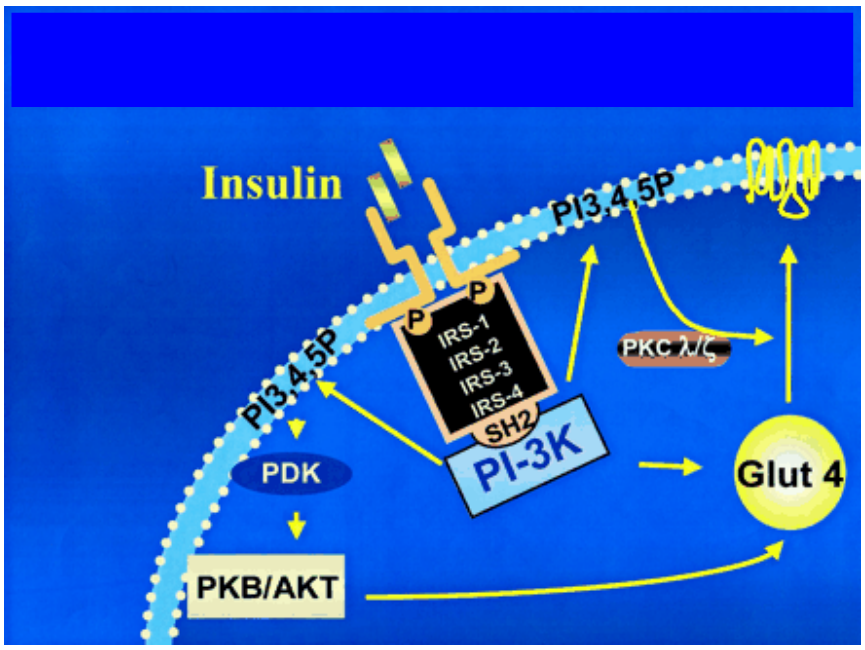

Figure 1.16: Molecular mechanism of insulin-stimulated transport. The insulin-dependent glucose transporter 4 (GLUT4) is translocated by a phosphatidylinositol 3-kinase (PI-3-K)-dependent pathway including PKB/AKT and PKC stimulation downstream of PI3K. PI3,4,5P, Phosphatidylinositol 3,4,5-phosphate; PDK, phosphatidylinositol-3,4,5-phosphate-dependent kinase; IRS, insulin receptor substrate; PKB, Protein kinase B; PKC, Protein kinase C (taken from Matthaei *et al*., 2000)

The PI-3-K, located near the cytosolic surface of the plasma membrane, catalyses the phosphorylation of inositol at position 3 of 4,5-diphosphophatidyl inositol ring producing phosphatidyl inositol 3,4,5-triphosphate (PIP_3). PIP_3 is embedded in the plasma membrane and is elevated during insulin signalling. It is clear that PI-3-K is able to control several signal pathway outcomes depending on the cell type: enhancement of transcription and translation, impairment of apoptosis, or the terminal dephosphorylation state of enzymes that are crucial for metabolic control (Gibson and Harris, 2002; Taniguchi *et al*., 2005).

PI-3-K then catalyses the phosphorylation of protein kinase B (PKB), thereby activating it, which in turn catalyses the binding of PIP_3 to the protein kinase B and Akt and initiates PKB and phosphatidyl inositol dependent kinase (PDK-1) to move

alongside one another in the plasma membrane. PKB and PDK-1 are responsible for inactivating glycogen synthase kinase (GSK-3), which normally phosphorylates and inactivates glycogen synthase. However with the GSK-3 enzyme activity decreased the opposing glycogen synthase-1G takes over. The protein phosphatase (PP1G), which is bound to glycogen through a regulatory protein (R_{GL}) brings about dephosphorylation of glycogen synthase, phosphorylase kinase, and glycogen phosphorylase thereby opposing the action of protein kinases, and promoting glycogen synthesis (Gibson and Harris, 2002). Akt kinase activates the forkhead family of transcription factors (FKHR). FKHR is a transcriptional enhancer that regulates genes involved in glucose production, cell cycle regulation, and apoptosis. It is found within the nucleus under basal conditions; however following insulin stimulation and phosphorylation, by Akt, it is excluded from the nucleus into the cytoplasm where insulin can down regulate a number of genes including IGF-binding protein-1, phosphoenolpyruvate carboxykinase (PEPCK), and glucose-6-phosphatase. (Nakae *et al*., 1999; Scheimann *et al*., 2001; Barthel *et al*., 2001; Yeagley *et al*., 2001; Lochhead *et al*., 2001; Rena *et al*., 2001; Cahill *et al*., 2001; Tomizawa *et al*., 2000; Tang *et al*., 1999; Guo *et al*., 1999). Akt also phosphorylates and regulates components of the glucose transporter 4 (GLUT4) complexes in skeletal muscle and adipose tissue thereby promoting glucose uptake (Czech *et al*., 1999; Farese *et al*., 2001; Shepherd *et al*., 1998; Ueki *et al*., 1998).

GLUT4 translocation independent of the PI-3-kinase pathway has also been identified through the tyrosine phosphorylation of IRS-2, Cbl, brought about by the autophosphorylation of the tyrosine residue of the insulin receptor β-subunit. The now active Cbl protein then complexes with the insulin receptor via an adaptor protein, CAP (Cbl-associated protein) (Ribon *et al*., 1998; Bjornholm and Zierath, 2005). The Cbl/CAP complex is then translocated to the plasma membrane domain, which is enriched in caveolae, where CAP associates with flotillin, a caveolar protein, to form a complex with a number of proteins including TC10, CRKII and other accessory proteins involved in vesicular trafficking and membrane fusion (Chiang *et al*., 2001).

- **The MAPK Pathway**

In this pathway the insulin activated receptor tyrosine kinase phosphorylates the tyrosines on the adaptor protein Shc, thereby activating it and catalysing the binding to SH2 domains on a second adaptor protein called Grb-2 (fig. 1.15). The Grb-2 protein amino acid sequence domain, SH3, binds to the proline rich regions of the next signal transduction protein Sos, thereby activating it. Sos is a guanosine nucleotide exchange protein (GEP) which continues the cascade of activation by converting a monomeric small G protein called Ras from its GDP-inactive mode to its GTP-active mode (Gibson and Harris, 2002; Taniguchi *et al*., 2005). In the presence of Sos bound GDP is replaced by the insertion of GTP from the cytosol. In the opposite direction are GAPs (GTPase activating proteins), which hydrolyse the bound GTP to GDP returning the system to a ground state. Ras is therefore an important regulatory protein (Gibson and Harris, 2002).

The now active Ras binds to the first of a series of linked protein kinases that phosphorylate (activate) and are themselves phosphorylated (activated) on specific serine, threonine, or tyrosine residues. Figure 1.15 indicates Raf-1, Mek and MAPK (ERK-endocrine receptor kinase) which are activated in response to insulin. They are representatives of three large families of kinases found in the various differentiated cells: MKKK (mitogen activating protein kinase-kinase-kinase), MKK (mitogen activating protein kinase-kinase), and MAPK (mitogen activating protein kinase), respectively. These three interlocked kinases are usually grouped together by scaffolding proteins, constituting a Raf-MAPK pathway module, and all of which are opposed by protein phosphatases. The final linkage to gene expression is through transcriptional factors which bind to the insulin responsive elements. The MAPK pathway is concerned with the transcription of enzymes catalysing glycolysis and the formation of fatty acids, as well as repression of liver enzymes catalysing gluconeogenesis (Gibson and Harris, 2002).

1.5.7.3. Internalization and Degradation of Insulin

Binding of the hormone to the cell membrane receptor is the initial step in the degradative process (1 in Fig. 1.17). Once bound, the insulin receptor, serves as a reservoir that can return intact insulin into circulation (2 in Fig. 1.17) or deliver it to an intact site. However for degradative purposes clustering of the receptor-ligand complexes occurs (3 in Fig. 1.17), followed by invagination of the coated pits (4 in Fig. 1.17), and pinching off of the pit to form an intracytoplasmic vesicle or an endosome (5 in Fig. 1.17). Degradation is initiated in these vesicles by the insulin degrading enzyme (IDE) prior to acidification of the vesicle and dissociation of the receptor-insulin complex (Duckworth *et al.*, 1997). The internal pH, of the endosome, then rapidly falls to pH6, resulting in the dissociation of the insulin- receptor complex (6A in Fig. 1.17). Further degradation to fragments can then occur, and intact insulin, partially degraded insulin, and insulin fragments can be translocated to various cellular sites (cytoplasm, nucleus, endoplasmic reticulum, lysosomes) (7A and 7B in Fig. 1.17) (Duckworth, 1988).

The insulin may also be delivered to lysosomes from certain subcellular sites such as the Golgi (8 in Fig 1.17). Some of the degraded insulin from the endosome as well as some intact insulin may cycle back to the membrane and fragments and intact insulin can be released (6B in Fig 1.17). In this case the receptor would be recycled back to the plasma membrane (9B in Fig 1.17).

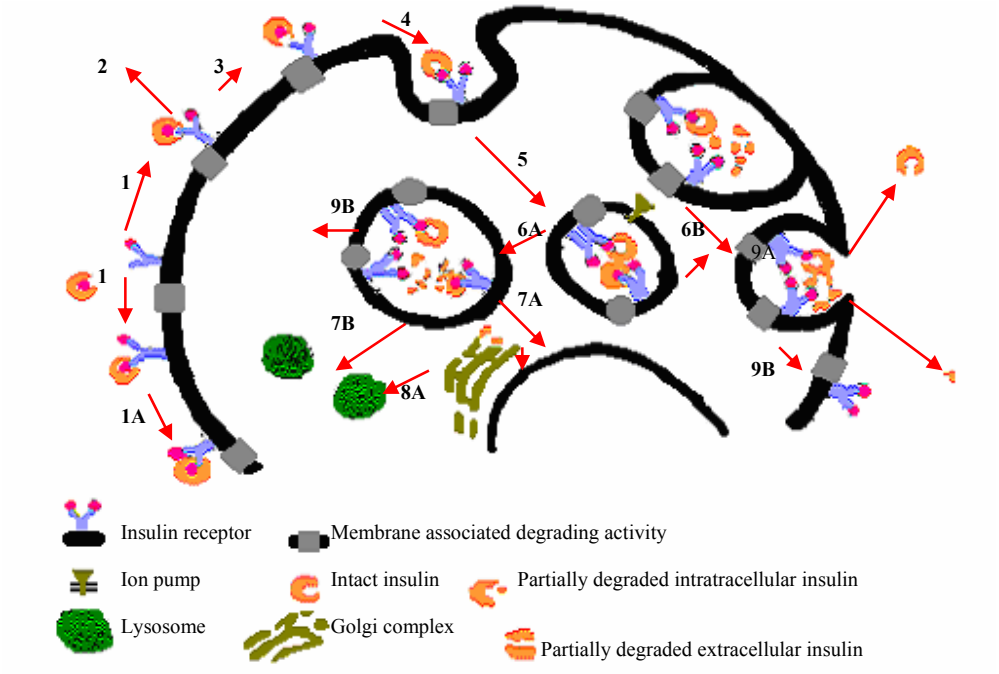

Figure 1.17: A model of cellular handling and insulin degradation (taken from Duckworth, 1988)

1.5.8. Insulin Clearance

The primary organs involved in the clearance of insulin from the circulation to the degradation of the hormone include the liver, kidney, and muscle (Duckworth *et al.*, 1998). Insulin uptake and degradation also occurs in adipocytes, fibroblasts, monocytes, lymphocytes, gastrointestinal cells, and all other tissues that contain insulin receptors. The liver is the predominant organ, for both normally secreted endogenous insulin, as well as exogenously administered insulin. Uptake is mediated primarily by the insulin receptor, at physiological concentrations, with a smaller contribution from non-specific processes. However at higher concentrations non-receptor processes assume greater importance. Insulin has a plasma half-life between 4 and 6 minutes due to the necessity for it to respond rapidly to changes in blood glucose. A brief summary of each of the major organs involved in insulin clearance follows:

(a) Liver

The liver removes approximately 50% of portal insulin. Since most uptake is a receptor mediated process, very high concentrations of insulin (500-2000μU/ml) result in a decrease in the fractional uptake, although total uptake is increased. Removal of circulating insulin does not imply immediate destruction of the hormone, a certain amount of receptor bound insulin is released from the cell and re-enters circulation. The clearance rate of the liver is decreased in individuals who suffer from obesity and type II diabetes (Duckworth *et al*., 1998).

(b) Kidney

Another important site of insulin clearance is the kidney, removing approximately 50% of peripheral insulin. The kidney is also responsible for removing 50% of circulating pro-insulin and 70% of C-peptide by glomerular filtration. Glomerular filtration and proximal tubular reabsorption and degradation are the two mechanisms for insulin clearance in the kidney. However during glomerular clearance more than 99% of the filtered insulin is reabsorbed, primarily by endocytosis. Therefore very little insulin is ultimately excreted into the urine. Insulin degradation by kidney cells is carried out by the same process as that of the liver. Insulin is internalized into endosomes where degradation is initiated (Duckworth *et al*., 1998). Some insulin may be released by retroendocytosis, from the cell. Lysosomes play a greater and earlier role in kidney insulin degradation, unlike liver. In the kidney most insulin and partially degraded insulin are delivered directly to lysosomes where degradation takes place (Duckworth *et al*., 1998).

(c) Other tissues

All insulin sensitive tissues remove and degrade insulin which is not cleared by the liver or kidney. The muscle also plays a large role in the removal of this hormone; the mechanism includes insulin binding to its receptor, internalization, and degradation. As already mentioned earlier adipocytes, fibroblasts, monocytes, lymphocytes, and gastrointestinal cells also degrade insulin. In short all cells that contain insulin receptors and internalization mechanisms can degrade insulin (Duckworth *et al.*, 1998).

1.5.9. Insulin Degrading Enzyme (IDE)

IDE is the primary insulin degrading enzyme in tissues and is a neutral thiol metalloproteinase (Duckworth, 1988; Eckman and Eckman, 2005). It has been difficult to obtain a stable enzyme preparation to study the properties of the enzyme. However the characteristics of the enzyme have now been studied in detail after investigators purified to homogeneity an IDE from human red blood cells in 1988. The enzyme showed inhibition by both sulfhydryl inhibitors, such as N-ethylmaleimide or *p*-chloromercuribenzoic acid as well as by chelators, such as EDTA, EGTA, and phenanthroline and therefore has a metal requirement. However which metal is involved is still unclear. Bacteriocin has also been proven to inhibit the enzyme (Duckworth, 1988).

The enzyme was also found to have an optimum pH of 7, and an isoelectric pH of 5.2. The enzyme has a molecular weight of 300 000 (Nelson and Cox, 2000). The substrate specificity is not only to insulin, but it has been shown that glucagon and insulin growth factor II are also degraded by the enzyme, while proinsulin and insulin growth factor I inhibit the enzyme, but are poor substrates (Duckworth, 1988).

The major portion of insulin degradation in tissues is cytosolic (Duckworth, 1988). However membrane degrading activity is also present with characteristics similar to that of the soluble enzyme. IDE also has regulatory functions for the activity of steroid receptors and proteasomes. Also the insulin control of cellular protein degradation and fat oxidation may be due to intracellular interactions of insulin with IDE (Duckworth *et al*., 1998).

1.5.9.1. Degradation products

The degradative products which are produced are a result of the action of the insulin degrading enzyme (IDE), which is the primary insulin degrading enzyme. The enzyme cleaves two peptide bonds in the A chain of intact insulin and seven bonds in the B chain with four major and three minor sites. The nature of the bonds cleaved do not allow a

simple classification of peptide bond specificity for the enzyme, but all the sites except B24-B25 and B25-B26 are in close proximity in the three dimensional structure of insulin, suggesting that the specificity is to the molecule itself rather than specific amino acid residues (Duckworth *et al.*, 1998), see figure 1.18.

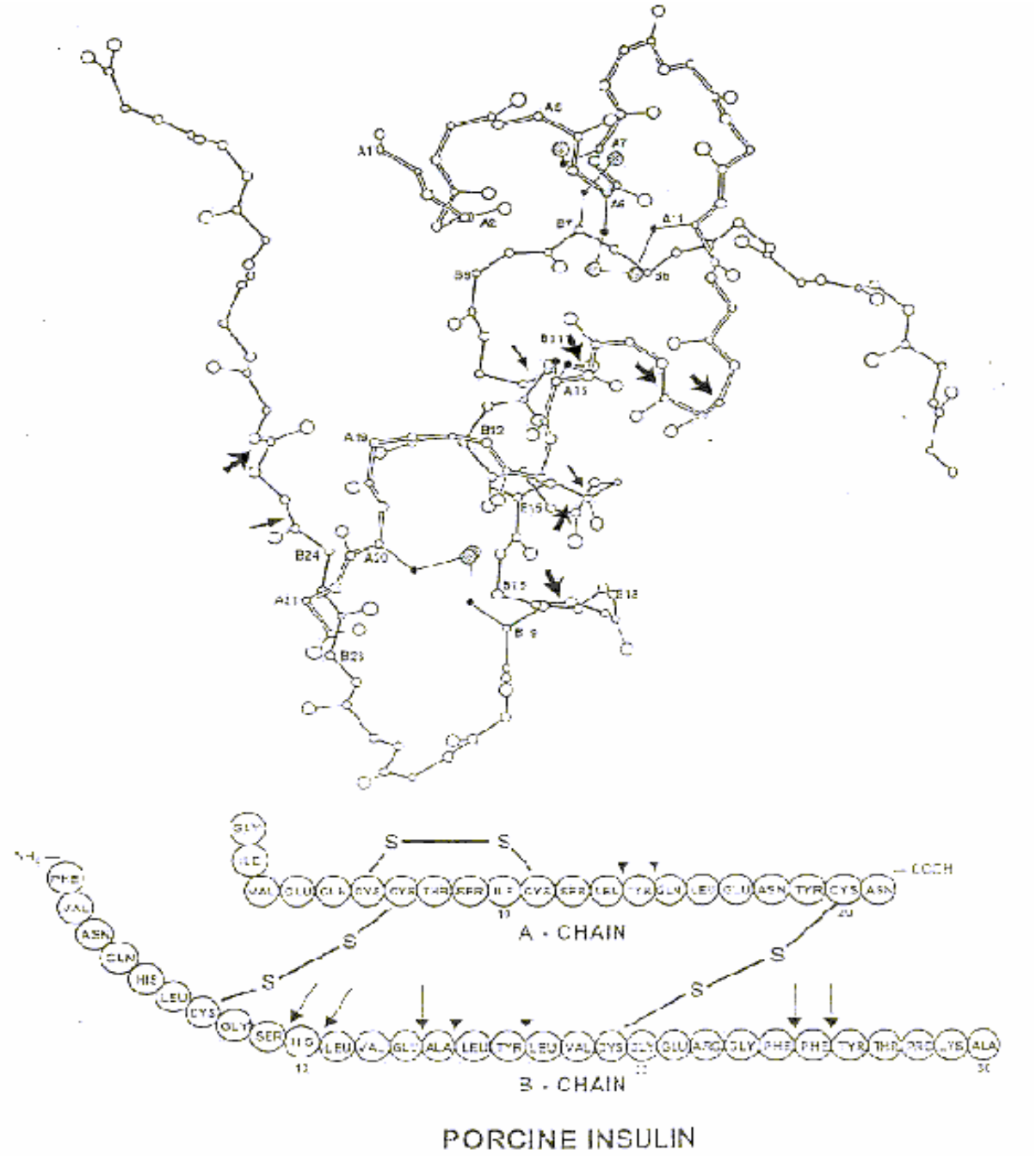

Figure 1.18: Cleavage sites of insulin for the insulin degrading enzyme (taken from Duckworth *et al.*, 1998)

1.6. ATP SENSITIVE POTASSIUM (K_{ATP}) CHANNELS: STRUCTURE, FUNCTION, AND REGULATION THEREOF

1.6.1. Introduction

Insulin secretion is a multi-step process involving transportation of the secretory vesicles to the plasma membrane, docking, priming and finally fusion of the vesicle with the plasma membrane. All of this is initiated by elevated intracellular ATP levels thereby instigating electrical depolarization of the β-cell which sets the entire process in motion. The elevated ATP levels are brought about by an increased concentration of serum glucose (above 5mM), which, in turn, is taken up by the cell's GLUT2 transporters and metabolized via glycolysis to produce ATP.

It has been shown that only a small portion of insulin stored in vesicles is released at a time, even with maximum stimulation, indicating that insulin levels are regulated by secretion instead of synthesis or storage pools. A large number of ion channels, pumps, and transporters contribute to intracellular calcium concentration, as well as other ions, to form the membrane potential (V_m) of the β-cell of ~ -70 mV when extracellular glucose is ~3 mM (Pittman *et al*., 2004).

ATP-sensitive potassium channels represent a family of potassium channels inhibited by intracellular ATP, and have been found in many tissues including the heart, pancreatic β-cells, skeletal muscles, smooth muscle, and the central nervous system. They have been associated with diverse cellular functions, such as shortening of action potential duration and cellular loss of potassium ions that occur during metabolic inhibition in heart, insulin secretion from pancreatic β-cells, smooth muscle relaxation, regulation of skeletal muscle excitability, and neurotransmitter release (Isomoto *et al*., 1996).

An increased concentration of ATP and certain glycolytic cycle intermediates initiate the closing of the ATP sensitive K^+ plasma membrane channels. This results in the subsequent decrease of K^+ conductance, leading to depolarization with subsequent

opening of the voltage dependant calcium channels. This process then ultimately leads to the secretion of insulin from the pancreatic β-cells. The ATP sensitive K^+ plasma membrane channels are therefore important and crucial for the release of insulin, and any form of mutation to these channels could affect insulin secretion. This entire process can be better understood by studying figure 1.19, which is a summary of insulin secretion in response to an elevated blood glucose concentration. The figure includes the K_{ATP} and calcium channels, and how they work together to bring about the exocytosis of insulin.

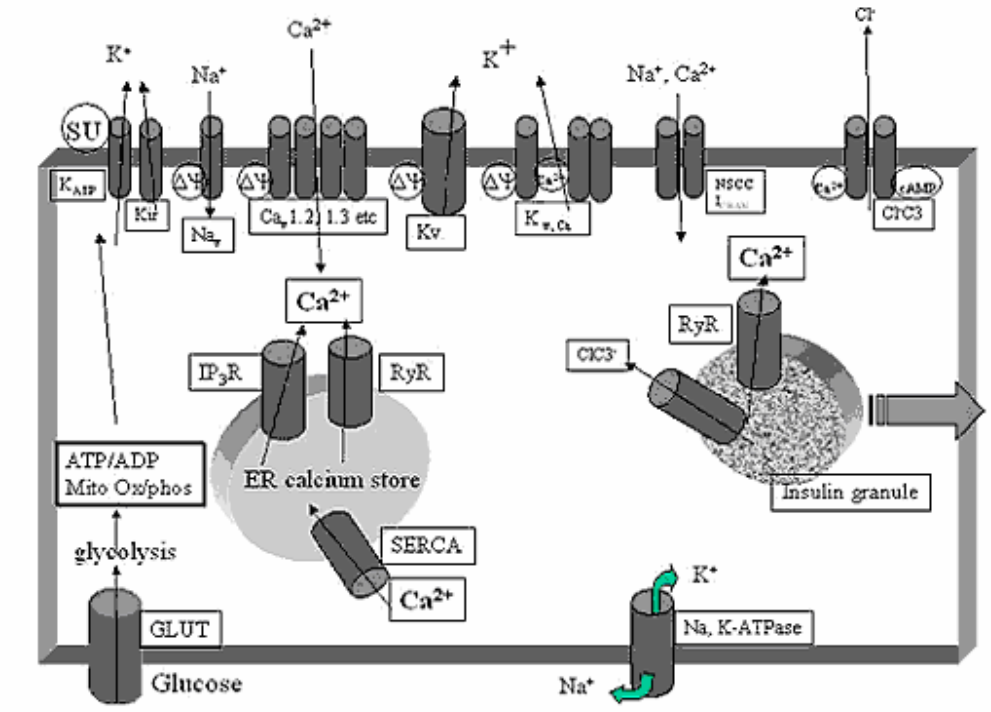

Figure 1.19: β-cell ion channels associated with insulin secretion (taken from Pittman *et al.*, 2004)

1.6.2. K_{ATP} Channel Structure

As already mentioned these channels are present in most, if not all, excitable tissues and are all inhibited by cytoplasmic ATP, thereby coupling cell metabolism to electrical activity and thus play an important role in the physiology and pathophysiology of many tissues. An example of functioning of the K_{ATP} channel is insulin secretion from pancreatic β-cells in response to glucose uptake. These channels must be able to respond to changes in ATP in the lower millimolar range (Baukrowitz and Fakler, 2000).

The molecular identity of the K_{ATP} channels has been elucidated: they are formed from an ATP binding cassette protein with several isoforms. The sulphonylurea receptor (SUR1, SUR2) which have two nucleotide binding folds (NBF-1 and NBF-2) in the cytoplasmic side, and a two segment type or Kir potassium channel (Kir6.2, Kir6.1) (Babenko *et al*., 1999; Uhde *et al*., 1999). There are Walker A and B motifs in both NBFs which are important for the functional activity of many ATP binding cassette proteins (Miki *et al*., 1999). After much experimentation it was found that the main constituents allowing this channel to function are SUR1and Kir6.2, a member of the inwardly rectifying potassium channel family (Miki *et al*., 1999). Both subunits assemble in a 4:4 stoichiometry, with four SUR1 and four Kir6.2 subunits required to form functional K_{ATP} channels, as illustrated in figure 1.20.

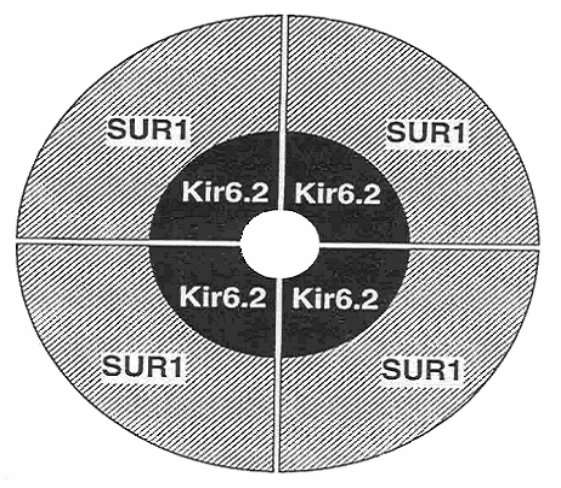

Figure 1.20: A structural representation of the K_{ATP} channel (taken from Miki *et al*., 1999)

While Kir6.2 acts as the pore forming subunit of the channel complex that determines its single channel conductance, its blockade by polyamines, and its inhibition by ATP, SUR1 has been identified as the regulatory subunit that confers sensitivity to sulfonylureas, channel openers and Mg-ADP, through the use of the two NBFs (Baukrowitz and Fakler, 2000). SUR1 also acts as a chaperone on the Kir6.2 subunits thereby allowing processing and transport of these proteins to the surface membrane (Ueda *et al*., 1997). A better understanding of the structural and functional relationship of these subunits may be obtained from studying figure 1.21.

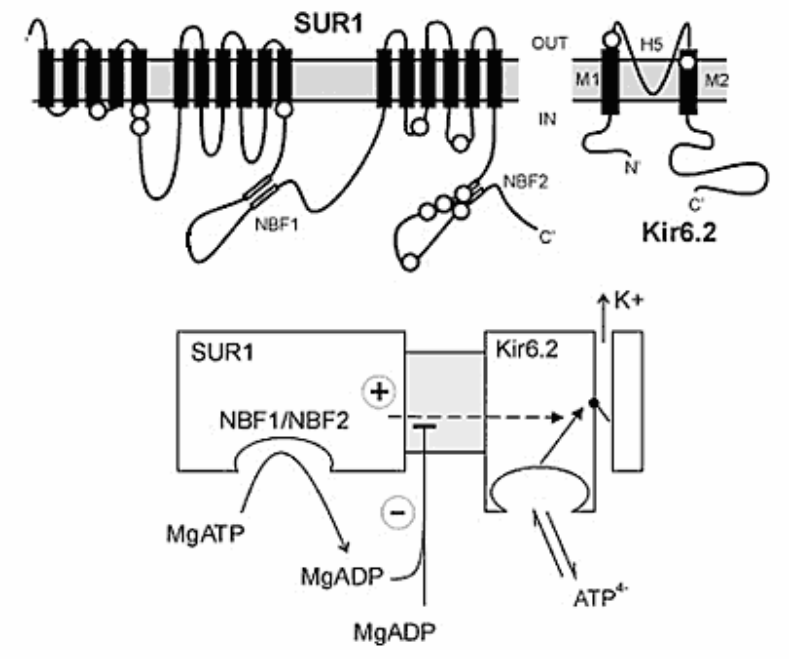

Figure 1.21: Structural and functional relationship of SUR1 and Kir6.2 (taken from Pittman *et al*., 2004)

The essential role of both subunits in regulating insulin secretion is supported by the characterization of mutations in either subunit that abrogate channel activity and cause persistent hyperinsulinemic hypoglycaemia of infancy characterized by constitutive insulin secretion despite the severe hypoglycaemia (Hernandez-Sanchez *et al*., 1999). A biochemical purification and amino terminal microsequencing of SUR1 indicates the presence of a glycosylation site near the amino terminus. It is also thought that the glycosylated form of the SUR1 protein is physically associated with Kir6.2, suggesting an extracellular localization for the amino terminus of the SUR1 subunit in the K_{ATP} channel (Raab-Graham *et al*., 1999).

Mutations have also been identified in Walker A (Lys719Arg and Lys719Met) in NBF-1 and Walker B (D854N) in NBF-1 of SUR1 which severely impair Mg^{2+} independent high affinity ATP binding. MgADP antagonizes ATP binding at NBF-1, and a mutation at NBF-2 reduces MgADP antagonism. Mutations in the K_{ATP} channel also exist which bring about hyperinsulaemia and hypoglycaemia (Miki *et al*., 1999).

1.6.3. Control of ATP Inhibition of K_{ATP} Channels by Phospholipids

Another important discovery involving the K_{ATP} channel has recently come of light: it has been shown that phospholipids such as phosphatidylinositol-4,5-biphosphate (PIP2) and phosphatidylinositol-4-phosphate (PIP) are able to shift ATP sensitivity of K_{ATP} channels from the micro- into the millimolar range and thus provide a mechanism for physiological activation of the channels (Baukrowitz and Fakler, 2000)

It was shown that the removal of the PIP2 phospholipid, in excised membrane patches, through the action of phospholipase C resulted in a loss of channel or transporter activity, which could be reversed with PIP2 and PIP (Baukrowitz and Fakler, 2000).

Two properties were found to be important for the functioning of the phospholipids, namely: (1) the negatively charged head group of the phospholipid, as it was found that PIP2 mediated shifts in ATP sensitivity could be abolished by the application of positively charged compounds such as poly-l-lysine, and (2) the requirement for the phospholipid is its insertion into the plasma membrane mediated by the lipid tail of the PIPs. It was found that PIPs are only effective when inserted into the inner leaflet of the membrane bilayer. Application of PIPs to the extracellular side of the membrane fails to affect channel properties (Baukrowitz and Fakler, 2000).

1.6.4. Control of K_{ATP} Activity on an Enzymatic Level

From the above information it can basically be concluded that PIPs are able to control ATP inhibition of K_{ATP} channels under cellular conditions. The entire process is certainly not as simple as it seems and involves a number of enzymes of the PIPs metabolism such as the phosphoinositide-kinases (PI-kinase), PIPs-phosphatases, and phospholipases. The activity of these enzymes is known to change in response to a multitude of biological responses such as activation of heteromeric G-proteins and protein tyrosine kinase receptors (Baukrowitz and Fakler, 2000).

1.6.5. Control of K_{ATP} Activity on a Genetic Level

Regulation of transcriptional activity of either SUR1 or Kir6.2 genes is important for determining the level of expression and therefore the activity of K_{ATP} channels. The mouse SUR1 gene proximal promoter region has already been characterized. The study revealed that there are no CAAT and TATA boxes or initiator elements that may mediate the initiation of transcription. Multiple transcription start sites do however exist, with the major site located 54 base pairs 5'-upstream of the translational start site (Hernandez-Sanchez *et al*., 1999).

Transient transfection experiments were run, with different constructs of the SUR1 promoter region, in the aid of determining where the basic elements required for significant basal transcriptional activity are located. The study revealed that these elements are found within the first 140 base pairs of the 5'-flanking region. There are multiple SUR1 promoter region binding sites that are responsible for SUR1 promoter region activation of SUR1 transcriptional activity in this particular region. Experiments have also shown that glucocorticoids down regulate the K_{ATP} channel levels by decreasing the SUR1 and Kir6.2 gene expression (Hernandez-Sanchez *et al*., 1999).

1.6.6. Drug Action on the Sulfonylurea Receptor

A common finding in individuals suffering from type II diabetes is variations occurring in the SUR1 gene. The nucleotide binding fold regions of the SUR1 gene were amplified with polymerase chain reaction and screened by the single strand conformational polymorphism analysis in 40 subjects with type II diabetes. The findings showed that there was one amino acid change, four silent substitutions, and three intron variants present in the nucleotide binding fold regions of the SUR1 gene (Rissanen *et al*., 2000).

The sulfonylurea class of drug, such as tolbutamide and glibenclamide, inhibit the activity of the channel, and are therefore important agents acting against type II diabetes. Evidence has accumulated that activation of the receptor by ADP and inhibition by the sulfonylurea class of drug is a property conferred by the sulfonylurea receptor on the

channel complex, while the site for ATP inhibition resides on the pore forming Kir6.2 subunit. Furthermore, the combined expression of the two proteins is required to generate current (Giblin *et al*., 1999).

1.7. TISSUES CONCENTRATED ON THROUGHOUT THE PROJECT: LIVER, MUSCLE, AND ADIPOSE TISSUE

1.7.1. Introduction

The tissues mainly affected by diabetes and obesity are adipose, muscle and liver tissue. To test the effectiveness of an anti diabetic remedy, it is necessary to know whether there is an accelerated glucose uptake occurring in a specific tissue. Each of the three tissues has a specific function in the body, expressing relevant biochemical pathways, as well as regulating these respective pathways.

1.7.2. Muscle

Skeletal muscle accounts for over 50% of the total oxygen consumption in a resting human being and up to 90% during very active muscular work. Skeletal muscle metabolism is primarily specialized to generate ATP as the immediate source of energy. Depending on the degree of muscular activity, skeletal muscles can use free fatty acids, ketone bodies, or glucose as fuel (Nelson and Cox, 2000)

.

Muscle is an efficiently controlled fuel driven machine, which is able to convert free energy, extracted by oxidation of organic nutrients into motion. In muscle several vital biochemical pathways are regulated, enabling muscle to meet its energy needs through a combination of aerobic glycolysis, fatty acid oxidation and oxidative phosphorylation (Gibson and Harris, 2002).

Glycolysis is arguably one of the most important biochemical pathways found in higher organisms, as it is responsible for producing energy in the form of ATP from a six carbon glucose molecule. The ATP produced is necessary to facilitate all energy driven reactions within the body. As already stated, other resources, such as fatty acids, may also be used by the body as a source of fuel, however these fuels are not suitable for the brain or erythrocytes which require glucose as an energy source. Glycolysis is a very delicate pathway, which consists of two phases, the preparatory phase and the payoff phase. The

preparatory phase consumes two ATP's while the pay off phase produces four ATP's per glucose molecule. The end products of anaerobic glycolysis are two pyruvate molecules for every glucose molecule oxidized (Nelson and Cox, 2000; Montgomery *et al*., 1996).

The two pyruvate molecules produced during this process are transported to the mitochondria were they take part in the citric acid cycle (Krebs cycle). Under aerobic conditions pyruvate is first oxidized to acetyl coenzyme A which then enters the citric acid cycle, and with the participation of the mitochondrial electron transport system is fully oxidised to carbon dioxide and water.

Once the entire process for a single glucose molecule is completed, under aerobic conditions, a total net yield of 36 or 38 ATP molecules is achieved. This is, however, not necessarily the fate of glucose in muscle. Under anaerobic conditions glucose is converted to two molecules of lactate per molecule of glucose in muscle, through the cytosolic process of anaerobic glycolysis. A nett yield of only two molecules of ATP per molecule of glucose is achieved, while lactate accumulates, enters the blood circulation and is transported to the liver for further oxidation. Muscle is also able to convert glucose into glycogen, for energy storage, once the body's ATP levels are saturated. Muscle is, however, unable to release glucose into the circulation as it lacks glucose 6-phophatase (Gibson and Harris, 2002).

These biochemical pathways are very well coordinated, for example, during exercise AMP concentrations are elevated which serves as a signal for increased glucose uptake, glycolysis and glycogen breakdown through positive effects on GLUT4 transport, 6-phosphofructo-1-kinase and glycogen phosphorylase respectively (Gibson and Harris, 2002).

1.7.3. Adipose tissue

Adipose tissue, which consists of adipocytes, is amorphous and widely distributed in the body: under the skin, around the deep blood vessels, and in the abdominal cavity. It

makes up about 15% of a young adult human being's body mass, with approximately 65% of this mass being in the form of triacylglycerols. Adipocytes are metabolically very active, and are fast to respond to hormonal stimuli (Nelson and Cox, 2000).

Adipocytes have an active glycolytic metabolism, oxidizing pyruvate and fatty acids via the citric acid cycle, and carrying out oxidative phosphorylation (Nelson and Cox, 2000). The principle flux of fatty acids and glucose is, however, directed towards the synthesis of triacylglycerols, during periods of high carbohydrate intake. Triacylglycerol synthesis is supported by the auxiliary flow of glucose through the pentose phosphate pathway, glycerol 3-phosphate synthesis, and through ATP synthesis, discussed in the preceding section (Gibson and Harris, 2002; Bays *et al*., 2004). The first step in fatty acid synthesis involves the enzyme, acetyl-CoA carboxylase, which catalyzes a 2-step reaction carboxylating acetyl-CoA to form malonyl-CoA.

The remaining reactions in the synthetic process are catalyzed by fatty acid synthase, which is a multienzyme complex consisting of seven enzymatically active sites (Nelson and Cox, 2000). The main final product of the fatty acid synthase system is palmitate (C16), which is the starting point for further modification reactions leading to the whole spectrum of fatty acids encountered in the adipose depots.

Fatty acids are in turn converted into triacylglycerides through the acylation of two free hydroxyl groups of glycerol-3-phosphate by two molecules of fatty acyl-CoA to yield diacylglycerol-3-phosphate. This in turn is hydrolysed by phosphatidate phosphatase to form 1,2-diacylglycerol, which is converted into triacylglycerols by transesterification with a third fatty acyl-CoA. The adipocytes behave more as a storage site for the triacylglycerides, which may also arrive from the liver or from the intestinal tract, usually after a meal rich in fat.

Excess fatty acids and carbohydrates obtained in the diet are converted into triacylglycerols in the liver and packaged with specific apolipoproteins into VLDL for export. In addition to triacylglycerols, VLDLs also contain some cholesterol and cholesteryl esters, as well as the apolipoproteins apoB-100, apoC-I, apoC-II, apoC-III,

and apo-E. These lipoproteins are transported in the blood from the liver to muscle and adipose tissue, where activation by lipoprotein lipase by apoC-II causes the release of free fatty acids from the triacylglycerols of the VLDL. The adipocytes take up these fatty acids, resynthesize triacylglycerols from them, and store the products in intracellular lipid droplets, whereas the myocytes oxidise them for an energy supply. Hepatocytes are responsible for removing most of the VLDL remnants from circulation through receptor mediated uptake and lysosomal degradation (Nelson and Cox, 2000).

Lipid stores in the form of triacylglycerides are important sources of energy, as they produce energy of complete oxidation (~38kJ/g) more than twice that for the same weight of carbohydrate or protein (Nelson and Cox, 2000).

Lipogenesis is very tightly regulated; during elevated plasma glucose and insulin levels, which accompany feeding, lipid synthesis is activated. However, without further consumption of food, plasma insulin levels fall as glucagon levels rise. The synthetic flux to triacylglycerides diminishes as glucagon signals the opening of the adipose hormone-sensitive lipase vents coincident with the down regulation of the activities of the lipogenic enzymes. The signal transduction circuitry for the insulin and glucagon hormones is directed towards a specific set of end point effector molecules (Gibson and Harris, 2002; Bays *et al*., 2004).

The leptin hormone mediates a negative feedback circuit that arises from adipose tissue as triacylglycerol stores accumulate. During starvation the dampening of the leptin signal promotes food consumption and conserves initial energy stores thereby minimizing uncoupled metabolism (Gibson and Harris, 2002).

1.7.4. The Liver

The liver is an extremely versatile organ, carrying out a number of tasks in the body and controlling many of the metabolic pathways:

- It synthesizes fat and cholesterol and ships them to peripheral tissues.

- It stores glycogen for later use by other tissues.
- It synthesizes bile acids and excretes them into the gut for lipid absorption.
- It synthesizes urea thereby preventing the build up of toxic levels of ammonia.
- The liver is glycogenic, glycolytic, and lipogenic in the fed state and glycogenolytic, gluconeogenic, and ketogenic in the starved state.

It is also of great importance that the liver has well developed regulatory mechanisms enabling it to switch rapidly between opposing metabolic pathways. Glukokinase serves as a glucose sensor enabling the liver to buffer the blood glucose concentration. Fructose 2,6-bisphosphate regulates flux from fructose 6-phosphate to fructose 1,6-bisphosphate by exerting opposite effects on the activities of 6-phosphofructo-1-kinase and the fructose 1,6-bisphosphatase (Gibson and Harris, 2002; Bays *et al*., 2004).

Fatty acid oxidation promotes gluconeogenesis by providing ATP for energy requiring steps and acetyl-CoA for activation of pyruvate carboxylase and inhibition of pyruvate dehydrogenase. The capacity of the liver for gluconeogenesis is dependent upon increased expression of the gene encoding phosphoenolpyruvate carboxykinase by glucagon and glucocorticoids. Malonyl-CoA inhibits fatty acid oxidation at the level of carnitine palmitoyltransferase I, this prevents futile cycling between fatty acid oxidation and synthesis (Gibson and Harris, 2002).

The liver is also able to produce ketone bodies from fat, as a source of energy for peripheral tissues during starvation. The synthesis of cholesterol is, in part, controlled by the end product negative feedback at the level of 3-hydroxy-3-methylglutaryl-CoA reductase expression. Bile acid synthesis is, in turn, controlled by end product negative feedback at the level of cholesterol 7 α-hydroxylase expression (Gibson and Harris, 2002).

1.8 SUMMARY AND MOTIVATION

Obesity is the gateway to many metabolic disorders including cardiovascular disease, type II diabetes, hypertension, gallbladder disease and stroke. This alone makes obesity an extremely expensive disorder, an economic burden many individuals cannot cope with.

The rapid increase of obesity in South Africa is associated with a swift increase in insulin resistance and cardiovascular diseases brought about by the westernised way of living in rural areas. Although the adoption of a westernised culture is the main instigator, certain genetic factors may be to blame, in some cases, and certain prescription medication may also cause excessive weight gain. The fact remains that insulin resistance associated with type II diabetes is a fast growing pandemic in Southern Africa, placing a large economic burden on the government for overpriced medication. It is for this reason that new avenues need to be investigated, including the potential use of traditional medicine. This may relieve the economic burden and open opportunities for export of an indigenous medication against type II diabetes.

CHAPTER 2

INTRODUCTION TO THE PRESENT STUDY

2.1. INTRODUCTION TO THE PRESENT STUDY

Obesity is among the more serious health care problems facing the westernised world to date, placing enormous economic and health costs on the government. This disorder is the gateway to many metabolic disorders including cardiovascular disease, type II diabetes, hypertension, gallbladder disease and stroke. The trends of obesity are expected to increase throughout the next half century if serious actions are not undertaken (Case *et al*., 2002). Although many cases of obesity are a result of a lack of exercise and bad eating habits, other factors are to blame such as environmental and physiological factors, as well as genetic and hormonal factors (section 1.1.3.). However certain forms of prescription medication may be the culprit for excessive weight gain, leading ultimately to obesity and the side effects thereof.

The tricyclic antidepressant, amitriptyline, is one such form of medication, which in many cases, has been accused of promoting excessive weight gain. Although many physicians prefer to prescribe alternative forms of antidepressants, such as selective serotonin reuptake inhibitors, tricyclics are still favoured by many due to their low cost and ability to be used as pain killer (Nowak and Handford, 1999) (see section 1.2.4.).

Many theories exist as to why amitriptyline is associated with excessive weight gain, shown in section 1.2.6, however many of these theories have since been proven false and many are still speculative. This project was therefore designed to determine the causative agent of the weight gain, if any, through the use of an animal model, in this case the male Wistar rat.

As previously mentioned, in section 1.4.1, type II diabetes is fast becoming a serious problem in developed counties worldwide, with children under the age of ten being diagnosed with the disease (Dyer, 2002). The incidence of type II diabetes is thought to be parallel with the growing rate of childhood obesity, a sad statistic considering the disease is easily preventable by following a healthy diet and by exercising regularly.

Various treatments are presently available for type II diabetes, as displayed in section 1.4.6, however these various forms of medication are expensive. It is also important to note that the medication is not a once off affair but instead is a daily necessity, thereby increasing the economic burden placed on the individual. It is therefore necessary to discover alternative forms of medication against type II diabetes. Through the use of an animal model, in the male Wistar rat, the alternative medication which was tested was derived from an indigenous plant, *Sutherlandia frutescens*, which is believed to be a hypoglycaemic agent by traditional healers in South Africa. If this plant is indeed a hypoglycaemic agent then it will certainly bring hope for the future to those individuals suffering from type II diabetes.

CHAPTER 3

METHODOLOGY

CONTENTS

3.1. ANTIDEPRESSANT STUDY

This study was approved by the Animal Ethics Committee of the Nelson Mandela Metropolitan University. Forty four male Wistar rats, 15 weeks of age, with an average weight of 350g, were received from the animal unit of the Diabetes Research Group of the Medical Research Council. The rats were randomly divided into two groups of 14 and 30 respectively. The former group served as the control receiving no medication. The other group served as test subjects, with one group, of 15, receiving 75mg/kg amitriptyline and the other 15 rats receiving 75mg/kg trimipramine, in their drinking water. All rats received dog pellets *ad lib* and medication was administered on a daily basis. Food and fluid consumption was also monitored on a daily basis. Rat weight was monitored weekly. All rats were housed in an environmental room with controlled temperature (22 ± 1^{o}C) with a 12 hour light – dark cycle (08h00-20h00). Principles of laboratory animal care were followed according to the Animal Ethics Committee of the Nelson Mandela Metropolitan University.

3.1.1. Preparation of Medication

Twenty-five mg amitriptyline / trimipramine tablets were employed throughout the experiment. The tablets were crushed with the aid of a pestle and mortar and stored in a dry environment. The dose was worked out relative to that prescribed to humans as per 'A consumers guide to prescription medicines' (Cooper and Gerlis, 1997) and the 'South African Medicines Formulary' (Gibbon, 2000) which states that the normal dose of amitriptyline / trimipramine is 75mg per day. The doses were then worked out assuming that an average adult human weighs approximately 75kg:

75mg amitriptyline or trimipramine /day / 75kg body weight
= 1mg amitriptyline or trimipramine / 1000g body weight/day
= 0.001mg amitriptyline or trimipramine /g body weight/day
Each tablet has a mass of 0.11g containing 25mg amitriptyline or trimipramine, therefore
25mg / 0.11g ≈ 0.001mg /*x*
= 0.0044mg amitriptyline or trimipramine tablet /g body weight/day

The dose was then dissolved in 1ml of a 0.1M HCl solution. This step was necessary, as the medications do not dissolve to form a homogenous solution with pure distilled water. The dissolved medicine was then made up to 200ml with distilled water, in the water bottles, and was added to the relevant cages. The amount of medication consumed was monitored on a daily basis by determining how much fluid was consumed and how much was lost to spillage.

3.1.2. Metabolic Rate

Principle

Resting metabolic rate was measured using the Amitec, an extremely accurate instrument used for measuring oxygen content from air samples. The apparatus contains an adjustable pump, which controls the amount of air to be pumped to the detector from the specific sample chamber. The sample chamber houses the animal under investigation, for a predetermined time, and is connected to the pump leading to the detector. The chamber also contains an inflow tube, from the surrounding environment, allowing air to move freely into the chamber. The average oxygen concentration in the air from the chamber gives an indication of the animals resting metabolic rate in relation to the predetermined incubation time.

Method

The resting metabolic rate of each rat was determined individually after 11 weeks medicational compliance. A 4680cm^3 chamber, which housed the rats throughout the experiment, was connected to the Amitec. Vaseline ensured the chamber was 'air tight'. As temperature fluctuations can give deceiving results, the entire chamber was partially submerged in a water bath, keeping the temperature at approximately 22^{o}C throughout the procedure. The temperature inside the chamber remained at approximately 24^{o}C.

The oxygen controller was calibrated for a day before each experiment, to determine the initial oxygen percentage in the air. Thereafter the rats were individually placed in the chamber for 40 minutes, allowing for their oxygen consumption to be determined. The air flowing to the reader was set to 3 liters/minute for this particular experiment. All results

were stored on a computer in volts and were interpreted from a standard curve obtained using pure oxygen, a 50/50 oxygen/nitrogen mixture, and pure nitrogen.

3.1.3. Food and Fluid Intake

Each rat received dog pellets, *ad lib*, on a daily basis. The remaining food was weighed every morning, at the same time, for a period of 14 weeks and recorded. The same volume of water was administered to each rat every evening. The amount consumed was recorded the following morning at the same time.

3.1.4. Sacrifice of Rats

The test groups for this study received either trimipramine or amitriptyline and consisted of 15 rats per test group. The control group, which received no medication, consisted of a total of 14 rats. All rats were sacrificed after a 12 hour fast, by an intramuscular injection of 3µl ketamine/g body weight. A blood drop was collected from the tail vein for blood glucose determination. Five rats from each group were sacrificed after 6 weeks medicational compliance, upon which blood was immediately removed from the heart for serum insulin determination. Muscle, liver, kidney, testicular fat pads and pancreas were harvested and fresh tissue not required for immediate experimentation were snap frozen in liquid nitrogen before being stored at -80^{o}C. A further 5 rats from each group were sacrificed after 14 weeks medicational compliance, once again blood was removed and organs were harvested. The remaining 5 rats from each test group and four rats from the control group were utilized for glucose disposal experiment, principle and methods are discussed in section 3.1.5.

3.1.5. Glucose Disposal

Glucose clearance was determined using glucose along with [^{3}H]-deoxy-glucose.

Principle

Past studies have shown that deoxy-glucose is taken up by tissues at the same rate as glucose (Utriainen *et al* 2000). Once inside the cell the deoxy-glucose is, however, unable to be metabolised, due to its unique structure. Deoxy-glucose is also unable to pass out of fat and muscle tissue due to the unavailability of GLUT 2 transporters (Nelson and Cox, 2000), allowing the degree of labelling by [^{3}H]-deoxy-glucose to serve as a measure of glucose uptake sensitivity.

3.1.5.1. Quench Correction Curves

Principle

Colours are able to absorb the visible light emitted by the secondary scintillator, M_2-POPOP, thereby decreasing the light detected by the scintillation counter. Tissues vary from one another with respect to colour. Due to the varying amount of blood within different tissues, each sample will display different degrees of quenching and will not be comparable to one another. A quench correction curve is therefore necessary to compensate for this.

Method

Rats used for this procedure were not from the antidepressant or diabetic study. One gram of muscle, liver, kidney and fat were removed and dissolved, over a Bunsen burner, in 1 ml 30% KOH containing 1000 dpm of 2-deoxy-D-[2,6-^{3}H] glucose (53Ci/mmol specific activity, Amersham Bioscience). Twenty, 40, 60, 80 and 100µl of the dissolved tissue was then, individually, added to 3ml of Packard Ultima Gold scintillation cocktail and counted in a Packard tri-carb 2300TR liquid scintillation analyzer. Counting windows were set to cover the full ^{3}H energy spectrum (A) and a narrower spectrum excluding the lower energy emissions (B). Quench correction curves were then plotted and counting efficiency was calculated using samples with known amounts of ^{3}H and increasing amounts of the respective tissue preparations. All samples were corrected for quenching by using the relevant quench correction curves.

Calculations

Plotting of the quench correction curve:

y-axis : % Efficiency = (cpm / dpm) x 100

x-axis : cpm window B / cpm window A

3.1.5.2. Glucose Clearance Experiments

To determine the rate of glucose clearance, four rats from each test group and six from the control group were anaesthetized, with an intramuscular injection of ketamine at 3µl/g body weight after a twelve hour starvation period. The femoral vein was exposed, by making an incision in the inner thigh. Basal blood glucose was determined using an Optium MediSense glucometer. One milliliter of 0.9% (m/v) saline, containing 0.4g/kg glucose and 1µCi/500g 2-deoxy-D-[2,6-^{3}H] glucose (53Ci/mmol specific activity, Amersham Bioscience) was injected over one minute into the femoral vein. Blood glucose was measured with the glucometer every five minutes, thereafter, for one hour. Glucose clearance was calculated from the area under the resulting progress curve for each rat.

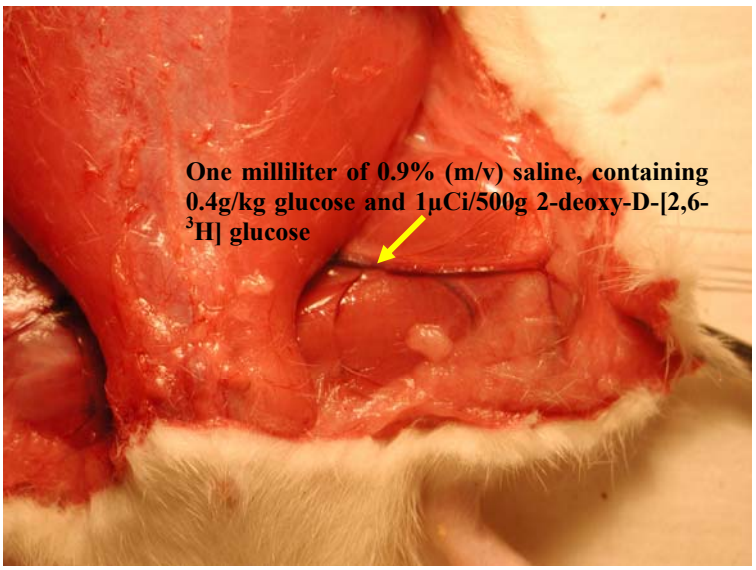

3.1.5.3. Quantification of Glucose Uptake by Various Tissues *in vitro*

To determine the tissue distribution of the glucose taken up, the rats from the glucose clearance experiment were immediately euthanased, after the hour incubation time, by injecting a further dose of ketamine straight into the heart. The liver, testicular fat pads, kidneys and a portion of the hind limb muscle were immediately removed and weighed. The organs were finely chopped and one gram of each was degraded by boiling in 1ml of 30% (m/v) KOH. One hundred µl of each extract was then counted for 15 minutes in 3ml Packard Ultima Gold scintillation cocktail in a Packard tri-carb 2300TR liquid scintillation analyzer. Urine was also removed from the bladder and 100µl of each sample was counted in 3ml Packard Ultima Gold scintillation cocktail.

3.1.6. Collection of Blood Samples

The remaining rats, in each group, were anaesthetized, after a 12 hour fast, by an intramuscular injection of 3µl ketamine/g body weight. All blood was removed from the heart using a 5ml syringe with a 22 gauge needle.

3.1.6.1. Determination of Blood Glucose Levels

Blood glucose was determined with an Optium MediSense glucometer.

3.1.6.2. Determination of Serum Insulin Levels

Insulin levels were determined using a standard radioimmunoassy kit for rat insulin (Linco, RI-13K).

Principle

A fixed concentration of labeled tracer antigen, [^{125}I] insulin, is incubated with a constant dilution of antiserum such that the concentration of antigen binding sites on the antibody is limited. If unlabeled antigen is added to the system, there is competition between labeled tracer and unlabeled antigen for the limited and constant number of binding sites on the antibody. Therefore the amount of tracer bound to the antibody will decrease as the amount of unlabeled antigen increases. This can be measured after separating free tracer from antibody bound and counting the latter using a gamma counter or a scintillation counter. A standard curve is set up with increasing concentrations of standard unlabelled antigen and from this curve the amount of antigen in unknown samples can be calculated.

Method

Blood was centrifuged at 2000 *g* at 4^{o}C for 20 minutes. Serum was collected and insulin levels determined using a radioimunoassy kit for rat insulin (Linco, RI-13K) as per manufacturer's instructions.

The following protocol was followed:

Day One						Day Two
Tube number	**Assay buffer**	**Standards & samples**	**[^{125}I] Insulin tracer**	**Rat insulin antibody**		**Precipitating reagent**
1, 2	-	-	100 µl	-		-
3, 4 (NSB)	200 µl	-	100 µl	-		1.0 ml
5, 6 (Bo)	100 µl	100µl 0.1ng/ml	100 µl	100 µl	**Vortex, cover and incubate at 4^{o}C for 24hrs**	1.0 ml
7, 8	-	100µl 0.2ng/ml	100 µl	100 µl		1.0 ml
9, 10	-	100µl 0.5ng/ml	100 µl	100 µl		1.0 ml
11, 12	-	100µl 1.0ng/ml	100 µl	100 µl		1.0 ml
13, 14	-	100µl 2.0ng/ml	100 µl	100 µl		1.0 ml
15, 16	-	100µl 5.0ng/ml	100 µl	100 µl		1.0 ml
17, 18	-	100µl 10ng/ml	100 µl	100 µl		1.0 ml
19 - ∞	-	Samples	100 µl	100 µl		1.0 ml

After the addition of the precipitating reagent the samples were vortexed and incubated for 20 minutes at 4^{o}C. The supernatant was then discarded and the pellet re-suspended in 1ml Beckman Ready Gel® liquid scintillation cocktail.

Calculation

The average of the non specific binding tubes (NSB), tubes 3–4, was subtracted from the average of each tube, except the total counts. The percent of tracer bound was calculated as follows:

%B = {Total binding counts (tubes 5–6)/Total counts (tubes 1–2)}x 100
(%B should be in the range of 35–50%)

The percent of total binding (% B/Bo) for each standard and sample was calculated as follows:

% B/Bo = (Sample or standard/Total binding) x 100

A log-log standard curve was then constructed by plotting the % B/Bo for each standard on the *y* – axis and the known concentrations on the *x*–axis. Insulin concentrations for

samples were then read from the standard curve (Morgan and Lazarow, 1963; Thorell and Lanner, 1973; Feldman and Rodbard, 1971; Westgard, 1981).

3.1.7. Glycogen Content in Muscle and Liver Samples

The building blocks of glycogen, glucose, were used to quantify the amount of glycogen in the test samples.

Principle

Glycogen is released from the tissue by heating with strong alkali and precipitated through the addition of ethanol. The polysaccharide is then hydrolysed in HCl and the released glucose is determined by the anthrone method (Plummer, 1987).

Method

Liver and hind limb muscle samples were removed and glycogen content was determined through an adaptation of previous methods (Suzuki *et al*., 2002). Liver or muscle tissue (0.5g) was degraded by boiling in 0.5ml 30% (m/v) KOH, for 5 minutes. Glycogen was precipitated with 1.2ml ethanol and centrifuged at 1900 *g* for 10 minutes in eppendorf tubes. The pellet was then dissolved in ddH_2O, 2ml for muscle and 4 ml for liver samples. Four hundred microliters of the resulting mixture was then added to 1ml anthrone reagent (2g/L concentrated H_2SO_4) and boiled for 10 minutes. Samples were read at 600nm and extrapolated using a glycogen standard curve.

3.1.8. Insulin Degradation

[^{125}I] insulin was used as a marker to determine the rate of insulin degradation in fresh sample tissue.

Principle

The [^{125}I] insulin binds to the insulin receptor on the sample tissue before being taken up and degraded, by the insulin degrading enzyme, thereby cleaving the protein into smaller peptides. After an incubation period the addition of trichloroacetic acid (TCA) to pre-removed aliquots causes denaturation and precipitation of intact or undegraded insulin. The amount of degraded insulin can

therefore be determined by analyzing the supernatant after centrifugation using a scintillation counter.

Method

The degradation of [^{125}I] insulin was followed by using an adaptation of the method of Powers *et al*., 1980 and Duckworth, 1979. Ten μCi of [^{125}I] insulin labeled at TyrA^{14} was reconstituted in 100μl distilled water, according to manufacturers instructions (AEC-Amersham®) to yield an insulin concentration of 5 x 10^{-8}M. Two and a half μl, of the diluted [^{125}I] insulin, was then mixed with 622.5μl of DMEM supplemented with 0.5% bovine serum albumin (BSA), to produce the binding buffer. All solutions which were to come in contact with the sample tissue were pre-warmed to 37^{o}C.

Insulin degradation studies were performed for both the 6 and 14 week sacrifice times. Liver was the only tissue tested after the 4 week sacrifice, while liver, kidney and muscle were tested after the 12 week sacrifice. On both occasions the tissue was immediately removed post mortem and washed in PBSA, warmed to 37^{o}C. The wash ensured the removal of any excess blood. The tissues were finely sliced, using a scalpel, and again washed with PBSA. Excess fluid was drained from the tissue and 2.5g of each sample was weighed out and incubated with 1000μl of the pre-mixed binding buffer solution. Control tubes contained no tissue.

The samples were incubated at 37^{o}C and 50μl aliquots of the binding buffer were removed at times 5, 10, 15, 20 and 30 minutes. The aliquots were immediately added to 100μl of cold 10% trichloroacetic acid (TCA), vortexed and kept on ice for a further 5 minutes, thereby ensuring the completion of the reaction and precipitation of undegraded insulin. The samples were then microfuged for 5 minutes before 80μl of the supernatant was added to a pony vial containing 3ml Packard Ultima Gold scintillation cocktail. Each of the samples was then counted for 15 minutes in a Packard tri-carb 2300TR liquid scintillation analyzer.

3.1.9. Insulin Degrading Enzyme Quantification

This procedure allowed for the quantification of the insulin degrading enzyme in muscle and liver tissue of control groups to be compared to that of the respective test groups.

3.1.9.1. Protein Extraction

Two hundred milligrams of previously frozen tissue was homogenized, using a Retsch mixer mill type 301, in 1ml homogenizing buffer, containing: 50mM HEPES, 10% glycerol, 1% Triton X-100 and 0.05ml/g protease inhibitor cocktail; pH 7.5. Samples were then centrifuged at 10 000 *g* for 10 minutes at 4^{o}C, and the resultant pellet was discarded.

3.1.9.2. Protein Separation through SDS-Page

Protein concentrations were determined using bicinchoninic acid (BCA) technique, see section 3.1.10. Thirty and 50µg total protein, for muscle and liver samples respectively, were separated on a 7.5% SDS-PAGE gel. The gel was made up as follows:

Stacking gel
- 3.213ml double distilled water
- 1.25ml 0.5M Tris-HCl, pH6.8
- 50µl 10% (w/v) Sodium dodecyl sulfate (SDS)
- 0.488ml Acrylamide/Bis (40% stock) (Bio-Rad)
- 25µl 10% Ammonium persulfate (fresh daily)
- 5µl TEMED

Separating gel
- 5.475ml Double distilled water
- 2.5ml 1.5M Tris-HCl, pH 8.8
- 100µl 10% (w/v) Sodium dodecyl sulfate (SDS)
- 1.875ml Acrylamide/Bis (40% stock) (Bio-Rad)

Degas for 15 minutes at room temperature
- 50µl 10% Ammonium persulfate (fresh daily)
- 5µl TEMED

The gel was run at 150V and 64mA for approximately 45 minutes.

3.1.9.3. Blotting Preparation

Nitrocellulose membranes were cut in accordance with the size of the separating gel, approximately 8.5cm by 5.5cm, always wearing powder free gloves and handling the membrane with forceps at all times to avoid contamination. The membranes were pre-wet in 5 – 10ml 100 % methanol for 1 – 2 seconds and then placed in 500ml double distilled water for 5 minutes to remove the methanol. The methanol allowed the hydrophobic surface to wet with aqueous solvents. The membrane was then equilibrated in 500ml transfer buffer for 30 minutes, which was made up from 48mM Tris, 39mM glycine and 20% methanol. Three pieces of extra thick filter paper, per membrane, were cut slightly bigger than the dimensions of the gel, and were completely saturated with transfer buffer. Once the protein separation had completed, the gel was allowed to equilibrate in transfer buffer for 30 minutes to remove electrophoresis buffer salts and detergents. These salts may increase the conductivity of the transfer buffer and the amount of heat generated during the transfer, if not removed. This step also ensured that the gel would not shrink during the transfer.

3.1.9.4. Unit Assembly

The safety cover and stainless steel cathode assembly was removed and a single sheet of thick pre-soaked filter paper was placed on the platinum anode. A roller was then used to exclude any air bubbles from under the sheet. The pre-wetted nitrocellulose membrane was placed on top of the filter paper. Once again air bubbles were excluded through the use of the roller. The equilibrated gel was carefully placed on top of the membrane, aligning the gel with the membrane exactly. Any air bubbles were once again removed with the roller. The two remaining sheets of filter paper were individually placed on top of the gel, once again ensuring no air bubbles were present between any of the layers. The stainless steel cathode and safety cover were carefully replaced, ensuring that the filter paper stacks were not disturbed in the process. The power supply was then set at 200mA and 25V over 2 hours for the transfer of 2 gels.

Once the transfer was complete the safety cover and stainless steel cathode assembly were removed, the filter paper discarded and the transfer efficiency monitored by staining

the gel with Coomassie blue R-250 protein stain. The membranes were then blocked in 5% bovine serum albumin (BSA) (100ml per membrane), primarily for an hour on a 3–D gel rocker before being transferred to 4^{o}C for an overnight incubation. The 5% BSA was made up in wash buffer, Tris–buffered saline (TBS), which consisted of 0.8% NaCl, 2% of a 1 M Tris HCl solution and 0.1% Tween 20; pH 7.6.

3.1.9.5. Primary and Secondary Antibody Binding

After the overnight block in 5% BSA the membranes were briefly rinsed in approximately 20ml of wash buffer. Care was taken not to wash too excessively as this would remove the blocking agent and cause excessive background on the X–ray film. The membrane was then subjected to a 2 hour incubation, in 5ml (1 : 5000) primary antibody {Rabbit anti-insulin degrading enzyme (116 kDa – Polyclonal antibody) - Merck Chemicals PC730}, in accordance to the pre-mentioned relevant dilutions. The incubation took place on a 3–D gel rocker, set to a very low speed.

The membranes were then, briefly, rinsed twice in wash buffer before being subjected to two fifteen minute washes and a further three 5 minute washes in approximately 100ml fresh wash buffer. The washes were done on a 3–D gel rocker system set on high speed.

The secondary antibody {ECL anti - rabbit IgG, peroxidase – linked species – specific whole antibody (from donkey) - Amersham NA934} was added to the washed membrane, at a volume of 5ml and a 1:2000 dilution. The 2 hour incubation took place on a 3–D gel rocker. All primary and secondary antibody dilutions were made in Tris–buffered saline (TBS), which consisted of 0.8% NaCl and 2% of a 1M Tris HCl solution; pH 7.6. The membranes were then subjected to the same washes as before, to ensure no non–specific binding of the secondary antibody to the nitrocellulose membrane.

3.1.9.6. Detection

Principle

A specific primary antibody binds to its corresponding antigen on the nitrocellulose membrane, namely the protein of interest. After a specified incubation period the membrane is washed so as to

eliminate any non–specific binding. The primary antibody provides a specific binding site for the secondary antibody, which in turn is bound to horse radish peroxidase (HRP). The addition of the detection reagent begins the reaction, HRP catalyses the oxidation of luminol under alkaline conditions. Immediately following the oxidation the luminol is in an excited state which proceeds to decay to a ground state via a light emitting pathway. Enhanced chemilluminescence is achieved by performing the oxidation of luminol by the HRP in the presence of chemical enhancers such as phenols. This has the effect of increasing the light output approximately 1000 fold and extending the time of the light emission. The light produce peaks after 5–20 minutes which gradually decay with a half life of approximately 60 minutes (Whitehead 1979, Isaccson and Watermark, 1974, Roswell and White (1978), Motensbocker (1968).

Method

All detection took place in a dark room using a specialized safety light. Equal volumes of detection solution 1 (Amersham RPN2106) and detection solution 2 (Amersham RPN 2109) were mixed, allowing sufficient total volume to cover both membranes entirely. The final volume required was 0.125 ml/cm^2. Excess wash buffer was drained from the membranes and they were placed protein side up on a clean surface. The mixed detection reagent was then pipetted onto the membrane and allowed to incubate at room temperature for 1 minute. Excess detection reagent was then drained off by holding the membrane gently with forceps and touching the edge against a tissue. The membranes were placed protein side down onto a clean, transparent sandwich bag of which two sides were cut open so it was able to flap open. The membrane is then placed on one of the open flaps. The bag was folded over and any bubbles were smoothed out. The bag containing the membrane was placed protein side up in a hypercassette autoradiography cassette (Amersham, RPN11642) and a sheet of ECL hyperfilm (Amersham, RPN2103K) was placed over the membrane. The film was exposed for five minutes after which it was removed and immediately added to developer for 2–5 minutes, the time for this depending on the relevant band density. The film was then rinsed in water and added to fixer for 10 minutes. The film was again rinsed and allowed to air dry before being analyzed using the Alpha Innotech, AlphaImager™ 3400 gel dock system.

3.1.10. Protein Determination

Bicinchoninic acid assay:

Fifty parts of reagent A, made up from 1% BCA-Na_2, 2% $Na_2CO_3.H_2O$, 0.16% Na_2 tartrate, 0.4% NaOH and 0.95% $NaHCO_3$ (pH 11.5), was mixed with 1 part of reagent B, 4% $CuSO_4.5H_2O$ to produce the BCA reagent. Two hundred µl BCA reagent was incubated with 10µl of sample / standard for 1 hour at 37^oC before the absorbance was read at 540 nm. A standard curve was prepared using 2mg/ml BSA, which was serially diluted with double distilled water.

DIABETES INVESTIGATIONS

3.2. INSULIN RESISTANT MODEL (Type II Diabetes)

This study was approved by the Animal Ethics Committee of the Nelson Mandela Metropolitan University. Thirty three male Wistar rats, 12 weeks of age and with an average weight of 319g, were obtained from the animal unit of the Diabetes Research Group (DRG) of the Medical Research Council (MRC). The rats were fed a specialized high fat diet after weaning which rendered them obese/insulin resistant (OB/IR), the diet was composed of 16.65% protein, 40.08% total fat and 43.27% carbohydrates (expressed as % energy per 100g). The rats remained on this diet for the remainder of the experiment. They were divided into three groups of eleven, one group served as the OB/IR control, the other group received a daily dose of metformin and served as the positive control and the third group received a daily dose of *S. frutescens* infusion and represented the test group. To save on animal lives, data obtained from the control rats of the antidepressant study was utilized as the lean control group. All rats were housed in an environmental room with controlled temperature (22 ± 1^{o}C) with a 12 hour light – dark cycle (08h00-20h00). Principles of laboratory animal care were followed according to the Animal Ethics Committee of the Nelson Mandela Metropolitan University.

3.2.1. Preparation of Medication

3.2.1.1. *Sutherlandia frutescens*

Sutherlandia frutescens subsp. *microphylla* was collected on a farm in the Murraysburg district. The *S. frutescens* infusion was prepared by weighing off 2.5g of dried, crushed leaves, adding 100ml boiling water and allowing this tea to brew overnight. The extract was then filtered through a sieve consisting of pores of approximately one millimeter in diameter. The rats received a dose concentration of 0.01ml/g rat weight, of the 100ml tea extract, in their drinking water. The amount consumed was monitored on a daily basis. The *S. frutescens* was made up fresh on a daily basis to prevent any fungal or bacterial growth in the tea. Water bottles were also washed and autoclaved daily.

3.2.1.1.1. Identification of Potential Bacterial Contamination in *S. frutescens* Extract

Identification of bacterial contamination in *Sutherlandia frutescens* infusion was done according to the methods of Gehringer *et al.* (1998) and Barrow and Feltham (1995). The bacterial identification was necessary as bacterial growth could be seen in the infusion after more than a day of standing at room temperature.

(a) Spread Plate and Streak Plate

One hundered µl of 0.025g/ml *Sutherlandia frutescens* infusion, as prepared in section 3.2.1.1, was transferred onto a petri dish containing nutrient agar. An L-shaped glass rod was placed into a beaker with 70% ethanol, covering the bent portion of the rod. The rod was then passed through the flame of a Bunsen burner for sterilization, allowing the ethanol to burn off completely. The *S. frutescens* extract was then spread, with the rod, over the entire surface of the agar and the plates incubated in an inverted position at 37^{o}C overnight.

The following day colonies of different morphologies were picked off with a flamed sterilized inoculation loop and each was streaked onto a fresh nutrient agar plate. Only one sector of the plate was initially streaked. The plates were then incubated in an inverted position at 37^{o}C overnight. Now that individual pure colonies were available identification of the bacteria could proceed.

(b) Preparation of a Bacterial Smear

Clean slides are essential for microbial smear preparations, and were therefore cleaned with 95% ethanol before use. An individual colony of bacteria was placed in a small drop of water on the slide, with a sterilized inoculation loop. The bacteria were slowly mixed with the water to create a milky suspension, which was allowed to air dry. Once dried the slides could be used for various stains to aid identification.

(c) Gram Stain Procedure

The smear was first covered with crystal violet for 30 seconds before being rinsed with distilled water. Then the smear was covered with Gram's iodine for 30 seconds, and then

decolourized with 95% ethanol. The slide was then washed with distilled water, covered in safranin for 30 seconds and allowed to air dry before viewing under a microscope. Purple stained bacteria indicates gram positive bacteria, while red stained bacteria indicates gram negative bacteria.

(d) Endospore Stain Procedure

Small pieces of tissue paper were torn and placed on fresh bacterial smears to reduce evaporation of the malachite green. The paper should be smaller than the stain. The slide and stain were then steamed for five minutes in order to drive the stain into the impermeable endospore. It was essential that the slide remained moist throughout the steaming process by adding more stain if necessary. The paper was then removed and the slides washed with distilled water and counter stained with safranin for 30 seconds. Thereafter the slides were again washed with distilled water, blotted dry and examined under the microscope. This technique yields a green endospore resting in a pink to red cell.

(e) Anaerobic Growth

This procedure determines whether a bacterium is able to grow under conditions where no oxygen is present. For this process the *Sutherlandia frutescens* infusion was streaked out, onto nutrient agar as previously mentioned and placed into an anaerobic container with a specialized GasPak. The GasPak is a sealed bag containing chemicals which remove oxygen from a sealed environment. The GasPak was then opened, 10ml of water was added to it and all was sealed in the anaerobic container. The palladium catalyst in the chamber lid catalysed the formation of water from hydrogen and oxygen, thereby removing oxygen from the sealed container. If growth is present on the agar dishes after one day's growth then the bacteria tests positive for anaerobic growth.

(f) Growth on 10% NaCl

Isolated bacterial colonies were picked off, with a sterilized inoculation loop, and streaked on specialized nutrient agar containing 10%NaCl. The plates were then incubated overnight at 37^{o}C in an inverted position. Any sign of growth was reported.

(g) Oxidase Test Procedure

In aerobic bacteria, cytochromes carry electrons to oxygen. The ability of bacteria to produce cytochrome oxidase can be determined by the addition of the test reagent tetramethyl-p-phenylenediamine dihydrochloride to colonies grown on a plate medium. This light pink reagent serves as an artificial substrate, donating electrons and thereby becoming oxidised to a blackish compound in the presence of the oxidase and the free oxygen. Following the addition of the test reagent, the development of pink, then maroon, and finally black colouration on the surface of the colonies is indicative of cytochrome oxidase production and represents a positive test. No colour change or a light pink colouration on the colonies is indicative of the absence of oxidase activity and is a negative test.

A streak plate of individual colonies, grown from the *Sutherlandia frutescens* infusion, was made and incubated overnight, as already mentioned. To test for cytochrome oxidase a drop of oxidase reagent was added to the colonies. A colour change to pink within one minute, then blue to black indicates a positive result. Negative results will have no colour change.

(h) Motility Test

Petroleum jelly was placed on all four corners of a cover slip with a drop of water placed in the center. A single bacterial colony was then picked, from a streak plate made from the *Sutherlandia frutescens* infusion, and mixed in with the water. A sterile microscope slide was then placed on top of the petroleum jelly, taking care that there was no contact between the slide and the droplet. The slide was then inverted forming a hanging drop from the cover slip. Bacterial motility could now be examined under the microscope.

3.2.1.2. Metformin

Five mg metformin tablets were employed throughout the experiment. The tablets were crushed with the aid of a pestle and mortar and stored in a dry environment. The doses were worked out relative to those prescribed to humans as per 'A consumers guide to prescription medicines' (Cooper and Gerlis, 1997) and 'South African Medicines Formulary' (Gibbon, 2000), which states that the normal dose for metformin is 500mg

every 8 hours or 850mg daily. The latter, lower dose was chosen for this study. The doses were then worked out assuming that an average adult human weighs approximately 75kg:

850mg metformin / 75kg body weight
= 11.33mg metformin / kg body weight/day
= 0.01133mg metformin / g body weight/day
Each tablet has a mass of 0.55g and has a concentration of 500mg, therefore
500mg/0.55g ≈ 0.01133mg/*x*
= 0.012mg metformin tablet /g body weight/day

The relevant dose was then dissolved in 1ml of a 0.1M HCl solution. This step was necessary, as the medication does not dissolve to form a homogenous solution with pure distilled water. The dissolved medicine was made up to 200ml with distilled water, in the water bottles, and was added to the relevant cages. The amount of medication consumed was monitored on a daily basis.

3.2.2. Metabolic Rate

The resting metabolic rate of each rat was determined individually after 7 weeks medicational compliance, refer to section 3.1.2.

3.2.3. Food and Fluid Intake

Each rat received the same amount of specialized OB/IR food, in the form of patties, on a daily basis. The food not consumed by each of the rats was weighed every morning, at the same time, for a period of 8 weeks and was recorded. The same volume of water was administered to each rat every evening at the same time, and the amount consumed was recorded at the same time each morning. Keeping in mind that certain groups received medication in their drinking water, the *S. frutescens* group received slightly less water than the other groups as they consumed less water due to the bitter taste of the infusion.

3.2.4. Glucose Clearance Experiment

The same method was followed as that described in section 3.1.5 for the sacrifice of the rats. Five rats from each group were anaesthetized, after 8 weeks medicational

compliance, with an intramuscular injection of ketamine at 3µl/g body weight after a twelve hour starvation period. Glucose clearance experiments and quantification of glucose uptake by various tissues were performed as described in sections 3.1.5.2 and 3.1.5.3.

3.2.4.1. Glucose Uptake in Anaesthetized Rats

Refer to section 3.1.5.3.

3.2.5. Collection of Blood Samples

The six remaining rats, in each group, were anaesthetized, after a 12 hour fast, by an intramuscular injection of 3µl ketamine/g body weight. All blood was removed from the heart using a 5 ml syringe with a 22 gauge needle.

3.2.5.1. Determination of Blood Glucose Levels

Blood glucose was determined with a Optium MediSense glucometer.

3.2.5.2. Determination of Serum Insulin Levels

Refer to section 3.1.6.2.

3.2.6. Tissue Glycogen Content

An alternate method was used in place of the anthrone method, employed in section 3.1.7, so as to avoid using concentrated H_2SO_4. The following method is also more sensitive.

Principle

Glycogen is released from the tissue by heating with strong alkali and precipitated through the addition of ethanol. Sodium sulfate is added as a co-precipitant giving a quantitative yield of glycogen. The polysaccharide is then hydrolysed in HCl and the released glucose determined through the glucose oxidase method (Plummer, 1987).

Method

Liver and hind limb muscle samples were removed and glycogen content was determined through an adaptation of previous methods (Suzuki *et al*., 2002 and Plummer 1987). Liver or muscle tissue (0.5g) was degraded by boiling in 0.5ml 30% (m/v) KOH, for 5 minutes. Glycogen was precipitated with 1.2ml ethanol and 0.06ml saturated Na_2SO_4. The precipitate was removed by centrifugation at 1900 *g* for 20 minutes in eppendorf tubes. To each pellet 0.3ml of 1.2M HCl was added and samples were boiled for two hours. The tubes were cooled and a drop of phenol red indicator was added to allow for neutralization with 0.5M NaOH. Glucose content was determined using a glucose oxidase kit (Glu-cinet, Bayer).

3.2.7. Intestinal Glucose Uptake

Intestinal glucose uptake was determined according to the previous method of Mizuma *et al*., 1997. Briefly, 10cm of the jejunum was removed, inverted, washed with cold PBS and clamped at one end. The jejunum was then filled with glucose free DMEM (Highveld Biological) and clamped at the other end. The inverted jejunum was placed in 30ml DMEM containing 20mM glucose and 20µl aliquots were taken from the DMEM within the intestine every 5 minutes for 30 minutes. Glucose concentration was determined with a glucose oxidase kit (Glu-cinet, Bayer), refer to section 3.2.7.1.

The [^{3}H]-deoxyglucose assay was run parallel with the glucose oxidase method, excepting that 1µl [^{3}H]-deoxyglucose (1µCi in 17.6µl distilled water) was added to the 30ml DMEM containing 20mM glucose. Twenty µl aliquots were taken from the DMEM within the intestine every 5 minutes for 30 minutes and added to 3ml of Packard Ultima Gold scintillation cocktail and counted using a Packard tri-carb 2300TR liquid scintillation analyzer.

3.2.7.1. Glucose Standard Curve

Firstly serial dilutions of a 2.5mM glucose concentration were made up, using DMEM without glucose, to dilute the samples. 50µl aliquots of these glucose concentrations were

then added, in triplicate, to wells in a 96 well plate and 200µl of a glu-cinet® reagent was added to each of the glucose concentrations. The wells were mixed and incubated at 37°C for 30 minutes. The absorbance was read at 492 nm, using a Multiskan® MR microtitre plate reader, Labsystems. A standard curve was run with each set of samples.

3.2.8. Insulin Signaling Pathway Analysis

Immediately after sacrifice the hind limb muscle, of each of the rats, was removed using a sharp scalpel blade. The tissue was washed, briefly, using PBSA, pre-warmed to 37°C, before being finely sliced with the scalpel ensuring to trim off any excess fat. The tissue was then washed, again using pre-warmed PBSA. Excessive moisture was removed from the tissue by draining it on filter paper. One gram of tissue was then weighed off and incubated with 1ml DMEM (pH 7.5) containing 10mM glucose, 60µU human insulin (Roche) and 0.05ml protease inhibitor cocktail (Sigma) for 1 hour in a 37°C water bath.

After the incubation the tissue was removed and briefly drained of the excess moisture using filter paper. The samples were then snap frozen in liquid nitrogen and stored at – 80°C until needed.

3.2.8.1. Protein Extraction

The frozen samples were individually ground into a fine powder, using a pestle and mortar and liquid nitrogen. The powder was homogenized in 10ml ice cold homogenizing buffer using a potter homogenizer. The homogenizing buffer was an alteration of that used by Mohammad *et al* (2002): 50mM HEPES, 150mM NaCl, 1.5mM $MgCl_2$, 1mM EGTA, 10% glycerol, 1% Triton X, 100mM NaF, 10mM $Na_4P_2O_7$, 1mM PMSF and 0.1ml/g tissue weight protease inhibitor cocktail (Sigma); pH 7.4. The tube was then rinsed using another 10ml of homogenizing buffer to ensure all extract was removed. The extracts were then centrifuged at 9000*g* for 20 minutes at 4°C and the pellet discarded. The supernatant was concentrated down, at 4°C, to approximately 5ml through the use of PEG 2000. The end product was stored at – 80°C.

3.2.8.2. Western Blots

3.2.8.2.1. Protein Separation through SDS-PAGE

Protein concentrations were determined using bicinchoninic acid (BCA) technique, see section 3.1.10. Eighty micrograms of total protein was separated using SDS-PAGE on a 7.5 % polyacrylamide gel. See sections 3.1.9.2, 3.1.9.3 and 3.1.9.4 for methods.

3.2.8.2.2. Primary and Secondary Antibody Binding

Eight proteins, namely: insulin receptor β-subunit, protein kinase Bα, p38, IP3 type II receptor, insulin receptor substrate-1 and 2, PI-3-kinase p85 subunit and GLUT4 were individually detected through the use of the following primary antibodies:

- Mouse anti-insulin receptor (β-subunit) (97 kDa) – Monoclonal antibody (Chemicon international MAB1139). Dilution – 1 : 1000
- Rabbit anti-protein kinase Bα (56 kDa) – Polyclonal antibody (Sigma P1601). Dilution – 1 : 4000
- Rabbit anti-ACTIVE® p38 (40 kDa) – Polyclonal antibody (Promega V1211). Dilution – 1 : 2000
- Rabbit anti-IP3 type II receptor (260 kDa) – Polyclonal antibody (Chemicon international AB3000). Dilution – 1 : 100
- Rabbit anti-insulin receptor substrate-1 (160-185 kDa) – Polyclonal antibody (Upstate Cell Signaling Solutions 06-248). Dilution – 1 : 1000
- Rabbit anti-insulin receptor substrate-2 (170-185 kDa) – Polyclonal antibody (Upstate Cell Signaling Solutions 06-506). Dilution – 1 : 1000
- Rabbit anti-PI-3-kinase p85 subunit (85kDa) - Polyclonal antibody (Upstate Cell Signaling Solutions 06-506). Dilution – 1 : 1000
- Rabbit anti-GLUT4 (43 kDa) – Polyclonal antibody (Chemicon International AB1346). Dilution – 1 : 4000

Secondary antibodies used were:

- ECL anti - rabbit IgG, peroxidase – linked species – specific whole antibody (from donkey) (Amersham NA934). Dilution – 1 : 2000
- ECL anti - mouse IgG, peroxidase – linked species – specific whole antibody (from sheep) (Amersham NXA931). Dilution – 1 : 2000

After the overnight block in 5% BSA the membranes were briefly rinsed in approximately 20ml of wash buffer, taking care not to wash excessively as this will remove the blocking agent and cause excessive background on the X–ray film. The membrane was then subjected to a 2 hour incubation, in 5ml of one of the above described primary antibodies, in accordance with the pre-mentioned relevant dilutions.

The incubation took place on a 3–D gel rocker, set to a very low speed. IRS-1 and IRS-2 antibodies were incubated for 1 hour on the 3-D rocker, at room temperature, before being incubated overnight at 4^{o}C. The remainder of the protocol and the detection protocol were as described in section 3.1.9.5 and 3.1.9.6, respectively.

3.2.9. Glucose-6-Phosphatase Activity

Principle

Glucose-6-phosphatase catalyses the hydrolysis of glucose-6-phosphate to glucose and phosphate, the phosphate is then determined in a separate experiment. EDTA is incorporated into the reaction mixture to chelate Mg^{2+} required for alkaline phosphatase activity.

Method

The method was followed according to Plummer (1987), 0.2 g liver was homogenized in homogenizing buffer: 0.25M sucrose, 5mM Tris, 0.1mM EDTA and 0.1ml/g tissue weight protease inhibitor cocktail (Sigma); pH 7.4. The extracts were centrifuged at 9000 *g* for 10 minutes and 0.2ml of the supernatant was added to 2ml of reaction buffer (0.1M sodium cacodylate buffer, 10mM EDTA and 50mM glucose-6-phosphate; pH 6.5) and incubated for 10 minutes at 37^{o}C. The reaction was stopped by adding 1ml, ice cold, 10% w/v TCA and tubes were centrifuged at 2000 *g* for 10 minutes at 4^{o}C. The supernatant was then used for inorganic phosphate determination (section 3.2.9.1).

3.2.9.1 Inorganic phosphate determination

Principle

Inorganic phosphate in solution reacts with ammonium molybdate in an acidic environment to form phosphomolybdic acid. Addition of reducing agent reduces the molybdenum in the phosphomolybdate to give a blue color. The reducing agent used is *p* – methylaminophenol sulfate. The presence of copper in the buffer solution increases the rate at which the color develops (Plummer, 1987).

Method

Inorganic phosphate for standards and samples were determined according to Plummer, 1987. Firstly a stock phosphate solution was made up by dissolving 438 mg potassium dihydrogen phosphate in 100ml double distilled water, this gives an equivalent of 100 mg phosphorus per 100ml. The above mentioned stock was then diluted 100 times with 50% TCA to give a working phosphate solution to be used for the standard curve. The starting phosphate concentration for the standard curve was 0.01mg/ml which was serially diluted to a final concentration of 0.000625mg/ml.

Copper acetate buffer was made up by dissolving 2.5g copper sulfate and 46g of sodium acetate in 1 liter of 2M acetic acid, pH 4.0. Twenty grams of p-methylaminophenol sulfate was dissolved in 100g/l solution sodium sulfate to produce the reducing reagent. Fifty grams/l ammonium molybdate was also required.

Three milliliters of the copper acetate buffer was added to 1ml sample / standard, along with 0.5ml of ammonium molybdate and 0.5ml reducing reagent, with thorough mixing after each addition. The tubes were then read at 800 nm using an Ultrospec 2100pro®, from Amersham Bioscience, after standing at room temperature for 10 minutes. The phosphate concentrations of the samples were obtained from the standard curve.

3.3. STREPTOZOTOCIN (STZ) MODEL (Type I Diabetes)

This study was approved by the Animal Ethics Committee of the Nelson Mandela Metropolitan University. A total of forty male Wistar rats, 12 weeks of age and with an average weight of 319g, were utilized for the following experiment. All rats were housed in the animal unit of the Diabetes Research Group of the Medical Research Council. Fourteen rats were randomly divided into 2 groups of 7, one group served as a control (not receiving STZ) and the other group received a daily dose of *S. frutescens* infusion and represented the test control group (not receiving STZ). The remaining 26 rats received a 36mg/kg STZ toxin, intramuscularly, and were randomly divided into three groups of 7 and one group of 5, the latter group served as the test group which received no medication and was sacrificed three days following STZ administration. From the remaining 3 groups of seven, one group received a daily dose of *S. frutescens* infusion (0.01ml/g rat weight in their drinking water), another group received a daily dose of insulin (Acraphane) intravenously and the third group received a combination of *S. frutescens* infusion and insulin. The concentration of insulin administered depended on each individual rat's blood glucose level 72 hours following STZ administration:

- Blood glucose between 10 & 12mM received 1 unit of insulin
- Blood glucose between 12 &15mM received 2 units of insulin
- Blood glucose between 15 &18mM received 3 units of insulin
- Blood glucose between 18 & 20mM received 4 units of insulin
- Blood glucose above 20mM received 5 units of insulin

All rats were fed dog pellets *ad lib* for the entire experiment and were housed in an environmental room with controlled temperature (22 ± 1^{o}C) with a 12 hour light – dark cycle (08h00-20h00).

Background: As already mentioned 36mg/kg of STZ was administered intramuscularly thereby initiating β-cell destruction, leading to the subsequent loss of circulating insulin which in turn resulted in severe hyperglycaemia and associated complications, as is common with type I diabetes.

Principle

STZ has been shown to cause increased, irreversible, O-glycosylation of β-cell proteins, through the inhibition of the enzyme *O*-GlcNAc-selective *N*-acetyl-b-d-glucosaminidase (OGlcNAcase). This particular enzyme is responsible for removing *O*-GlcNAc (N-Acetylglucosamine) from proteins, and is thus the final enzyme in the pathway of O-glycosylation in the β-cell (Roos *et al*., 1998; Liu *et al*., 2000). Nuclear and cytosolic β-cell O-glycosylation occurs with O-linkage of the monosaccharide *O*-GlcNAc at the serine and threonine residues of proteins. It has been proposed that β-cells display increased expression of the enzyme *O*-GlcNAc transferase, responsible for transferring the *O*-GlcNAc to proteins, which increases their sensitivity to the STZ toxin (Konrad *et al*., 2001). The structures of STZ and *O*-GlcNAc are shown in figure 3.1.

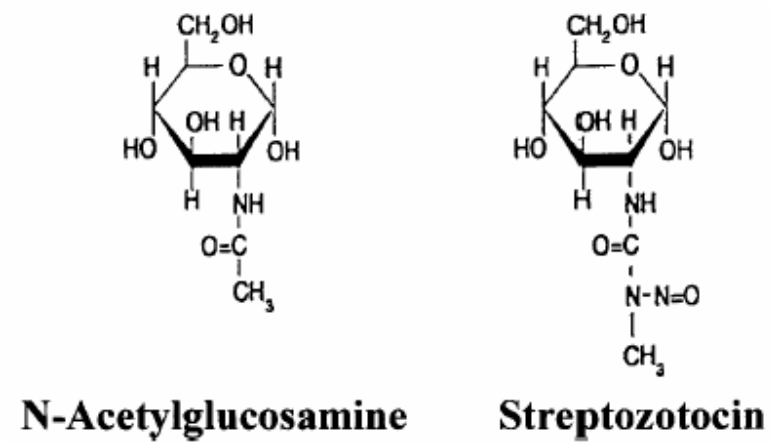

Figure 3.1: Chemical structures of N-Acetylglucosamine and STZ (taken from Konrad *et al*., 2001).

3.3.1. Collection of Blood Samples

Rats were anaesthetized, after an 8 hour fast, by an intramuscular injection of 3µl ketamine/g body weight. All blood was removed from the heart using a 5 ml syringe with a 22 gauge needle.

3.3.1.1. Determination of Blood Glucose Levels

Blood glucose was measured on days 0, 3 and 6. Day 0 indicates the start of the experiment, 72 hours after STZ administration. The blood was collected from the tail vein of the rat and the glucose concentration was determined with an Optium MediSense glucometer.

3.3.1.2. Determination of Serum Insulin Levels

The 35 rats were anaesthetized, on day 6 after a 12 hour fast, by an intramuscular injection of 3µl ketamine/g body weight, upon which all blood was removed from the heart using a 5 ml syringe with a 22 gauge needle. Serum insulin levels were then determined according to 3.1.6.2.

3.3.2. Tissue Glycogen Content

Refer to section 3.2.6.

3.3.3. Jejunum Mucosa Na^+K^+ ATPase Activity

Na^+K^+ ATPase activity was determined according to Madsen *et al*. (1996). The jejunum was removed and flushed with ice cold PBSA. The mucosa was separated from the underlying muscle by scraping with a glass slide, weighed, and then homogenized in a 1:10 volume of extraction buffer, containing 50mM Tris-HCl and 0.05ml/g tissue weight protease inhibitor cocktail (Sigma); pH 8.0.

The protein concentration of each extract was then determined through the Bradford assay (see section 3.3.4.) and 50µg protein / ml was incubated in a 1ml mixture of 25mM imadazole, 1mM EGTA and 0.6mg deoxycholate / mg protein for 15 minutes at 37^oC. This ensured the disruption of the membranes for ligand access to all ouabain binding sites. One ml of a buffer containing 50mM histidine, 130mM NaCl, 20mM KCl, 4mM MgCl and 3mM ATP (pH 7.4) was added to 1ml of the homogenate, to start the reaction. The reaction was allowed to proceed for 15 minutes at 37^oC before being quenched by the addition of 1ml of 50% ice cold TCA. The samples were centrifuged at 2000 *g* for 10 minutes. Samples to which protein was added after the reaction was terminated served as the blanks. Each sample was run in triplicate and the entire experiment was run in duplicate with the one half of samples containing 1mM ouabain added to the 1ml mixture of 25mM imadazole, 1mM EGTA and 0.6mg deoxycholate / mg protein. Ouabain inhibits Na^+K^+ ATPase pump, therefore the Na^+K^+ ATPase activity can be calculated by

subtracting the final inorganic phosphate levels from samples incubated without ouabain from those incubated with ouabain.

3.3.3.1. Inorganic phosphate determination

Refer to section 3.2.9.1.

3.3.4. Protein Determination

Bradford assay:

Five µl sample / standard was added to 200µl Bradford reagent (Sigma, B-6916) in a 96 well plate and allowed to stand for 10 minutes at room temperature before being read at a wavelength of 600 nm. A standard curve was prepared using 1mg/ml BSA, which was serially diluted with double distilled water.

3.4. CELL STUDIES

3.4.1. Cell Culture

C_2C_{12} cells were routinely maintained in 10cm culture dishes (Sarstedt) in RPMI1640 (Highveld Biological, South Africa) supplemented with 10% heat inactivated fetal calf serum (FCS) (Highveld Biological, South Africa). The cells were kept in a humidified 37^{o}C incubator supplemented with 5% CO_2. The cells were sub-cultured at a 1:3 ratio before they reached 70% confluence. For experimental purposes the cells were subcultured at 70% confluence and seeded into sterile 24 well culture plates (Nunclon) at a density of 37 500 cells per well. The cells were then left for a period of three and a half days to differentiate. No differentiation inducers were added to the medium at any time during the experiment. The medium was also not changed during this time period.

3.4.2. Binding Studies

Binding studies allowed insulin receptor binding efficiency of *S. frutescens* to be determined through displacement of [^{125}I] insulin.

Principle

The binding study integrated the displacement of the detecting agent, [^{125}I] insulin, by varying concentrations of native insulin or *S. frutescens* after an incubation period with C_2C_{12} muscle cells.

Method

Two 24 well plates with C_2C_{12} cells were grown up, as described above. One plate would contain native insulin at various concentrations: 0.01nM, 0.1nM, 1nM, 10nM, 1000nM. The second plate contained various concentrations of freeze dried *S. frutescens* infusion: 0.025, 0.25, 2.5, 25 and 250µg/ml. A *S. frutescens* infusion was made up as previously described (section 3.2.1.1), and then freeze dried overnight to produce a fine powder of pure extract. All dilutions were added to a 0.7nM concentration of [^{125}I] insulin (Linco 9011) in RPMI1640 supplemented with 0.1% BSA.

The growth medium was aspirated and each plate was divided into 6 lanes of 4 wells each. Incubation media were then added as follows:

Plate 1
Lane 1: 200µl 0.7nM [^{125}I] insulin (Total binding)
Lane 2: 200µl 0.01nM native insulin in 0.7nM [^{125}I] insulin
Lane 3: 200µl 0.1nM native insulin in 0.7nM [^{125}I] insulin
Lane 4: 200µl 1nM native insulin in 0.7nM [^{125}I] insulin
Lane 5: 200µl 10nM native insulin in 0.7nM [^{125}I] insulin
Lane 6: 200µl 1000nM native insulin in 0.7nM [^{125}I] insulin {Non-specific binding (NSB)}

Plate 2
Lane 1: 200µl 0.7nM [^{125}I] insulin (Total binding)
Lane 2: 0.025µg/ml *S. frutescens* extract dissolved in 200µl 0.7nM [^{125}I] insulin
Lane 3: 0.25µg/ml *S. frutescens* extract dissolved in 200µl 0.7nM [^{125}I] insulin
Lane 4: 2.5µg/ml *S. frutescens* extract dissolved in 200µl 0.7nM [^{125}I] insulin
Lane 5: 25µg/ml *S. frutescens* extract dissolved in 200µl 0.7nM [^{125}I] insulin
Lane 6: 250µg/ml *S. frutescens* extract dissolved in 200µl 0.7nM [^{125}I] insulin {Non-specific binding (NSB)}

The plates were incubated in a 20^{o}C water bath for 20 minutes. The low temperature and short incubation period eliminate insulin degradation, but have no effect on insulin binding to receptors (Verspohl and Ammon, 1980).

After incubation the medium was immediately aspirated and wells were washed, twice, with ice cold RPMI1640, supplemented with 0.1% BSA to remove all unbound [^{125}I] insulin. Cells were lifted by the addition of 100µl, ice cold, 1M NaOH. Cells were removed from wells and individually added to 1.5ml eppendorfs. Wells were washed out with a further 50µl 1M NaOH to ensure that all cells were removed from the wells. One and a half ml scintillation cocktail was then added to each eppendorf tube. The tubes were mixed before each sample was counted for 30 minutes using a Packard tri-carb 2300TR liquid scintillation analyzer. The experiment was done in triplicate.

Calculations
Specific [^{125}I] insulin binding
= (cpm in presence of displacer – NSB) / (cpm in absence of displacer – NSB) x 100% [^{125}I] insulin displaced
= 100 - % [^{125}I] insulin bound

3.4.3. GLUT4 Translocation

Cells incubated with an external stimulus, such as native insulin, will promote translocation of GLUT4 to the plasma membrane by intracellular transverse tubules, thereby facilitating glucose uptake.

Principle

Cells were incubated with either insulin or *S. frutescens* at 37°C in glucose free medium, to facilitate GLUT4 translocation, before being flash frozen in homogenizing buffer and fractionated to isolate cellular membrane fractions for GLUT4 quantification.

Method

The same culturing conditions which were described earlier were employed to culture C_2C_{12} cells to confluency in fifteen, 10cm culture dishes. Five plates were to receive insulin treatment, another five would receive *S. frutescens* treatment and the remaining five would receive no treatment, serving as the control. Medium was removed from the cells and they were washed with pre-warmed 5ml wash buffer (PBSA containing 0.1% BSA). Cells were pre-incubated, at 37°C, with incubation buffer (PBSA containing 1% BSA) for 10 minutes. Buffer was removed and 5 plates received 10ml incubation buffer supplemented with 1µM insulin, another 5 plates received 10ml incubation buffer supplemented with 250µg/ml *S. frutescens* extract and the remaining 5 plates were incubated with 10ml incubation buffer for 8 minutes.

Incubation buffer was removed and 1ml ice cold homogenizing buffer {10mM $NaHCO_3$, 0.25M sucrose and 10µl/ml protease inhibitor cocktail (sigma); pH 7.5} was added before plates were placed into a -80°C freezer for 3 freeze thaw cycles. Cells were then passed through a 22 gauge needle ten times and centrifuged at 1000 *g* for 10 minutes to remove nuclear material. The supernatant was centrifuged at 190 000 *g* for an hour and pellet was dissolved in 80µl homogenizing buffer. The protein concentration was determined using the BCA assay (section 3.1.10).

Thirty micrograms total protein was loaded onto a 7.5% polyacrylamide gel which was subsequently transferred to a nitrocellulose membrane for 2 hours (section 3.1.9.2 – 3.1.9.4). The membrane was blocked in 5% BSA containing 0.04% nonidet P40 overnight at 4^{o}C. A 1:2000 dilution of primary GLUT4 antibody was used (section 3.2.8.2.2); the remainder of the method is described in sections 3.1.9.5 and 3.1.9.6.

3.5. STATISTICAL ANALYSIS

Data are expressed as mean ± SD. Differences between the experimental groups were evaluated using the unpaired Student's *t* test for several independent observations. A *p* value of less than 0.05 was considered significant. For glucose clearance curves, the area under the curve was calculated using GraphPad Prism 3.0.

3.6. TWO DIMENSIONAL GEL ELECTROPHORESIS, PROTEIN ANALYSIS AND PROTEIN IDENTIFICATION

All gels were run by Dr. S. Roux at the Center for Proteome Analysis (CPA) in Odense, Denmark. Image analysis was performed by Dr. S. Roux and the author at CPA and results were interpreted by the author.

3.6.1. Sample preparation

Frozen liver samples were homogenized in special glass homogenizing tubes in 100µl ice cold DNase / RNase buffer (20mM Tris-HCl buffer, pH 7.5, 30mM NaCl, 5mM $CaCl_2$, 5mM $MgCl_2$, 25µg/ml DNase I and 25µg/ml RNase I). After homogenization the samples were freeze dried and then dissolved in 120µl of lysis buffer (7M urea, 2M thiourea, 2% CHAPS, 0.4% dithiothreitol, 0.5% Pharmalyte 3-10 and 0.5% Pharmalyte 6-11) by shaking, for approximately 3 hours (Hojlund *et al*., 2003). Protein concentration was determined using the Bradford method, refer to section 3.3.4.

3.6.2. Two Dimensional Gel Electrophoresis

First dimension gel electrophoresis was performed on IPG covering the pH range from 4-7 and 6-9 (Amersham Biosciences). Re-hydration buffer for the IPG strips was identical to the lysis buffer used during sample preparation, and sample was applied by in-gel re-hydration. Three hundred and fifty micrograms total protein was loaded onto each gel. Focusing was performed on a Multiphor II at 20^{o}C using a voltage time profile linearly increasing from 0-600V for 2:15hrs, 600-3500V for 8hrs, 3500V for 9:25hrs for acidic gels and 0-600V for 2:15hrs, 600-3500V for 4hrs, 3500V for 1:28hrs for basic gels. After focusing the gels were equilibrated twice, each for 15 minutes, in equilibration buffer (6M urea, 2% SDS, 30% glycerol, 50mM Tris-HCl, pH 8.8, 1% dithiothreitol). Gels were frozen at -80^{o}C between the equilibration steps. SDS-PAGE second dimension was performed using the Protean™ II Multi Cell 2-D electrophoresis system (Bio-Rad) and laboratory-made single percentage12.5% acrylamide gels. The gels were run overnight at

20^{o}C at constant current. Running buffer was re-circulated to maintain pH, SDS, temperature and salt concentrations (Hojlund *et al*., 2003).

3.6.3. Protein visualization and computer analysis

After the second dimension, hepatic proteins were visualized by sypro-ruby staining. All images were analyzed by Dr. S. Roux and by the author using a Bio Image computer program (version 6.1; Bob Luton, Ann Arbor, MI) at CPA. For comparison three 2-D gels from the OB/IR control group were compared to three 2-D gels from the lean control, metformin treated and *S. frutescens* treated groups. It was decided to only do three per group due to the high cost involved in running and visualizing these gels. The expression of each protein was measured and expressed as a percentage integrated optical density (% IOD – this is interpreted as the sum of all the pixel grey level values on and within the boundary of the spot in question and compared with that of all detected spots). Images from each group were then matched, edited and compared statistically. The average value of the spots % IOD and standard deviations were then calculated for each protein in each group and then compared using the two-sided Student's *t* test. Protein spots whose expression was found different between the two groups at the significance level $p < 0.05$ were selected for further analysis (Hojlund *et al*., 2003).

3.6.4. Mass spectrometry and protein identification

Proteins of interest were cut out from the gels and, after in-gel digestion, analyzed by mass spectrometry using a Bruker REFLEX matrix-assisted laser desorption / ionization time-of-flight (MALDI-TOF) mass spectrometer. The mass spectra obtained were internally calibrated using trypsin autodigestion peptides, and the masses were used to search the NCBI data base using the ProFound, FindPept and FindMod programs (www.proteomics.com). Data base searches were performed using the following attributes with minor modifications needed for each program: all species, no restrictions for molecular weight and protein pI, trypsin digest, one missed cleavage allowed, cysteines modified by acrylamide, oxidation of methionines possible and mass tolerance

between 0.1 and 0.5 Da. Identification was considered positive when at least 5 peptides matched the protein with no sequence overlap (Hojlund *et al*., 2003).

CHAPTER 4

RESULTS

CONTENTS

4.1. ANTIDEPRESSANT INVESTIGATIONS

The results of the amitriptyline treated rats (referred to as "amitriptyline group") and the trimipramine treated rats (referred to as "trimipramine group") were compared with the results of the control rats ("control group"). The amitriptyline group and the trimipramine group are also collectively referred to as the "test groups"

4.1.1. Rat Body Weight (refer to section 3.1)

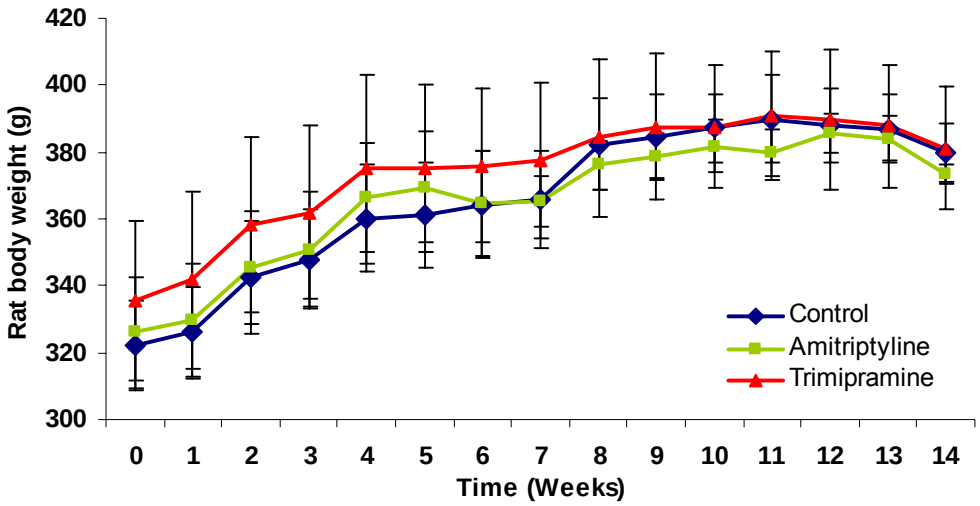

Figure 4.1: Rat body weight monitored on a weekly basis over 14 weeks of medicational compliance. Data are the mean ±SD (n = 15 test rats/group and n = 14 control rats/group).

Figure 4.1 shows no significant difference between either of the test groups when compared to the control group. All groups displayed equivalent weight gains throughout the experimentation, concluding that both antidepressants had no significant effect on weight gain or loss, relative to the control group.

4.1.2. Food and Fluid Consumed per Gram Rat Body Weight (refer to section 3.1.3)

The fluid and food consumption was monitored on a daily basis and the weekly average was plotted on a graph. Food and fluid consumption was calculated by correcting for the relevant rat weight.

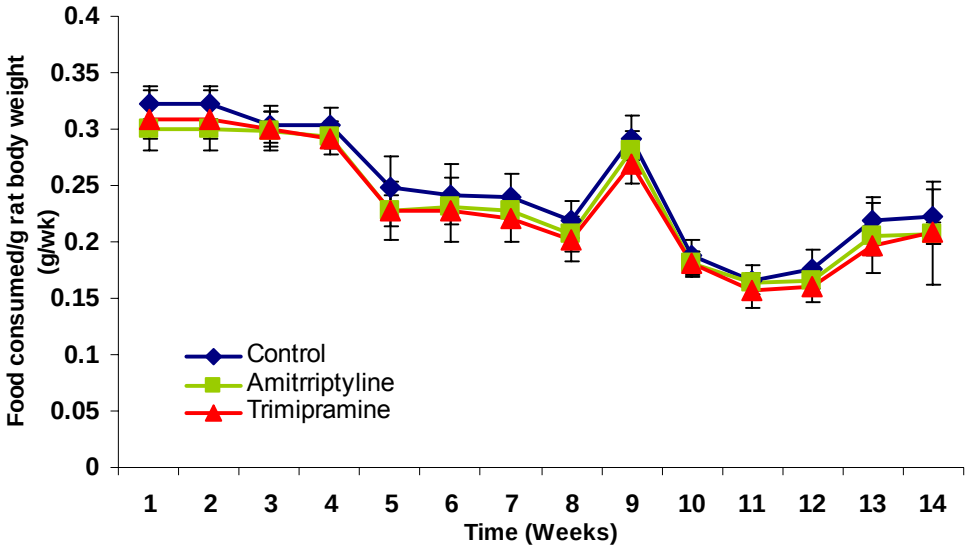

Figure 4.2: The weekly summary of the amount of food consumed per gram body weight throughout the 14 week experiment. Data are the mean ±SD (n = 15 test rats/group and n = 14 control rats/group).

Figure 4.2 shows no significant difference in food consumption per gram body weight between either of the test groups in comparison to the control group. It is evident that none of the medications had a significant effect on appetite throughout the experiment; thus contradicting the hypothesis put forward by Fava (2000), which states that tricyclics may alter hypothalamic sensitivity thereby causing an excessive craving for carbohydrates, leading to weight gain. Rigler *et al*., (2001) also proposed that tricyclics may promote appetite by acting on the neurotransmitter systems at the hypothalamic level.

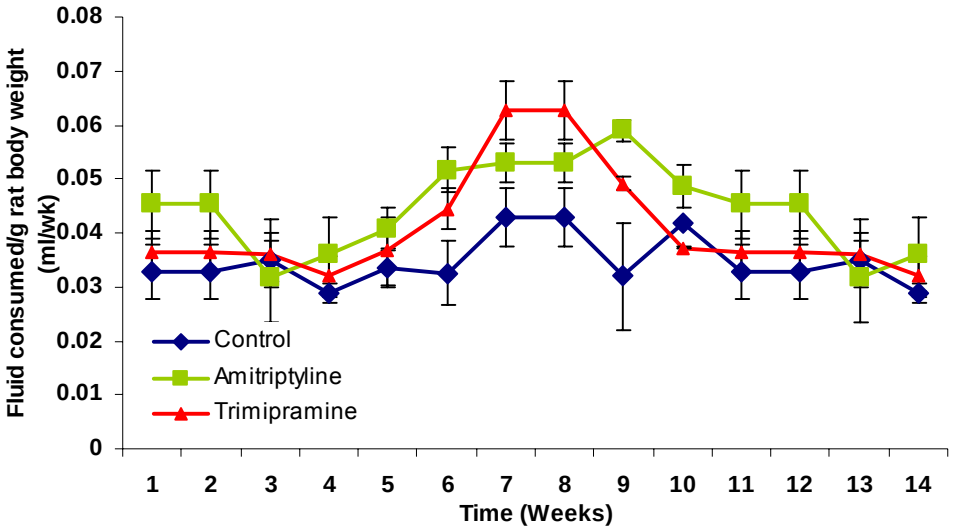

Figure 4.3: Weekly summary of the amount of fluid consumed during the day per gram body weight throughout the 14 week experiment. Data are the mean ±SD (n = 15 test rats/group and n = 14 control rats/group).

A significant increase in day time fluid consumption became evident after 5 weeks medicational treatment for the amitriptyline group, 0.041 ± 0.0039ml compared to the 0.33 ± 0.0036ml of the control group ($p < 0.05$) (fig. 4.3). This increase remained significant, for amitriptyline, right through to week 10 (see fig. 4.4 – fig. 4.9). Trimipramine also displayed a significant increase in fluid consumption, in comparison to the control group ($p < 0.01$), between week 7 and week 9 of treatment (fig. 4.6 – fig. 4.8). On week 10 the trimipramine group seemed to consume significantly less fluid than those rats in the control group, 0.037 ± 0.00018ml and 0.042 ± 0.00017ml respectively ($p < 0.05$) (fig. 4.9). No significant difference, for day time fluid consumption, was evident for the remainder of the experiment between either of the test groups compared to the control group (see fig. 4.3).

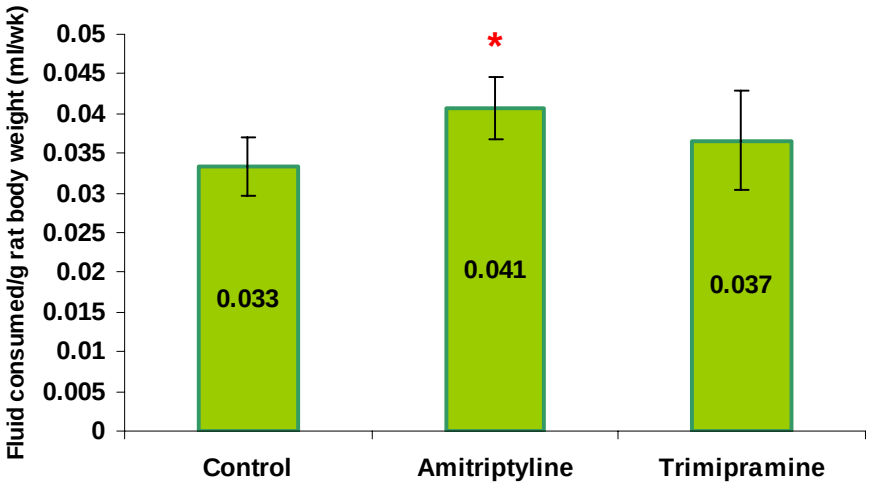

Figure 4.4: Day time fluid consumed per gram body weight at 5 weeks of medicational treatment. Data are the mean ±SD (n = 15 test rats/group and n = 14 control rats/group). * $p < 0.05$ compared to the control group by student's *t*-test.

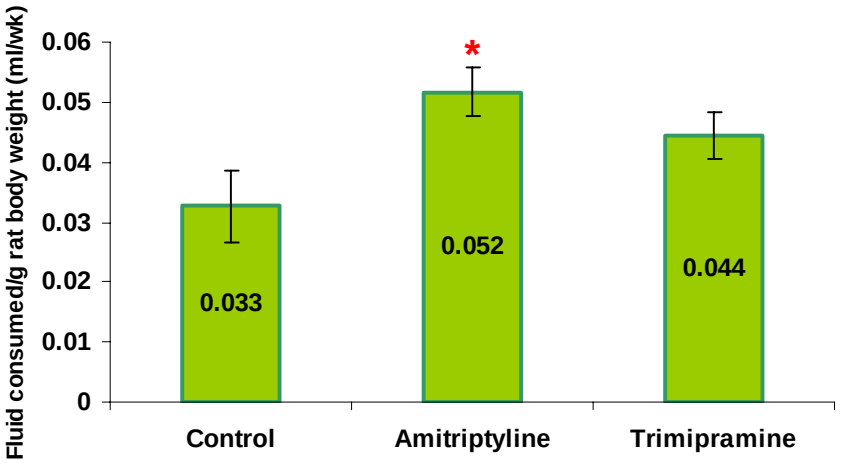

Figure 4.5: Day time fluid consumed per gram body weight during the day at 6 weeks of medicational treatment. Data are the mean ±SD (n = 15 test rats/group and n = 14 control rats/group). * $p < 0.05$ compared to the control group by student's *t*-test.

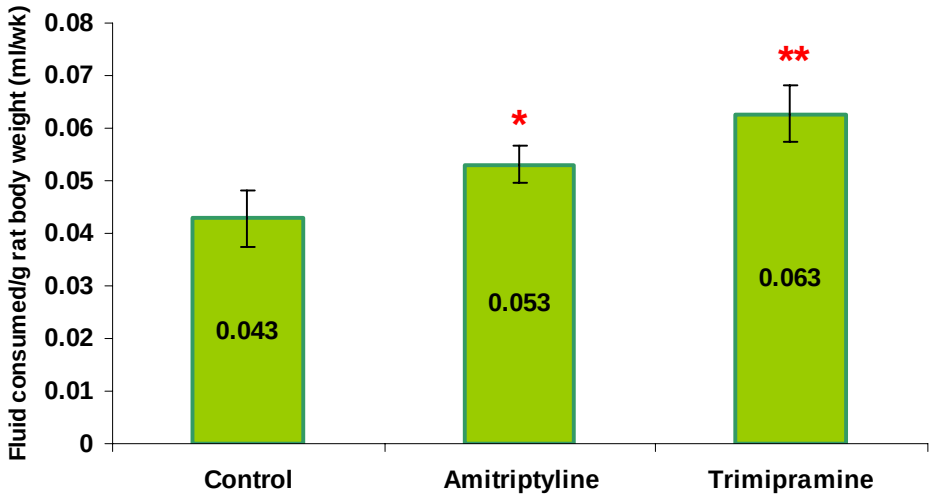

Figure 4.6: Day time fluid consumed per gram body weight at 7 weeks of medicational treatment. Data are the mean ±SD (n = 15 test rats/group and n = 14 control rats/group). * $p < 0.05$, ** $p < 0.01$ compared to the control group by student's *t*-test.

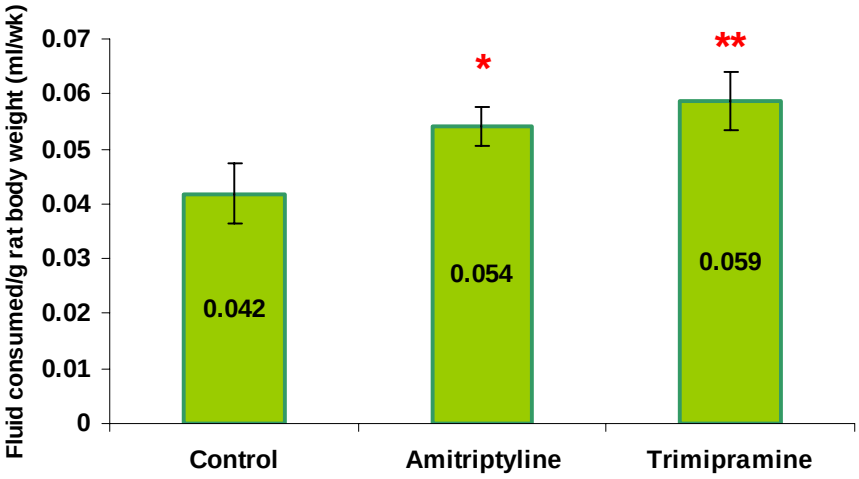

Figure 4.7: Day time fluid consumed per gram body weight at 8 weeks of medicational treatment. Data are the mean ±SD (n = 15 test rats/group and n = 14 control rats/group). * $p < 0.05$, ** $p < 0.01$ compared to the control group by student's *t*-test.

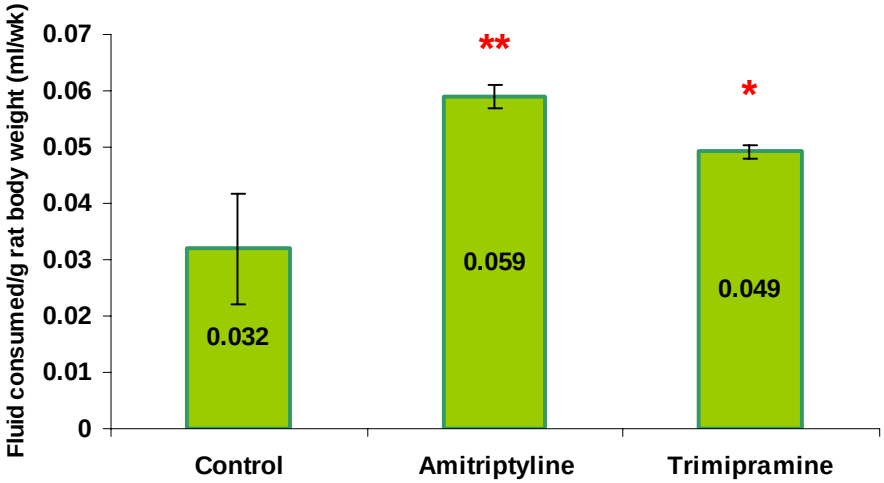

Figure 4.8: Day time fluid consumed per gram body weight at 9 weeks of medicational treatment. Data are the mean ±SD (n = 15 test rats/group and n = 14 control rats/group). * $p < 0.05$, ** $p < 0.01$ compared to the control group by student's *t*-test.

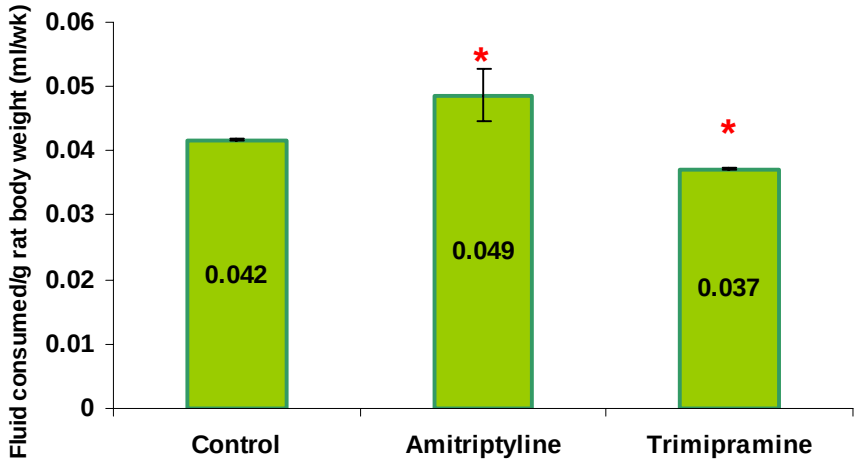

Figure 4.9: Day time fluid consumed per gram body weight at 10 weeks of medicational treatment. Data are the mean ±SD (n = 15 test rats/group and n = 14 control rats/group). * $p < 0.05$ compared to the control group by student's *t*-test.

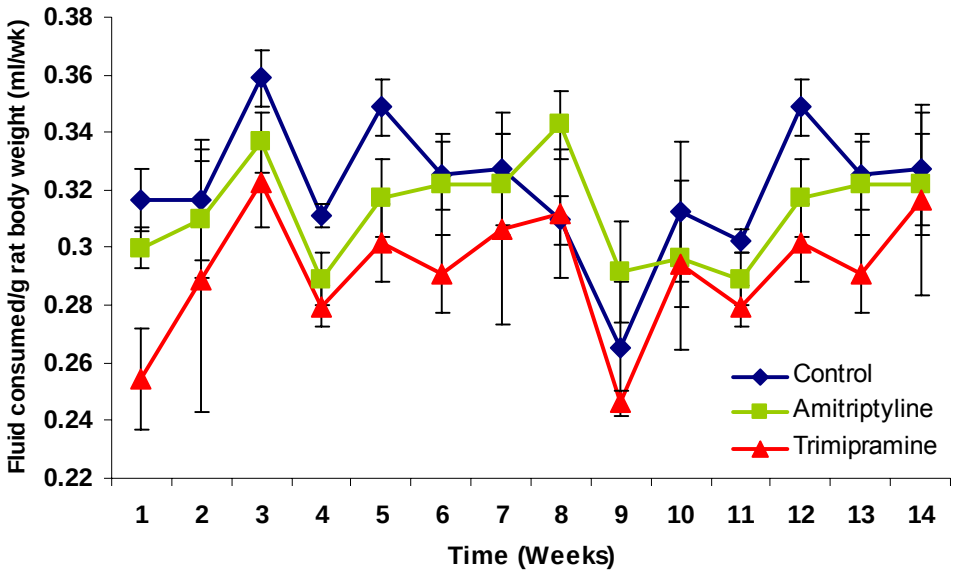

Figure 4.10: Weekly summary of the amount of fluid consumed during the night per gram body weight throughout the 14 week experiment. Data are the mean ±SD (n = 15 test rats/group and n = 14 control rats/group).

The night time fluid consumption was found to be contradictory to that of the day time consumption. The amitriptyline group starting consuming significantly less fluid, compared to the control group, after 4 weeks of medicational treatment, $p < 0.05$ (fig. 4.12). The decrease was again evident at week 5, $p < 0.05$ (fig. 4.13), and week 12, $p < 0.05$ (fig. 4.15) for control and amitriptyline groups respectively. The trimipramine group consumed significantly less fluid at night, in comparison to the control group, after 3, 4, 5, 6 and 12 weeks medicational treatment (fig. 4.11 – fig. 4.15).

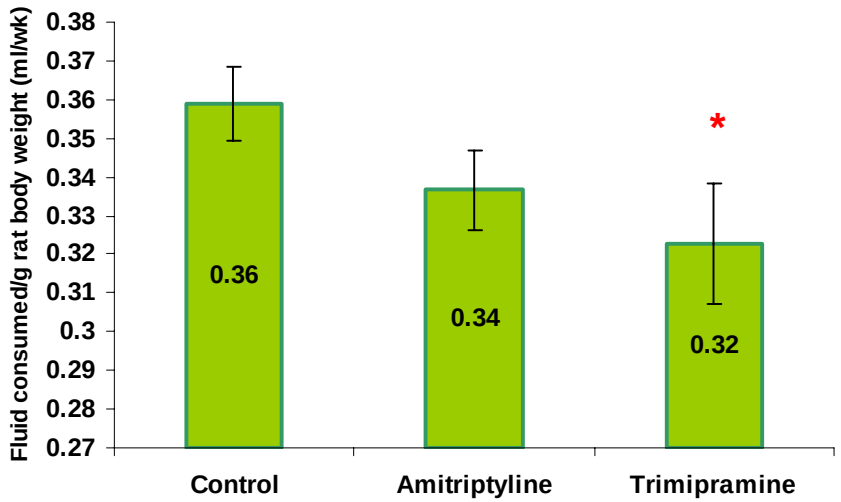

Figure 4.11: Night time fluid consumed per gram body weight at 3 weeks of medicational treatment. Data are the mean ±SD (n = 15 test rats/group and n = 14 control rats/group). * $p < 0.05$ compared to the control group by student's *t*-test

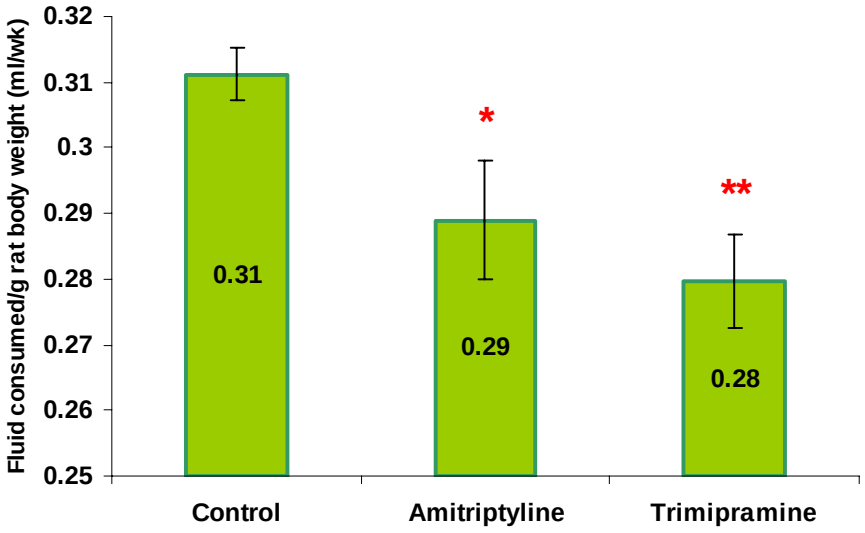

Figure 4.12: Night time fluid consumed per gram body weight at 4 weeks of medicational compliance. Data are the mean ±SD (n = 15 test rats/group and n = 14 control rats/group). * $p < 0.05$, ** $p < 0.01$ compared to the control group by student's *t*-test.

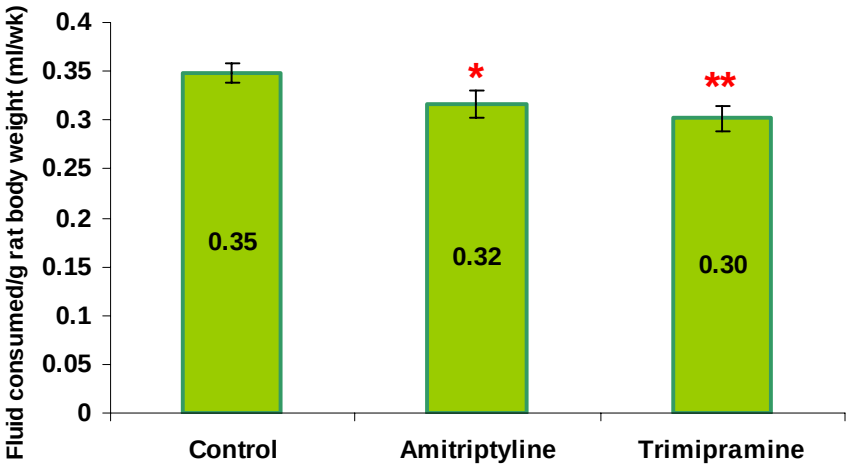

Figure 4.13: Night time fluid consumed per gram body weight at 5 weeks of medicational treatment. Data are the mean ±SD (n = 15 test rats/group and n = 14 control rats/group). * $p < 0.05$, ** $p < 0.01$ compared to the control group by student's *t*-test.

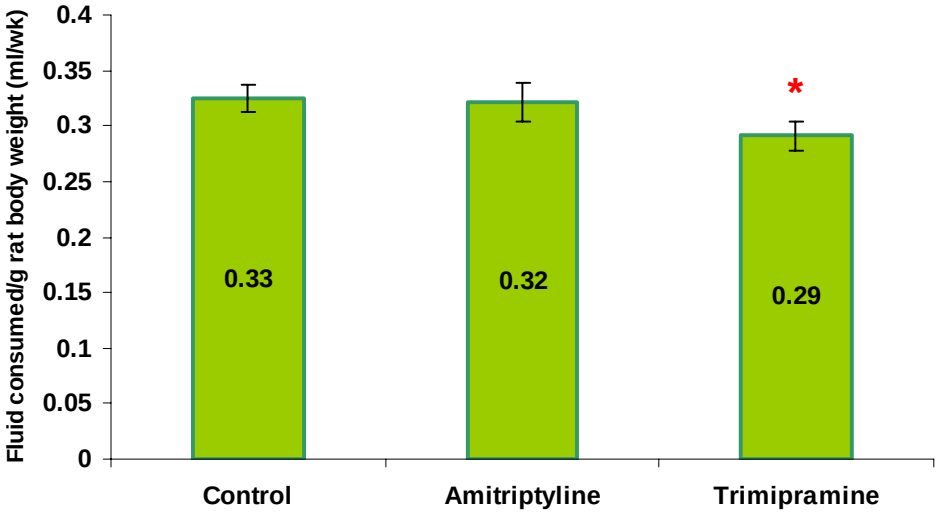

Figure 4.14: Night time fluid consumed per gram body weight at 6 weeks of medicational treatment. Data are the mean ±SD (n = 15 test rats/group and n = 14 control rats/group). * $p < 0.05$ compared to the control group by student's *t*-test

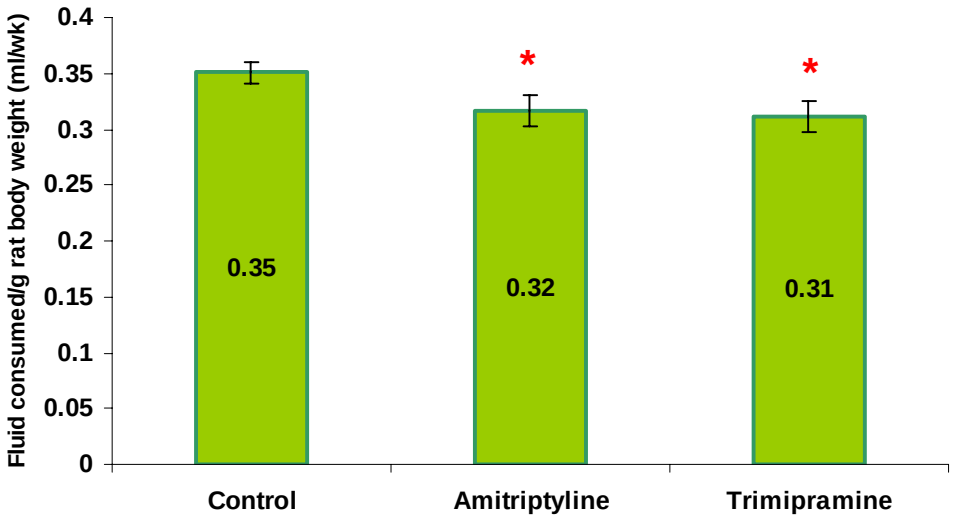

Figure 4.15: Night time fluid consumed per gram body weight at 12 weeks of medicational treatment. Data are the mean ±SD (n = 15 test rats/group and n = 14 control rats/group). * $p <$ 0.05 compared to the control group by student's *t*-test

4.1.3. Resting Metabolic Rate (refer to section 3.1.2)

In figure 4.16 no significant difference in oxygen consumption can be seen between amitriptyline (0.0097 ± 0.00117ml O_2/g/min) or trimipramine (0.0101 ± 0.00124ml O_2/g/min) treated rats when compared to the control group (0.0099 ± 0.00136ml O_2/g/min). The results displayed in figure 4.16 contradicts the hypothesis put forward by Garland *et al*., (1988), in which it was proposed that tricyclic antidepressants promoted weight gain by significantly reducing the basal metabolic rate (energy expenditure).

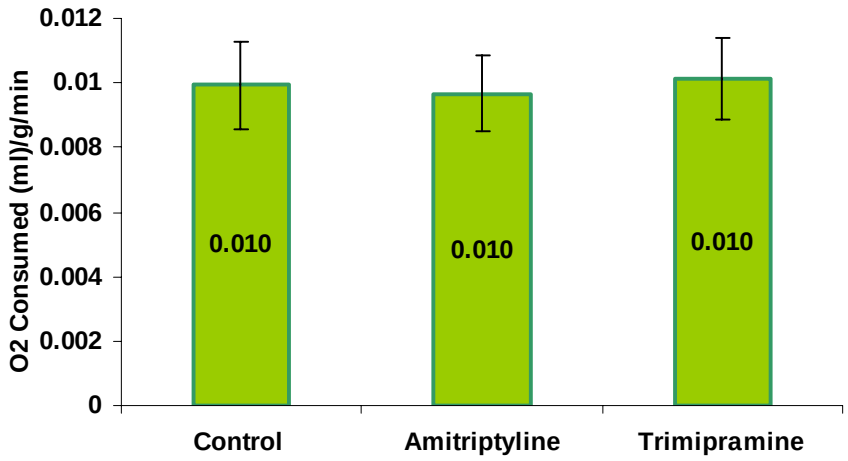

Figure 4.16: Oxygen consumed per gram body weight, per minute after 14 weeks. The flow rate was 3L/min over a period of 40 minutes. Data are the mean ± SD (n = 10 test rats/group and n = 9 control rats/group).

4.1.4. Blood Glucose (refer to section 3.1.4)

Twenty minutes after the ketamine was administered, each rat was pinched between the toes, in order to test if it was still conscious; if not blood was then collected from the tail through a small incision made using a scalpel. During the test trials it was found that the blood glucose levels were elevated when the chest cavity was opened and blood was drawn from the heart. This was probably due to the fact that the lungs collapse as soon as the chest cavity is opened, causing anoxia whereby the adrenal gland is then stimulated to release adrenaline and glucocorticoids. Both these stress hormones would contribute to a glucose elevating effect. It was therefore decided to collect blood from the tail and not directly from the heart.

The blood glucose for the amitriptyline (5.10 ± 0.37mM) and trimipramine group (5.38 ± 0.38mM) was found to be significantly higher when compared to that of the control group (4.0 ± 0.71mM, $p < 0.01$ in both cases) at the 6 week sacrifice (fig. 4.17). Both test groups similarly displayed significant increases in the blood glucose values, in comparison to the control group, at the 14 week sacrifice (fig. 4.18). Blood glucose values for the trimipramine group proved to be more elevated as compared to that displayed by the amitriptyline or control groups, 7.22 ± 0.72mM compared to 5.5 ±

0.81mM ($p < 0.05$) and 4.53 ± 0.49mM ($p < 0.01$) respectively (fig. 4.18). From figure 4.17, it seems evident that a definite trend existed at the six week sacrifice which carried through to the 14 week sacrifice. There was also no great change in blood glucose values for the amitriptyline or control groups between the 6 week and 14 week sacrifice times. A difference of 1.84mM ($p < 0.1$) was found for the trimipramine groups between the 6 week and 14 week sacrifice times.

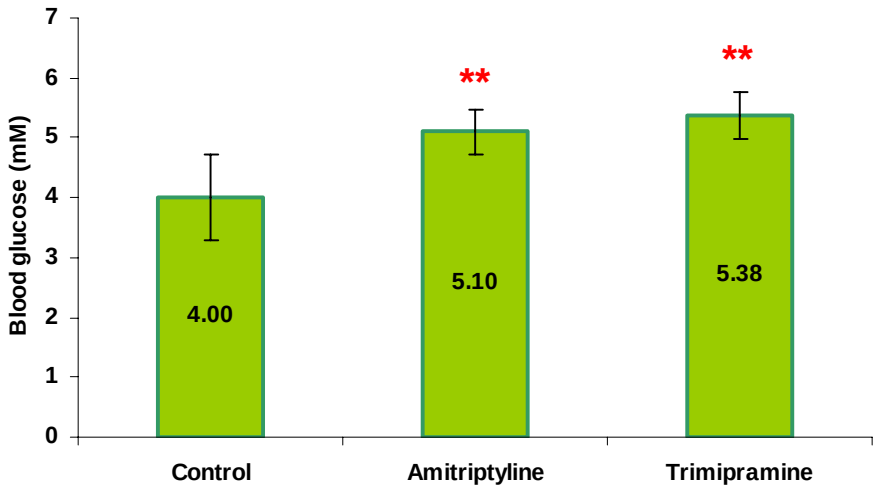

Figure 4.17: Blood glucose levels at the 6 week sacrifice, after 12 hour starvation. Data are the mean ±SD (n = 5 rats/group) ** $p < 0.01$ compared to the control group by student's *t*-test

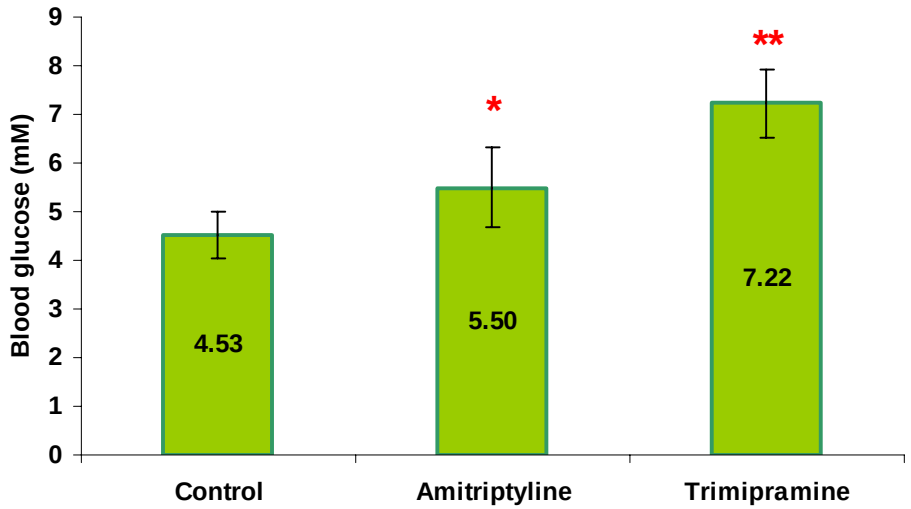

Figure 4.18: Blood glucose levels at the 14 week sacrifice, after 12 hour starvation. Data are the mean ±SD (n = 5 rats/group) * $p < 0.05$, ** $p < 0.01$ compared to the control group by student's *t*-test

The significantly higher blood glucose levels found for each of the test groups, relative to the control group, contradict the theory of antidepressants causing hypoglycaemic-induced hunger (Garland *et al*., 1988).

4.1.5. Glucose Clearance (refer to section 3.1.5.2)

As can be seen in figure 4.19, no significant difference is apparent between either test groups, in relation to the control group, for the rate of glucose clearance. Results are represented as the area under each of the relevant glucose clearance curves (results not shown). This may imply that the medication did not have a significant effect on insulin-receptor sensitivity or any post receptor proteins activated through insulin stimulation.

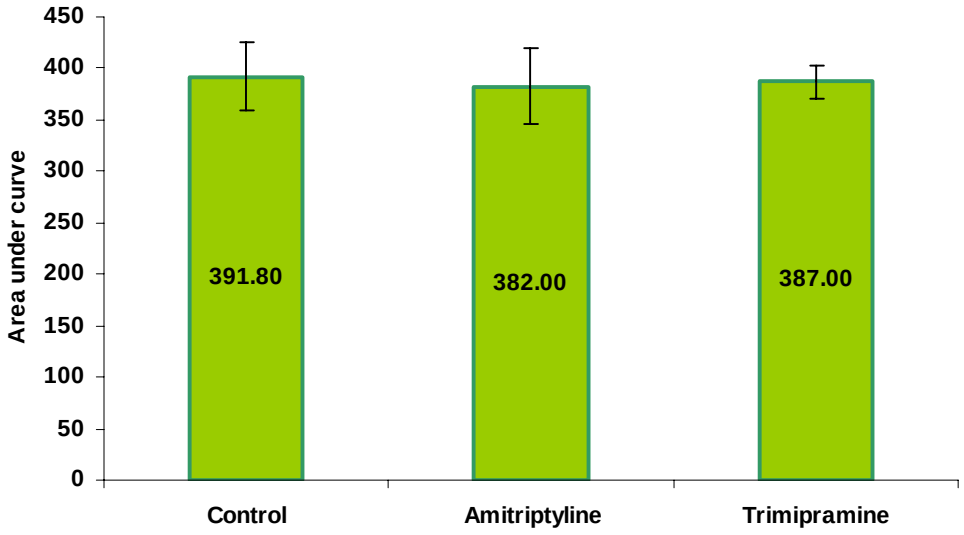

Figure 4.19: Effects of amitriptyline and trimipramine on blood glucose clearance. Values are expressed as mean ± SD (n = 5 rats/group). The y-axis represents arbitrary units.

4.1.6. Glucose Uptake (refer to section 3.1.5.3)

An indication of glucose uptake for muscle, liver, fat and kidney can be obtained from figure 4.20. Glucose uptake into muscle showed no significant difference for the amitriptyline (160 ± 13.8dpm/g) or trimipramine groups (151.2 ± 20dpm/g) relative to that of the control group (141.1 ± 13.8dpm/g). The control group seemed to have a higher

concentration of ^{3}H in the liver, 315.5 ± 135dpm/g, than the amitriptyline, 254.0 ±75dpm/g, or trimipramine groups, 133 ± 74dpm/g. This result was however, not significant due to high standard deviations brought about by the [^{3}H] deoxyglucose being able to enter and leave the liver tissue freely through GLUT2 transporters, which are not present in the other tissues under investigation. No difference in ^{3}H distribution, in adipose tissue, could be found between the control, amitriptyline or trimipramine group, 78.3 ± 5.42dpm/g, 79.1 ± 2.69dpm/g and 80.05 ± 2.80dpm/g respectively.

A significant reduction in [^{3}H] deoxyglucose can be seen in the kidney of the amitriptyline, 593.8 ± 200dpm/g, and trimipramine groups, 517.4 ± 150dpm/g, in comparison to that found within the control group, 1525 ± 100dpm/g.

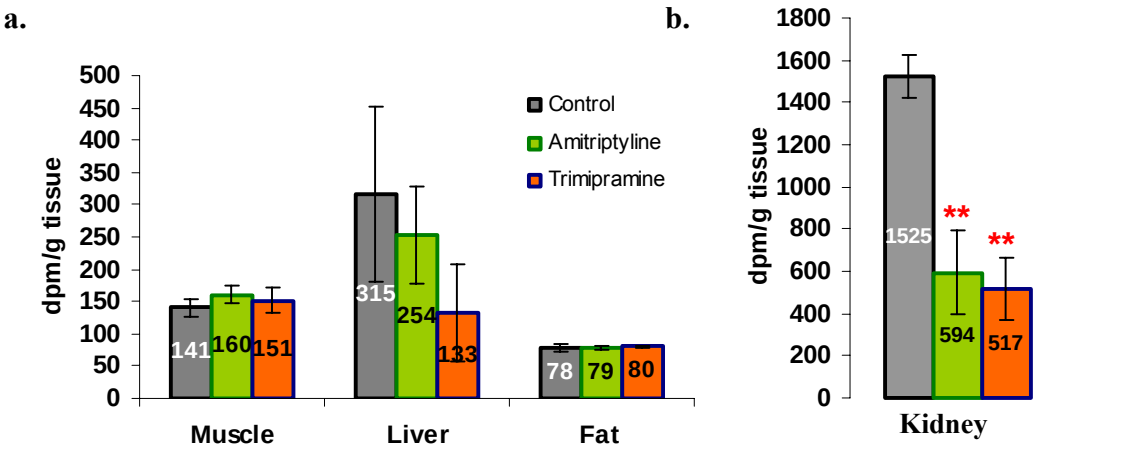

Figure 4.20: ^{3}H counts in muscle, liver and epididymal fat (a) and kidney (b) one hour after an intravenous glucose load supplemented with 2-deoxy-D-[2,6-^{3}H] glucose. Values are expressed as mean ± SD, ** $p < 0.001$ compared to the control (n = 5 test rats/group and n = 4 control rats/group).

4.1.7. Tissue Glycogen Content (refer to section 3.1.7)

Figure 4.21 represents the tissue glycogen content following the 6 and 14 week antidepressant treatment. The figure illustrates a significant decrease in glycogen content for both test groups, relative to that of the control group, for liver and muscle tissue at both sacrifice periods. Reasons for the lower glycogen levels found in the liver relative to that found in the muscle may be attributed to the overnight starvation endured by the

animals prior to the sacrifice. Under normal circumstances liver should of course hold the highest concentration of glycogen, as this is the primary organ involved in glycogen metabolism and storage. However, the liver is the primary source for glycogen breakdown during starvation. This would be the reason for the muscle having a significantly higher concentration of glycogen relative to the liver. If the starvation was prolonged the glycogen in the muscle would be the next source of glucose for the body.

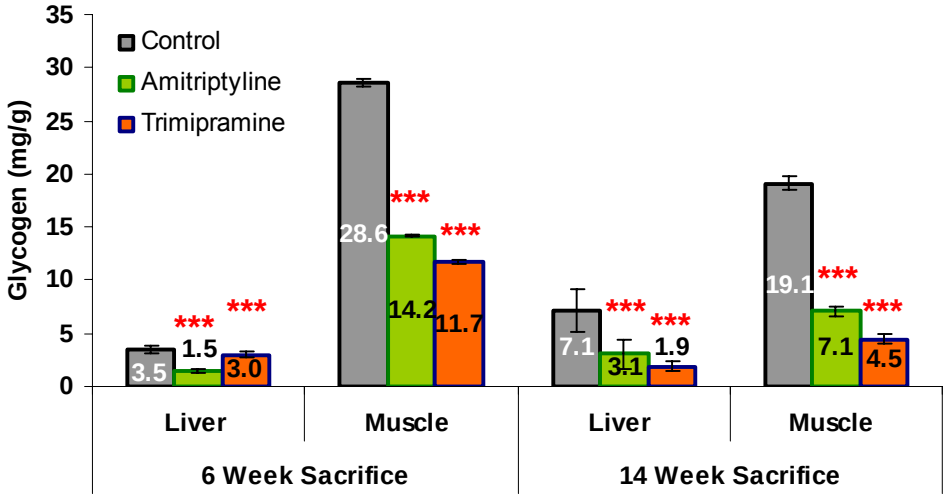

Figure 4.21: Effects of amitriptyline and trimipramine on tissue glycogen levels. Values are expressed as mean ± SD (n = 5 rats/group). *** $p < 0.001$ compared with control group.

A significant decrease in liver glycogen content can be observed for both the amitriptyline, 1.5 ± 0.17mg/g ($p < 0.001$), and trimipramine group, 3.0 ± 0.22mg/g ($p < 0.001$), in comparison to that of the control group, 3.5 ± 0.36mg/g, following the six week sacrifice. An even greater decrease in glycogen content can be observed in the muscle at the same sacrifice period, for the amitriptyline and trimipramine groups, 14.2 ± 0.16mg/g ($p < 0.001$) and 11.7 ± 0.14mg/g ($p < 0.001$) respectively, compared to the 28.6 ± 0.39mg/g glycogen found in the control group.

The 14 week sacrifice follows the same trend for both tissues tested. The amitriptyline and trimipramine treated groups, again, contained a significantly lower liver glycogen concentration, 3.1 ± 1.4mg/g ($p < 0.001$) and 1.9 ± 0.42mg/g ($p < 0.001$) respectively, compared to that found for the control group 7.1 ± 2.0mg/g. The muscle glycogen

followed the same trend as found for the previous sacrifice with a significant reduction in glycogen for the amitriptyline, 7.1 ± 0.46mg/g ($p < 0.001$), and trimipramine groups, 4.5 ± 0.54mg/g ($p < 0.001$), relative to that found within the control group, 19.1 ± 0.70mg/g.

The glycogen content for the trimipramine group was found to be significantly reduced in comparison to that found within the amitriptyline group for the muscle, following the 6 week sacrifice period, and both the muscle and liver, following the 14 week sacrifice period ($p < 0.001$).

4.1.8. Serum Insulin Levels (refer to section 3.1.6.2)

Due to budget constraints only the amitriptyline serum insulin levels could be determined. The serum insulin of the control group is within the normal range for fasting rats, 75 – 150pmol/l (Morgan and Lazarow, 1963; Feldman and Rodbard, 1971; Thorell and Lanner, 1973; Westgard, 1981). As can be seen from figure 4.22 the amitriptyline group's serum insulin, 91.11 ± 11.40pmol/l, is insignificantly lower than that of the control, 102.17 ± 14.94pmol/l.

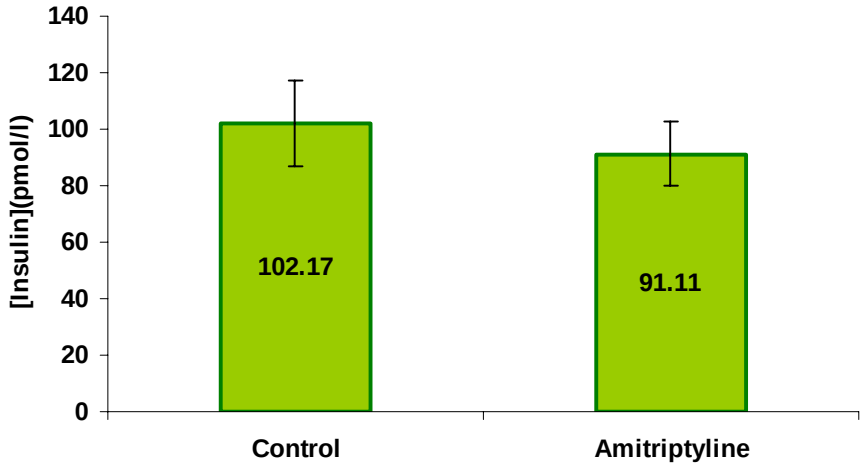

Figure 4.22: Effects of amitriptyline treatment on serum insulin levels, following 14 weeks medicational compliance. Values are expressed as mean ± SD (n = 5 rats/group).

4.1.9. Insulin Degradation (refer to section 3.1.8)

Both the amitriptyline and trimipramine groups showed an increase in insulin degradation, within the liver, in comparison to the control group. The trimipramine showed the highest insulin degradation at 10 (51.7 ± 1.34%; $p < 0.01$), 15 (52.6 ± 2.30%; $p < 0.01$), 20 (52.9 ± 2.47%; $p < 0.01$) and 30 (52.9 ± 2.56%; $p < 0.05$) minutes incubation, relative to that of the control group (fig. 4.23) over the same respective time periods (49.2 ± 1.15%, 48.4 ± 1.76%, 48.1 ± 2.08% and 48.9 ± 2.39%). Insulin degradation, for the trimipramine group, seems to peak after the 15 minute incubation period and then plateaus from there for the remainder of the experiment. The control group reaches its maximum as soon as the 10 minute incubation period (49.1 ± 1.15%) after which it remains relatively stable throughout the remainder of the experiment.

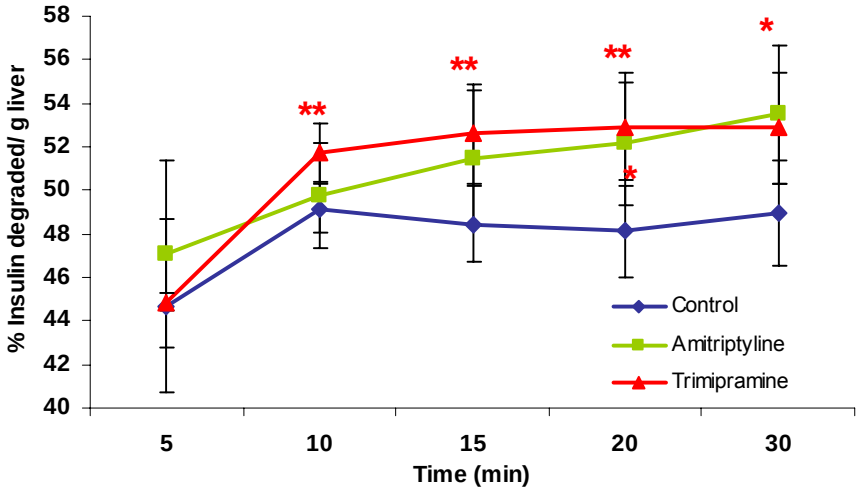

Figure 4.23: Insulin degradation in rat liver, following 6 weeks amitriptyline or trimipramine treatment. Values are expressed as mean ± SD (n = 5 rats/group). * $p < 0.05$ and ** $p < 0.01$ compared to the control group by student's *t*-test.

Although amitriptyline treatment also contributed to an increase in insulin degradation only one value was significantly different from the control group. This was found to be at the 20 minute incubation period, 52.1 ± 2.9% ($p < 0.05$) compared to the control group's 48.1 ± 2.08%. The insulin degradation was also found to be higher after the 15 (51.5 ± 3.06%) and 30 (53.5 ± 2.55%) minute incubation periods for the amitriptyline group in relation to that of the control group, but with a $p < 0.1$ difference it was not considered to

be significant. The amitriptyline treatment did not seem to reach a plateau, as it did for the trimipramine group, but instead seemed to be steadily on the increase over the 30 minute incubation period.

An increase in insulin degradation was once again found for both test groups following the 14 week sacrifice, as can be seen in figure 4.24. Both the amitriptyline and the trimipramine group displayed significant increases in insulin degradation after the 15 (43.3 ± 1.82%; $p < 0.005$ and 42.9 ± 2.51%; $p < 0.005$, respectively), 20 (42.9 ± 1.93%; $p < 0.001$ and 42.8 ± 1.43%; $p < 0.001$, respectively) and 30 (41.6 ± 2.17%; $p < 0.005$ and 45.1 ± 2.20%; $p < 0.001$, respectively) minute incubation periods when compared to the same incubation periods for the control group (37.9 ± 2.03%, 37.4 ± 1.51% and 35.1 ± 1.03% respectively).

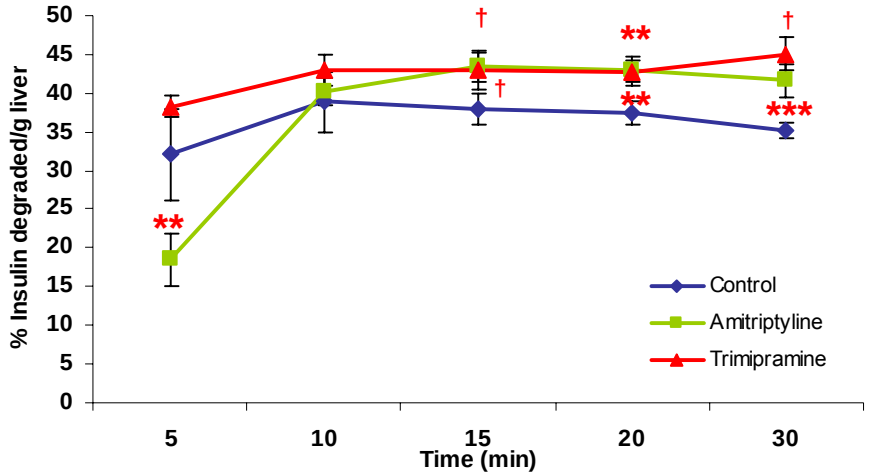

Figure 4.24: Insulin degradation in rat liver, following 14 weeks amitriptyline or trimipramine treatment. Values are expressed as mean ± SD (n = 5 rats/group). ** $p < 0.01$, † $p < 0.005$ and *** $p < 0.001$ compared to the control group by student's *t*-test.

Insulin degradation in the amitriptyline group was significantly lower, relative to that of the control group after the 5 minute incubation period, 18.47 ± 3.48% compared to 32.0 ± 5.88% ($p < 0.01$) respectively. Insulin degradation for the trimipramine group seems to plateau at 10 minutes while the amitriptyline group only reaches a plateau after the 15 minute incubation period. The average percent insulin degradation, for all groups, is

undoubtedly lower here than that found following the 6 week sacrifice experiment (fig. 4.23), even though the protocol was accurately replicated.

Amitriptyline and trimipramine treatment clearly increased insulin degradation in liver (figures 4.23 and 4.24) and it was therefore decided to determine whether other tissues implicated in insulin degradation were affected in a similar way. Kidney and muscle samples were therefore tested as well, following the same protocol as before. Suspicions were confirmed; figures 4.25 and 4.26 revealed that both amitriptyline and trimipramine treatment caused an increase in insulin degradation relative to the control group.

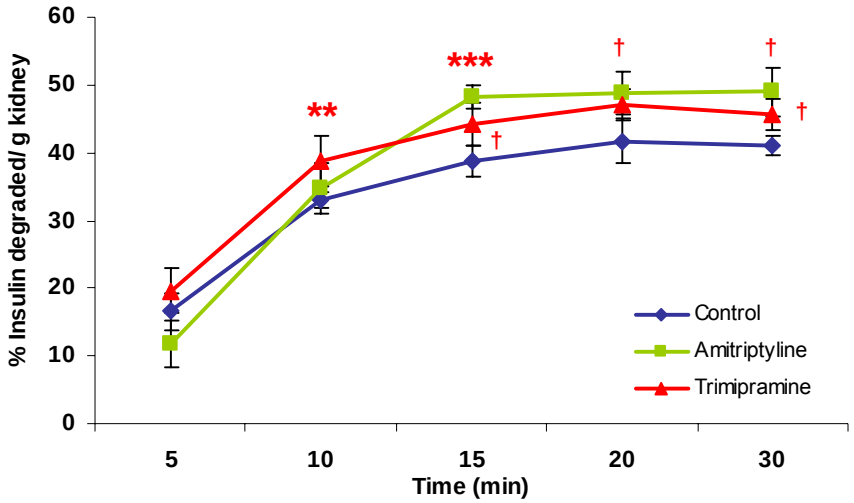

Figure 4.25: Insulin degradation in rat kidney, following 14 weeks amitriptyline or trimipramine treatment. Values are expressed as mean ± SD (n = 5 rats/group). ** $p < 0.01$, † $p < 0.005$ and *** $p < 0.001$ compared to the control group by student's *t*-test.

The amitriptyline group's insulin degradation (11.8 ± 3.47%) was once again lower than the control group (16.6 ± 2.71%), after 5 minutes incubation, this result was however not significant. The degradation increased significantly after 15 minutes, 48.2 ± 1.76% ($p < 0.001$), where it reached a plateau at the 20 and 30 minute incubation periods, 48.7 ± 3.19% ($p < 0.005$) and 50.0 ± 3.51% ($p < 0.005$), respectively, in comparison to that of the control group (38.8 ± 2.19%, 41.7 ± 3.29% and 41.0 ± 1.44% respectively).

The trimipramine group displayed increased insulin degradation at the 10 minute mark, 38.8 ± 3.63% ($p < 0.01$) in comparison to that of the control group, 32.9 ± 1.16%. This

significant trend continued after 15 minutes, 44.2 ± 3.14% ($p < 0.005$) and decreased slightly after 30 minutes, 45.5 ± 2.30% ($p < 0.005$) but remained significantly higher than that of the control group for this time point, 41.0 ± 1.44%.

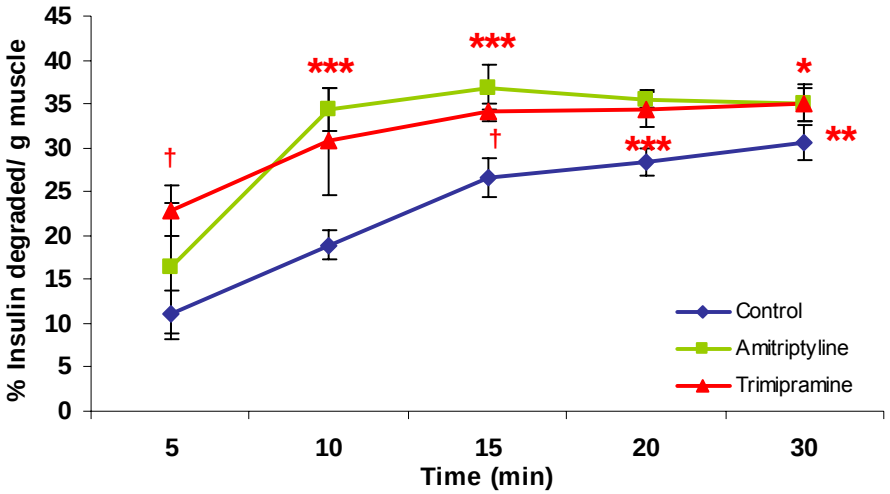

Figure 4.26: Insulin degradation in rat muscle, following 14 weeks amitriptyline or trimipramine treatment. Values are expressed as mean ± SD (n = 5 rats/group). * $p < 0.05$, ** $p < 0.01$, † $p < 0.005$ and *** $p < 0.001$ compared to the control group by student's *t*-test.

The average percent degradation in figure 4.26 is slightly lower for all groups in comparison to the other tissues. This is not surprising as liver and kidneys are the primary sites for insulin degradation, whereas the muscle is more a secondary site. Both test groups still display significantly increased insulin degradation, relative to the control group.

The amitriptyline significantly increased insulin degradation after 10 (34.3 ± 2.47%; $p < 0.005$), 15 (36.9 ± 2.53%; $p < 0.001$), 20 (35.5 ± 0.91%; $p < 0.001$) and 30 (35.1 ± 2.10%, $p < 0.05$) minutes compared to that of the control group (18.9 ± 1.71%, 26.6 ± 2.25%, 28.4 ± 1.54% and 30.7 ± 2.03%). The trimipramine showed a significant increase over all the time periods plotted; 5 (22.75 ± 2.91%; $p < 0.005$), 10 (30.7 ± 6.06%, $p < 0.001$), 15 (34.0 ± 1.09%; $p < 0.005$), 20 (34.4 ± 2.13%; $p < 0.001$) and 30 (35.0 ± 1.90%; $p < 0.01$) minutes.

4.1.10. Quantification of Insulin Degrading Enzyme (refer to section 3.1.9)

The results obtained from the blots for the insulin degrading enzyme (figures A1 a & b) are graphically displayed in figure 4.27 as percentages. These percentages were calculated by obtaining each band's integrated density value, subtracting the background and dividing by the relative band area. Figure 4.27 shows that both the trimipramine and the amitriptyline group have significantly higher levels of insulin degrading enzyme, 12.62 ± 2.1% ($p < 0.001$) and 11.48 ± 0.52% ($p < 0.001$) respectively, in comparison to the control group, 9.25 ± 1.3%.

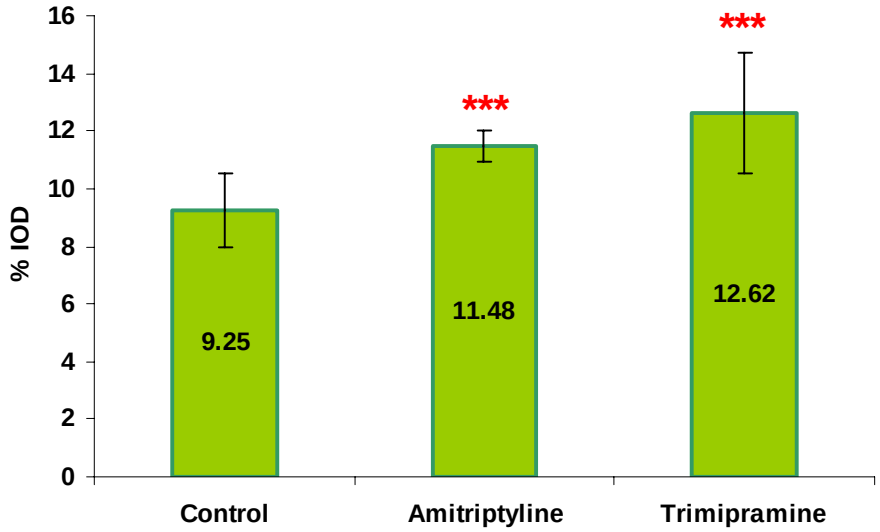

Figure 4.27: Band density of liver IDE after 6 weeks treatment, expressed as a percentage of integrated optical density (IOD) obtained from Western blots. Values are expressed as mean ± SD (n = 5 rats/group).*** $p < 0.001$ compared to control group.

Figure 4.28 clearly indicates an increased concentration of muscular insulin degrading enzyme for both the amitriptyline, 12.80 ± 0.64% ($p < 0.001$), and trimipramine groups, 11.58 ± 0.73% ($p < 0.001$), in comparison to the control group, 8.75 ± 2.27%. It seems evident that the accelerated rate of insulin degradation for the amitriptyline and trimipramine groups, observed in figures 4.24 and 4.26, is attributed to a significantly higher concentration of insulin degrading enzyme in their respective tissues.

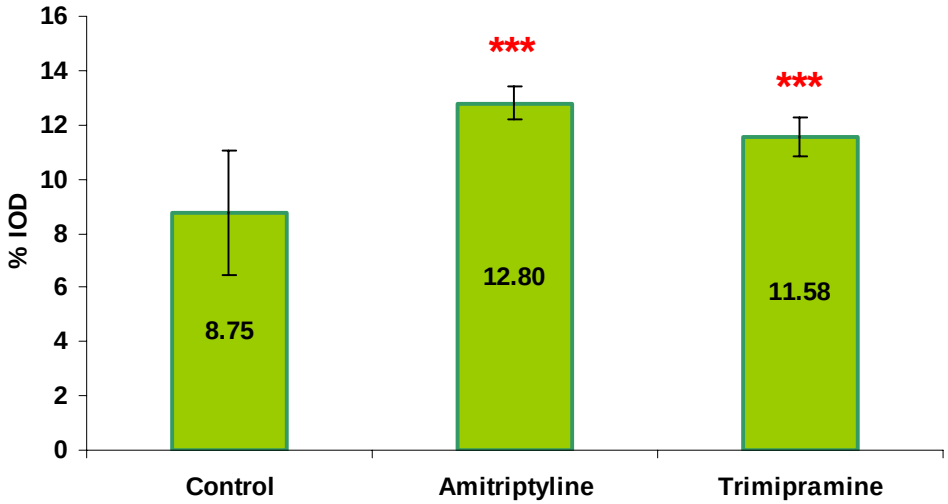

Figure 4.28: Band density of muscle IDE after 6 weeks treatment as a percentage of integrated optical density (IOD) obtained from Western blots. Values are expressed as mean ± SD (n = 5 rats/group).*** $p < 0.001$ compared to control group.

Although insulin degradation was tested only in the liver, for the 6 week sacrifice (fig. 4.23), muscle insulin degrading enzyme levels were determined in the muscle tissue from this sacrifice (6 weeks) due to the accelerated insulin degradation observed in this tissue over the 14 week sacrifice period, figure 4.26. The -80^{o}C freezer holding the samples from the 14 week sacrifice malfunctioned, allowing samples to defrost and protein to denature, it is for this reason that samples from the previous sacrifice were employed for this experiment (figs. 4.27 and 4.28).

The concentration of insulin degrading enzyme in the muscle seems to be slightly higher, but not significantly so, in comparison to that of the liver for the amitriptyline group (12.80 ± 0.64%, figure 4.28, and 11.48 ± 0.52%, figure 4.27, respectively). The reverse is true for the trimipramine treated group, which displayed an insignificantly higher concentration of insulin degrading enzyme in the liver in comparison to the muscle tissue (12.62 ± 2.1%, figure 4.27, and 11.58 ± 0.73%, figure 4.28, respectively). Unfortunately, as no insulin degradation experiments were performed on muscle tissue during the 6 week sacrifice no comparison can be made with regards to the percent insulin degraded and insulin degrading enzyme concentration in the relevant tissues. A comparison can

however be made between the percent insulin degraded and the insulin degrading enzyme concentration within the liver for the trimipramine and amitriptyline treated groups. The average percentage of insulin degraded seems to be slightly higher for the trimipramine treated group relative to the amitriptyline group (figure 4.24). A reason for this increase may be due to the trimipramine group having a slight, but insignificant, increase in insulin degrading enzyme in comparison to the amitriptyline treated group in liver (figure 4.27).

DIABETES STUDY

4.2. Identification of Potential Bacterial Contaminants in the *S. frutescens* Extract
(refer to section 3.2.1.1.1)

The total bacterial count was 88 000 colony forming units per ml of the *Sutherlandia frutescens* infusion, as determined from the spread plate. Three morphologically different colonies were identified, from the spread plate, and were isolated into single colonies through the streak plate technique. These individual colonies were then used for further identification of the bacteria.

All three colonies stained purple for the gram stain, indicating they were all gram positive bacteria. The three different colonies contained endospores, were rod shaped, and were motile. The morphology of these bacteria under the microscope along with the above mentioned information allowed all three colonies to be grouped into the *Bacillus* genus. More than sixty different valid *Bacillus* species have been identified in the past, and all except two, are non-pathogenic (Barrow and Feltham, 1995). It was therefore decided not to further identify the bacteria but to rather confirm that they were not of a pathogenic nature. All the other *Bacillus* species are commonly found in the soil and do not have any pathogenic effects.

The two pathogenic bacteria in the *Bacillus* group are *B. anthracis* and *B. cereus*. The simplest way of elimination was to determine whether the bacteria, isolated from the *Sutherlandia* infusion, grew on 10% NaCl and under anaerobic conditions, as the pathogenic *Bacillus* species are known to grow under both these conditions. After an overnight incubation at 37^{o}C, all three colonies from the infusion were negative for anaerobic growth and for growth on 10% NaCl. One species was oxidase positive, while the other two species were oxidase negative. These results suggested that none of the bacteria isolated from the infusion was either *B. anthracis* or *B. cereus* and was therefore not of a pathogenic nature. All bacterial identification was determined with the aid of Cowan and Steel's Manual for the Identification of Medical Bacteria (Barrow and Feltham, 1995).

4.3. INSULIN RESISTANT MODEL (Type II Diabetes)

4.3.1. Rat Body Weight

Figure 4.29 depicts the rat weights prior to and during experimentation from week 1. Rats with similar body weights were put into the same groups for experimentation. The reason for this was to reduce large standard deviations between groups so that even a slight change in body weight brought about by medication or diet could be detected.

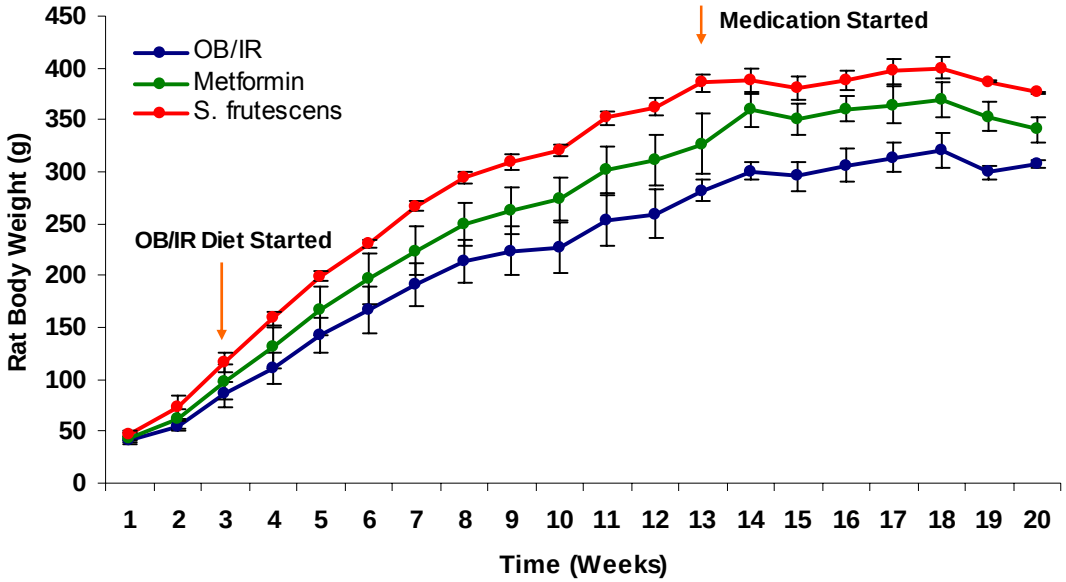

Figure 4.29: Rat weights from time of administration of OB/IR diet, followed through to the completion of the experiment. Values are expressed as mean ± SD (n = 11 rats/group).

Previous experiments have shown that metformin is successful in promoting weight loss in humans through inhibition of food intake and a reduction in the rate of glucose absorption through the intestine (Paolisso *et al.*, 1998). However once again the subjects used for the experiment were obese and obese diabetics, which was not the case with the Wistar rats. Work done by Suzuki *et al.*, (2002), using Wistar rats, showed that they displayed a slight weight increase after being administered a dose of 300mg/kg per day of metformin. Many studies have been undertaken involving metformin, most of which show the drug promoting weight loss, however it is important to note that these studies involved obese subjects. Figures 4.30 and 4.31 allow for a more detailed look at the

effects the medications had on body weight changes from the start of administration of medication until the sixth week and eigth week of experimentation, respectively

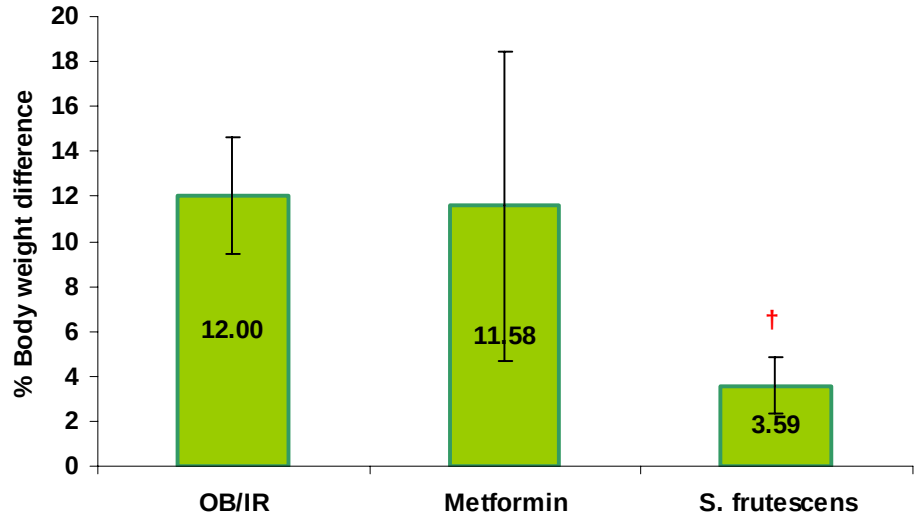

Figure 4.30: Percentage body weight gained from time of administration of medication until 18th week of experimention. Values are expressed as mean ± SD (n = 11 rats/group). † $p < 0.005$ compared to control group.

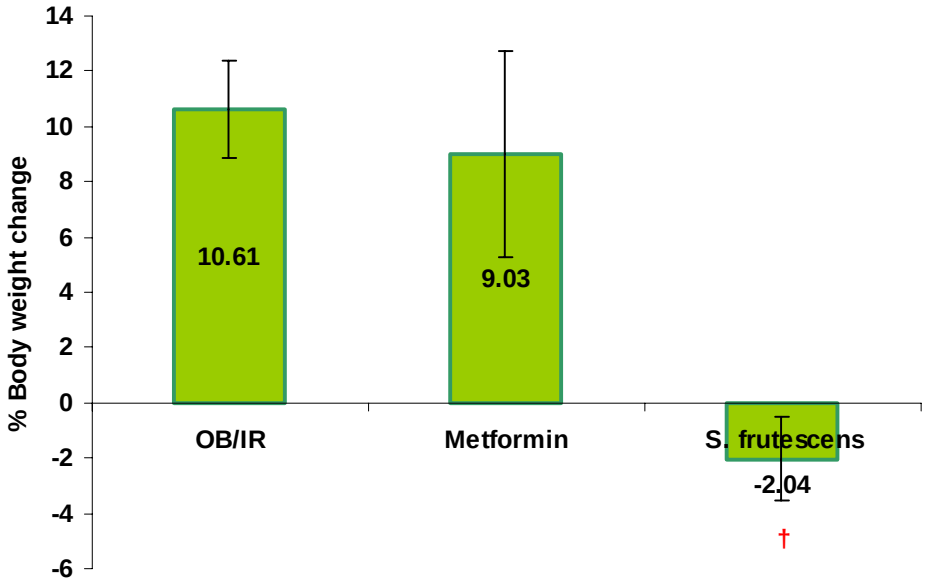

Figure 4.31: Percentage body weight gained from time of administration of medication until completion of the experiment. Values are expressed as mean ± SD (n = 11 rats/group). † $p < 0.005$ compared to control group.

4.3.2. Food and Fluid Consumed (refer to section 3.2.3)

As mentioned in the methodology, the rats received a specialized diet to render them insulin resistant. This specialized diet came in the form of patties, of which each rat received a half on a daily basis. As each rat consumed the entire patty each day and the lean control group received dog pellets, *ad lib*, comparisons between different groups' food consumption could not be made.

A comparison between the different groups' fluid consumption was also not made for various reasons. Firstly the *S. frutescens* group consumed less fluid than the other groups due to the water which was supplemented with the bitter extract. Secondly the lean control group consumed the most fluid due to the nature of the dry food they received *ad lib*, no conclusions could therefore be drawn regarding food and fluid consumption.

4.3.3. Resting Metabolic Rate (refer to section 3.2.2)

A significant decrease in oxygen consumption was observed for the *S. frutescens* group, 0.009 ± 0.0015ml O_2/g/min, in comparison to the OB/IR group, 0.013 ± 0.0017ml O_2/g/min ($p < 0.01$) (fig. 4.32). The oxygen consumption also seemed to be lower for rats from the lean control group, 0.011 ± 0.0023ml O_2/g/min. This lowering was however not significant. A similar trend was obtained from a previous study (Chadwick, 2003), in which male Wistar rats, on a normal diet, received the same dose of *S. frutescens* extract, in their drinking water, over a period of 19 weeks.

No significant changes in oxygen consumption were found between the other groups. The OB/IR group seemed to have a slightly higher rate of oxygen consumption, 0.013 ± 0.0017ml O_2/g/min, compared to the lean control, 0.011 ± 0.002ml O_2/g/min but this trend was not significant (fig. 4.32). The metformin group also displayed a non-significant decreased trend in oxygen consumption, 0.011 ± 0.00048ml O_2/g/min, compared to the OB/IR group, 0.013 ± 0.0017ml O_2/g/min. The reading was similar to that of the lean control group, 0.011 ± 0.002ml O_2/g/min (fig. 4.32).

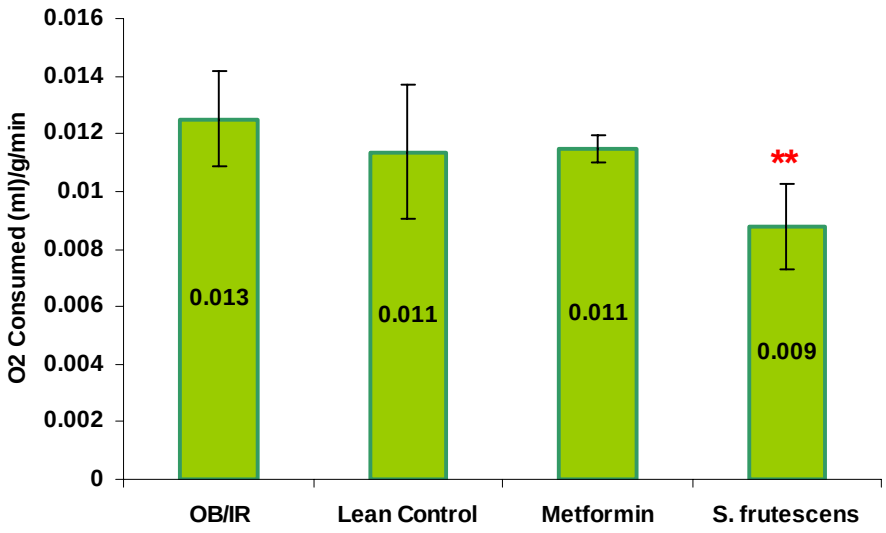

Figure 4.32: Resting metabolic rate, measured as oxygen consumed per gram body weight, per minute after 8 weeks medicational treatment. The flow rate was 3l/min over a period of 40 minutes. Data are the mean ± SD (n = 11 rats/group). ** $p < 0.01$ compared with the OB/IR group by Dunnett's test.

4.3.4. Blood Glucose (refer to section 3.2.5.1)

Figure 4.33 displays blood glucose values for the various test and control groups. It is clear that no significant differences exist between *S. frutescens* or metformin or the OB/IR group; 4.79 ± 0.38mM, 4.76 ± 0.28mM and 4.83 ± 0.51mM respectively. It is also obvious, from fig. 4.33, that the lean control's blood glucose, 4.28 ± 0.38mM, does not differ significantly from that of the OB/IR group, 4.83 ± 0.51mM. One may conclude from the above results that OB/IR rats do not seem to suffer from diabetes, when comparing their blood glucose values with the healthy lean controls. Type II diabetes is a disease that occurs in stages, the first stage, insulin resistance, is compensated for by an over active pancreas which doubles or triples insulin production and secretion, resulting in normoglycaemia. The second stage, the diabetes stage, occurs when the pancreas is exhausted leading to a subsequent loss in insulin production and secretion and, ultimately, hyperglycaemia. At the time of sacrifice the rats in this experiment were assumed to be in the first stage of diabetes where hyperinsulinaemia compensates for insulin resistance resulting in normoglycaemia. To confirm this theory serum insulin levels were determined.

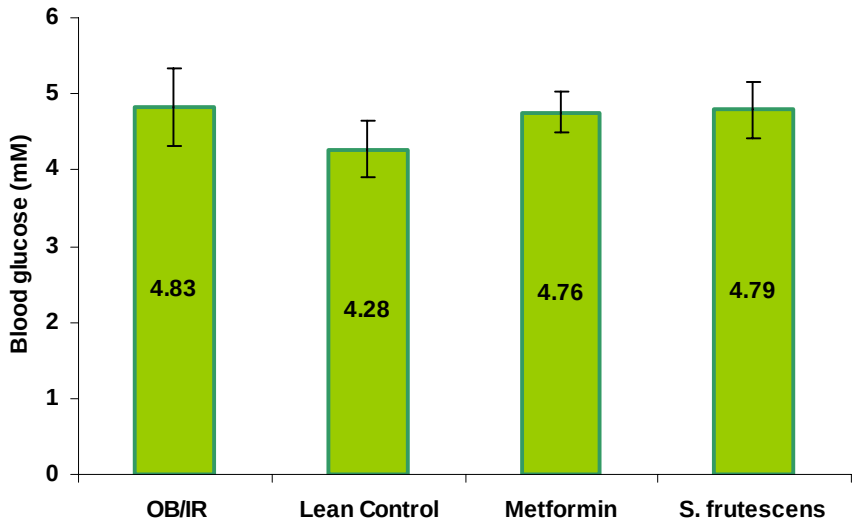

Figure 4.33: Blood glucose levels after 8 weeks medicational treatment, following a 12 hour starvation period. Data are the mean ±SD (n = 11 rats/group).

4.3.5. Serum Insulin Levels (refer to section 3.2.5.2)

The serum insulin levels, in figure 4.34, confirm the suspicion that the OB/IR diet induced insulin resistance. It seems clear that the normoglycaemic levels of the OB/IR group (fig. 4.33) were brought about by hyperinsulinaemia, 222 ± 35.7pmol/l, in comparison to that of the lean control group, 102 ± 14.9pmol/l, (fig. 4.34). It is encouraging to note that the serum insulin levels of the *S. frutescens* group, 95 ± 41.7pmol/l, are within the same range as the lean control group, 102 ± 14.9pmol/l, and is significantly lower than that of the OB/IR group, 222 ± 35.7pmol/l, ($p < 0.01$). The fact that the *S. frutescens* group was able to maintain normoglycaemic (fig. 4.33) and normoinsulinaemic levels (fig. 4.34) while being fed an OB/IR diet, suggests that the treatment has a positive effect in alleviating the burden of insulin resistance.

The observed effect of metformin on serum insulin levels was, however, quite unexpected. The metformin group displayed a significant increase in serum insulin levels, 402 ± 78.5pmol/l, in comparison to the lean control group, 102 ± 14.9pmol/l, ($p < 0.01$) and were even significantly increased when compared with the OB/IR group; 402 ± 78.5pmol/l versus 222 ± 35.7pmol/l respectively ($p < 0.05$) (fig. 4.34). This was unexpected as metformin is not known to stimulate insulin secretion (Davidson and

Peters, 1997). Previous studies have shown metformin treatment to have no effect on serum insulin levels in Wistar rats fed a high fat diet (Davidson and Peters 1997; Minassian *et al*. 1998, Suzuki *et al*. 2002, Mithieux *et al*. 2002).

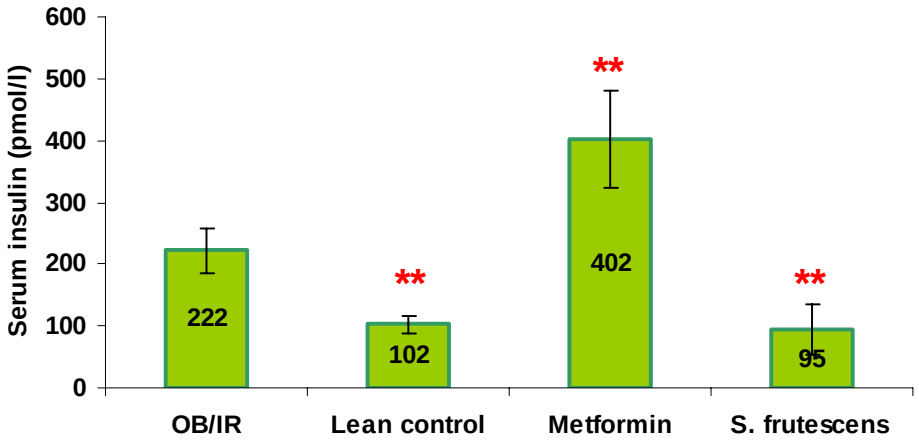

Figure 4.34: Effects of metformin and *S. frutescens* treatment on serum insulin levels. Values are expressed as mean ± SD (n = 11 rats/group). ** $p < 0.01$ compared with the OB/IR group by student *t*-test.

A study undertaken by Jackson *et al*., (1987) on non-insulin dependent diabetic patients also showed that metformin treatment did not significantly reduce serum insulin levels. Minassian *et al*. (1998) and Mithieux *et al*. (2002) maintained their rats on the high fat diet for 21 days and 6 weeks, respectively. On both occasions the metformin treatment (50mg/kg/day) only lasted for 7 days before serum insulin levels were recorded, and in both cases the serum insulin levels were only insignificantly lowered as compared to the high fat diet control group. Suzuki *et al*. (2002) maintained metformin treatment on fatty rats for a period of 15 days at a concentration of 300mg/kg/day and measured serum insulin levels which were identical to that of the fatty control group. It must be kept in mind, however, that the concentration of metformin used in the present study was only 12mg/kg/day (the equivalent of 850mg/day for an average human adult). Clearly further studies are needed before any conclusions can be drawn about the effect of metformin on blood insulin levels.

4.3.6. Glucose Clearance (refer to section 3.2.4)

Figure 4.35 gives an indication of the rate of a 0.4g/kg intravenous glucose load clearance over a 30 minute period. The lean control displayed a significantly accelerated rate of glucose clearance (reduced area under curve), 392 ± 33.17, in comparison to the OB/IR group, 492 ± 36.82, ($p < 0.001$). The insulin resistance, brought about by the OB/IR diet reduced the rate of blood glucose clearance. The high serum insulin levels associated with the OB/IR group (see fig. 4.34) was not enough to compensate for their insulin resistance and glucose clearance, which was still delayed.

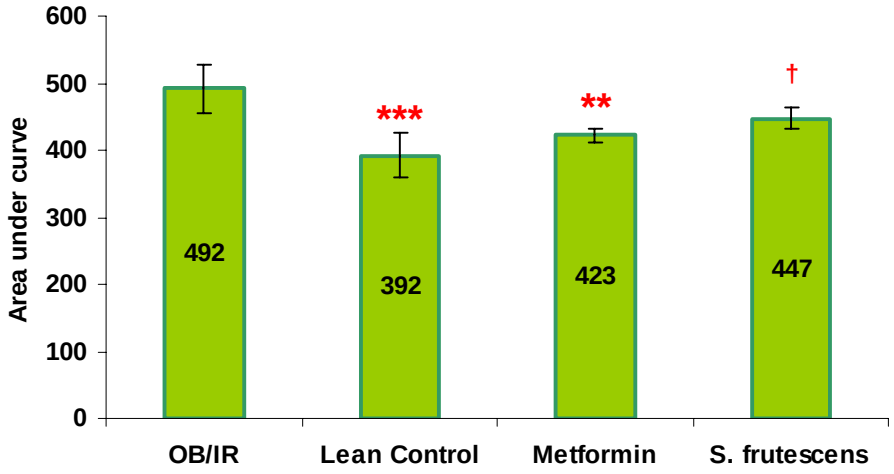

Figure 4.35: Effects of metformin and *S. frutescens* on blood glucose clearance over 60 minutes. Values are expressed as mean ± SD (n = 5 rats/group). † $p < 0.05$, ** $p < 0.005$ and *** $p < 0.001$ compared with the OB/IR group by student *t*-test.

The metformin group displayed a significantly accelerated rate of glucose clearance compared to the OB/IR group, 423 ± 10.2 versus 492 ± 36.8 respectively ($p < 0.005$). Past studies have shown metformin to increase peripheral insulin sensitivity, thereby promoting glucose uptake (Jackson *et al*., 1987; Klip and Leiter, 1990). Metformin's rate of glucose clearance, 423 ± 10.2, is slightly delayed in comparison to the lean control's rate, 392 ± 33.2, this delay is, however, not significant.

The *S. frutescens* group also showed a significantly accelerated rate of glucose clearance of 447 ± 15.74, compared to the 492 ± 36.82 of the OB/IR group ($p < 0.05$). This

significant result suggests that the *S. frutescens* extract is alleviating the burden of insulin resistance by either promoting insulin sensitivity, in peripheral tissue, or, through some active ingredient, which is supporting the role of insulin.

4.3.7. Glucose Uptake (refer to section 3.2.4)

Figure 4.36a and b gives an indication of the effects of the various treatments on the uptake of glucose into the different tissues. Since deoxy-glucose is not metabolised by the tissue, but is taken up at the same rate as glucose (Utriainen *et al*., 2000), the amounts of ^{3}H in the tissue gives an indication of whether any of the treatments affect the glucose uptake into the different tissues. It can be noted that the ^{3}H counts in the muscle tissue of the lean control are significantly higher than those of the OB/IR group, 141 ± 13.7dpm versus 106 ± 4.3dpm respectively ($p < 0.01$). The lower ^{3}H counts associated with the OB/IR group are a result of the insulin resistance associated with the tissue. The hyperinsulinaemia of the OB/IR group (fig. 4.34) is not enough to compensate for the insulin insensitivity when comparing the lean control's ^{3}H counts to that of the OB/IR group.

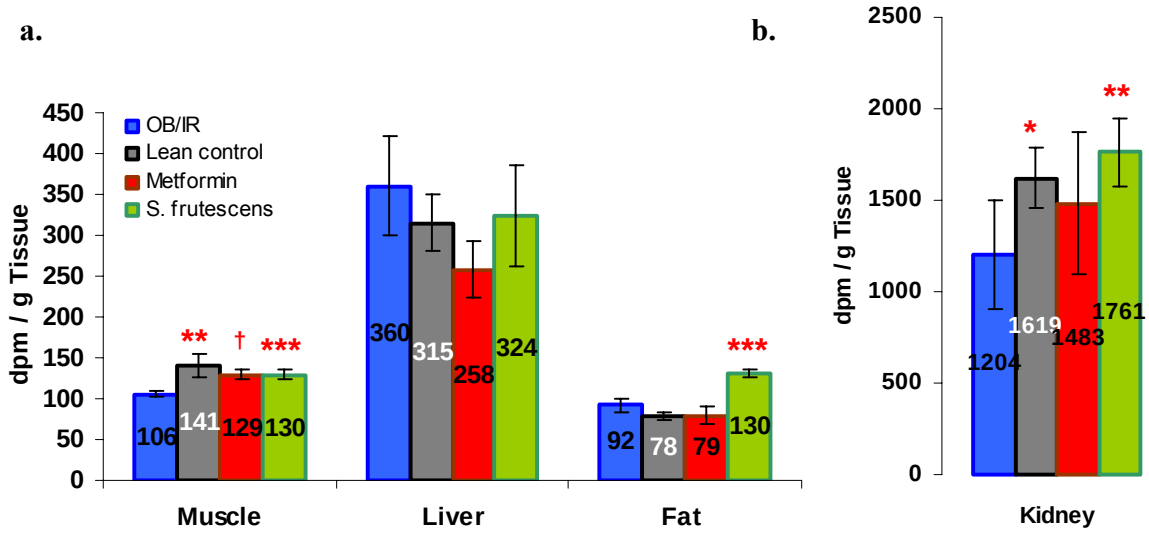

Figure 4.36: ^{3}H counts in muscle, liver and epididymal fat (a) and kidney (b) one hour after an intravenous glucose load supplemented with 2-deoxy-D-[2,6-^{3}H] glucose. Values are expressed as mean ± SD (n = 5 rats/group). * $p < 0.05$, ** $p < 0.01$, † $p < 0.005$ and *** $p < 0.001$ compared with the OB/IR group by student *t*-test.

The metformin and *S. frutescens* groups displayed a significant increase in ^{3}H counts within the muscle tissue in comparison to the OB/IR group, 129 ± 6.7dpm ($p < 0.05$) and 130 ± 6.0dpm ($p < 0.001$) compared to 106 ± 4.3dpm (fig. 4.36a). The significantly higher ^{3}H counts, in these test groups, may be due to increased insulin sensitivity, promoting GLUT4 translocation to the cellular membrane, resulting in accelerated glucose uptake. Although the lean control's ^{3}H counts, 141 ± 13.7dpm, were higher than those of the metformin, 129 ± 6.7dpm, and *S. frutescens* groups, 130 ± 6.0dpm, this difference was insignificant.

In the epididymal fat tissue no significant differences, in ^{3}H counts, were found between the OB/IR, metformin or lean control groups; 92 ± 9.0dpm, 78 ± 10.9dpm and 78 ± 5.4dpm respectively. The *S. frutescens* group did however appear to have a significantly higher ^{3}H concentration compared to the OB/IR group; 130 ± 5dpm versus 92 ± 9.0dpm ($p < 0.05$) (fig. 4.36a). As with the muscle tissue, this may once again be attributed to the plant extract promoting insulin sensitivity, thereby increasing GLUT4 translocation to the cellular membrane.

No significant differences could be seen with ^{3}H counts in the liver tissue due to the high standard deviations accompanying the data (see figure 4.36a). The reason for this may be due to the chemical nature of the [^{3}H] deoxy-glucose. As mentioned previously, the deoxy-glucose is taken up with the same sensitivity as native glucose (Utriainen *et al*., 2000), but due to its chemical make up cannot be phosphorylated and therefore will not enter the glycolysis pathway. The [^{3}H] deoxy-glucose is therefore trapped inside the cell of tissues which do not contain GLUT2 transporters, such as the muscle and fat cells. GLUT2 transporters are able to transport glucose in and out of the cell. The liver, which contains these glucose transporters, constantly moved the [^{3}H] deoxy-glucose in and out of the cell, resulting in differences in ^{3}H counts within specific groups, thereby not allowing for accurate quantification. Therefore the ^{3}H counts found within the liver will be ignored.

Figure 4.36b displays the [^{3}H] deoxy-glucose counts for the kidney. The relatively high counts, in comparison to the other tissues, is an indication of the large volumes of blood flowing through this organ. The lower ^{3}H counts associated with the OB/IR group 1204 ± 295dpm compared to the lean control 1619 ± 164dpm, $p < 0.05$, may be due to insulin resistance. The elevated counts in the kidney of the metformin group (fig. 4.36b) may be attributed to the ability of this agent to decrease blood pressure as well as the enzyme activity which converts dopamine to norepinephrine in the kidney (Davidson & Peters, 1997; Gibbon, 2000; Tortora & Grabowski, 2003). Both these aspects reduce the flow of blood through the kidney as the pressure for glomerular filtration is severely reduced. This will allow the blood to remain in the kidney for a longer period of time, thereby allowing an extended time for glucose uptake in this organ. This may also be the case for the *S. frutescens* treated group although further studies need to confirm this.

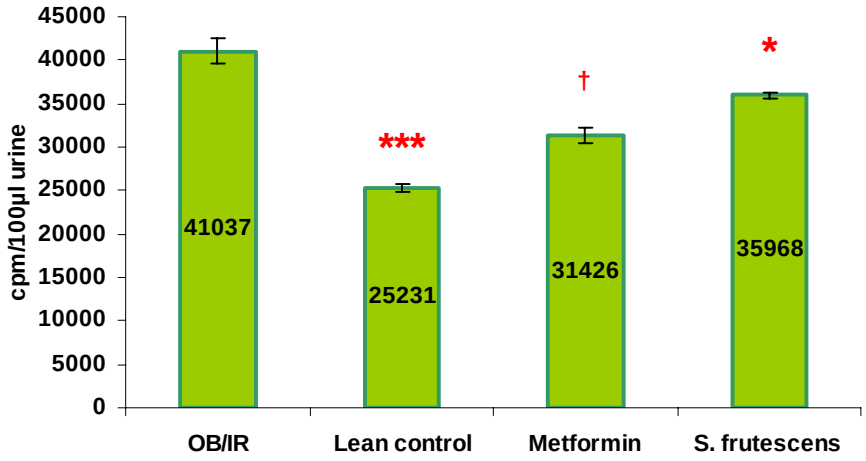

Figure 4.37: Urine ^{3}H counts one hour after intravenous glucose infusion supplemented with 2-deoxy-D-[2,6-^{3}H] glucose**.** Values are expressed as mean ± SD (n = 5 rats/group). * $p < 0.05$, † $p < 0.005$ and *** $p < 0.001$ compared with the OB/IR group by student *t*-test.

^{3}H counts were taken in the urine one hour after intravenous glucose infusion supplemented with 2-deoxy-D-[2,6-^{3}H] glucose. The urine removed from the bladders of the OB/IR diet group displayed significantly higher counts, 41037 ± 1391cpm, in comparison to the lean control, 25231 ± 487.6cpm, ($p < 0.001$)(fig. 4.37). Determination of 2-deoxy-D-[2,6-^{3}H] glucose in the urine is a very sensitive method and even small traces of it can be determined very easily. Glucose should only be detectable in the urine when the blood glucose levels are higher than the Tm value. In this case the blood

glucose values were not significantly different between the various groups (see fig. 4.33), though figure 4.37 displays a clear distinction between the groups, the explanation can only be speculative at this stage and needs further investigation. Both the metformin and *S. frutescens* groups were shown to have significantly lower [^{3}H] deoxy-glucose counts in the urine in comparison to the OB/IR group; 31426 ± 488cpm and 35968 ± 269cpm versus 41037 ± 1391cpm, respectively.

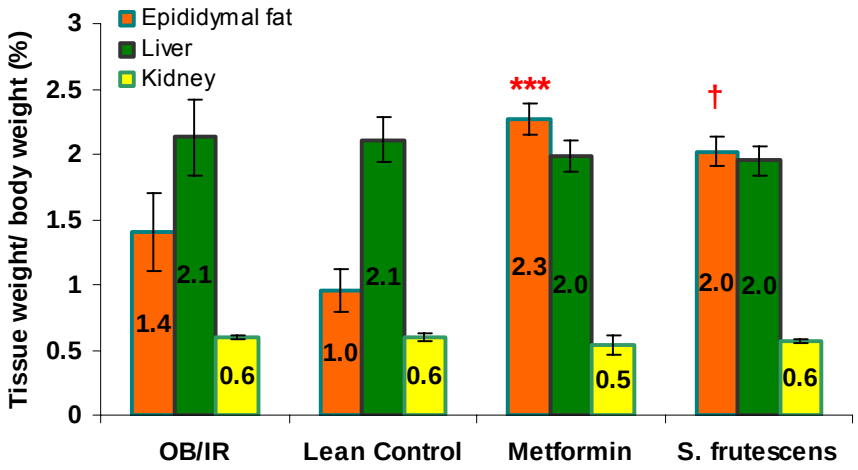

Figure 4.38: Tissue weight relative to the respective body weight. Values are expressed as a mean ± SD (n = 5 rats/group). † $p < 0.005$ and *** $p < 0.001$ compared with the OB/IR group by student *t*-test.

After the 0.4g/kg glucose intravenous infusion experiment, the liver, kidney and epididymal fat removed for [^{3}H] deoxy-glucose counts were first weighed and calculated relative to the rat's body weight (fig. 4.38). No significant difference can be seen between any of the groups with regard to liver or kidney weight, as could be expected.

The epididymal fat pads did, however differ between the various groups. The OB/IR group's fat pads were slightly heavier than those of the lean control groups, 1.4 ± 0.3% versus 1.0 ± 0.17%. This trend was, however not significant due to the high standard deviation accompanying the data. Both metformin and the *S. frutescens* group were found to have a significantly higher percentage of epididymal fat pads in comparison to the OB/IR group; 2.3 ± 0.12% ($p < 0.001$) and 2.0 ± 0.11% ($p < 0.005$) versus 1.4 ± 0.3%. The reason for the increased weight associated with the test groups may be that they are

facilitating the action of peroxisome proliferator-activated receptor-γ ligands (PPARγ). If the medications did act as ligands, for the PPARγ, this would promote adipocyte differentiation which would explain the increased fat pad weights.

4.3.8. Tissue Glycogen Content (refer to section 3.2.6)

Hepatic glycogen levels were significantly lower in the OB/IR diet rats, 1.0 ± 0.014mg/g, in comparison to the lean controls, 1.3 ± 0.028mg/g ($p < 0.001$). Liver glycogen content has been reported to be lower in individuals suffering from type II diabetes when compared to healthy individuals (Magnusson *et al*., 1992). The liver glycogen for the metformin group was found to be significantly higher in comparison to the OB/IR control, 1.1 ± 0.020mg/g and 1.0 ± 0.014mg/g respectively ($p < 0.001$) (fig. 4.39). Past studies have shown metformin to favor the non-oxidative metabolism of glucose, such as glycogen synthesis, in both diabetic patients and non-diabetic insulin resistant subjects (Ricco *et al*., 1991; Johnson *et al*., 1993 and DeFronzo *et al*., 2003). Studies undertaken by Mithieux *et al*. (2002) showed that fatty rats treated with metformin for a week, at a dose of 50mg/kg/day, displayed significantly elevated hepatic glycogen levels in comparison to fatty controls ($p < 0.01$).

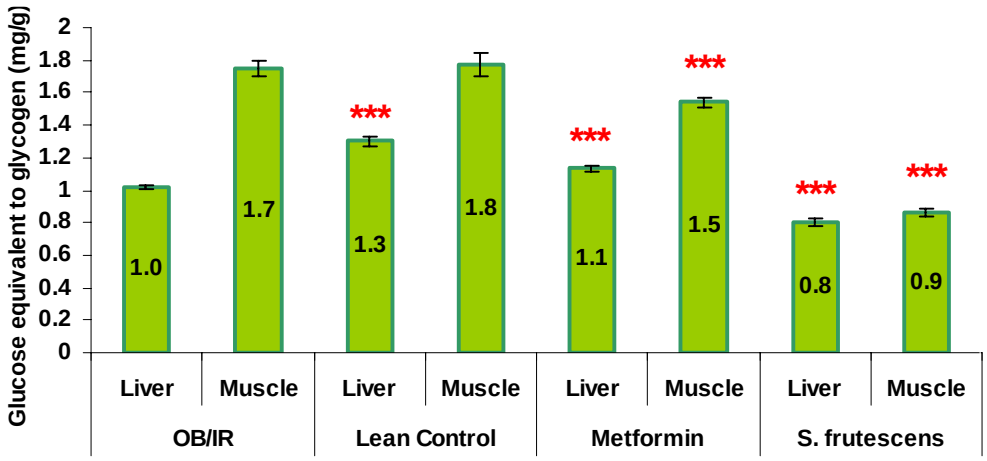

Figure 4.39: Effects of metformin and *S. frutescens* on tissue glycogen levels. Values are expressed as mean ± SD (n = 6 rats/group). *** $p < 0.001$ compared with the OB/IR group by student t-test.

The metformin treated group also showed no change in glycogen synthase a or glycogen phosphorylase b activity suggesting the likely reason for elevated glycogen levels, in this

group, may be due to either an increased availability of glucose-6-phosphate or a putative activation of glycogen synthase a by glucose-6-phosphate. The *S. frutescens* hepatic glycogen levels (fig. 4.39) were drastically and significantly decreased in comparison to the OB/IR diet group, 0.8 ± 0.021mg/g and 1.0 ± 0.014mg/g respectively ($p < 0.001$), and also in comparison to the lean control, 1.3 ± 0.029mg/g ($p < 0.001$). The glycogen levels were consistently higher in the skeletal muscle than the liver of all four groups. A possible reason for the higher skeletal muscle glycogen levels in comparison to hepatic glycogen levels is the overnight fast prior to sacrifice.

No significant difference was evident between the lean control and the OB/IR muscle glycogen levels, 1.8 ± 0.074mg/g and 1.7 ± 0.043mg/g (fig. 4.39). A significant decrease in muscle glycogen content was observed for the metformin group, 1.5 ± 0.026mg/g, in comparison to the OB/IR diet group, 1.7 ± 0.043mg/g ($p < 0.001$). A similar, but insignificant, trend was found for the muscle glycogen content of fatty rats treated with metformin, in a study undertaken by Suzuki *et al*., (2002). The dose of metformin used was 300mg/kg/day for a period of 15 days. A longer exposure or higher concentration of metformin, such as the one used during the present study (500mg/kg/day), may have rendered the trend in the present experiment significantly lower. The *S. frutescens* muscle glycogen content was also found to be significantly lower than that of the OB/IR and lean control groups; 0.9 ± 0.021mg/g, 1.7 ± 0.043mg/g and 1.8 ± 0.074mg/g ($p < 0.001$) respectively. The observation that the *S. frutescens* group showed significantly lower glycogen content in both muscle and liver tissue in comparison to both control groups does not favour *S. frutescens* as an ideal anti-diabetic medication. The glucose may have been utilized for the production of lipids for the purpose of adipocyte differentiation. Okuno *et al*., (1998) reported that thiazolidinediones (PPARγ antagonists) cause an increase in the number of small adipocytes from larger ones. This process may be the mechanism through which thiazolidinediones reduce insulin resistance, because large adipocytes produce insulin resistance-related substances such as tumor necrosis factor-α (TNF-α) and non esterfied fatty acids, whereas small ones do not.

4.3.9. Glucose-6-Phosphatase Activity (refer to section 3.2.9)

Figure 4.40 compares glucose-6-phosphatase activity between the various test groups and the control group. The activity of the enzyme for the OB/IR group is significantly higher than that for the lean control group, 15.83 ± 0.43µmol/min/g versus 12.25 ± 0.84µmol/min/g ($p < 0.001$). The increased activity implies accelerated glycogen degradation (glycogenolysis), and/or gluconeogenesis; a common trait associated with insulin resistance. Under normal physiological conditions glucose-6-phosphatase activity is inhibited by insulin and activated by glycogen. During the fasting state, as is the case here, glucose-6-phosphatase is elevated, as can be seen from figure 4.40.

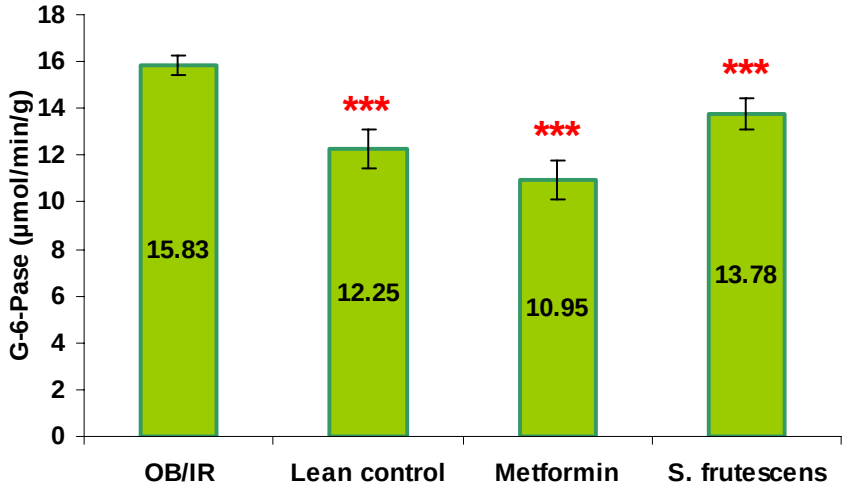

Figure 4.40: Effects of metformin and *S. frutescens* on liver glucose-6-phosphatase activity. Values are expressed as mean ± SD (n = 6 rats/group). *** $p < 0.001$ compared with the OB/IR group by student *t*-test.

The glucose-6-phosphatase activity for the metformin (10.95 ± 0.81µmol/min/g, $p < 0.001$) and *S. frutescens* groups (13.78 ± 0.64µmol/min/g, $p < 0.001$) were also significantly lower relative to that of the OB/IR group (15.83 ± 0.43µmol/min/g), metfromin has been shown to inhibit gluconeogenesis (Klip and Leiter, 1990). The decreased enzyme activity for the two test groups may be a result of the specific treatments increasing insulin sensitivity. Even a slight decrease in glucose-6-phosphatase activity would favour hypoglycaemia. Metformin is able to significantly suppress

glucose-6-phosphatase activity relative to that of the lean control group, 10.95 ± 0.81µmol/min/g versus 12.25 ± 0.84µmol/min/g, $p < 0.05$.

4.3.10. Intestinal Glucose Uptake (refer to section 3.2.7)

Figure 4.41 and 4.42 depict results from two different methods used to quantify the rate of intestinal glucose uptake. The first method, figure 4.41, used glucose oxidase to measure the movement of glucose across the intestinal epithelial layer. The second method used [^{3}H] deoxy-glucose integrated in the glucose mixture, as a radiolabelled marker, to measure glucose movement across the intestine. Keeping in mind that deoxy-glucose is taken up at the same rate and with the same sensitivity as native glucose (Utriainen *et al*., 2000); this method was used as a precautionary measure in case glucose oxidase was not sensitive enough to pick up variations between the different groups. Both figure 4.41 and 4.42 give the same trends for the various groups, indicating that both methods are suitable for intestinal glucose uptake quantification. The [^{3}H] deoxy-glucose does however display more significant data at the sampled time points. Each data point also seems to have lower standard deviations compared to the glucose oxidase method. The [^{3}H] deoxy-glucose method may therefore be a more sensitive method, as it seems to be able to pick up smaller variations between the different groups.

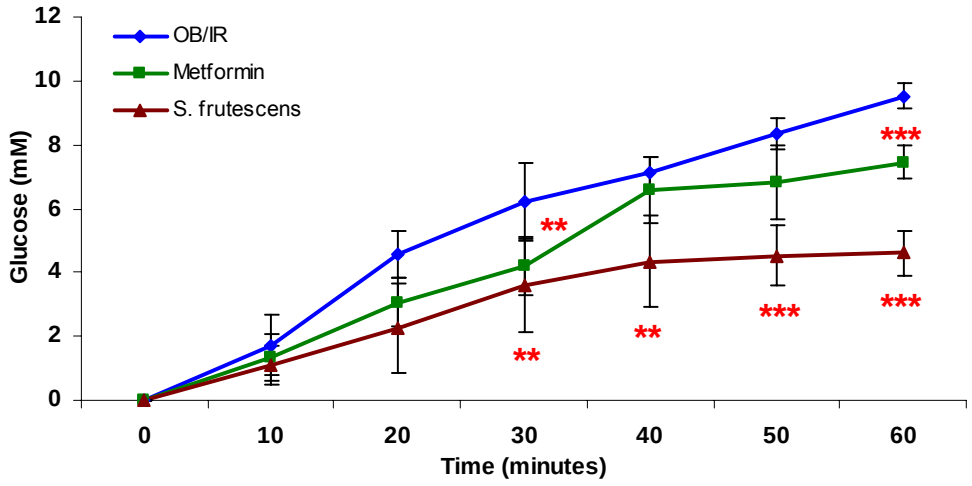

Figure 4.41: Effects of metformin and *S. frutescens* on intestinal glucose uptake, using inverted jejenums with native glucose, measured using the glucose oxidase method. Values are expressed as mean ± SD (n = 6 rats/group). ** $p < 0.01$ and *** $p < 0.001$ compared with the OB/IR group by student *t*-test.

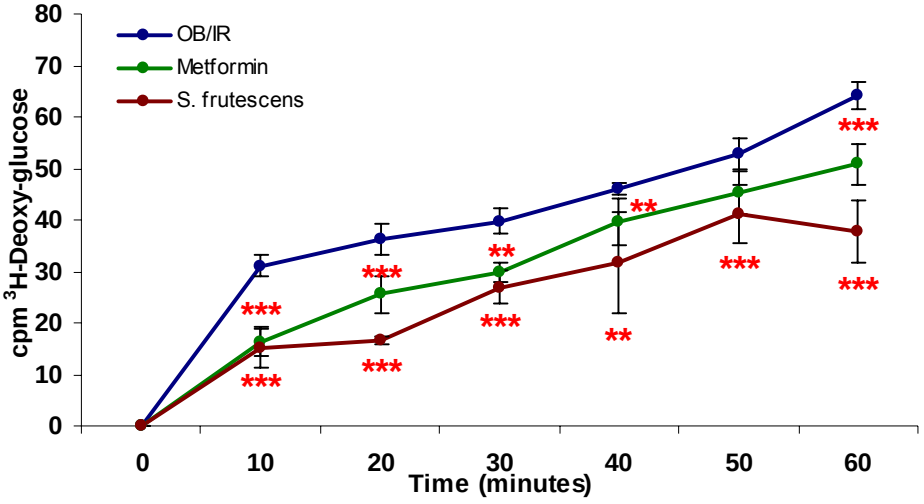

Figure 4.42: Effects of metformin and *S. frutescens* on intestinal glucose uptake, using inverted jejunums with native glucose and [^{3}H] deoxy-glucose as a radiolabelled marker. Values are expressed as mean ± SD (n = 6 rats/group). ** $p < 0.01$ and *** $p < 0.001$ compared with the OB/IR group by student *t*-test.

It is clear from figure 4.41 and 4.42 that both test groups, metformin and *S. frutescens*, significantly inhibit intestinal glucose uptake when compared to the OB/IR group. The glucose oxidase method only picked up two significant differences for metformin, at times 30 (4.21 ± 0.91mM; $p < 0.01$) and 60 minutes (7.45 ± 0.51mM; $p < 0.001$), for the metformin groups with reference to the OB/IR group (6.21 ± 1.24mM, 30 minutes and 9.5 ± 0.39mM, 60 minutes) (fig. 4.41). The [^{3}H] deoxy-glucose method found significant differences for the metformin group, compared against the OB/IR group, at 10 minutes (16.4 ± 2.69cpm versus 31.1 ± 2.1cpm; $p < 0.001$), 20 minutes (25.6 ± 3.64cpm versus 36.13 ± 3.0cpm; $p < 0.001$), 30 minutes (29.7 ± 1.80cpm versus 39.7 ± 2.50cpm; $p < 0.01$), 40 minutes (39.7 ± 4.6cpm versus 46.1 ± 1.10cpm; $p < 0.01$) and 60 minutes (50.8 ± 4.0cpm versus 64.1 ± 2.70cpm; $p < 0.001$) (refer to fig. 42). Metformin has long since been known for inhibiting the gastrointestinal absorption of glucose (Jackson *et al.*, 1987; Klip and Leiter, 1990), so this result was not unexpected.

The *S. frutescens* group displayed an even greater inhibition of gastrointestinal glucose uptake than the metformin group, when compared to the OB/IR group (fig. 4.41 and 4.42). Once again the [^{3}H] deoxy-glucose method (fig. 4.42) proved to be more sensitive

in comparison to the glucose oxidase method (fig. 4.41). The glucose oxidase, for the *S. frutescens* group, displayed significance, when compared to the OB/IR group, at 30 minutes (3.57 ± 1.46mM versus 6.21 ± 1.24mM; $p < 0.01$), 40 minutes (4.35 ± 1.42mM versus 7.10 ± 0.53mM; $p < 0.01$), 50 minutes (4.52 ± 1.42mM versus 8.33 ± 0.48mM; $p < 0.001$) and 60 minutes (4.61 ± 0.70mM and 9.53 ± 0.39mM; $p < 0.001$) (refer to fig. 4.41). The [^{3}H] deoxy-glucose method, however, once again showed more or greater significant values between the *S. frutescens* and OB/IR group at all the analysed sample data points; 10 minutes (15.18 ± 3.80cpm versus 31.13 ± 2.1cpm; $p < 0.001$), 20 minutes (16.62 ± 0.82cpm versus 36.13 ± 3.0cpm; $p < 0.001$), 30 minutes (26.98 ± 3.12cpm versus 39.73 ± 2.5cpm; $p < 0.001$), 40 minutes (31.62 ± 9.87cpm versus 46.13 ± 1.1cpm; $p < 0.01$), 50 minutes (41.16 ± 5.63cpm versus 52.87 ± 3.0cpm; $p < 0.001$) and 60 minutes (37.63 ± 6.01cpm versus 64.07 ± 2.7cpm; $p < 0.001$) (refer to fig. 4.42).

The inhibition of gastrointestinal glucose uptake is an effective measure in ensuring that a type II diabetic individual takes up less glucose in an already insulin resistant environment.

4.3.11. Muscle Protein Isolation (refer to section 3.2.8.1)

A typical gel obtained following the separation of muscle samples on a 7.5% polyacrylamide gel can be seen in appendix 1, figure A3. These gels were used for the Western blots which follow.

4.3.12. Western Blots (refer to section 3.2.8.2)

Figure 4.43 is a graphical interpretation of the blots displayed in figures A4a and b. The data is represented as percentages which are calculated by obtaining the integrated density value of each band, subtracting the background and dividing by the area of the relevant band. The results obtained, from figure 4.43, show a clear and significant decrease in the concentration of the β-subunit of the insulin receptor for the OB/IR group, 3.75 ± 1.63% IOD, in comparison to the lean control group, 14.53 ± 5.64% IOD ($p < 0.001$). Both the metformin and the *S. frutescens* groups showed no increase in β-subunit

concentration relative to that of the OB/IR group, 3.83 ± 2.11% IOD and 3.73 ± 2.23% IOD respectively. These values are significantly lower in comparison to that of the lean control ($p < 0.001$).

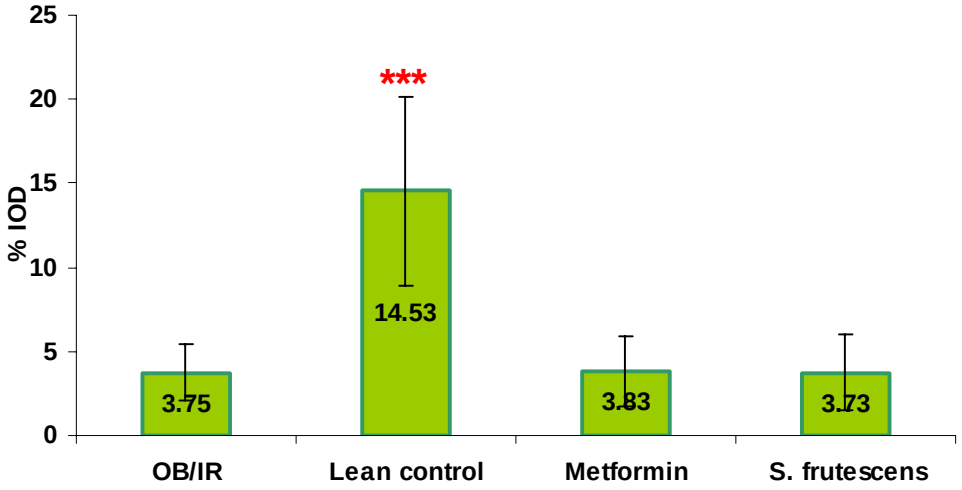

Figure 4.43: Muscle insulin receptor-β subunit band density expressed as a percentage of integrated optical density (IOD). Values are expressed as mean ± SD (n = 5 rats/test group or 4 rats/control group). *** $p < 0.001$ compared with the OB/IR group by student *t*-test.

Figure 4.44 shows that the unmedicated, OB/IR group, displayed a significantly lower concentration of muscular IRS-1, 9.73 ± 2.11% IOD, in comparison to the lean control group, 13.47 ± 0.4% IOD ($p < 0.05$). The metformin group also revealed a higher concentration of muscular IRS-1 relative to the OB/IR group, this result was however not significant, 12.77 ± 1.43% IOD ($p < 0.07$). Not enough protein extract for a rat from the metformin treated group could be obtained for this particular experiment and could therefore not be included for IRS-1 quantification; this could be the reason for the insignificant result obtained for this group.

The *S. frutescens* treated group did, however, display a significantly higher concentration of IRS-1, 16.28 ± 5.61% IOD ($p < 0.05$), in comparison to the OB/IR group. The result was even higher than that found for the lean control group, but due to the *S. frutescens* high standard deviation this result was not significant.

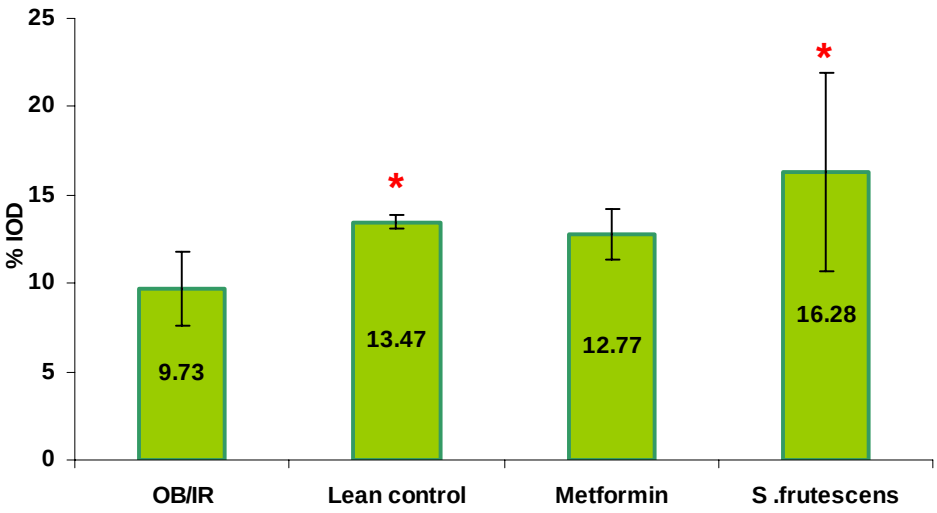

Figure 4.44: Muscle IRS-1 band density expressed as a percentage of integrated optical density (IOD). Values are expressed as mean ± SD (n = 5 rats/*S. frutescens* group, 4 rats/metformin group or 4 rats/control and metformin group). * $p < 0.05$ compared with the OB/IR group by student *t*-test.

The results obtained in figure 4.45 show that although the muscular IRS-2 concentration is higher for the lean control, 11.53 ± 3.0% IOD, in comparison to the OB/IR group, 8.07 ± 1.25% IOD, this result is not significant. This is clearly a result of the high standard deviation obtained from the lean control group.

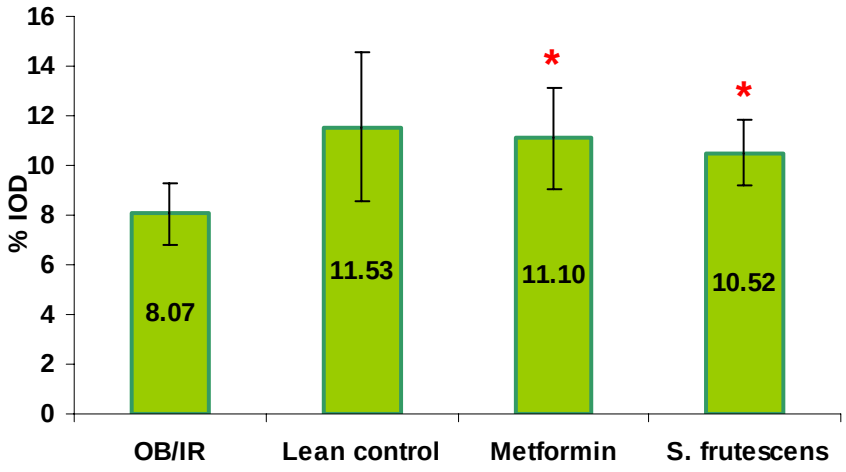

Figure 4.45: Muscle IRS-2 band density expressed as a percentage of integrated optical density (IOD). Values are expressed as mean ± SD (n = 5 rats/test group or 4 rats/control group). * $p < 0.05$ compared with the OB/IR group by student *t*-test.

Both the metformin and the *S. frutescens* groups do however display significantly higher concentrations of muscular IRS-2 relative to the OB/IR group, 11.1 ± 2.04% IOD; $p < 0.05$; and 10.52 ± 1.35% IOD; $p < 0.05$; respectively (fig. 4.45). Both these results are very similar to that of the lean control group.

The concentration of the p85 subunit of the PI-3-kinase is significantly reduced in the OB/IR group, 8.50 ± 0.26% IOD, in comparison to the lean control group, 10.43 ± 0.81% IOD ($p < 0.05$), for figure 4.46. Both the metformin and *S. frutescens* groups also displayed significant increases ($p < 0.05$) in the p85 subunit in comparison to the OB/IR group, 13.73 ± 2.5% IOD and 10.26 ± 0.85 % IOD, respectively.

The p85 subunit concentration for the metformin and *S. frutescens* groups are higher than that of the lean control group, but not significantly so. These differences indicate the significant effect both medications may have on post receptor insulin signaling.

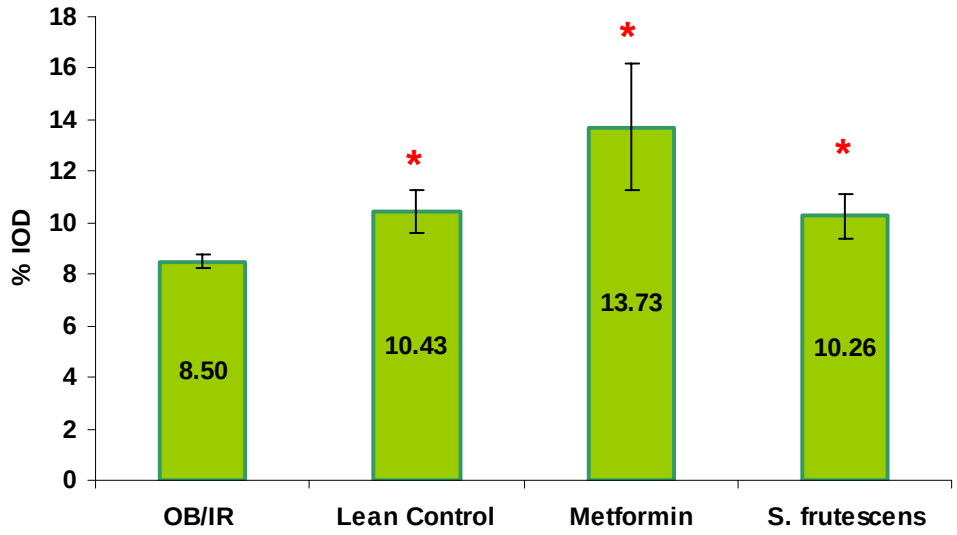

Figure 4.46: Muscle PI-3-kinase, p85 subunit band density expressed as a percentage of integrated optical density (IOD). Values are expressed as mean ± SD (n = 5 rats/test group or 4 rats/control group). * $p < 0.05$ compared with the OB/IR group by student *t*-test.

As can be seen in figure 4.47 no significant differences were evident for the phosphorylated p38 residue. The p38 residue is situated on the MAPK protein and is activated through tyrosine phosphorylation.

The results show that there is an insignificant increase in p38 phosphorylation resulting from the OB/IR diet, 7.30 ± 3.22% IOD, in comparison to the lean control, 5.25 ± 1.91% IOD. A reduction in phosphorylation was also found to be associated with both groups receiving medication; 3.80 ± 1.17% IOD for metformin, and 5.02 ± 2.06% IOD for the *S. frutescens* treated group.

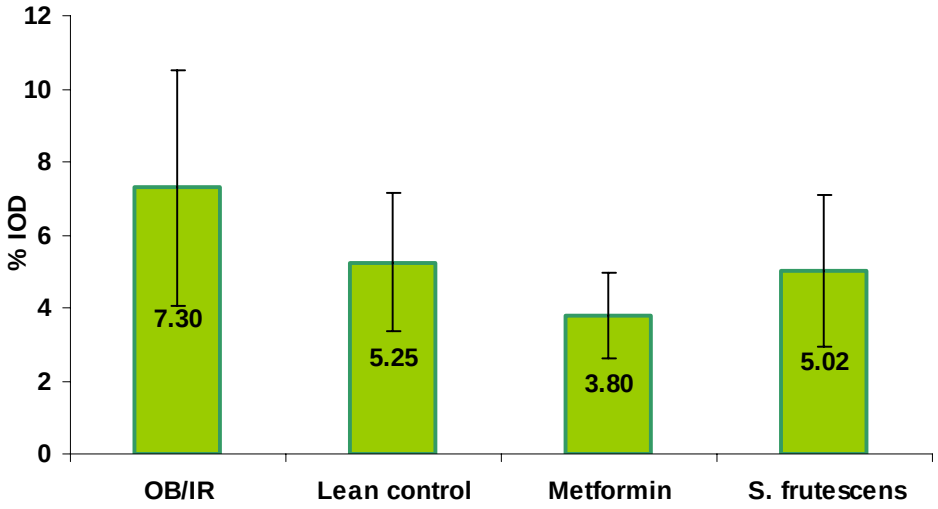

Figure 4.47: Muscle phosphorylated p38 residue band density expressed as a percentage of integrated optical density (IOD). Values are expressed as mean ± SD (n = 5 rats/test group or 4 rats/control group).

Figure 4.48 shows the relative band percentages for inositol 1,4,5-triphosphate receptor. The OB/IR group has a lower concentration of cellular inositol 1,4,5-triphosphate receptor compared to the lean control group, 3.98 ± 0.87% and 5.23 ± 0.85% respectively, however this difference was not significant. Both the metformin and the *S. frutescens* groups have a significantly higher concentration of the receptor in comparison to that of the OB/IR group; 6.38 ± 1.12% ($p < 0.001$) and 5.88 ± 1.21% ($p < 0.05$). The metformin and the *S. frutescens* groups appear to have higher concentrations of the receptor in comparison to the lean control group. These differences are however not significant.

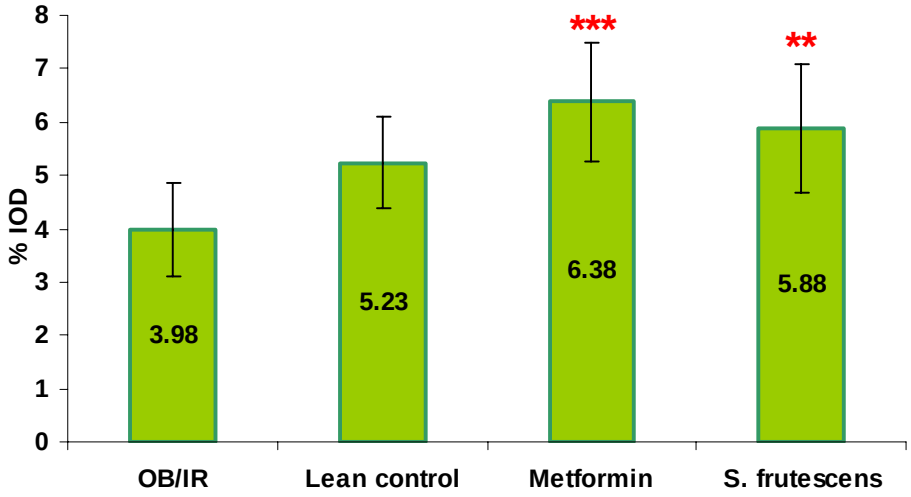

Figure 4.48: Muscle inositol 1,4,5 triphosphate receptor band density expressed as a percentage of integrated optical density (IOD). Values are expressed as mean ± SD (n = 5 rats/test group or 4 rats/control group). ** $p < 0.05$ and *** $p < 0.001$ compared with the OB/IR group by student *t*-test.

Figure 4.49 displays the integrated density values for protein kinase B. Protein kinase B is a family of threonine/serine kinases considered to play an important role in the control of cell cycle, cell proliferation and differentiation and apoptosis (Coffer and Woodgett, 1991; Jones *et al*., 1991; Bellacosa *et al*. 1991). As can be seen from figure 4.49 the lean control group displays a significant increase in this kinase, 5.97 ± 0.57% ($p < 0.05$), in comparison to the OB/IR group, 4.25 ± 0.4%. The metformin and *S. frutescens* groups were also found to have significantly higher concentrations of protein kinase B, 5.40 ± 0.86% and 5.43 ± 0.94% ($p < 0.05$), respectively, relative to the OB/IR group.

It is clear from figure 4.50 that the total cellular GLUT4 concentration for the OB/IR group is significantly lower than that for both test groups and that of the lean control, 10.95 ± 1.79% ($p < 0.05$). The decreased GLUT4 concentration found within the OB/IR group, 8.08 ± 1.21%, is one of the factors contributing to the decreased rate of glucose clearance seen in figure 4.35, for this group. More importantly it is directly related to the decreased counts of the [^{3}H] deoxyglucose in tissue, for the OB/IR group, observed in figure 4.36a, 141 ± 13.7dpm versus 106 ± 4.3dpm respectively ($p < 0.01$).

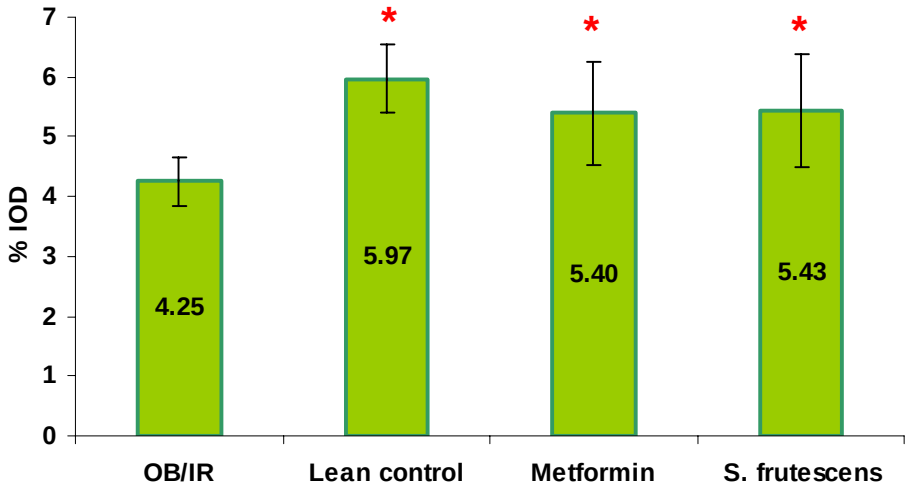

Figure 4.49: Muscle protein kinase B band density expressed as a percentage of integrated optical density (IOD). Values are expressed as mean ± SD (n = 5 rats/test group or 4 rats/control group). * $p < 0.05$ compared with the OB/IR group by student *t*-test.

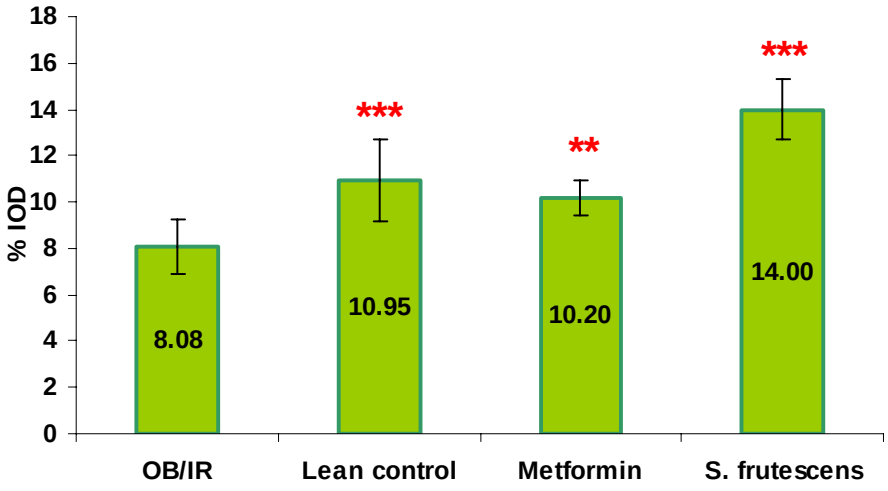

Figure 4.50: Total cellular muscle GLUT4 band density expressed as a percentage of integrated optical density (IOD). Values are expressed as mean ± SD (n = 5 rats/test group or 4 rats/control group). ** $p < 0.05$ and *** $p < 0.001$ compared with the OB/IR group by student *t*-test.

The metformin and the *S. frutescens* groups also contain a significantly higher concentration of total cellular GLUT4, 10.20 ± 0.74% ($p < 0.05$) and 14,00 ± 1.31% ($p < 0.001$), respectively, relative to that of the OB/IR group(fig. 4.50). This increased GLUT4 concentration is undoubtedly the reason for the significantly increased [^{3}H] deoxyglucose counts in the tissue for both these groups in comparison to that of the OB/IR group, in

figure 4.36a (*S. frutescens*: 130 ± 6.0dpm, $p < 0.001$, and metformin: 129 ± 6.7dpm, $p < 0.05$, compared to 106 ± 4.3dpm for the OB/IR group). The elevated GLUT4 concentration brought about by both these test groups may be due to these medications acting at specific molecular sites, the mechanism of which would require further investigation.

4.4. STREPTOZOTOCIN (STZ) MODEL (Type I Diabetes)

A brief investigation was undertaken to determine whether *S. frutescens* could effectively promote hypoglycaemia in rats exposed to streptozotocin toxin, which actively attacks and destroys pancreatic β cells, thereby mimicking a type I diabetic rat model. The main aim of the study was to determine whether *S. frutescens* could be used to control type I diabetes. Blood glucose levels of rats exposed to STZ, were therefore followed over a period of six days to determine whether the extract could effectively bring about normoglycaemia from the hyperglycaemic condition.

4.4.1. Blood Glucose Levels (refer to section 3.3.1.1)

The blood glucose values in figure 4.51 for rats that were not exposed to STZ display the ideal blood glucose values in healthy rats. No difference was evident between the normal control rats and the healthy rats that received the *S. frutescens* extract. It is evident from figure 4.51 that the STZ toxin was effective in destroying the pancreatic β cells, thereby inhibiting the production, storage and secretion of insulin leading ultimately to severe hyperglycaemia. The first set of STZ rats received insulin treatment, the most common and effective treatment for type I diabetes. Before the insulin was administered the blood glucose level was dangerously high, 19.0 ± 5.1mM. The blood glucose had decreased on day 3, after a daily insulin administration, to 13.5 ± 3.9mM and on day 6 the blood glucose had significantly decreased to 11.7 ± 4.0mM ($p < 0.001$), when compared to the blood glucose concentration on day 0.

The STZ rats that were medicated with *S. frutescens* extract were also dangerously hyperglycaemic on day zero, 19.9 ± 5.2mM, prior to being medicated. After the rats received a daily dose of *S. frutescens* the blood glucose reading taken on day 3 was significantly reduced to 12.2 ± 5.2mM ($p < 0.001$) and a further significant reduction was observed on day six, 7.9 ± 4.2mM ($p < 0.001$), when compared to the readings taken on day 0. The extract almost returned the rats' blood glucose levels to that found in the normal control rats. The *S. frutescens* extract seemed to reduce the blood glucose more effectively than the insulin when comparing the blood glucose levels on day six, 7.9 ±

4.2mM compared to 11.7 ± 4.0mM respectively. With further experimentation the *S. frutescens* extract could eventually take the place of native insulin therapy for type I diabetes. The two obvious advantages of this would be a more cost effective and a non intravenous drug, with the same efficacy of native insulin.

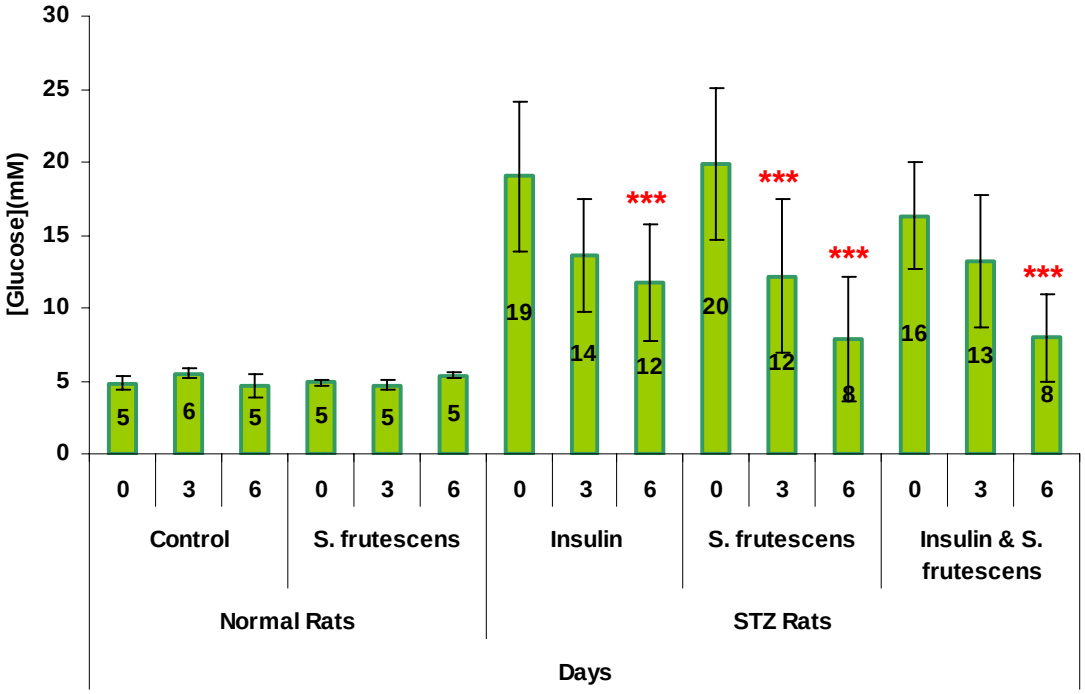

Figure 4.51: Blood glucose values of normal and STZ rats followed over a six day window (n = 14 rats per group). *** $p < 0.001$ relative to day 0 glucose level.

The combinational therapy of *S. frutescens* and native insulin also proved to effectively reduce the blood glucose levels from 16.3 ± 3.7mM, on day 0, to 13.2 ± 4.5mM, on day 3. A further and significant decrease was observed after 6 days medicational compliance, leaving the blood glucose levels at 7.9 ± 3mM ($p < 0.001$). These results are also encouraging as figure 4.51 implies that there is no contra-indication between the combined insulin and *S. frutescens* treatment. However, the addition of insulin did not produce any significant hypoglycaemic effect over and above that of the *S. frutescens* extract alone in the STZ rats.

4.4.2. Serum Insulin Levels (refer to section 3.3.1.2)

To ensure that the STZ toxin was working effectively, the rats' serum insulin levels were measured on day six. The serum insulin levels for rats exposed to the STZ toxin were compared to the serum insulin levels of the lean control rats used in the pre-diabetic study. The reason for this was to reduce the cost of the experiment, as this particular method of insulin determination involves a rather expensive kit. This also allowed for triplicate serum insulin readings to be taken for the STZ rats, thereby increasing the accuracy of the assay.

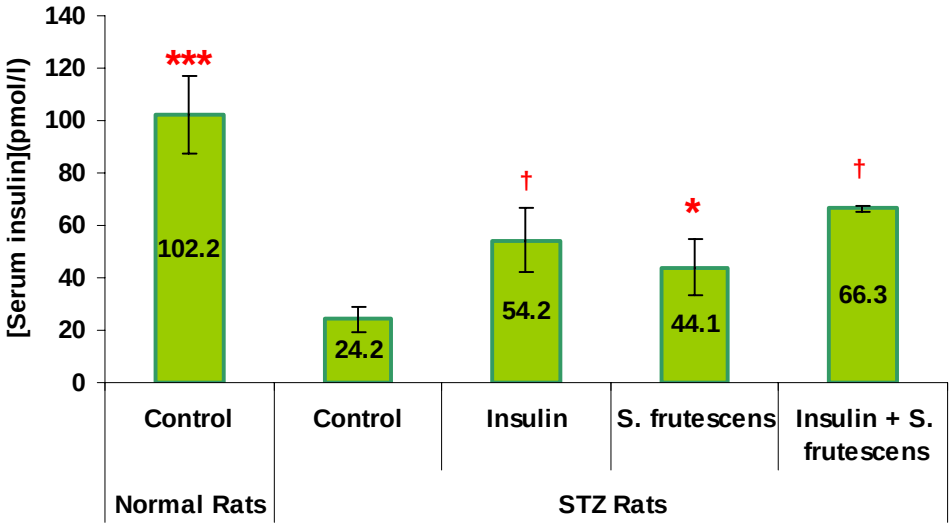

Figure 4.52: Serum insulin levels taken 6 days after STZ exposure and compared to healthy control rat used during pre-diabetic study (n = 14 rats per group). * $p < 0.05$, † $p < 0.005$, *** $p < 0.001$ compared with the STZ control group by student *t*-test.

Figure 4.52 displays the serum insulin levels of the rats which were exposed to STZ toxin and compares them to that of healthy rats. The STZ control group could only be kept alive for 2 days due to the severity of their hyperglycaemia for which they received no medication. As can be seen from figure 4.52 the serum insulin levels for the STZ control group is significantly reduced, 24.2 ± 4.6pmol/L, when compared to that of the healthy controls, 102.2 ± 14.9pmol/l ($p < 0.001$).

The STZ rats that received native insulin treatment, for their hyperglycaemia, showed significantly elevated serum insulin levels, 54.2 ± 12.2pmol/L, in comparison to the STZ

control group, 24.2 ± 4.6pmol/L ($p < 0.005$). Researchers have found that insulin administered to STZ rats stimulated an increase in β cell volume and insulin content (McEvoy, *et al*., 1979; Rabinovitch *et al*., 1982). The STZ rats receiving the *S. frutescens* extract also displayed elevated serum insulin levels, 44.1 ± 10.8pmol/L ($p < 0.05$). The reasons for this effect are not clear and would require further investigation. The combinational therapy of insulin and *S. frutescens* extract also promoted the circulating serum insulin levels, 66.3 ± 0.79pmol/L ($p < 0.005$).

4.4.3. Tissue Glycogen Content (refer to section 3.3.2)

Immediately after sacrifice, muscle and liver tissue were removed and tested for glycogen content as before. Insulin's contribution to tissue glycogen synthesis has already been discussed in great detail, and it is clear from figure 4.53 that a lack of circulating insulin greatly affects tissue glycogen content, as seen for the STZ control groups which received no medication; 0.033 ± 0.0027mg/g for muscle and 0.027 ± 0.0012mg/g for the liver.

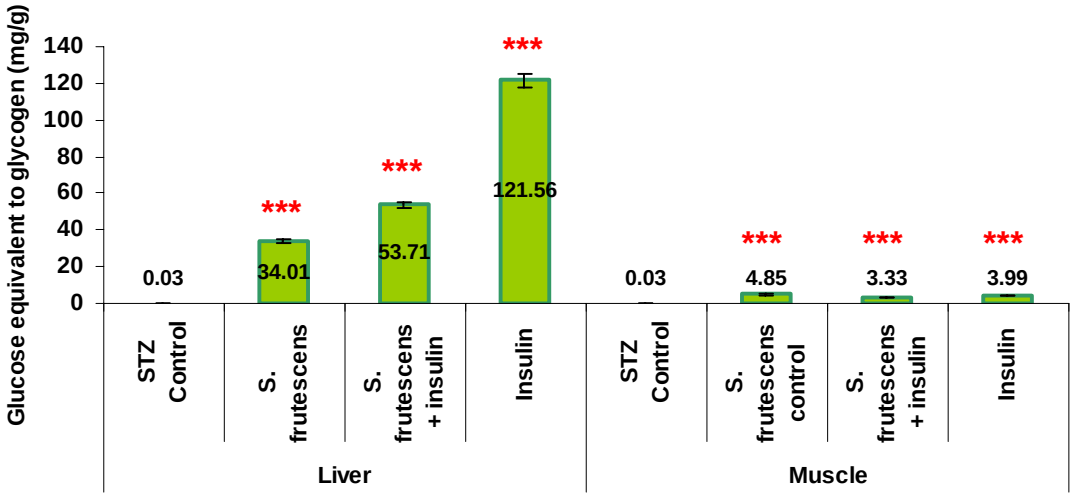

Figure 4.53: Tissue glycogen levels taken 6 days after STZ exposure. Results compared to relevant tissue control group (n = 14 rats per group). *** $p < 0.001$ compared with the STZ control group by student *t*-test

The tissue glycogen content values, for this experiment, are generally higher than any found during the high fat diet experimentation, figure 4.39. Reasons for this lie in the fact

that the rats for this experiment were subjected to a shorter fasting period prior to sacrifice, whereas rats for the high fat diet study had a much longer fasting period, prior to their sacrifice, resulting in severe glycogenolysis. The fact that the liver glycogen content in figure 4.39 was much lower than that for the muscle proves this, as the liver is the first tissue to undergo glycogenolysis and gluconeogenesis under severe hypoglycaemia.

Referring back to figure 4.53, the STZ group that received insulin treatment displayed a significant increase in liver and muscle glycogen content in comparison to the STZ control groups; 121.56 ± 3.71mg/g versus 0.027 ± 0.0012mg/g ($p < 0.001$) and 3.99 ± 0.060 versus 0.033 ± 0.0027mg/g ($p < 0.001$) respectively. As insulin is the positive control for this experiment the significant increase in tissue glycogen content was expected. The STZ group which were medicated with *S. frutescens* extract also showed elevated liver and muscle glycogen content in comparison to the unmedicated control group; 34,01 ± 1.12mg/g versus 0.027 ± 0.0012mg/g ($p < 0.001$) and 4.85 ± 0.19mg/g versus 0.033 ± 0.0027mg/g ($p < 0.001$) respectively. The combination of *S. frutescens* and insulin also significantly increased the liver and muscle glycogen content; 53.71 ± 1.65 mg/g versus 0.027 ± 0.0012mg/g ($p < 0.001$) and 3.33 ± 0.059mg/g versus 0.033 ± 0.0027mg/g ($p < 0.001$) respectively.

4.4.4. Jejunum Sodium/Potassium ATPase Activity (refer to section 3.3.3)

During the high fat diet study the *S. frutescens* extract displayed its capabilities of significantly decreasing the amount of glucose taken up by the jejunum, figure 4.41 and 4.42, a trait which promotes hypoglycaemia within the body. A reason for the reduced intestinal glucose uptake was thought to lay in a decreased intestinal sodium/potassium ATPase activity. As no intestine from the previous experiment was kept, fresh intestine from the STZ experiment was used to test for Na^+K^+ ATPase activity.

We see from figure 4.54 that insulin significantly inhibits the sodium/potassium ATPase activity in the jejunum, 0.88 ± 0.15 Pi ng/min/µg protein ($p < 0.005$), in comparison to

the STZ control group 1.70 ± 0.2 Pi ng/min/µg protein. Chronic diabetes, as is the case with the STZ control group, results in the enhanced absorption of glucose across the small intestinal epithelium as a result of mucosal hypertrophy coupled with an increased number of transporters in both the brush border (Burant *et al*., 1994; Debnam *et al*., 1995) and the basolateral membranes of enterocytes (Cheeseman and Maenz, 1989).

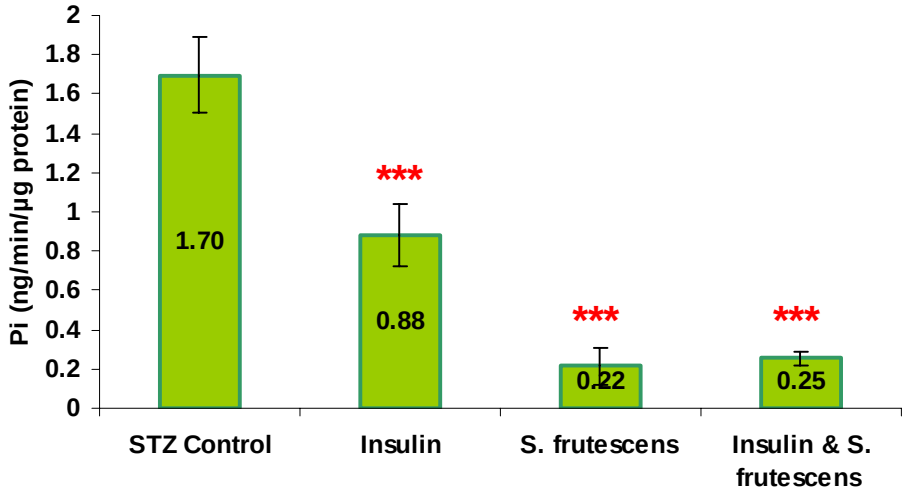

Figure 4.54: Effects of *S. frutescens* and insulin on intestinal Na^+K^+ ATPase activity. Values are expressed as mean ± SD (n = 6 rats/group). *** $p < 0.001$ compared to STZ control group by student *t*-test.

The *S. frutescens* group displayed an even greater decrease in the intestinal Na^+K^+ ATPase pump activity, 0.22 ± 0.096 Pi ng/min/µg protein, which could contribute to the decreased intestinal glucose uptake displayed for this group in figures 4.41 and 4.42. The group which received the combination of *S. frutescens* and insulin treatment also showed a significant reduction in the intestinal Na^+K^+ ATPase pump activity, 0.25 ± 0.033 Pi ng/min/µg protein; $p < 0.001$.

4.5. CELL STUDIES

4.5.1. Binding Studies (refer to section 3.4.2)

Each data point, for both experiments, represents the average obtained from three independent experiments, each done in quadruplicate. Each well was seeded with 37 500 C_2C_{12} cells at the beginning of the experiment. As mentioned in the methodology the cells were allowed to differentiate prior to experimentation. Figure 4.55 demonstrates the displacement of [^{125}I] insulin bound to C_2C_{12} muscle cells by an increasing concentration of native insulin. As would be expected displacement of the [^{125}I] insulin increases as the concentration of native insulin increases.

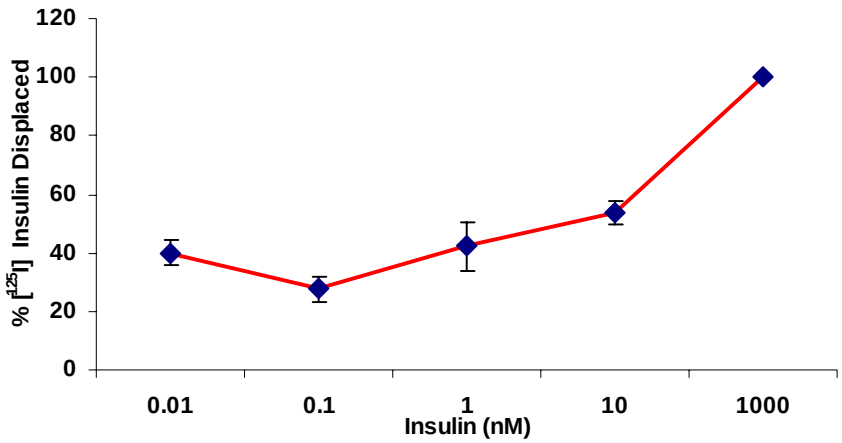

Figure 4.55: Competitive insulin receptor binding for [^{125}I] insulin versus native insulin in C_2C_{12} muscle cells. Each data point represents the average obtained from three independent experiments, each done in quadruplicate.

Figure 4.56 displays the effect that increasing concentrations of *S. frutescens* extract has on the binding of a fixed concentration, 2.4nM, of [^{125}I] insulin. From the graph it is apparent that the *S. frutescens* extract influences receptor binding of the [^{125}I] insulin in a bimodal concentration dependent manner. Minimal displacement of about 11 ± 3.9% is observed at a concentration of 2.5µg/ml of *S. frutescens* extract with increasing levels of displacement at both lower and higher concentrations of the extract (approximately 41 ± 1.6% at the lowest concentration of 0.025µg/ml and 100% displacement at 250µg/ml of extract).

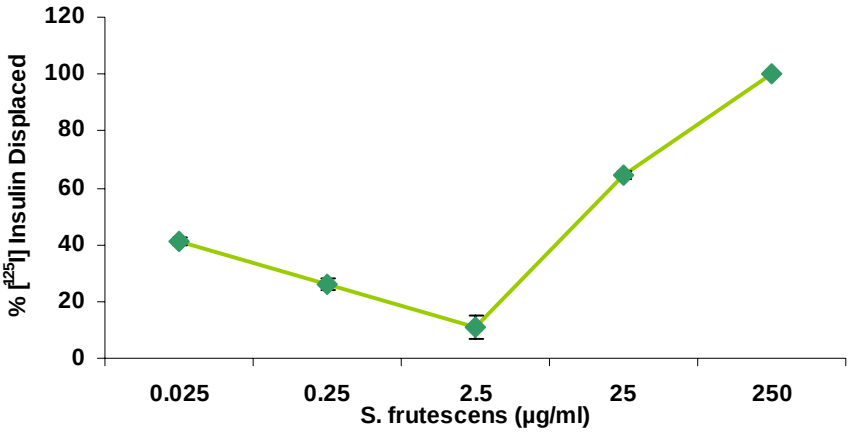

Figure 4.56: Influence of increasing concentrations of an *S. frutescens* extract on the binding of [^{125}I] insulin to C_2C_{12} muscle cells. Each data point represents the average obtained from three independent experiments, each done in quadruplicate.

4.5.2. GLUT4 Translocation (refer to section 3.4.3)

Figure 4.57a & b clearly show that *S. frutescens* causes, independent, translocation of GLUT4 to the plasma membrane, in comparison to the control cells which received no external supplements. The insulin treated cells served as the positive control, and as was expected caused translocation of GLUT4 to the plasma membrane.

Discontinuous sucrose gradient centrifugation was used in an attempt to isolate transverse tubules, intracellular membrane and plasma membrane fractions for GLUT4 quantification. BCA quantification showed that protein fractions were obtained from each of the different sucrose gradients; however, not enough protein could be obtained for Western blot analysis. It was then decided to isolate the entire plasma membrane and transverse tubules fraction through ultracentrifugation for GLUT4 quantification. Due to low protein yields samples had to be pooled allowing for only one lane for each sample to be quantified, this leaves no room for statistical analysis. The experiment is being repeated at present, with a greater amount of starting material, which will allow for statistical analysis. However the data seems to imply that *S. frutescens* is able to independently cause GLUT4 translocation to the plasma membrane.

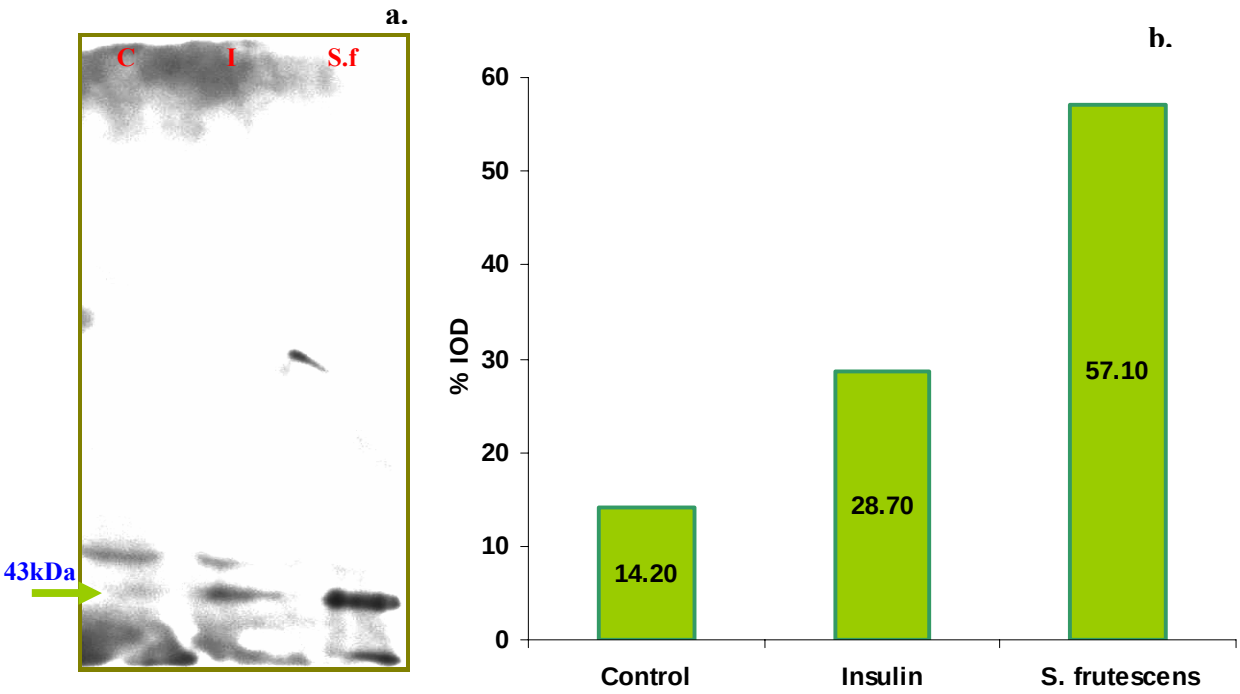

Figure 4.57: Translocation of GLUT4 to the plasma membrane in C2C12 cells. **a.)** ECL hyperfilm after 5 minutes exposure to anti-rabbit IgG, peroxidase secondary antibody (1:2000) bound to rabbit anti-GLUT4 primary antibody (1:2000). Each lane contains 30 µg total protein loaded on 7.5% SDS gel, followed by a 2 hour semi-dry transfer and an overnight block in 5% BSA. As described earlier, cells were incubated in PBSA containing 1% BSA (control-C) or PBSA containing 1% BSA supplemented with 1µM native insulin (I) or PBSA containing 1% BSA supplemented with 250µg/ml *S. frutescens* (S.f). **b.)** Plasma membrane muscle GLUT4 band density expressed as a percentage of integrated optical density (IOD).

4.6. TWO DIMENSIONAL ELECTROPHORESIS

After the second dimension, liver proteins were visualized by sypro-ruby staining. All gel images were analyzed using a Bio Image computer program. The expression of each protein was measured and expressed as its percentage integrated optical density (%IOD). The %IOD is a percentage of the sum of all the pixel level values compared with that of all detected spots. Images from each of the groups was matched, edited and compared statistically. Protein spots, whose expressions were significant, at a level of $p < 0.05$, were selected for further analysis (refer to section 3.6 for methodology).

For simplicity this section will be presented in a series of tables, each table represents the proteins significantly affected within each group for the basic and acidic gels, figures 4.58 and 4.59. The tables include a brief description of the proteins and whether their integrated optical density is increased (up) or decreased (down) relative to a comparative group in each table. AA: 99.5% student t-test with equal variance ($p < 0.005$), BB: 97.5% student t-test with equal variance ($p < 0.025$), CC: 99.5% student t-test with unequal variance ($p < 0.005$) and DD: 97.5% student t-test with unequal variance ($p < 0.025$).

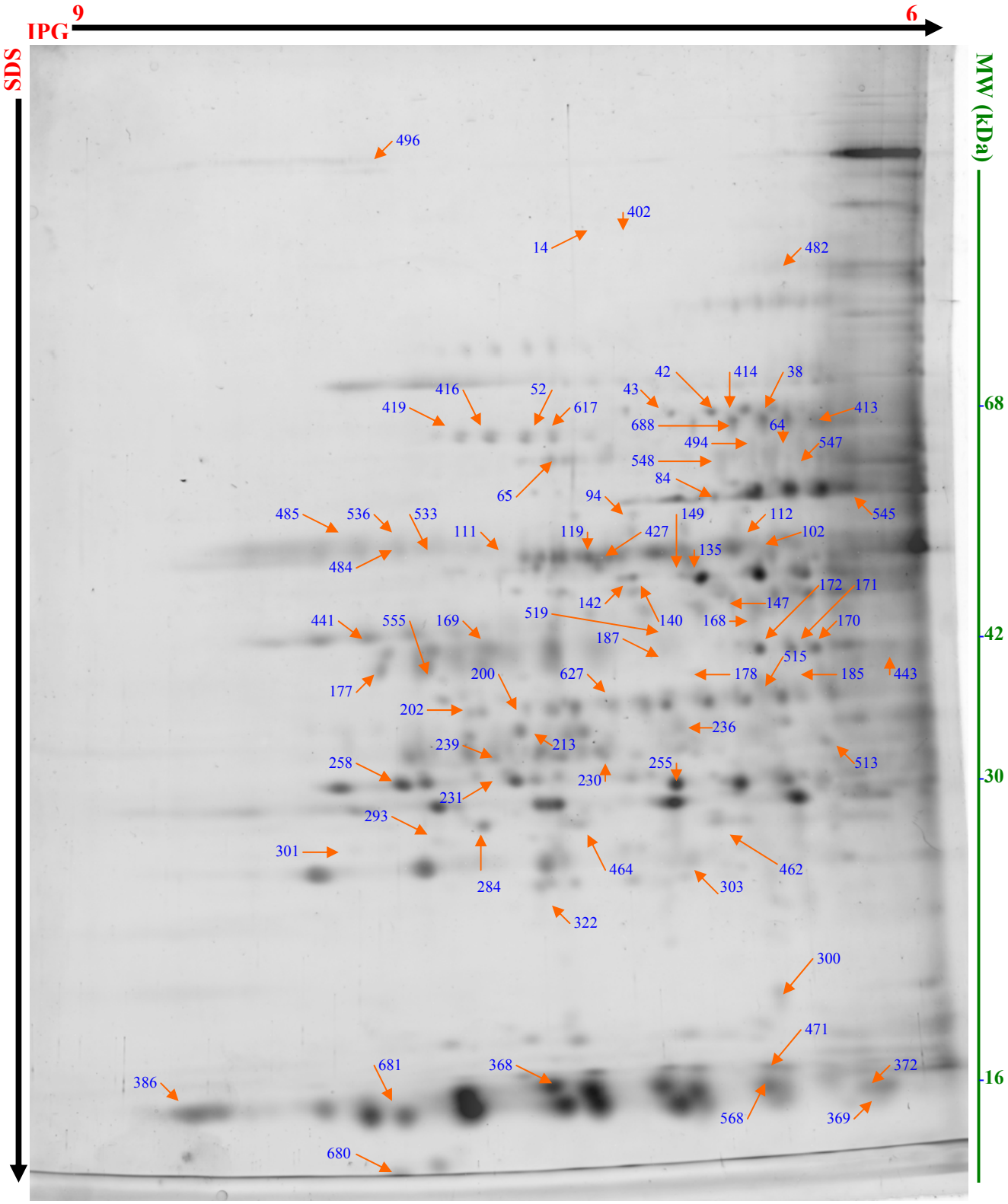

Figure 4.58: Representative 2-D gel image of rat liver protein, separated in the first dimension by IPG gels (covering the pH range from 6 to 9) and by a 12 % polyacrylamide gel in the second dimension, arrows indicate spot # positions on the gel. Spots visualized by sypro-ruby staining

Table 4.6.1: MALDI-TOF MS identification of OB/IR rat liver proteins, from basic gels, for spots which displayed a significant difference relative to the lean control group.

Effects	Swiss protein name & code	Description	Accession # (NCBI)	MW (kDa) (NCBI)	pI (NCBI)	Location
UpBB (Spot # 519)	Aldolase B (364 aa)	Involved in glycolysis, catalyses the conversion of fructose-1,6-bisphosphate into dihydroxyacetone and glyceraldehyde-3-phosphate (Nelson and Cox, 2000). The relative position on the gel implies this enzyme's activity is severely reduced. Aldolase B has been shown to degrade, from the carboxyl terminal, resulting in a positively charged C-terminal arginine which is indicative of its relative position on the gel in this case (Chappel *et al*., 1978).	gi|1619606	40	8.66	Cytolsol
UpAA (Spot # 52)	Citrin (676 aa) Active (Ca^{2+} bound)	Mitochondrial membrane protein which functions as an aspartate/glutamate carrier during amino acid deamination (necessary for gluconeogenesis) and is an important component of the malate aspartate NADH shuttle (Tamamori *et al*., 2002; Ohura *et al*., 2003, Sinasac *et al*., 2004). These carriers contain an N-terminal domain in the intermembrane space that contains four Ca^{2+}-binding hands. Thus, they are activated by an increase in Ca^{2+} binding at these sites (Roesch *et al*., 2004).	gi|62646841	74	8.86	Mitochondria
DownBB (Spot # 416)	Citrin (676 aa) Less active (Less Ca^{2+} bound)	Same as above.	gi|62646841	74	8.86	Mitochondria
DownBB (Spot # 419)	Citrin (676 aa) Less active (Less Ca^{2+} bound)	Same as above.	gi|62646841	74	8.86	Mitochondria
UpBB (Spot # 617)	Citrin (676 aa) Active (Ca^{2+} bound)	Same as above.	gi|62646841	74	8.86	Mitochondria
DownAA (Spot # 496)	Enoyl-Coenzyme A, hydratase/3-hydroxyacyl Coenzyme A dehydrogenase complex (722 aa)	Mitochondrial enzymes involved in β-oxidation of long chain fatty acids. Enzymes isolated and identified as a complex which may imply they are inactive. (Holden and Banaszakg 1983; Nelson and Cox, 2000).	gi|59809132	79	9.28	Mitochondria

DownBB (Spot # 255)	S-Glutathiolated Carbonic Anhydrase III (260 aa)	Occurs under oxidative stress (Mallis *et al*., 2000).	gi|10120584	29	6.74	Cytosol
UpBB (Spot # 568)	Hba-a1 protein	Haemoglobin contamination.	gi|60688619	15	8.45	
UpBB (Spot # 102)	3-hydroxy-3-methylglutaryl-CoA synthase 2 (508 aa)	Catalyses the reversible condensation of acetyl-CoA and acetoacetyl-CoA during the second step of cholesterol synthesis (Nelson and Cox, 2000).	gi|51259246	57	8.86	Mitochondria
UpCC (Spot # 236)	3-hydroxyacyl-CoA dehydrogenase (314 aa) Active (NAD^+ bound)	Mitochondrial enzyme involved in β-oxidation of long chain fatty acids, it catalyzes the NAD dependent oxidation of L-3-Hydroxyacyl-CoA to β-Ketoacyl-CoA (Holden and Banaszakg 1983; Nelson and Cox, 2000).	gi|17105336	34	8.83	Mitochondria
UpBB (Spot # 464)	3-Hydroxyacyl-CoA Dehydrogenase, binary complex (314 aa) Active (NAD^+ bound)	Same as above.	gi|14488727	27	8.91	Mitochondria
DownAA (14)	17-β-hydroxysteroid dehydrogenase, type IV (735 aa) Inactive (No NAD^+ bound)	Multifunctional peroxisomal hormone possessing separable 17-hydroxysteroid/fatty acyl-CoA dehydrogenase, fatty acyl-CoA-hydratase and sterol transfer activities (Leenders *et al.* 1996). Also involved in degradation of branched chain fatty acids (Dieuaide-Noubhani *et al.* 1997*a*) and the side chain of cholesterol (Dieuaide-Noubhani *et al.* 1997*b*). Inactivate sex steroid hormones by catalyzing the production of keto forms (Fan *et al*., 1998). Functions with the cofactor NAD^+.	gi|1881831	79	8.77	Peroxisomes
DownBB (Spot # 202)	11-β-Hydroxysteroid dehydrogenase-1 (288 aa) Inactive (No NADPH or $NADP^+$ bound)	Acts *in vivo* mainly as a NADP-dependent reductase, activating glucocorticoids from circulating 11-oxo precursors (cortisone in humans, and 11-dehydrocorticosterone in rodents) to the respective 11b-OH receptor ligands (cortisol, corticosterone). Also catalyses the reverse reaction (Benediktsson *et al*., 1992; Davani *et al*., 2000).	gi|50927643	32	8.55	Peroxisomes
DownAA (Spot # 200)	Malate dehydrogenase 2	Mitochondrial enzyme that catalyses the oxidation of L-malate to oxaloacetate during the citric acid cycle. The reaction is reversible and requires NAD^+ as a cofactor (Lehininger *et al*., 2000).	gi|42476181	36	8.93	Mitochondria

DownBB (Spot # 494)	Methylmalonate semialdehyde dehydrogenase (535 aa) Less active (No NAD^+ or CoA bound)	Mitochondrial enzyme that catalyzes the irreversible oxidative decarboxylation of malonate and methylmalonate semialdehydes to acetyl- and propionyl-CoA, respectively. This activity is part of the valine and pyrimidine catabolic pathways (Chambliss *et al.*, 2000). Methylmalonate semialdehyde dehydrogenase is the only aldehyde dehydrogenase known to require CoA and NAD^+ for activity (Goodwin *et al*., 1989).	gi|13591997	58	8.47	Mitochondria
DownAA (Spot # 38)	Transketolase (623 aa) Inactive (no thiamine pyrophosphate bound)	Involved in the non-oxidative pentose phosphate pathway, converting pentose phosphates into hexose phosphates, thereby promoting continual NADPH formation for fatty acid synthesis. Thiamine pyrophosphate dependent enzyme, catalyzes the transfer of a 2 carbon fragment of xylulose-5-phosphate to ribose-5-phosphate, forming sedoheptulose-7-phosphate and glyceraldehyde-3-phosphate. It later converts xylose-5-phosphate and erythrose-4-phosphate into glyceraldehydes-3-phosphate and fructose-6-phosphate (Lehiniger *et al*. 2000).	gi|1729977	68	7.23	Cytosol

Up/down refers to either an increase or decrease, respectively, in protein spot density for the relevant test group in relation to a comparative group in each table. AA: 99.5% student t-test with equal variance ($p < 0.005$), BB: 97.5% student t-test with equal variance ($p < 0.025$), CC: 99.5% student t-test with unequal variance ($p < 0.005$) and DD: 97.5% student t-test with unequal variance ($p < 0.025$).
NCBI - data base (ProFound, FindPept and FindMod programs) www.proteomics.com

Table 4.6.2: MALDI-TOF MS identification of metformin rat liver proteins, from basic gels, for spots which displayed a significant difference relative to the OB/IR group

Effects	Swiss protein name & code	Description	Accession # (NCBI)	MW (kDa) (NCBI)	pI (NCBI)	Location
UpBB (Spot # 177)	Aldolase B (364 aa)	Involved in glycolysis, catalyses the conversion of fructose-1,6-bisphosphate into dihydroxyacetone and glyceraldehyde-3-phosphate (Nelson and Cox, 2000). The relative position on the gel implies this enzyme is intact and is active. Aldolase B has been shown to degrade, from the carboxyl terminal, resulting in a positively charged C-terminal arginine (Chappel *et al*., 1978). However, no C-terminal degradation seems evident with regard to its relative position on the gel.	gi|1619606	40	8.66	Cytosol
DownBB (Spot # 519)	Aldolase B	Involved in glycolysis, catalyses the conversion of fructose-1,6-bisphosphate into dihydroxyacetone and glyceraldehyde-3-phosphate (Nelson and Cox, 2000). The relative position on the gel implies this enzyme's activity is severely reduced. Aldolase B has been shown to degrade, from the carboxyl terminal, resulting in a positively charged C-terminal arginine which is indicative of its relative position on the gel in this case (Chappel *et al*., 1978).	gi|1619606	40	8.66	Cytosol
UpBB (Spot # 555)	Aldolase B (364 aa)	Involved in glycolysis, catalyses the conversion of fructose-1,6-bisphosphate into dihydroxyacetone and glyceraldehydes-3-phosphate (Nelson and Cox, 2000). The relative position on the gel implies this enzyme is intact and is active. Aldolase B has been shown to degrade, from the carboxyl terminal, resulting in a positively charged C-terminal arginine (Chappel *et al*., 1978). However, no C-terminal degradation seems evident with regard to its relative position on the gel.	gi|1619606	40	8.66	Cytosol
UpBB (Spot # 168)	Aldo-keto reductase family 1, member A1 (325 aa)	Catalyzes the reduction of aflatoxin dialdehyde to its corresponding diol and represents an important detoxification route for aflatoxin (Burczynski *et al*., 1999)	gi|13591894	36	6.84	Cytosol
UpBB (Spot #	Aldo-keto reductase family 1, member D1 (326 aa)	Catalyzes the reduction of the delta 4 double bond of bile acid intermediates and steroid hormones carrying the delta 4-	gi|20302063	37	6.18	Cytosol

443)		3-one structure in the A/B cis configuration (Kondo *et al*., 1994).				
DownAA (Spot # 427)	Betaine-homocysteine methyltransferase (407 aa)	Catalyzes the conversion of betaine and homocysteine to dimethylglycine and methionine, respectively and is also essential for the regulation of methionine and catabolism of choline in mammalian tissues (Heil *et al*., 2000).	gi|50926806	45	8.01	Mitochondria
UpBB (Spot # 147)	Bile acid co-enzyme A, amino acid N-acyltransferase (420 aa)	Catalyzes the conjugation of bile acids with glycine or taurine, a reaction which favors the fat and fat soluble vitamins A, D, E and K in the acidic environment of the small intestine by lowering the pKa of bile acids and in doing so maintaining their stability (Sfakianos *et al*., 2002).	gi|56789149	46	6.97	Microsomes
UpAA (Spot # 413)	Catalase / Ba1-651 (527 aa)	Expressed under conditions of stress brought about by reactive oxygen species: catalyses the conversion of H_2O_2 to O_2 and $2H_2O$ (Nelson and Cox, 2000).	gi|6978607	60	7.07	Peroxisome
UpBB (Spot # 414)	Catalase (527 aa)	Same as above.	gi|51980301	60	7.07	Peroxisome
UpAA (Spot # 505)	Chain B, Crystal Structure Of A Mammalian 2-Cys Peroxiredoxin, Hbp23 (199 aa)	Expressed under conditions of stress brought about by reactive O_2 and reactive N_2 species. Also associated with proliferation, differentiation, immune response and oxidative stress (Hirotsu *et al*., 1999).	gi|6435548	22	8.34	Mitochondria
UpBB (Spot # 65)	Choline dehydrogenase (441 aa)	Choline dehydrogenase localizes to the matrix side of the mitochondrial inner membrane and is responsible for catalyzing the dehydrogenation of choline to betaine aldehyde. It functions as an iron sulfur flavoprotein via two redox centers: FAD and an iron sulfur cluster. One molecule of choline oxidized through the respiratory chain yields two molecules of ATP in the coupled mitochondria (Huang and Lin, 2003).	gi|1154950	49	7.78	Mitochondria
DownBB (Spot # 617)	Citrin (676 aa) Active (Ca^{2+} bound)	Mitochondrial membrane protein which functions as an aspartate/glutamate carrier during amino acid deamination (necessary for gluconeogenesis) and is an important component of the malate aspartate NADH shuttle (Tamamori *et al*., 2002; Ohura *et al*., 2003, Sinasac *et al*., 2004). These carriers contain an N-terminal domain in the intermembrane space that contains four Ca^{2+}-binding hands. Thus, they are activated by an increase in Ca^{2+} binding	gi|62646841	74	8.86	Mitochondria

		at these sites (Roesch *et al*., 2004).				
DownAA (Spot # 231)	2,4-dienoyl CoA reductase 1 (335 aa)	Involved in β-oxidation of polyunsaturated fatty acids (Nelson and Cox, 2000).	gi|37748456	36	9.18	Mitochondria
DownAA (Spot # 372)	Fatty acid binding protein 1 (127 aa)	Member of the fatty acid binding group of proteins that are involved in the intracellular transport of bioactive fatty acids and participate in intracellular signaling pathways, cell growth and differentiation (Lawrie *et al*., 2004). Liver fatty acid binding proteins were found to be increased in fatty Zucker rats, implying an increased rate of fatty acid utilization. These proteins are delipidated at pH 9. (Ocher and Manning, 1982).	gi|56541250	14	7.79	Cytosol
DownBB (Spot # 681)	α-2-globin chain (142 aa)	Hemoglobin contamination.	gi|3367720	15	8.45	
DownBB (Spot # 471)	B-1 globin (146 aa)	Hemoglobin contamination	gi|546056	16	7.98	
DownBB (Spot # 386)	III β-3 globin (147 aa)	Hemoglobin contamination.	gi|395943	16	9.04	
UpBB (Spot # 441)	Glutamate oxaloacetate transaminase 2 (430 aa) Active (pyridoxal bound)	Catalyzes the transfer of an amino group from an amino acid (Glu) to an 2-keto-acid to generate a new amino acid and the residual 2-keto-acid of the donor amino acid, reaction is reversible and requires pyridoxal phosphate as a cofactor (Nelson and Cox, 2000).	gi|38197424	47	9.13	Mitochondria
DownBB (Spot # 293)	Glutathione S-transferase, mitochondrial (226 aa)	Confers protection against genotoxic and cytotoxic electrophiles in the mitochondrial compartment (Singh *et al*., 2004). May be lower due to decreased β-oxidation occurring in the mitochondria.	gi|31077128	26	9.13	Mitochondria
UpAA (Spot # 258)	Glutathione S-transferase,-α (226 aa)	Cytosolic detoxification enzymes that catalyze the conjugation reaction of glutathione with a variety of endogenous electrophiles and xenobiotics. The enzyme catalyzes the reaction by lowering the p*Ka* of the sulfhydryl group of the enzyme-bound glutathione. The conjugation products are more watersoluble, usually less toxic, and can be degraded or	gi|7188365	26	8.98	Cytosol

		transported outside of the cell (Wang *et al.*, 2000; Whalen *et al.*, 2004).				
DownBB (Spot # 303)	Glutathione transferase YA subunit (222 aa)	Glutathione *S*-transferases catalyze the nucleophilic addition of the thiol moiety of reduced glutathione to a variety of electrophiles. They also bind with high affinity to a variety of hydrophobic compounds such as heme, bilirubin, hormones, and drugs, acting as intracellular carrier proteins for the transport of various ligands. They are also known to be involved in the antioxidant protection of cells by reducing toxic organic hydroperoxides, i.e., non-selenium glutathione peroxidase activity (Reddy *et al.*, 1995).	gi|58331251	26	8.89	Cytosol
UpAA (Spot # 178)	Glyceraldehyde-3-phosphate dehydrogenase, chain G (334 aa) Active (NAD^+ bound)	Catalyses the first step in the pay-off phase of glycolysis; producing 1,3-bisphosphoglycerate through the oxidation of glyceraldehyde-3-phosphate. Reaction is reversible and this enzyme may also be used for gluconeogenesis (Nelson and Cox, 2000).	gi|230868	36	6.60	Cytosol
UpBB (Spot # 515)	Glyceraldehyde-3-phosphate dehydrogenase, phosphorylating (332 aa) Active (phosphorylating)	Same as above.	gi|65987	36	9.90	Cytosol
DownAA (Spot # 236)	3-hydroxyacyl-CoA dehydrogenase (314 aa) Active (NAD^+ bound)	Mitochondrial enzyme involved in β-oxidation of long chain fatty acids, it catalyzes the NAD dependent oxidation of L-3-Hydroxyacyl-CoA to β-Ketoacyl-CoA (Holden and Banaszakg 1983; Nelson and Cox, 2000).	gi|17105336	34	8.83	Mitochondria
UpBB (Spot # 402)	17-β-hydroxysteroid dehydrogenase, type IV (735 aa) Active (NAD^+ bound)	Multifunctional peroxisomal hormone possessing separable 17-hydroxysteroid/fatty acyl-CoA dehydrogenase, fatty acyl-CoA-hydratase and sterol transfer activities (Leenders *et al.* 1996). Also involved in degradation of branched chain fatty acids (Dieuaide-Noubhani *et al.* 1997*a*) and the side chain of cholesterol (Dieuaide-Noubhani *et al.* 1997*b*). Inactivate sex steroid hormones by catalyzing the production of keto forms (Fan *et al.*, 1998). Functions with the cofactor NAD^+.	gi|1881831	79	8.77	Peroxisomes
UpAA (Spot #	Malate dehydrogenase 2	Mitochondrial enzyme that catalyses the oxidation of L-malate to oxaloacetate during the citric acid cycle. The	gi|42476181	36	8.93	Mitochondria

200)		reaction is reversible and requires NAD^+ as a cofactor (Lehininger *et al*., 2000).				
UpBB (Spot # 494)	Methylmalonate semialdehyde dehydrogenase (535 aa) Inactive (No NAD^+ or CoA bound)	Methylmalonate semialdehyde dehydrogenase catalyzes the irreversible oxidative decarboxylation of malonate and methylmalonate semialdehydes to acetyl- and propionyl-CoA, respectively. This activity is part of the valine and pyrimidine catabolic pathways (Chambliss *et al.*, 2000). Methylmalonate semialdehyde dehydrogenase is the only aldehyde dehydrogenase known to require CoA and NAD^+ for activity (Goodwin *et al*., 1989).	gi|13591997	58	8.47	Mitochondria
UpBB (Spot # 547)	Methylmalonate semialdehyde dehydrogenase (535 aa) Active (NAD^+ and CoA bound)	Same as above.	gi|13591997	58	8.47	Mitochondria
UpBB (Spot # 170)	Ornithine transcarbamylase (350 aa) Active (Zn^{2+} bound)	Catalyses carbamoyl phosphate to donate its carbamoyl group to ornathine to form citrulline and release Pi during the urea cycle (Nelson and Cox, 2000). This enzyme requires Zn^{2+} for activation and has an optimal pH of 10 (De Mars *et al*., 1976; Riggio *et al*., 1992).	gi|56789151	40	9.25	Mitochondria
UpBB (Spot # 185)	Rhodanese (295 aa)	Mitochondrial enzyme that catalyzes the detoxification of cyanide and thiosulfate or other suitable sulfur donors into thiocynate (Saidu, 2004).	gi|57069	33	7.84	Mitochondria
UpBB (Spot # 485)	Translation elongation factor 1 α-1-like 14 (398 aa)	Cytosolic protein which binds to mRNA to facilitate scanning of the mRNA to locate the first AUG region (Nelson and Cox, 2000).	gi|15277711	43	8.94	Cytosol
UpBB (Spot # 533)	Translation elongation factor 1 α-1-like 14 (398 aa)	Same as above.	gi|15277711	43	8.94	Cytosol
UpAA (Spot # 627)	Urate oxidase (303 aa)	Peroxisomal enzyme catalyzing the oxidation of uric acid, a product of purine metabolism, to allantoin (Oda *et al*., 2002; Xiangwei *et al*., 1989).	gi|56971244	35	8.20	Peroxisome

Up/down refers to either an increase or decrease, respectively, in protein spot density for the relevant test group in relation to a comparative group in each table. AA: 99.5% student t-test with equal variance ($p < 0.005$), BB: 97.5% student t-test with equal variance ($p < 0.025$), CC: 99.5% student t-test with unequal variance ($p < 0.005$) and DD: 97.5% student t-test with unequal variance ($p < 0.025$).
NCBI - data base (ProFound, FindPept and FindMod programs) www.proteomics.com

Table 4.6.3: MALDI-TOF MS identification of *S. frutescens* rat liver proteins, from basic gels, for spots which displayed a significant difference relative to the OB/IR group

Effects	Swiss protein name & code	Description	Accession # (NCBI)	MW (kDa) (NCBI)	pI (NCBI)	Location
UpBB (Spot # 169)	Aldolase B (364 aa)	Involved in glycolysis, catalyses the conversion of fructose-1,6-bisphosphate into dihydroxyacetone and glyceraldehyde-3-phosphate (Nelson and Cox, 2000). The relative position on the gel implies this enzyme is intact and is active. Aldolase B has been shown to degrade, from the carboxyl terminal, resulting in a positively charged C-terminal arginine (Chappel *et al*., 1978). Decreased C-terminal degradation seems evident with regard to its relative position on the gel.	gi|1619606	40	8.66	Cytosol
DownBB (Spot # 519)	Aldolase B	Involved in glycolysis, catalyses the conversion of fructose-1,6-bisphosphate into dihydroxyacetone and glyceraldehyde-3-phosphate (Nelson and Cox, 2000). The relative position on the gel implies this enzyme's activity is severely reduced. Aldolase B has been shown to degrade, from the carboxyl terminal, resulting in a positively charged C-terminal arginine which is indicative of its relative position on the gel in this case (Chappel *et al*., 1978).	gi|1619606	40	8.66	Cytosol
UpBB (Spot # 443)	Aldo-keto reductase family 1, member D1 (326 aa)	Catalyzes the reduction of the delta 4 double bond of bile acid intermediates and steroid hormones carrying the delta 4-3-one structure in the A/B cis configuration (Kondo *et al*., 1994).	gi|20302063	37	6.18	Cytosol
UpBB (Spot # 135)	Arginosuccinate synthetase	Involved in the "Krebs bicycle". The enzyme catalyzes the formation of argininosuccinate from aspartate (product of Krebs cycle) and citrulline (product of urea cycle) in the cytosol (Nelson and Cox, 2000).				Mitochondria
UpBB (Spot # 482)	Apoptosis-inducing factor (608 aa)	Found in the mitochondrial intermembrane space, translocated to the nucleus upon induction of apoptosis. Oxidoreductase that acts as a caspase-independent mitochondrial effector of apoptotic cell death. Extramitochondrial AIF induces nuclear chromatin condensation and large scale DNA fragmentation. FAD^+ dependent (Nelson and Cox, 2000).	gi|14279176	66	9.10	Mitochondria

DownCC (Spot # 112)	Betaine-homocysteine methyltransferase 2 (407 aa)	Involved in the regulation of homocysteine metabolism. Converts betaine and homocysteine to dimethylglycine and methionine, respectively. This reaction is also required for the irreversible oxidation of choline. Homocysteine is formed by S-adenosylmethionine-dependent methylation reactions and removed by remethylation to methionine by either methionine synthase or betaine:homocysteine methyltransferase (BHMT) or by transsulfuration to cysteine via cystathionine-□-synthase (CBS). CBS synthesis and activity are downregulated by insulin and are upregulated by glucocorticoids. Methionine synthase is unaffected by diabetes or by insulin treatment. BHMT activity and mRNA levels are reportedly increased by diabetes (Brosnan *et al*., 2003).	gi|50926806	45	8.01	Cytosol
UpBB (Spot # 147)	Bile acid co-enzyme A, amino acid N-acyltransferase (420 aa)	Catalyzes the conjugation of bile acids with glycine or taurine, a reaction which favors the fat and fat soluble vitamins A, D, E and K in the acidic environment of the small intestine by lowering the pKa of bile acids and in doing so maintaining their stability (Sfakianos *et al*., 2002).	gi|56789149	46	6.97	Microsomes
UpBB (Spot # 688)	Catalase (527 aa)	Expressed under conditions of stress brought about by reactive oxygen species: catalyses the conversion of H_2O_2 to O_2 and $2H_2O$ (Nelson and Cox, 2000).	gi|51980301	60	7.07	Peroxisome
DownBB (Spot # 52)	Citrin (676 aa) Active (Ca^{2+}bound)	Mitochondrial membrane protein which functions as an aspartate/glutamate carrier during amino acid deamination (necessary for gluconeogenesis) and is an important component of the malate aspartate NADH shuttle (Tamamori *et al*., 2002; Ohura *et al*., 2003, Sinasac *et al*., 2004). These carriers contain an N-terminal domain in the intermembrane space that contains four Ca^{2+}-binding hands. Thus, they are activated by an increase in Ca^{2+} binding at these sites (Roesch *et al*., 2004).	gi|62646841	74	8.86	Mitochondria
UpAA (Spot # 419)	Citrin (676 aa) Less active (Less Ca^{2+} bound)	Same as above.	gi|62646841	74	8.86	Mitochondria
UpBB	2-Cys Peroxiredoxin (199 aa)	Expressed under conditions of stress brought about by reactive O_2 and reactive N_2 species.	gi|6435548	22	8.34	Mitochondria

(Spot # 322)		Also associated with proliferation, differentiation, immune response and oxidative stress (Hirotsu *et al*., 1999).				
DownBB (Spot # 231)	2,4-dienoyl CoA reductase 1 (335 aa)	Involved in β-oxidation of polyunsaturated fatty acids (Nelson and Cox, 2000).	gi|37748456	36	9.18	Mitochondria
UpBB (Spot # 484)	Elongation factor-1-α (207 aa)	Cytosolic protein responsible for the GTP-dependent binding of aminoacyl-tRNAs to ribosomes, it is composed of four subunits: the alpha chain, which binds GTP and aminoacyl-tRNAs, the gamma chain that probably plays a role in anchoring the complex to other cellular components and the beta and delta (or beta') chains (Nelson and Cox, 2000).	gi|203992	22	9.47	Cytosol
DownAA (Spot # 471)	B-1 globin	Hemoglobin contamination.	gi|546056	16	7.98	
UpBB (Spot # 178)	Glyceraldehyde-3-phosphate dehydrogenase, chain G (334 aa) Active (NAD^+ bound)	Catalyses the first step in the pay-off phase of glycolysis; producing 1,3-bisphosphoglycerate through the oxidation of glyceraldehyde-3-phosphate. Reaction is reversible and this enzyme may also be used for gluconeogenesis (Nelson and Cox, 2000).	gi|230868	36	6.60	Cytosol
UpBB (Spot # 255)	S-Glutathiolated Carbonic Anhydrase III (260 aa)	Occurs under oxidative stress (Mallis *et al*., 2000).	gi|10120584	29	6.74	Cytosol
DownBB (Spot # 568)	Hba-a1 protein (142 aa)	Hemoglobin contamination.	gi|60688619	15	8.45	
UpBB (Spot # 119)	3-hydroxy-3-methylglutaryl-CoA synthase 2 (508 aa)	Catalyses the reversible condensation of acetyl-CoA and acetoacetyl-CoA during the second step of cholesterol synthesis (Nelson and Cox, 2000).	gi|51259246	57	8.86	Mitochondria
UpBB (Spot # 284)	3-Hydroxyacyl-CoA dehydrogenase, binary complex (314 aa) Inactive (No NAD^+ bound)	Mitochondrial enzyme involved in β-oxidation of long chain fatty acids, it catalyzes the NAD dependent oxidation of L-3-Hydroxyacyl-CoA to β-Ketoacyl-CoA (Holden and Banaszakg 1983; Nelson and Cox, 2000).	gi|14488727	27	8.91	Mitochondria
UpBB (Spot # 64)	Methylmalonate semialdehyde dehydrogenase (535 aa) Active (NAD^+ and CoA bound)	Methylmalonate semialdehyde dehydrogenase catalyzes the irreversible oxidative decarboxylation of malonate and methylmalonate semialdehydes to acetyl- and propionyl-CoA, respectively. This activity is part of the	gi|13591997	58	8.47	Mitochondria

		valine and pyrimidine catabolic pathways (Chambliss *et al.*, 2000). Methylmalonate semialdehyde dehydrogenase is the only aldehyde dehydrogenase known to require CoA and NAD^+ for activity (Goodwin *et al.*, 1989).				
UpAA (Spot # 548)	Methylmalonate semialdehyde dehydrogenase (535 aa) Inactive (No NAD^+ or CoA bound)	Same as above.	gi|13591997	58	8.47	Mitochondria
UpBB (Spot # 330)	Nucleoside diphosphate kinase β isoform (152 aa)	Plays regulatory roles in various cellular functions such as signal transduction (exist as a complex with G protein in membranes and to regulate G protein function by supplying GTP in its immediate vicinity), tumor metastasis, morphogenesis, and cell growth and differentiation. It seems plausible in one sense that this enzyme is related with multiple cellular events because the reaction products, dinucleoside triphosphates, of the enzyme are consumed for syntheses of many cellular components including nucleic acids, polysaccharides, lipids, and proteins. This enzyme also holds tumor metastatic properties, and was demonstrated to be located in contact with tubulin network (Shimada *et al.*, 1993).	gi|286232	17	5.96	Cytosol
UpAA (Spot # 172)	Ornithine transcarbamylase (350 aa) Least active form (No Zn^{2+} bound)	Catalyses carbamoyl phosphate to donate its carbamoyl group to ornathine to form citrulline and release Pi during the urea cycle (Nelson and Cox, 2000). This enzyme requires Zn^{2+} for activation and has an optimal pH of 10 (De Mars *et al.*, 1976; Riggio *et al.*, 1992).	gi|56789151	40	9.25	Mitochondria
UpAA (Spot # 42)	Transketolase (623 aa) Active (thiamine pyrophosphate bound)	Involved in the non-oxidative pentose phosphate pathway, converting pentose phosphates into hexose phosphates, thereby promoting continual NADPH formation for fatty acid synthesis. Thiamine pyrophosphate dependent enzyme, catalyzes the transfer of a 2 carbon fragment of xylulose-5-phosphate to ribose-5-phosphate, forming sedoheptulose-7-phosphate and glyceraldehyde-3-phosphate. It later converts xylose-5-phosphate and erythrose-4-phosphate into glyceraldehyde-3-phosphate and fructose-6-	gi|1729977	68	7.23	Cytosol

		phosphate (Lehiniger *et al.* 2000).				
UpAA (Spot # 43)	Transketolase (623 aa) Active (thiamine pyrophosphate bound)	Same as above.	gi|1729977	68	7.23	Cytosol
DownBB (Spot # 111)	Translation elongation factor 1 α-1 (462 aa)	Cytosolic protein responsible for the GTP-dependent binding of aminoacyl-tRNAs to ribosomes, it is composed of four subunits: the alpha chain, which binds GTP and aminoacyl-tRNAs, the gamma chain that probably plays a role in anchoring the complex to other cellular components and the beta and delta (or beta') chains (Nelson and Cox, 2000).	gi|28460696	50	9.10	Cytosol
UpBB (Spot # 536)	Translation elongation factor 1-α-1 (462 aa)	Same as above.	gi|28460696	50	9.10	Cytosol
UpAA (Spot # 533)	Translation elongation factor 1-α-1-like 14 (398 aa)	Cytosolic protein which binds to mRNA to facilitate scanning of the mRNA to locate the first AUG region (Nelson and Cox, 2000).	gi|15277711	43	8.94	Cytosol
UpAA (Spot # 627)	Urate oxidase (303 aa)	Peroxisomal enzyme catalyzing the oxidation of uric acid, a product of purine metabolism, to allantoin (Oda *et al.*, 2002; Xiangwei *et al.*, 1989).	gi|56971244	35	8.20	Peroxisome

Up/down refers to either an increase or decrease, respectively, in protein spot density for the relevant test group in relation to a comparative group in each table. AA: 99.5% student t-test with equal variance ($p < 0.005$), BB: 97.5% student t-test with equal variance ($p < 0.025$), CC: 99.5% student t-test with unequal variance ($p < 0.005$) and DD: 97.5% student t-test with unequal variance ($p < 0.025$).
NCBI - data base (ProFound, FindPept and FindMod programs) www.proteomics.com

Table 4.6.4: MALDI-TOF MS identification of *S. frutescens* rat liver proteins, from basic gels, for spots which displayed a significant difference relative to the lean control group

Effects	Swiss protein name & code	Description	Accession # (NCBI)	MW (kDa) (NCBI)	pI (NCBI)	Location
UpBB (Spot # 142)	Acetyl-coA acetyltransferase 1 (424 aa)	Catalyzes the conversion of 2 acetyl-CoA molecules to acetoacetyl-CoA plus CoA (Fukao *et al*., 1989).	gi|8392836	45	8.92	Mitochondria
UpBB (Spot # 94)	Aldehyde dehydrogenase (501 aa)	Microsomal NAD/NADP dependent enzyme that acts on long chain aliphatic substrates. It has an important biological role in oxidizing and detoxifying long chain aldehydes produced during the peroxidation of microsomal membranes (Demozay *et al*., 2004).	gi|974168	54	7.14	Microsome
UpBB (Spot # 149)	Calreticulin (398 aa)	Calreticulin plays an important role in quality control during protein synthesis, folding, and posttranslational modification. Calreticulin binds Ca^{2+} and affects cellular Ca^{2+} homeostasis. The protein increases the Ca^{2+} storage capacity of the endoplasmic reticulum and modulates the function of endoplasmic reticulum Ca^{2+}-ATPase. Calreticulin also plays a role in the control of cell adhesion and steroid-sensitive gene expression (Michalak *et al*., 1998; Treves *et al*., 1990).	gi|8393215	44	8.20	Cytosol
UpBB (Spot # 419)	Citrin (676 aa) Less active (Less Ca^{2+}bound)	Mitochondrial membrane protein which functions as an aspartate/glutamate carrier during amino acid deamination (necessary for gluconeogenesis) and is an important component of the malate aspartate NADH shuttle (Tamamori *et al*., 2002; Ohura *et al*., 2003, Sinasac *et al*., 2004). These carriers contain an N-terminal domain in the intermembrane space that contains four Ca^{2+}-binding hands. Thus, they are activated by an increase in Ca^{2+} binding at these sites (Roesch *et al*., 2004).	gi|62646841	74	8.86	Mitochondria
DownBB (Spot # 496)	Enoyl-CoA, hydratase/3-hydroxyacyl CoA dehydrogenase complex (722 aa)	Mitochondrial enzymes involved in β-oxidation of long chain fatty acids. Enzymes isolated and identified as a complex which may imply they are inactive. (Holden and Banaszakg 1983; Nelson and Cox, 2000).	gi|59809132	79	9.28	Mitochondria
UpAA (Spot # 84)	F1-ATPase (510 aa) (Active)	Inner mitochondrial membrane enzyme consisting of 6 subunits containing binding sites for ATP and ADP, including the	gi|6729934	55	8.28	Mitochondria

		catalytic site for ATP synthesis (Nelson and Cox, 2000).				
DownBB (Spot # 545)	F1-ATPase (510 aa) (Less active)	Same as above.	gi|6729934	55	8.28	Mitochondria
DownBB (Spot # 369)	Fatty acid binding protein 1	Member of the fatty acid binding group of proteins that are involved in the intracellular transport of bioactive fatty acids and participate in intracellular signaling pathways, cell growth and differentiation (Lawrie *et al*., 2004). Liver fatty acid binding proteins were found to be increased in fatty Zucker rats, implying an increased rate of fatty acid utilization. These proteins are delipidated at pH 9. (Ocher and Manning, 1982).	gi|56541250	14	7.79	Cytosol
DownAA (Spot # 471)	B-1 globin (147 aa)	Haemoglobin contamination.	gi|204570	16	7.88	
UpBB (Spot # 178)	Glyceraldehyde-3-phosphate dehydrogenase, chain G (334 aa) Active (NAD^+ bound)	Catalyses the first step in the pay-off phase of glycolysis; producing 1,3-bisphosphoglycerate through the oxidation of glyceraldehyde-3-phosphate. Reaction is reversible and this enzyme may also be used for gluconeogenesis (Nelson and Cox, 2000).	gi|230868	36	6.60	Cytosol
UpAA (Spot # 187)	Similar to glyceraldehyde-3-phosphate dehydrogenase (334 aa)	Same as above.	gi|51766262	28	8.66	Cytosol
DownAA (Spot # 301)	Glutathione S-transferase, mitochondrial (226 aa)	Confers protection against genotoxic and cytotoxic electrophiles in the mitochondrial compartment (Singh *et al*., 2004). May be lower due to decreased β-oxidation occurring in the mitochondria.	gi|31077128	26	9.13	Mitochondria
UpAA (Spot # 513)	Glycine N-methyltransferase (293 aa)	Cytosolic protein which catalyzes the methylation of glycine by S-adenosylmethionine to form N-methylglycine and S-adenosylhomocysteine. Important folate binding protein. Folate functions as a precursor of nucleic acids (Cook and Wagner, 1984; Yeo and Wagner, 1993).	gi|8567354	33	7.10	Cytosol
DownAA (Spot # 368)	β-haemoglobin (147 aa)	Haemoglobin contamination.	gi|204570	16	7.88	

UpBB (Spot # 119)	3-Hydroxy-3-methylglutaryl-CoA synthase 2 (508 aa)	Catalyses the reversible condensation of acetyl-CoA and acetoacetyl-CoA during the second step of cholesterol synthesis, also involved in ketone body synthesis (Nelson and Cox, 2000).	gi|51259246	57	8.86	Mitochondria
UpAA (Spot # 230)	3-Hydroxyacyl-CoA dehydrogenase, short chain (314 aa) Inactive (No NAD^+ bound)	Mitochondrial enzyme involved in β-oxidation of long chain fatty acids, it catalyzes the NAD dependent oxidation of L-3-Hydroxyacyl-CoA to β-Ketoacyl-CoA (Holden and Banaszakg 1983; Nelson and Cox, 2000).	gi|17105336	34	8.83	Mitochondria
UpAA (Spot # 239)	3-Hydroxyacyl-CoA dehydrogenase (314 aa) Inactive (No NAD^+ bound)	Same as above.	gi|17105336	34	8.83	Mitochondria
UpBB (Spot # 284)	3-Hydroxyacyl-Coa dehydrogenase, binary complex (314 aa) Inactive (No NAD^+ bound)	Same as above.	gi|14488727	27	8.91	Mitochondria
UpAA (Spot # 201)	Hydroxysteroid 11-beta dehydrogenase 1 (288 aa) Active ($NADP^+$ bound)	Acts *in vivo* mainly as a NADPH-dependent reductase, activating glucocorticoids from circulating 11-oxo precursors (cortisone in humans, and 11-dehydrocorticosterone in rodents) to the respective 11b-OH receptor ligands (cortisol, corticosterone). (Benediktsson *et al*., 1992; Davani *et al*., 2000). The relevant position of this protein on the gel indicates that it may be bound to $NADP^+$ implying that it is catalyzing the reverse reaction by which cortisol or corticosterone are oxidised to inactive precursors.	gi|50927643	32	8.55	Peroxisomes
UpAA (Spot # 213)	Lactate dehydrogenase	Mitochondrial enzyme which catalyses the conversion of lactate into pyruvate (Nelson and Cox, 2000)	gi|38014570	30	9.16	Mitochondria
UpBB (Spot # 64)	Methylmalonate semialdehyde dehydrogenase (535 aa) Active (NAD^+ and CoA bound)	Methylmalonate semialdehyde dehydrogenase catalyzes the irreversible oxidative decarboxylation of malonate and methylmalonate semialdehydes to acetyl- and propionyl-CoA, respectively. This activity is part of the valine and pyrimidine catabolic pathways (Chambliss *et al.*, 2000). Methylmalonate semialdehyde dehydrogenase is the only aldehyde dehydrogenase known to require CoA and NAD^+ for activity (Goodwin *et al*., 1989).	gi|13591997	58	8.47	Mitochondria

UpDD (Spot # 548)	Methylmalonate semialdehyde dehydrogenase (535 aa) Inactive (No NAD^+ or CoA bound)	Same as above.	gi|13591997	58	8.47	Mitochondria
DownBB (Spot # 680)	Multifunctional acyl-CoA-binding protein (87 aa)	Binds medium- and long-chain acyl-CoA esters with very high affinity and may function as an intracellular carrier of acyl-CoA esters. It is also able to displace diazepam from the benzodiazepine recognition site located on the GABA type A receptor. It is therefore possible that this protein also acts as a neuropeptide to modulate the action of the GABA receptor (Nelson and Cox, 2000).	gi|1228089	10	8.78	Cytosol
UpBB (Spot # 171)	Ornithine transcarbamylase (350 aa) Less active (No Zn^{2+} bound)	Catalyses carbamoyl phosphate to donate its carbamoyl group to ornaihine to form citrulline and release Pi during the urea cycle (Nelson and Cox, 2000). This enzyme requires Zn^{2+} for activation and has an optimal pH of 10 (De Mars *et al*., 1976; Riggio *et al*., 1992).	gi|56789151	40	9.25	Mitochondria
UpBB (Spot # 140)	Phosphoglycerate kinase 1 (417 aa)	Second step in the pay off phase of glycolysis, cytosolic enzyme. Catalyses the transfer of a high energy phosphate group to the carboxyl group of 1,3-bisphosphoglycerate to ADP, forming ATP and 3-phosphoglycerate. Requires Mg^{2+} for activation. (Nelson and Cox, 2000).	gi|40254752	45	8.02	Cytosol
UpBB (Spot # 462)	Quinoid dihydropteridine reductase (241 aa)	Recycles tetrahydrobiopterin works with phenylalanine hydroxylase to ensure the proper metabolism of phenylalanine in the body. Tetrahydrobiopterin also helps produce neurotransmitters (Wild *et al*., 2003).	gi|11693160	26	7.67	Mitochondria
UpBB (Spot # 627)	Urate oxidase (303 aa)	Peroxisomal enzyme catalyzing the oxidation of uric acid, a product of purine metabolism, to allantoin (Oda *et al*., 2002; Xiangwei *et al*., 1989).	gi|56971244	35	8.20	Peroxisome

Up/down refers to either an increase or decrease, respectively, in protein spot density for the relevant test group in relation to a comparative group in each table. AA: 99.5% student t-test with equal variance ($p < 0.005$), BB: 97.5% student t-test with equal variance ($p < 0.025$), CC: 99.5% student t-test with unequal variance ($p < 0.005$) and DD: 97.5% student t-test with unequal variance ($p < 0.025$).
NCBI - data base (ProFound, FindPept and FindMod programs) www.proteomics.com

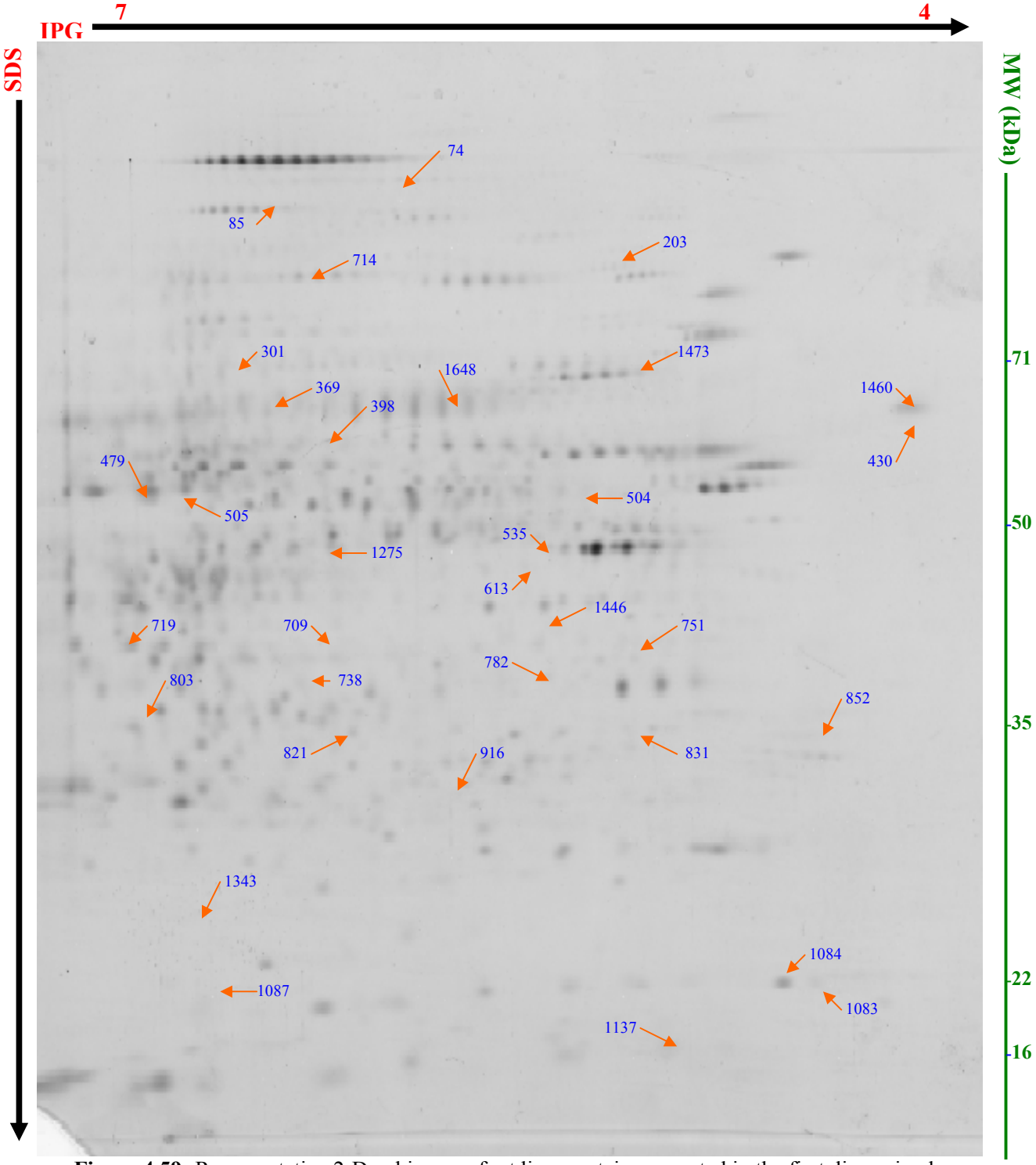

Figure 4.59: Representative 2-D gel image of rat liver protein, separated in the first dimension by IPG gels (covering the pH range from 4 to 7) and by a 12 % polyacrylamide gel in the second dimension, arrows indicate spot # positions on the gel. Spots visualized by sypro-ruby staining

Table 4.6.5: MALDI-TOF MS identification of OB/IR rat liver proteins, from acidic gels, for spots which displayed a significant difference relative to the lean control group

Effects	Swiss protein name & code	Description	Accession # (NCBI)	MW (kDa) (NCBI)	pI (NCBI)	Location
UpBB (831)	Albumin (607 aa)	Blood contamination.	gi|162648	69	5.82	
UpAA (504)	Aldehyde dehydrogenase 2 (488 aa)	Primarily responsible for oxidizing acetaldehyde, as well as several aldehydes generated by lipid peroxidation. Like Class 1 aldehyde dehydrogenases, Class 2 aldehyde dehydrogenase uses NAD and preferentially functions at micromolar concentrations of small aliphatic aldehydes (Boesch *et al*., 1996).	gi|25990263	53	5.07	Mitochondria
UpAA (74)	Carbamoyl-phosphate synthetase 1, mitochondrial (1500 aa)	Is the first rate-limiting step of the urea synthesis and catalyzes the removal of ammonia, a by-product of amino acid catabolism (Corvi *et al*., 2001; Nelson and Cox, 2000).	gi|8393186	16	6.33	Mitochondria
Down AA (1084)	Chain A, solution structure of oxidized rat microsomal cytochrome b_5 (94 aa)	Smooth endoplasmic reticulum protein. Involved in the desaturation of palmitate and stearate to produce palmitoleate, 16:1(Δ^9) and oleate, 18:1(Δ^9) (Nelson and Cox, 2000). Oxidized form indicates excess positive charge due to no electrons bringing about reduction. Oxidized form is indicative of a decrease in activity of cytochrome b_5, implying a decrease in the production of monounsaturated fatty acids.	gi|6980893	11	5.13	Endoplasmic reticulum
UpAA (505)	α-Enolase	Catalyses the reversible dehydration of 2-phosphoglycerate to phosphoenolpyruvate in glycolysis. This enzyme seems to be active for the reverse reaction. The enzyme forms a stable complex with 2-phosphoglycerate through strong ionic interactions with Mg^{2+} ions in the enzyme's active site. These interactions cause a drastic decrease in its pKa which is not the case here (Nelson and Cox, 2000).	gi|21674774	47	7.53	Cytosol
UpAA (613)	Fatty acid binding protein (133 aa)	Member of the fatty acid binding group of proteins that are involved in the intracellular transport of bioactive fatty acids and participate in intracellular signaling pathways, cell growth and differentiation	gi|13162363	15	5.90	Cytosol

		(Lawrie *et al*., 2004).				
UpBB (1446)	Fructose-1,6-bisphosphatase (363 aa)	Regulatory gluconeogenic enzyme catalyzing the irreversible hydolysis of fructose-1,6-bisphosphate to fructose-6-phosphate (Nelson and Cox, 2000).	gi|51036635	40	5.54	Cytosol
DownAA (821)	3-Hydroxyisobutyrate dehydrogenase Inactive/reverse reaction (No NAD^+ bound)	Catalyses the conversion of 3-hydroxyisobutyrate into methylmalanoate semialdehyde (Nelson and Cox, 2000).	gi|62647280	35	8.73	Mitochondria
UpBB (476)	Glutamate dehydrogenase (558 aa)	Catalyzes the conversion of glutamate into α-ketoglutarate (Nelson and Cox, 2000).	gi|6980956	61	8.05	Mitochondria
UpAA (709)	Ornithine carbamoyltransferase (354 aa) Active (Zn^{2+} bound)	A mitochondrial matrix enzyme found in the liver of ureotelic animals, where it catalyzes the dephosphorylation of carbamoyl phosphate and the subsequent binding of the remaining carbamoyl group to ornithine, forming citrulline (Nissim *et al*., 2002, Nelson and Cox, 2002).	gi|6981312	40	9.12	Mitochondria
UpAA (719)	Ornithine transcarbamylase (354 aa) Inactive (No Zn^{2+} bound)	A mitochondrial matrix enzyme found in the liver of ureotelic animals, where it catalyzes the dephosphorylation of carbamoyl phosphate and the subsequent binding of the remaining carbamoyl group to ornithine, forming citrulline (Nissim *et al*., 2002, Nelson and Cox, 2002).	gi|6981312	40	9.12	Mitochondria
UpBB (1087)	Peroxiredoxin 5 (213 aa)	Cytosolic antioxidant enzyme (Hirotsu *et al*., 1999).	gi|51261175	22	8.94	Cytosol
UpAA (916)	Peroxiredoxin 4 (273 aa)	Cytosolic antioxidant enzyme. Directly binds to a nonreceptor tyrosine kinase, c-Abl. The expression is coupled with the cell cycle, as is that of c-Abl, suggesting that high levels of peroxiredoxin expression may counteract the cytostatic activity of c-Abl. Phosphorylaton on thr-90 leads to a more than 80% decrease in enzymatic activity (Hirotsu *et al*., 1999).	gi|16758274	31	6.18	Cytosol
UpAA (535)	Phenylalanine hydroxylase (453 aa)	Catalyses the hydroxylation of phenylalanine to tyrosine , in order to remove excess phenylalanine from circulation (Davis *et al*., 1997).	gi|50926235	52	5.76	Mitochondria
UpBB (85)	Pyruvate carboxylase (1178 aa)	First regulatory enzyme in gluconeogenesis that converts pyruvate to oxaloacetate (Nelson and Cox, 2000).	gi|929988	13	6.25	Mitochondria

DownBB (398)	Serum abumin (608 aa)	Blood contamination.	gi|55391508	69	6.09	
UpBB (852)	Tropomyosin alpha 4 chain (247 aa)	Implicated in stabilizing cytoskeleton actin filaments (Tortora and Grabowski, 2003).	gi|52353308	29	4.79	Cytosol
UpAA (301)	Tumor necrosis factor α (706 aa)	Tumor necrosis factor-alpha is associated with the loss of insulin sensitivity and the pathogenesis of insulin resistance in diabetic animal models and human patients (Solomon *et al*., 1997; Duckworth, 1997, Miyazaki *et al*., 2003).	gi|54035509	80	6.56	Cytosol

Up/down refers to either an increase or decrease, respectively, in protein spot density for the relevant test group in relation to a comparative group in each table. AA: 99.5% student t-test with equal variance ($p < 0.005$), BB: 97.5% student t-test with equal variance ($p < 0.025$), CC: 99.5% student t-test with unequal variance ($p < 0.005$) and DD: 97.5% student t-test with unequal variance ($p < 0.025$).
NCBI - data base (ProFound, FindPept and FindMod programs) www.proteomics.com

Table 4.6.6: MALDI-TOF MS identification of metformin rat liver proteins, from acidic gels, for spots which displayed a significant difference relative to the OB/IR control group

Effects	Swiss protein name & code	Description	Accession # (NCBI)	MW (kDa) (NCBI)	pI (NCBI)	Location
UpBB (831)	Albumin (607 aa)	Blood contamination.	gi|162648	69	5.82	
UpBB (430)	Calreticulin (416 aa)	Calreticulin plays an important role in quality control during protein synthesis, folding, and posttranslational modification. Calreticulin binds Ca^{2+} and affects cellular Ca^{2+} homeostasis. The protein increases the Ca^{2+} storage capacity of the endoplasmic reticulum and modulates the function of endoplasmic reticulum Ca^{2+}-ATPase. Calreticulin also plays a role in the control of cell adhesion and steroid-sensitive gene expression (Michalak *et al*., 1998).	gi|11693172	48	4.33	Cytosol
DownAA (1137)	Cytochrome c oxidase subunit Va	Smooth endoplasmic reticulum protein. Involved in the desaturation of palmitate and stearate to produce palmitoleate, 16:1(Δ^9) and oleate, 18:1(Δ^9) (Nelson and Cox, 2000). Reduced form (neutral) due to electron reduction indicating an active form of cytochrome b_5 (Nelson and Cox, 2000).	gi|224985	10	5.23	Endoplasmic reticulum
DownBB (1343)	Expressed in non-metastatic cells 2 (152 aa)	Kinase involved in synthesis of nucleoside triphosphates.	gi|55926145	17	6.92	Cytosol
DownBB (1473)	Heat shock cognate 71kDa (646 aa)	Mediate essential cell survival strategy. The stresses that can trigger this response vary widely, and include heat or cold, osmotic imbalance, toxins, heavy metals and pathophysiological signals such as cytokines and eicosanoids. These proteins are synthesized in response to such environmental stresses (Ranford *et al*., 2000).	gi|56385	71	5.43	Cytosol

Up/down refers to either an increase or decrease, respectively, in protein spot density for the relevant test group in relation to a comparative group in each table. AA: 99.5% student t-test with equal variance ($p < 0.005$), BB: 97.5% student t-test with equal variance ($p < 0.025$), CC: 99.5% student t-test with unequal variance ($p < 0.005$) and DD: 97.5% student t-test with unequal variance ($p < 0.025$).
NCBI - data base (ProFound, FindPept and FindMod programs) www.proteomics.com

Table 4.6.7: MALDI-TOF MS identification of *S. frutescens* rat liver proteins, from acidic gels, for spots which displayed a significant difference relative to the OB/IR control group

Effects	Swiss protein name & code	Description	Accession # (NCBI)	MW (kDa) (NCBI)	pI (NCBI)	Location
DownBB (504)	Aldehyde dehydrogenase (488 aa)	Class 2 aldehyde dehydrogenase is localized to the mitochondria. This isoform appears to be primarily responsible for oxidizing acetaldehyde, as well as several aldehydes generated by lipid peroxidation. Like Class 1 aldehyde dehydrogenases, Class 2 aldehyde dehydrogenase uses NAD and preferentially functions at micromolar concentrations of small aliphatic aldehydes (Boesch *et al*., 1996).	gi|25990263	53	5.70	Mitochondria
DownBB (74)	Carbamoyl-phosphate synthetase 1, mitochondrial (1500 aa)	Mitochondrial protein, carbamoyl-phosphate synthetase is the first and rate-limiting step of the urea synthesis and catalyzes the removal of ammonia, a by-product of amino acid catabolism (Corvi *et al*., 2001; Nelson and Cox, 2000).	gi|8393186	16	6.33	Mitochondria
DownAA (505)	α-Enolase	Catalyses the reversible dehydration of 2-phosphoglycerate to phosphoenolpyruvate in glycolysis. This enzyme seems to be active for the reverse reaction. The enzyme forms a stable complex with 2-phosphoglycerate through strong ionic interactions with Mg2+ ions in the enzymes active site. These interactions cause a drastic decrease in its pKa which is not the case here (Nelson and Cox, 2000).	gi|21674774	47	7.53	Cytosol
DownBB (1343)	Expressed in non-metastatic cells 2 (152 aa)	Kinase involved in synthesis of nucleoside triphosphates.	gi|55926145	17	6.92	Cytosol
DownBB (1446)	Fructose-1,6-bisphosphatase (363 aa)	Regulatory gluconeogenic enzyme catalyzing the irreversible hydolysis of fructose-1,6-bisphosphate to fructose-6-phosphate (Nelson and Cox, 2000).	gi|51036635	40	5.54	Cytosol
DownBB (476)	Glutamate dehydrogenase (558 aa)	Mitochondrial, catalyzes the conversion of glutamate into α-ketoglutarate (Nelson and Cox, 2000).	gi|6980956	61	8.05	Mitochondria
DownBB (1473)	Heat shock cognate 71kDa (646 aa)	Mediate essential cell survival strategy. The stresses that can trigger this response vary widely, and include heat or cold, osmotic imbalance, toxins, heavy metals and pathophysiological signals such as cytokines and	gi|56385	71	5.43	Cytosol

		eicosanoids. These proteins are synthesized in response to such environmental stresses (Ranford *et al*., 2000).				
UpBB (821)	3-Hydroxyisobutyrate dehydrogenase Inactive/reverse reaction (No NAD^+ bound)	Catalyses the conversion of 3-hydroxyisobutyrate into methylmalanoate semialdehyde (Nelson and Cox, 2000).	gi|62647280	35	8.73	Mitochondria
DownBB (709)	Ornithine carbamoyltransferase (354 aa)	A mitochondrial matrix enzyme found in the liver of ureotelic animals, where it catalyzes the dephosphorylation of carbamoyl phosphate and the subsequent binding of the remaining carbamoyl group to ornathine, forming citrulline (Nissim *et al*., 2002, Nelson and Cox, 2002).	gi|6981312	40	9.12	Mitochondria
UpBB (751)	Oxidase IV cytochrome (97 aa)	Integral mitochondrial membrane protein associated with oxidative phosphorylation. Carries out 4 electron reductions of O_2, forming $2H_2O$, without producing free radical intermediates. This process also causes the net movement of protons from the matrix to the intermembrane space thereby contributing to the proton motive force (Nelson and Cox, 2000).	gi|223590	11	6.46	Mitochondria
DownBB (1087)	Peroxiredoxin 5 (213 aa)	Cytosolic antioxidant enzyme (Hirotsu *et al*., 1999).	gi|51261175	22	8.94	Cytosol
DownAA (85)	Pyruvate carboxylase (1178 aa)	Mitochondrial, first regulatory enzyme in gluconeogenesis that converts pyruvate to oxaloacetate (Nelson and Cox, 2000).	gi|929988	13	6.25	Mitochondria
UpBB (398)	Serum albumin (608 aa)	Blood contamination.	gi|55391508	69	6.09	
DownBB (852)	Tropomyosin-α-4 chain (247 aa)	Implicated in stabilizing cytoskeleton actin filaments (Tortora and Grabowski, 2003).	gi|52353308	29	4.79	Cytosol
DownAA (301)	Tumor necrosis factor α (706 aa)	Tumor necrosis factor-alpha is associated with the loss of insulin sensitivity and the pathogenesis of insulin resistance in diabetic animal models and human patients (Solomon *et al*., 1997; Duckworth, 1997, Miyazaki *et al*., 2003).	gi|54035509	80	6.56	Cytosol

Up/down refers to either an increase or decrease, respectively, in protein spot density for the relevant test group in relation to a comparative group in each table. AA: 99.5% student t-test with equal variance ($p < 0.005$), BB: 97.5% student t-test with equal variance ($p < 0.025$), CC: 99.5% student t-test with unequal variance ($p < 0.005$) and DD: 97.5% student t-test with unequal variance ($p < 0.025$).
NCBI - data base (ProFound, FindPept and FindMod programs) www.proteomics.com

Table 4.6.8: MALDI-TOF MS identification of *S. frutescens* rat liver proteins, from acidic gels, for spots which displayed a significant difference relative to the lean control group

Effects	Swiss protein name & code	Description	Accession # (NCBI)	MW (kDa) (NCBI)	pI (NCBI)	Location
DownBB (1460)	Calreticulin (416 aa)	Calreticulin plays an important role in quality control during protein synthesis, folding, and posttranslational modification. Calreticulin binds Ca^{2+} and affects cellular Ca^{2+} homeostasis. The protein increases the Ca^{2+} storage capacity of the endoplasmic reticulum and modulates the function of endoplasmic reticulum Ca^{2+}-ATPase. Calreticulin also plays a role in the control of cell adhesion and steroid-sensitive gene expression (Michalak *et al*., 1998).	gi|11693172	48	4.33	Cytosol
UpBB (74)	Carbamoyl-phosphate synthetase 1, mitochondrial (1500 aa)	Mitochondrial protein, carbamoyl-phosphate synthetase is the first and rate-limiting step of the urea synthesis and catalyzes the removal of ammonia, a by-product of amino acid catabolism (Corvi *et al*., 2001; Nelson and Cox, 2000).	gi|8393186	16	6.33	Mitochondria
DownDD (1084)	Chain A, Solution Structure Of Oxidized Rat Microsomal Cytochrome b_5 (94 aa)	Smooth endoplasmic reticulum protein. Involved in the desaturation of palmitate and stearate to produce palmitoleate, 16:1(Δ^9) and oleate, 18:1(Δ^9) (Nelson and Cox, 2000). Oxidized formed indicates excess positive charge due to no electrons bringing about reduction. Oxidized form is significant of a decrease in activity of cytochrome b_5, implying a decrease in the production of monounsaturated fatty acids.	gi|6980893	11	5.13	Cytosol
UpBB (1083)	Cytochrome b_5 (90 aa)	Smooth endoplasmic reticulum protein. Involved in the desaturation of palmitate and stearate to produce palmitoleate, 16:1(Δ^9) and oleate, 18:1(Δ^9) (Nelson and Cox, 2000). Reduced form (neutral) due to electron reduction indicating an active form of cytochrome b_5.	gi|224985	10	5.23	Cytosol
DownBB (1343)	Expressed in non-metastatic cells 2 (152 aa)	Kinase involved in synthesis of nucleoside triphosphates.	gi|55926145	17	6.92	Cytosol
UpAA (613)	Fatty acid binding protein (133 aa) (Active form)	Member of the fatty acid binding group of proteins that are involved in the intracellular transport of bioactive fatty acids and participate in intracellular signaling	gi|13162363	15	5.90	Cytosol

		pathways, cell growth and differentiation (Lawrie *et al*., 2004).				

Up/down refers to either an increase or decrease, respectively, in protein spot density for the relevant test group in relation to a comparative group in each table. AA: 99.5% student t-test with equal variance ($p < 0.005$), BB: 97.5% student t-test with equal variance ($p < 0.025$), CC: 99.5% student t-test with unequal variance ($p < 0.005$) and DD: 97.5% student t-test with unequal variance ($p < 0.025$).
NCBI - data base (ProFound, FindPept and FindMod programs) www.proteomics.com

Table 4.6.9: Summary of changes observed for OB/IR in comparison to lean control group for basic gels

	Glycolysis	Krebs Cycle	Oxidative Phosphorylation	Pentose Phosphate Pathway	β-Oxidation	Stress Proteins	Gluconeogenesis	Bile Synthesis	Urea Cycle	Detoxification	Fatty Acid Transport	Amino Acid Metabolism	Protein Synthesis	Ketone Body Synthesis	Structural Proteins	Cytokines	Lipid Synthesis	Cholesterol	Protein Degradation
Aldolase B	↓						↑												
Citrin							↑					↑	↓						↑
Enoyl-CoA, hydratase/3-hydroxyacyl CoA dehydrogenase complex					↑												↓		
S-Glutathiolated Carbonic Anhydrase III						↓													
3-Hydroxy-3-methylglutaryl-CoA synthase 2																		↑	
3-Hydroxyacyl-CoA Dehydrogenase	↓	↑	↑		↑		↑										↓		
17-β-hydroxysteroid dehydrogenase, type IV													↑						
Hydroxysteroid 11-β dehydrogenase 1					↓		↓												↓
Malate dehydrogenase 2	↓				↑		↑					↑							↑
Methylmalonate semialdehyde dehydrogenase												↓							↓
Transketolase				↓													↓		

Key: ↓ Direct decrease, ↑ Direct increase, ↑ or ↓ Indirectly causes an increase/decrease

Table 4.6.10: Summary of changes observed for OB/IR in comparison to lean control group for acidic gels

	Glycolysis	Krebs Cycle	Oxidative Phosphorylation	Pentose Phosphate Pathway	β-Oxidation	Stress Proteins	Gluconeogenesis	Bile Synthesis	Urea Cycle	Detoxification	Fatty Acid Transport	Amino Acid Metabolism	Protein Synthesis	Ketone Body Synthesis	Structural Proteins	Cytokines	Lipid Synthesis	Cholesterol	Protein Degradation
Aldehyde dehydrogenase					↑					↑									
Carbamoyl-phosphate synthetase 1	↓	↑					↑		↑			↑							↑
Chain A, Microsomal Cytochrome b_5					↑												↓		
α-Enolase	↓						↑												
Fatty acid binding protein 1					↑						↑						↑		
Fructose-1,6-bisphosphatase	↓		↓				↑					↑							
3-Hydroxyisobutyrate dehydrogenase												↓							↓
Glutamate dehydrogenase	↓	↑					↑					↑							
Ornithine carbamoyltransferase	↓	↑					↑		↑			↑							↑
Peroxiredoxin 4						↑													
Peroxiredoxin 5						↑													
Phenylalanine hydroxylase												↑							↑
Pyruvate carboxylase	↓		↓	↓			↑												
Tropomyosin α 4 chain															↑				
Tumor necrosis factor α																↑			

Key: ↓Direct decrease, ↑Direct increase, ↑or↓Indirectly causes an increase/decrease

Table 4.6.11: Summary of changes observed for OB/IR in comparison to metformin group for basic gels

	Glycolysis	Krebs Cycle	Oxidative Phosphorylation	Pentose Phosphate Pathway	β-Oxidation	Stress Proteins	Gluconeogenesis	Bile Synthesis	Urea Cycle	Detoxification	Fatty Acid Transport	Amino Acid Metabolism	Protein Synthesis	Ketone Body Synthesis	Structural Proteins	Cytokines	Lipid Synthesis	Cholesterol	Protein Degradation
Aldolase B	↑						↓												
Aldo-keto reductase family 1, member A1										↑									
Aldo-keto reductase family 1, member D1								↑											
Betaine-homocysteine methyltransferase												↓							
Bile acid CoA, amino acid N-acyltransferase								↑											
Catalase						↑													
Chain B, 2-Cys Peroxiredoxin, Hbp23						↑													
Choline dehydrogenase			↑																
Citrin							↓					↓	↑						↓
2,4-dienoyl CoA reductase 1, mitochondrial	↑				↓		↓										↑		
Fatty acid binding protein 1					↓						↓						↑		
Glutamate oxaloacetate transaminase 2							↓					↓	↑						↓
Glutathione S-transferase						↓				↓									
Glutathione S-transferase-α						↑				↑									
Glutathione S-transferase YA subunit						↓													
Glyceraldehyde-3-phosphate dehydrogenase	↑	↑	↑				↓												
3-hydroxyacyl-CoA dehydrogenase	↑	↓	↓		↓		↓										↑		
17-β-hydroxysteroid dehydrogenase, type IV													↓						
Malate dehydrogenase 2	↑				↓		↓					↓							↓
Methylmalonate semialdehyde dehydrogenase												↑							↑
Ornithine transcarbamylase									↑										↑
Rhodanese										↑									
Translation elongation factor 1 alpha 1-like 14													↑						↓
Urate oxidase									↑										

Key: ↓Direct decrease, ↑Direct increase, ↑or↓Indirectly causes an increase/decrease

Table 4.6.12: Summary of changes observed for OB/IR in comparison to metformin group for acidic gels

	Glycolysis	Krebs Cycle	Oxidative Phosphorylation	Pentose Phosphate Pathway	β-Oxidation	Stress Proteins	Gluconeogenesis	Bile Synthesis	Urea Cycle	Detoxification	Fatty Acid Transport	Amino Acid Metabolism	Protein Synthesis	Ketone Body Synthesis	Structural Proteins	Cytokines	Lipid Synthesis	Cholesterol	Protein Degradation
Calreticulin													↑						
Cytochrome c oxidase subunit Va			↓																
Heat shock cognate 71kDa						↓													

Key: ↓Direct decrease, ↑Direct increase, ↑or↓Indirectly causes an increase/decrease

Table 4.6.13: Summary of changes observed for OB/IR in comparison to *S. frutescens* group for basic gels

	Glycolysis	Krebs Cycle	Oxidative Phosphorylation	Pentose Phosphate Pathway	β-Oxidation	Stress Proteins	Gluconeogenesis	Bile Synthesis	Urea Cycle	Detoxification	Fatty Acid Transport	Amino Acid Metabolism	Protein Synthesis	Ketone Body Synthesis	Structural Proteins	Cytokines	Lipid Synthesis	Cholesterol	Protein Degradation
Aldolase B	↑						↓												
Aldo-keto reductase family 1, member D1								↑											
Arginosuccinate synthetase		↑							↑			↑							
Betaine-homocysteine methyltransferase 2												↓							
Bile acid co-enzyme A, amino acid N-acyltransferase								↑											
Catalase						↑													
Citrin							↓					↓	↑						↓
2-Cys Peroxiredoxin, Hbp23						↑													
2,4-dienoyl CoA reductase 1					↓												↑		
Glyceraldehyde-3-phosphate dehydrogenase	↑	↑	↑				↓												
S-Glutathiolated Carbonic Anhydrase III						↑													
3-hydroxy-3-methylglutaryl-Coenzyme A synthase 2																		↑	
3-hydroxyacyl-CoA dehydrogenase					↓												↑		
Methylmalonate semialdehyde dehydrogenase												↑							↑
Nucleoside diphosphate kinase beta isoform													↑		↑				
Translation elongation factor 1 alpha 1													↑						↓
Translation elongation factor 1 alpha 1-like 14													↑						↓
Transketolase				↑													↑		
Ornithine transcarbamylase									↓										↓
Urate oxidase									↑										

Key: ↓Direct decrease, ↑Direct increase, ↑or↓Indirectly causes an increase/decrease

Table 4.6.14: Summary of changes observed for OB/IR in comparison to *S. frutescens* group for acidic gels

	Glycolysis	Krebs Cycle	Oxidative Phosphorylation	Pentose Phosphate Pathway	β-Oxidation	Stress Proteins	Gluconeogenesis	Bile Synthesis	Urea Cycle	Detoxification	Fatty Acid Transport	Amino Acid Metabolism	Protein Synthesis	Ketone Body Synthesis	Structural Proteins	Cytokines	Lipid Synthesis	Cholesterol	Protein Degradation
Aldehyde dehydrogenase					↓					↓									
Carbamoyl-phosphate synthetase 1	↑		↑	↑			↓		↓			↓							↓
α-Enolase	↑		↑	↑			↓												
Fructose-1,6-bisphosphatase	↑	↑	↑				↓												
Glutamate dehydrogenase	↑	↓					↓					↓							
Heat shock cognate 71kDa						↓										↓			
3-Hydroxyisobutyrate dehydrogenase												↑							↑
Ornithine carbamoyltransferase									↓			↓							
Oxidase IV cytochrome	↑	↑	↑				↓												
Peroxiredoxin 5						↓													
Pyruvate carboxylase	↑	↑	↑				↓												
Tropomyosin α 4 chain															↓				
Tumor necrosis factor α																↓			

Key: ↓ Direct decrease, ↑ Direct increase, ↑ or ↓ Indirectly causes an increase/decrease

Table 4.6.15: Summary of changes observed for lean control in comparison to *S. frutescens* group for basic gels

	Glycolysis	Krebs Cycle	Oxidative Phosphorylation	Pentose Phosphate Pathway	β-Oxidation	Stress Proteins	Gluconeogenesis	Bile Synthesis	Urea Cycle	Detoxification	Fatty Acid Transport	Amino Acid Metabolism	Protein Synthesis	Ketone Body Synthesis	Structural Proteins	Cytokines	Lipid Synthesis	Cholesterol	Protein Degradation
Acetyl-CoA acetyltransferase 1																		↑	
Aldehyde dehydrogenase										↑									
Calreticulin													↑						
Citrin												↑							
F1-ATPase	↑	↑	↑																
Fatty acid binding protein 1											↓								
D-Glyceraldehyde-3-Phosphate Dehydrogenase	↑	↑	↑				↓												
Glutathione S-transferase						↓				↓									
Glycine N-methyltransferase													↑						
3-hydroxy-3-methylglutaryl-CoA synthase 2					↑													↑	
3-hydroxyacyl-CoA dehydrogenase					↓												↑		
Lactate dehydrogenase		↑																	
Methylmalonate semialdehyde dehydrogenase												↑	↓						↑
Multifunctional acyl-CoA-binding protein											↑								↑
Ornithine transcarbamylase									↑			↑							
Phosphoglycerate kinase 1	↑	↑	↑				↓												
Quinoid dihydropteridine reductase												↑							
Urate oxidase									↑										

Key: ↓ Direct decrease, ↑ Direct increase, ↑ or ↓ Indirectly causes an increase/decrease

Table 4.6.16: Summary of changes observed for lean control in comparison to *S. frutescens* group for acidic gels

	Glycolysis	Krebs Cycle	Oxidative Phosphorylation	Pentose Phosphate Pathway	β-Oxidation	Stress Proteins	Gluconeogenesis	Bile Synthesis	Urea Cycle	Detoxification	Fatty Acid Transport	Amino Acid Metabolism	Protein Synthesis	Ketone Body Synthesis	Structural Proteins	Cytokines	Lipid Synthesis	Cholesterol	Protein Degradation
Calreticulin													↓						↑
Carbamoyl-phosphate synthetase 1, mitochondrial							↑		↑			↑							↑
Chain A, Microsomal Cytochrome b_5																	↓		
Cytochrome b5																	↑		
Fatty acid binding protein											↑						↑		

Key: ↓ Direct decrease, ↑ Direct increase, ↑ or ↓ Indirectly causes an increase/decrease

CHAPTER 5

DISCUSSION AND CONCLUSIONS

CONTENTS

5.1. DISCUSSION AND CONCLUSIONS

Obesity is an increasing problem in the western society and many studies have proven that a westernised diet and a sedentary lifestyle need to be blamed for the problem. However other factors like a genetic predisposition and certain drugs need to share the blame. Several studies indicated that tricyclic antidepressants cause weight gain (Ansseau *et al*., 1989; Garland *et al*., 1988; Berken *et al*., 1984).

This study investigated the metabolic changes brought about by tricyclic antidepressants and a high fat diet and the effect these two factors have on obesity and insulin resistance. Since obesity, insulin resistance and diabetes are increasing in westernised and developing countries, it was further investigated whether *Sutherlandia frutescens*, a South African medicinal plant, can be used to reverse or counteract the metabolic changes. Metformin, a well known hypoglycaemic agent, used for type II diabetes, was also included in the study as a positive control.

5.1.1. Antidepressant Study

Results presented in figure 4.1 of the antidepressant study show that neither amitriptyline nor trimipramine caused any significant weight gain in normal Wistar rats, at a dosage of 1mg/kg, despite contradictory reports which state otherwise. Ansseau *et al*. (1989) reported significant weight gain after only 5 weeks in patients receiving amitriptyline treatment. Garland *et al*. (1988) also reported an average weight gain of between 0.57kg and 1.37kg per month in patients receiving amitriptyline treatment (100-200mg/day). A study undertaken by Berken *et al*. (1984) showed that a mean increase in weight of 1.3 to 2.9lb per month was the net result of six months amitriptyline therapy (maximum doses of 150mg/day), implying that a greater risk of an increase in weight gain is achieved with prolonged tricyclic antidepressant treatment. Fernstorm and Kupfer (1988) also reported amitriptyline related weight gain after 1 month therapy in 73 hospitalized patients receiving a dose of 150-300mg/day. Remick and colleagues (1982) reported a significant increase in weight gain in patients receiving amitriptyline treatment over a 4 week period.

On the other side of the coin Nakra *et al*. (1977) found no weight gain in 6 healthy volunteers after 1 month treatment with amitriptyline and other tricyclic antidepressants. In another study rats receiving 2.5mg/kg amitriptyline for 20 days displayed no change in caloric intake or any significant weight gain in comparison to a control group (Storlien *et al*., 1985). Nobrega and Coscina (1987) confirm these results in their study, which also subjected rats to amitriptyline treatment ranging from 2.5-17mg/kg. In Nobrega and Coscina's study (1987) the treatment produced either no significant increase in weight gain or caloric intake, or slightly reduced levels in comparison to a control group.

There are three clear differences between the groups where the investigators reported weight gain or no weight gain:

- Experiments done with depressed patients or healthy subjects/rats
- Duration of treatment
- Dosage of antidepressants given

Experimentation which resulted in weight gain after amitriptyline therapy focused only on clinically depressed subjects, whereas those studies which did not find weight gain following tricyclic antidepressant treatment, used healthy volunteers or rats. Ansseau *et al*., (1989) Garland *et al*., (1988), Berken *et al*., (1984), Fernstorm and Kupfer (1988) and Remick *et al*. (1982) all used patients diagnosed with depression as subjects for their studies.

The duration of tricyclic antidepressant therapy may also play a role in whether these drugs are responsible for excessive weight gain. Although Berken *et al*., (1984) reported weight gain after 6 months antidepressant treatment and Ansseau *et al*., (1989) after 5 weeks, Fernstorm and Kupfer (1988) and Remick and colleagues (1982) reported a significant increase in weight gain in patients after only one month and four weeks repectively. The healthy volunteers used by Nakra *et al*. (1977) in their study did not show any weight gain after 1 month. The rats used in Nobrega and Coscina's (1987) study also did not display any significant weight gain after a month of amitriptyline

treatment. In the present study the rats did not show any weight gain after 14 weeks and therefore the lack of weight gain was not because of the duration of the experiment.

A reason that no weight gain was found in the present study may be due to the relatively low dose of medication administered to the rats, namely 1mg/kg body weight. Weight gain was reported by Garland *et al*. (1988), Berken *et al*. (1984) and Fernstorm and Kupfer (1988) when depressed patients used 100-200mg/day, 150mg/day and 150-300mg/day amitriptyline respectively. If the average patient weighs 70kg, then all these patients received more than 1mg/kg body weight per day. However rats used by Storlien *et al*., (1985) and Nobrega and Coscina (1987), receiving 2.5mg/kg/day for twenty days and 2.5-17mg/kg/day amitriptykine respectively, did not gain any weight. In the present study 1mg/kg body weight per day was chosen, because this is the dosage given to patients nowadays when tricyclic antidepressants are used to treat depression, pain or sleeplessness. This dosage was lower than any dosage reported to cause weight gain. On the other hand even a much higher dose of amitriptyline (2.5–17mg/kg body weight) given to normal rats by Nobrega and Coscina (1987) did not cause weight gain. It seems therefore that 1mg/kg body weight per day amitriptyline or trimipramine does not contribute to any weight gain in normal rats. The dosage of the two tricyclic antidepressants mentioned is however responsible for certain metabolic changes which are highlighted in the following discussion.

Appetite is controlled by the hypothalamus which is suppressed by factors like the blood glucose levels, the stretching of the stomach and neurotransmitters present in the brain (Tortora and Grabowski, 2003). Figures 4.17 and 4.18 both show an increase in blood glucose levels of tricyclic antidepressant treated rats compared with the control rats. An increase in blood glucose levels should suppress carbohydrate craving that was reported in literature (Ansseau *et al*., 1989; Garland *et al*., 1988). Figure 4.2 also show that tricyclic antidepressant treated rats did not have any difference in appetite compared to control rats. There was also no significant difference in body weights between control groups and tricyclic antidepressant treated rats. A study was undertaken, by Makino *et al*. (2000), to determine the effects that desipramine has on the regulation of neuropeptide Y

mRNA expression. Desipramine is a tricyclic antidepressant with the same mechanism of action as for amitriptyline and trimipramine. Neuropeptide Y is a key neuropeptide which modulates the hypothalamic pituitary adrenal cortex and controls food intake. Neuropeptide Y increases the secretion of corticotrophin-releasing hormone, adrenocorticotropic hormone and corticosterone and also increases food intake (Dallman *et al*., 1993; Stanley *et al*., 1985). Desipramine treated rats showed a reduction in neuropeptide Y mRNA expression in the arcuate nucleus and a significant decrease of this neuropeptide in the locus coeruleus (Makino *et al*., 2000), thus again implying the reduction in appetite brought about by tricyclic antidepressants.

This study did not measure any neuropeptides and no comments can be made on this aspect, though if the appetite of the rats in this study was not suppressed the reason may be linked to the dosage of the tricyclic antidepressants the rats received. The compelling evidence surrounding this debate is endless. Although both sides of the argument provide sufficient scientific evidence supporting their respective hypotheses a possibly important difference is apparent in the subjects used for each study.

In the present study no difference in oxygen consumption, which is related to resting metabolic rate, was found for either test group receiving amitriptyline or trimipramine treatment, in comparison to the control group (figure 4.16). These results confirm results obtained by Dullo and Miller (1987) who conducted a study using 33 drugs known to stimulate the sympathetic nervous system, including amitriptyline and trimipramine. However, in this case the aim of the study was not to determine the effects these drugs may have on weight gain, but rather what thermogenic properties these drugs hold. The drugs were tested on 5 animal models of obesity; genetic mice and rats, hypothalamic mice, dietary mice and rats and finally lean mice. A significant weight loss was found for all the obese animal models receiving tricyclic antidepressant treatment in comparison to their relevant control groups. The weight loss was attributed to a significant increase in metabolic rate brought about by the drug treatment. A reduction in norepinephrine, which plays an important role in the regulation of energy balance, may underlie the development of obesity. The appropriate long term stimulation of norepinepharine action,

such as that brought about by amitriptyline or trimipramine, may reduce body fat by restoring levels of thermogenesis and in so doing returning an energy balance to the body. The lean mouse control however displayed no weight loss or alteration in resting metabolic rate. This result would be expected if obesity is due to a metabolic defect. The drugs would therefore correct the defect in the obese animals by increasing thermogenesis, whereas they would have relatively no effect on the lean controls which have no metabolic defect, once again emphasizing that experimental results are a consequence of the subjects used. All rats used for the present antidepressant study were normal or lean and were not altered through any genetic manipulation or dietary intake, as was the case for Dullo and Miller's (1987) experiment. The amitriptyline or trimipramine treatment does not in any way seem to significantly reduce the resting metabolic rate (figure 4.16), in the present case, which was proposed by Garland *et al*. (1988) as a possible mechanism of tricyclic antidepressant weight gain.

The blood glucose values for both the amitriptyline and trimipramine group were significantly elevated in comparison to the control group after the six and twelve week sacrifice (figures 4.17 and 4.18). The blood glucose of normal lean rats is the same as normal humans therefore the blood glucose levels of rats are comparable with humans. The blood glucose of the trimipramine treated rats after 14 weeks were in the range of 7mM, according to table 1.3 the rats should be diabetic, though their insulin levels were not in the range of diabetic patients.

The elevated serum glucose levels for both test groups may result from the effect that these drugs have on the concentration of norepinephrine in the synaptic cleft. These drugs increase biogenic amine release and block their neuronal reuptake. The net result of this is elevated blood glucose levels brought about by increased glucagon secretion, a direct effect of the biogenic amines, this is speculatory and further investigation is necessary to confirm this. A co-student, in this laboratory, showed however, that amitriptyline promoted insulin secretion (Wilson, 2005). An insulin producing and secreting pancreatic beta cell line, INS-1, was incubated with amitriptyline for various time intervals after which time the surrounding medium was tested and revealed the presence of insulin

secreted by the INS-1 cells (results not shown). The amitriptyline appeared to have directly promoted insulin secretion from these β-cells. The results for the circulating serum insulin (fig. 4.22), however, show the amitriptyline group to have slightly suppressed (but not significant) insulin levels, after 14 weeks medicational compliance, (91.1 ± 11.4pmol/l) in comparison to the control group (102.2 ± 14.9pmol/l). The increased norepinephrine may not be able to compensate for the direct action of the tricyclic antidepressants on the pancreas. The increased norepinephrine or tricyclic antidepressant itself may instead cause an accelerated rate of insulin clearance resulting from the excess insulin being produced and secreted by the β-cells of the pancreas. This possibility is supported by the increased concentration of insulin degrading enzyme found in the liver and muscle of amitriptyline and trimipramine treated groups in comparison to the control group (figures 4.27 & 4.28). Unfortunately only muscle and liver samples from the six week sacrifice could be analyzed as these are the only samples which could be salvaged following the -80^{o}C freezer malfunction. The results obtained from the Western blots displayed significantly higher concentrations of insulin degrading enzyme for both test groups in comparison to the control group at the six week sacrifice period, for liver (9.25 ± 1.3% for control group compared to 12.62 ± 2.1% and 11.48 ± 0.52% for the trimipramine and the amitriptyline group; $p < 0.001$; respectively) and muscle tissue (8.75 ± 2.27% for the control group compared to 11.58 ± 0.73%; $p < 0.001$ and 12.8 ± 0.644%; $p < 0.001$; for trimipramine and the amitriptyline respectively).

An increase in norepinephrine also promotes glycogenolysis which would explain the significantly lower tissue glycogen content at both the 6 and 14 week sacrifice period for both test groups in comparison to the controls (fig. 4.21). The degree of apparent glycogenolysis seems consistent with the blood glucose levels for both time periods, indicating that the excess circulating blood glucose for both test groups is a result of glycogen breakdown. The trimipramine group which displayed the most significant hyperglycaemia at the 14 week sacrifice was also found to have the lowest liver glycogen content. As already mentioned reasons for lower liver glycogen content, relative to that of the muscle, is a result of the overnight fast.

No difference was found for the glucose clearance experiment for either test group in comparison to the control group (fig. 4.19). There was however slight differences in the distribution of the ^{3}H labeled deoxyglucose between the control and test groups, these differences were not significant and only represented trends (fig. 4.20). Norepinephrine and epinephrine cause dilation of blood vessels flowing to major organs such as the brain, heart, liver, skeletal muscle and fat (Tortora and Grabowski, 2003). A slight increase in the [^{3}H] deoxyglucose is apparent in the muscle for both test groups but not the epididymal fat. There is too much variation in the liver samples due to the presence of excess blood in the surrounding vessels and capillaries, which masks the true concentration of [^{3}H] deoxyglucose in the hepatocytes. GLUT2 transporters, in the hepatocytes, allow the deoxyglucose to move in and out of the cells freely thereby contributing to the variation among samples of the same group.

The results obtained during this study indicate that neither of the tricyclic antidepressants, amitriptyline nor trimipramine, are directly related to weight gain through carbohydrate craving or alteration of the resting metabolism, at least under the experimental conditions used for this study. It therefore seems likely, that the weight gain reported by Ansseau *et al*., (1989), Berken *et al*., (1984) and others may be an indirect result of the antidepressant therapy rather than a direct one. As already mentioned depression is associated with many side effects, one such side effect being a decreased appetite and resting metabolic rate. The tricyclic antidepressants such as amitriptyline and / or trimipramine may restore the resting metabolic rate while simultaneously increasing the mood of the patient. An increased appetite may soon follow as a result of the mood change. It is likely to be expected that similar considerations may not apply to the rat model used in the present study.

The conclusion arising from this section of the work seems to be that the tricyclic antidepressants, amitriptyline and trimipramine, do not alter a normal, healthy metabolism to bring about excessive weight gain. However, an already altered metabolism, such as an individual with a predisposition to obesity or a clinically depressed individual, may experience alterations or corrections in their metabolism as a

result of tricyclic antidepressant therapy. Further investigations along this avenue, using clinically depressed human subjects paralleled with healthy volunteers are needed and may answer some questions on this subject, and finally bring an end to the heated debate surrounding it. What is however clear, is that amitriptyline and imiprimine increase blood glucose levels and increase insulin degration. Medical practinioners should therefore be aware of this fact when prescribing tricyclic antidepressants, especially trimiprimine to patients who can be predisposed to develop diabetes.

5.1.2. Diabetes Study

Insulin resistance is a complex disease and mimicking such a disease in an animal model, although challenging, allows for an in depth look into the development of the metabolic syndrome and how it would become established in an individual following an unhealthy diet and lack of exercise lifestyle. The rats for this study were fed a high fat diet (OB/IR diet) in an attempt to bring about insulin resistance. The diet was started immediately following weaning, allowing sufficient time for the development of insulin resistance when the rats reach maturity. The rats also were not exposed to any physical activity, which has been well documented to alleviate or reverse the effects brought about by insulin resistance. A combination of comparative results, obtained from the present study, confirmed that insulin resistance was achieved by the OB/IR diet after 13 weeks:

1. Hyperinsulinaemia combined with normoglycaemia (figs. 4.34 and 4.33 respectively).
2. Reduced glucose clearance (fig. 4.35).
3. Reduced muscle glucose uptake (figs. 4.36a).
4. Reduced insulin signaling proteins (4.43, 4.44, 4.45, 4.46, 4.48, 4.49 & 4.50)
5. Increased hepatic gluconeogenic enzymes (fig. 4.40 & tables 4.6.1. and 4.6.5.).
6. Increased enzymes involved in β-oxidation (tables 4.6.1. and 4.6.5).

The resulting hyperinsulinaemia associated with the OB/IR diet would typically result in an increase in circulating free fatty acids. The increase in free fatty acids eventually make their way into the β-cells, via the fatty acid binding protein 2, where they are converted into malonyl-CoA, which inhibits carnitine palmitoyl transferase-1 and in so doing

impairs the transport of fatty acyl-CoAs into the mitochondria where they can be oxidised by the citric acid cycle. The resulting build up of the fatty acyl-CoA within the cytosol of the β-cells is the reason for the increased insulin secretion associated with high fat diets. The resulting hyperinsulinaemia is then brought about by a combination of three mechanisms (McGarry, 2002; Shimabukuro *et al*., 1998, Matschinsky, 1996; Newgard and McGarry, 1995):

1. Enhanced exocytosis of stored insulin via the activation of protein kinase C resulting from the increased production of phosphatidic acid and diacylglycerol.
2. An increase in intracellular calcium concentration resulting from the stimulation of endoplasmic reticulum calcium adenosine triphosphatase.
3. Depolarization of the β-cell membrane due to closure of K^+-ATP channels, resulting in an increase in intracellular calcium concentration, which in turn promotes exocytosis of insulin containing granules.

Due to budget constraints, the determination of serum free fatty acids was not part of the original research protocol. Results of the present study strongly recommend that serum free fatty acid determination should be done in future studies to confirm the mechanism of development of insulin resistance as is suggested by the present study.

An increase in plasma free fatty acids promotes hepatic free fatty acid uptake, which leads to an acceleration in lipid oxidation and an accumulation of acetyl-CoA (Bays *et al*., 2004). The accumulation of intracellular acetyl-CoA stimulates the gluconeogenic rate limiting enzymes, pyruvate carboxylase and fructose-1,6-bisphosphatase, and also activates glucose-6-phosphatase, the rate controlling enzyme for hepatic glucose release. This process, which is most probably the early start of this tragic disease, is masked by the hyperinsulinaemia keeping the individual within the normoglycaemic range. A significant reduction in liver glycogen content was evident for the OB/IR fed rats relative to the lean control group (fig. 4.39). Glycogen is the storage form of excess glucose, especially in liver and muscle. The liver glycogen is utilized during times of starvation (Baron *et al*., 1987; Nelson and Cox, 2000; Matsuda *et al*., 2002). The reduced liver glycogen content, for the OB/IR group (fig. 4.39) results from the increased

glycogenolysis as has been confirmed as well by the increased levels of glucose-6-phosphatase activity (fig. 4.40). The increased levels of fructose-1,6-bisphosphatase (table 4.6.5) would reflect increased liver gluconeogenesis (from non-carbohydrate precursors) in the OB/IR groups as compared to the lean controls. Note that both enzymes, fructose-1,6-bisphosphatase and glucose-6-phosphatase, are present in liver, whereas only the former is present in muscle. Liver is also the primary site for gluconeogenesis as well as glycogenolysis. Lowering of liver glycogen in OB/IR rats would thus result from glycogenolysis, which could/would be accompanied by subsequent gluconeogenesis as well, thus explaining elevated levels of both enzymes in liver in OB/IR relative to lean controls. The OB/IR group's muscle glycogen content was not affected in the same way as for the liver in comparison to the lean control group (fig. 4.39). Although the glucose uptake in the muscle was significantly lower for the OB/IR rats (fig. 4.36a) the muscle glycogen did not alter significantly (fig. 4.39). It needs to be remembered that glycogen represents the amount of glucose stored in tissue. By comparing figures 4.39 and 4.36 it becomes clear that the glycogen content of a tissue does not only indicate the glucose uptake or for that matter insulin resistance, but is rather a function of both the glucose uptake and utilization of glucose in the tissue concerned.

Gluconeogenesis is energetically costly. For each molecule of glucose formed from pyruvate, 6 high energy phosphate groups are required (4 from ATP and 2 from GTP) as well as 2NADH molecules (Nelson and Cox, 2000). The high energy requirement for this pathway is to ensure that it stays irreversible, avoiding any futile cycling with glycolysis. The increase in 3-hydroxyacyl-CoA dehydrogenase activity (table 4.6.1) implies an increase in β-oxidation, which is the removal of two carbon units from the carboxyl end of a fatty acid chain in the form of acetyl-CoA. The acetyl-CoA is then able to enter the citric acid cycle producing NADH and $FADH_2$ which drives ATP synthesis by participating in the electron transfer chain of oxidative phosphorylation. A total of 131 ATP molecules are able to be produced from the oxidation of palmitoyl-CoA. β-oxidation is an alternative source of ATP production when glycolysis is hindered, as it is in the case of insulin resistance. The large quantities of ATP produced from fatty acid oxidation is able to drive gluconeogenesis allowing the brain, nervous system, kidney medulla, testes

and erythrocytes to function normally, with glucose as their major fuel source (Nelson and Cox, 2000). The relative decrease in the OB/IR group's Cytochrome b_5 concentration (table 4.6.5) implies a decrease in fatty acid production. Cytochrome b_5 is involved in the desaturation of palmitate and stearate to produce palmitoleate, 16:1(Δ^9) and oleate, 18:1(Δ^9) (Nelson and Cox, 2000). An increase in β-oxidation would ensure that any lipid synthesis would be suppressed as to avoid loss of energy through futile cycling.

The reduction in liver transketolase concentration (table 4.6.1) for the OB/IR control group implies a decrease in the nonoxidative pentose phosphate pathway. The oxidative pentose phosphate pathway constitutes part of the secondary metabolism of glucose, producing the products; NADPH, necessary for fatty acid synthesis, and ribose-5-phosphate, utilized for nucleic acid biosynthesis. The nonoxidative pathway recycles the ribose-5-phosphate produced back into glucose-6-phosphate in an attempt to increase the output of NADPH. The decreased activity of the nonoxidative pathway implies a decrease in fatty acid synthesis. Fatty acid synthesis is hormonally affected by insulin, glucagon and norepinephrine, with insulin promoting the synthesis of fatty acids and the latter two hormones promoting lipid catabolism (Nelson and Cox, 2000). The insulin resistance associated with the OB/IR control group, refered to at the beginning of this section, would therefore be the reason for the decrease in fatty acid synthesis.

The muscle insulin resistance resulting from the OB/IR diet, represented through the inhibition of the PI-3-kinase pathway (fig. 4.46), is again believed to result from elevated free fatty acids. Randle *et al*., (1963) proposed that increased fatty acid oxidation restrains glucose oxidation in muscle by altering the redox potential of the cell and by inhibiting key glycolytic enzymes (Bays *et al*., 2004; Randle *et al*., 1963). Randle *et al*., (1963) proposed the mechanism of this muscular insulin resistance (Randle cycle) to occur as follows:

> The elevated concentration of free fatty acids leads to an increase in their oxidation, causing an elevation of the intracellular acetyl-CoA and citrate concentration and of the NADH/NAD^+ ratio. The increased acetyl-CoA and citrate concentrations result in the inhibition of pyruvate dehydrogenase and phosphofructokinase, respectively, while the elevated NADH/NAD^+ ratio results

> in the slowing of the citric acid cycle. Phosphofructokinase inhibition results in the accumulation of glucose-6-phosphate, which in turn inhibits hexokinase II, causing a decrease in glucose phosphorylation leading to an elevation in intracellular free glucose which restrains glucose transport into the cell via GLUT4. The resultant decrease in glucose transport impairs glycogen synthesis, although a direct inhibitory effect of fatty acyl-CoAs on glycogen synthase has been demonstrated by Wititsuwannakul and Kim (1977) (Bays *et al*., 2004).

The product inhibition theory, forming the backbone of the Randle theory, was however found to be flawed when investigators observed an increase in glucose-6-phosphate and citrate levels followed by a decrease in phosphofructokinase when insulin stimulated glucose metabolism was inhibited by a lipid infusion leading to an elevation in circulating free fatty acids (Boden *et al*., 1994; Roden *et al*., 1999; Boden, 1999). This proved that alternate factors other than product accumulation were the causative agent associated with insulin resistance. Studies performed on human skeletal muscle implicate increased intramuscular concentrations of fatty acyl-CoAs and diacylglycerol, resulting from elevated free fatty acids, activating protein kinase Cθ, which increases serine phosphorylation with the subsequent inhibition of IRS-1 tyrosine phosphorylation, which impairs the signaling of the remaining proteins situated downstream of the insulin signaling cascade. A direct effect of long chain fatty acyl-CoAs on the inhibition of glucose transport, glucose phosphorylation and glycogen synthase has also been demonstrated in muscle (Schmitz-Peiffer *et al*., 1999; Chavez *et al*., 2003).

The significant reduction in insulin receptor β-subunit concentration for the OB/IR group in muscle (fig. 4.43) would imply a potential decrease in phosphorylation sites, of the tyrosine kinase domains on the carboxy terminus, ultimately leading to a decline in intracellular insulin signaling. A decrease in the β-subunit would almost certainly imply a similar decrease in the α-subunit concentration brought about by the hyperinsulinaemia (fig. 4.34) which would result in down-regulation of the insulin receptor (Tortora and Grabowski, 2003; Taylor, 1992; Olefsky, 1976). The hyperinsulinaemia will eventually lead to β-cell exhaustion and apoptosis resulting in an insulin dependent diabetic state.

Both the muscle IRS-1 and the IRS-2 proteins were found to be reduced for the OB/IR group in comparison to the lean control, however only the IRS-1 protein was significantly

reduced (figs. 4.44 and 4.45 respectively). IRS-1 and IRS-2 proteins have been found to be significantly suppressed in diabetic animals and human subjects (Taniguchi *et al*., 2005). Under normal circumstances the IRS tyrosine domains would become phosphorylated as part of the insulin receptor activation cascade. As already discussed, in section 1.5.8.1, IRS-1 knockout mice showed signs of insulin resistance, β-cell hyperplasia and glucose intolerance, while IRS-2 knockout mice displayed liver and peripheral tissue insulin resistance, impaired β-cell functioning and developed overt type II diabetes. IRS-2 is known to play a more prominent role in the liver, while IRS-1 is predominantly involved in muscle insulin activation (Taniguchi *et al*., 2005).

A significant increase in hepatic TNFα was found for the OB/IR group relative to the lean control group (refer to table 4.6.5), which implies an increase in TNFα production from mature adipocytes. TNFα is a pro-inflammatory cytokine which has been implicated, along with plasma free fatty acids, to interfere in the early steps of insulin signaling, as demonstrated in the accompanying figure (Gual *et al*., 2005). TNFα has been shown to decrease insulin stimulated glucose transport through decreasing the expression of the insulin receptor, IRS-1 and GLUT4 (Bjornholm and Zierath, 2005), all of which were significantly suppressed for the OB/IR group in this study. Increased TNFα levels, associated with obesity, have also been implicated in reducing insulin stimulated tyrosine phosphorylation of IRS-1 through promoting its serine phosphorylation. The serine phosphorylation brings about a conformational change in the IRS-1 protein resulting in a decrease in its potential interaction with the insulin receptor (Ferri *et al*., 1995; Hotamisligil, 1999). Increased concentrations of muscle fatty acyl-CoAs and diacylglycerol have lead to the activation of protein kinase Cθ which has also been shown to increase the serine phosphorylation of IRS-1 proteins (De Fea and Roth, 1997; Kelly and Mandarino, 2002). The increased TNFα levels, associated with OB/IR diet, reduced post receptor insulin signaling through decreasing the IRS-1 protein expression and/or

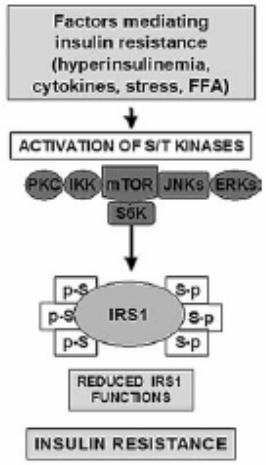

(Gual *et al*., 2005)

decreasing its substrate interaction capabilities with the insulin receptor by promoting serine phosphorylation.

The p85 regulatory subunit of the PI-3-kinase protein is next to be stimulated by the tyrosine phosphorylated IRS proteins in the insulin signaling cascade. PI-3-kinase is activated by insulin, insulin-like growth factor-1 and other growth factors. PI-3-kinase consists of a regulatory p85 subunit, which binds to the IRS proteins, and a catalytic subunit which phosphorylates phosphatidylinositol-4,5-biphosphate to produce phosphatidyl inositol 3,4,5-triphosphate (PIP_3). PIP_3 acts as a secondary messenger by recruiting PI-3-kinase-dependent serine/threonine kinases (PDK1) and protein kinase B from cytoplasm to the plasma membrane by binding to the "pleckstrin homology domain" (PH domain) of the kinases. Lipid binding and membrane translocation lead to conformational changes in protein kinase B that is subsequently phosphorylated on Thr 308 and Ser 473 by PDK1. Phosphorylation by PDK1 leads to full activation of protein kinase B, which phosphorylates and, in so doing, regulates the activity of certain downstream proteins involved in numerous aspects of cellular physiology. Protein kinase B also phosphorylates and regulates components which are essential to insulin mediated metabolism, such as the GLUT4 complex, protein kinase C (PKC) isoforms, and GSK3 (Shepherd *et al*., 1998; Ueki *et al*., 1998; Czech and Corvera, 1999; Farese, 2001). Inhibition of PI-3-kinase was found to significantly reduce the formation of PIP_3, which in turn decreased the translocation of GLUT 4 (Kanai *et al*., 1993; Okada *et al*., 1994; Clarke *et al*., 1994; Cheatham *et al*., 1994; Bjornholm and Zierath, 2005). The decreased PIP_3 concentration associated with the OB/IR diet (fig. 4.46) is as a result of the decreased p85 regulatory subunit, which would ultimately lead to the formation of PIP_3. Insulin resistance is known to alter the catalytic activities of PI-3-kinase and protein kinase B and in so doing attenuate the metabolic syndrome, however the decreased concentration of these proteins (including total GLUT4 content) found to be associated with the OB/IR diet is more likely to be a result of insulin resistance rather than the reason for it. Whole body GLUT4 knockout mice have been shown to display slight hyperglycaemia and experienced a shortened lifespan, whereas muscular GLUT4 disruption lead to insulin resistance and glucose intolerance (Katz *et al*., 1995). The

reduction in glucose clearance for the OB/IR group (fig. 4.35) is due to the decreased insulin signaling cascade protein concentrations and/or conformational changes resulting from incorrect phosphorylations.

No significant difference in the phosphorylated p38 MAPK residue was found between either of the control or test groups (fig. 4.47). Kumar and Dey (2002) found that insulin stimulated p38 phosphorylation was impaired in insulin resistant C2C12 muscle cells and they implicated p38 as an important component in glucose uptake when the PI-3-kinase pathway is inactivated. Fujishiro *et al*., (2001) demonstrated that this was possible because p38 activation increased GLUT1 expression; and since p38 MAPK has also been reported to be activated by TNFα, interleukin-1 and hyperosmotic shock (Kulisz *et al*., 2002; Kundua *et al.*, 2005), implicates p38 activation as a method in which cells are able to meet their energy demands during times of stress. The high standard deviations do not allow any conclusion to be drawn, although it seems that the p38 for the OB/IR group could show a tendency to be increased, which would imply an increased GLUT1 expression, further investigations are however needed.

The overactive phenylalanine hydroxylase (table 4.6.5), resulting from the OB/IR diet, implies an increased concentration in circulating phenylalanine, which may be the result of increased protein degradation. The overactive citrin carrier protein (aspartate / glutamate shuttle) (table 4.6.1), for the OB/IR group, represents an increase in the shuttling of aspartate and glutamate between the cytosol and the mitochondrial matrix. Once glutamate has entered the mitochondrial matrix, in exchange for aspartate, it is converted into α-ketoglutarate, by glutamate dehydrogenase, which may then enter the citric acid cycle. The activity of glutamate dehydrogenase is increased for the OB/IR group (table 4.6.5) relative to that of the lean control group, implying an increase in α-ketoglutarate production. The cytosolic aspartate may now be converted into oxaloacetate by aspartate aminotransferase which in turn may be converted into malate by cytosolic malate dehydrogenase. The malate is then able to enter the mitochondrial matrix through the oxoglutarate / malate carrier in exchange for the α-ketoglutarate. The mitochondrial malate can now be converted into oxaloacetate by mitochondrial malate dehydrogenase

(table 4.6.1) (Scholz *et al*., 1998; Nelson and Cox, 2000). This enzyme is however significantly reduced for the OB/IR group in comparison to the lean control group, which would result in a significant reduction in mitochondrial oxaloacetate concentration. The reduction in mitochondrial malate dehydrogenase may imply a reduction in malate / oxoglutarate shuttling, which would result in a build up of mitochondrial α-ketoglutarate, which may be utilized for the citric acid cycle instead of being utilized for malate shuttling. The mitochondrial aspartate aminotransferase (glutamate oxaloacetate transaminase 2) activity was also found to be reduced for the OB/IR group in comparison to that of the lean control group, this result is however not significant; 0.117 ± 0.048% IOD versus 0.149 ± 0.069% IOD respectively (result not shown). The reduction in this aminotransferase activity implies that less oxaloacetate is being converted into aspartate. Since the mitochondrial malate dehydrogenase concentration is severely reduced, allowing for less oxaloacetate to be produced, it would make sense that the aspartate aminotransferase concentration is also lower. Less substrate for the enzyme would cause a decrease in its activity.

The main function of the malate / oxoglutarate shuttle is to provide a transport system for cystolic NADH, produced during glycolysis, to the mitochondrial matrix where it can be utilized for oxidative phosphorylation. However, if glycolysis is impaired (significant reduction in aldolase B), as is anticipated, in the OB/IR group, due to insulin resistance, then this shuttle would no longer need to function. The overactive aspartate / glutamate shuttle and glutamate dehydrogenase enzyme imply an increase in intracellular α-ketoglutarate for the citric acid cycle, which may then enter the gluconeogenic pathway.

The conversion of glutamate into α-ketoglutarate, by glutamate dehydrogenase, produces ammonia as a by product. As ammonia is toxic to living organisms it needs to be excreted, this is achieved through the urea cycle. First, the ammonia is converted into carbamoyl phosphate by carbamoyl phosphate synthetase-1, which is increased for the OB/IR treated group (table 4.6.5). The carbamoyl phosphate now enters the urea cycle by donating its carbamoyl group to ornithine to form citrulline and simultaneously releasing a phosphate group in a reaction catalysed by ornithine carbamoyltransferase, which also

is significantly increased (table 4.6.5) for the OB/IR treated group (Nelson and Cox, 2000).

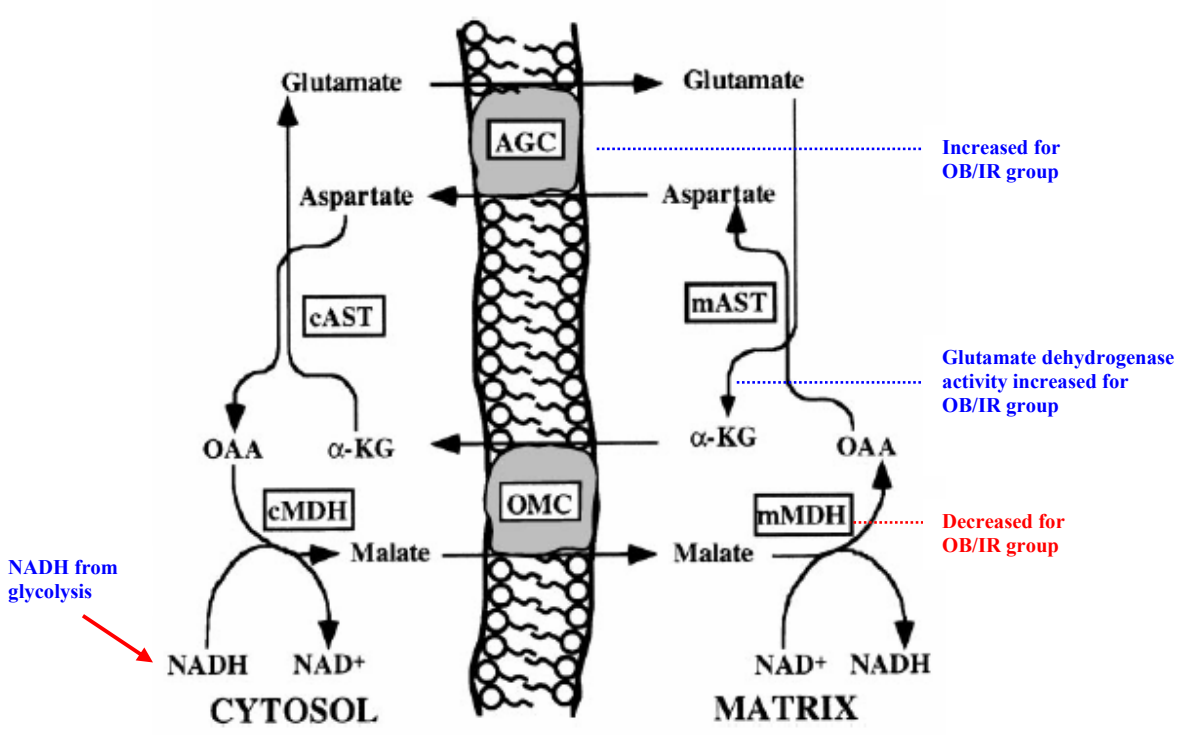

Figure 5.1: Malate-aspartate shuttle, a section of the inner mitochondrial membrane separates the cell's cytosol from the mitochondrial matrix (Scholz *et al*., 1998).
Key: AGC – aspartate/glutamate carrier, cAST & mAST – cytosolic and mitochondrial aspartate aminotransferase, α-KG – α-ketoglutarate, cMDH & mMDH – cytosolic and mitochondrial malate dehydrogenase, OAA – oxaloacetate, OMC – oxoglutarate/malate carrier.

The increased phenylalanine hydroxylase and glutamate dehydrogenase (table 4.6.5), for the OB/IR group, imply an increase in amino acid metabolism through the citric acid cycle. The ammonia produced as a by product of these reactions are then removed by the urea cycle, this is confirmed by the increased carbamoyl phosphate synthase-1 and ornithine carbamoyltransferase. An increase in amino acid oxidation implies an increase in citric acid cycle intermediates for gluconeogenic reactions.

Amino acid degradation is commonly associated with diabetes and insulin resistance but only accounts for approximately 10-15% of the body's total energy production. The activities of these catabolic pathways vary greatly, between the 20 amino acids, and

depend upon the balance between requirements for biosynthetic processes and amounts of a given amino acid availability (Nelson and Cox, 2000). The valine catabolic pathway seems to be decreased for the OB/IR treated group through a decrease in both the methylmalonate semialdehyde dehydrogenase (MMSD) (table 4.6.1) and 3-hydroxyisobutyrate dehydrogenase (3-HBD) (table 4.6.5) concentration (Nelson and Cox, 2000). The reaction catalysed by thes enzymes are shown below.

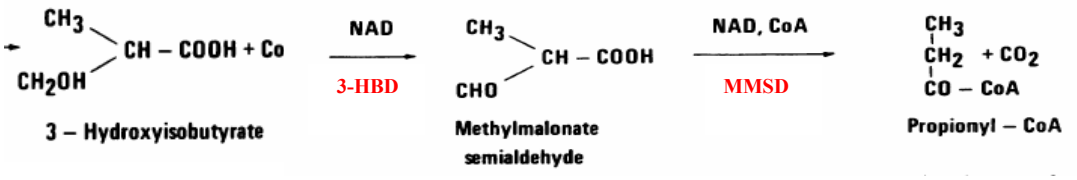

(Taken from Marshall and Sokatch, 1972)

Propionyl-CoA would then be converted to methylmalonyl-CoA which in turn would be converted into succinyl-CoA, a citric acid cycle intermediate. Valine is an essential amino acid which can only be obtained from the diet (Nelson and Cox, 2000). Wijekoon *et al*., (2004) showed that serum and hepatic branched chain amino acids were elevated in Zucker fatty rats during the insulin resistant pre-diabetic stage and the type II diabetic stage (Wijekoon *et al*., 2004).

The concentration of hydroxysteroid 11-β dehydrogenase-1 (table 4.6.1) is significantly reduced for the OB/IR group in comparison to that found for the lean control group, this enzyme catalyzes the reduction of inactive11-deoxycortisol to its active form cortisol.

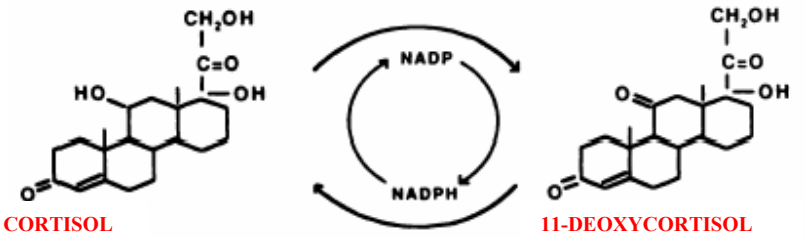

(Taken from Monder, 1991)

Although cortisol is known to increase β-oxidation and gluconeogenesis it is also known to significantly inhibit insulin release (Tortora and Grabowski, 2003) as discussed in section 1.6.5. Both the metabolic effects of glucocorticoids, namely, insulin resistance

and hepatic glucose production, result in increased serum insulin levels (Davani *et al*., 2000). This is however attenuated by the direct inhibitory effects glucocorticoids have on insulin release both *in vitro* and *in vivo* (Davani *et al*., 2000). A study undertaken by Davani *et al*., (2000) showed that 11-β-hydroxysteroid dehydrogenase 1 (11-β-HSD-1) knockout *ob/ob* mice showed decreased hyperglycaemic levels due to enhanced insulin release as a result of the 11-β-HSD-1 -/-. The reduction in 11-β-HSD-1 (table 4.6.1) found for the OB/IR treated group may be a result of the extremely high serum insulin levels, which may effect the 11-β-HSD-1 expression:

↓ 11-β-HSD-1 → ↓ Glucocorticoids → Hyperinsulinaemia → Insulin Resistance

17-β-hydroxysteroid dehydrogenase, type IV, concentration was suppressed in the OB/IR group. This enzyme is responsible for inactivating testosterone by catalyzing the production of keto forms (Fan *et al*., 1998). Significant fluctuations in circulating testosterone levels have been implicated in the development of peripheral tissue insulin resistance. A study undertaken by Holmang and Bjorntorp (1992) on orchidectomized rats, which are unable to produce their own testosterone, showed that skeletal muscle insulin resistance to both glucose uptake and glycogen synthesis was achieved following either chronic testosterone treatment or no treatment at all. The altered testosterone levels mainly affected peripheral tissue insulin sensitivity and seemed to enhance glycogen phosphorylase while inhibiting glycogen synthase activity. When low levels of testosterone was administered to the rats all metabolic abnormalities were reversed, indicating that physiological concentrations of testosterone promote insulin sensitivity while deleterious concentrations impair the action of insulin (Livingstone and Collison, 2002). The decrease in 17-β-hydroxysteroid dehydrogenase, type IV, levels associated with the OB/IR control group (table 4.6.1) will lead to a decrease in the inactivation of testosterone leading to an increase in concentration of the steroid hormone which would augment skeletal muscle insulin resistance. However, a significant decrease in this enzyme's activity may be a result of a reduction in circulating testosterone levels, in other words a decrease in the enzyme due to a decrease in substrate availability. Studies have shown that obese men suffering from insulin resistance and hyperinsulinaemia have a significant reduction in circulating testosterone levels. Testosterone replacement in these

men alleviated insulin resistance, shown by a glucose clamp technique (Haffner *et al*., 1993). None of these studies took into account whether the resulting circulating testosterone levels were due to an over production of 17-β-hydroxysteroid dehydrogenase or due to a faulty deactivation process of the hormone.

Studies have shown that animal cells incubated with high levels of steroids have a reduction in intracellular IRS-1, IRS-2 and PI-3-kinase concentrations and a reduction in GLUT4 translocation, leading to a significant reduction in glucose clearance (Clark *et al*., 2000). Since these proteins were found to be significantly reduced in the skeletal muscle of the OB/IR control group (figs. 4.44, 4.45, 4.46) the decreased levels of 17-β-hydroxysteroid dehydrogenase may account for an increase in testosterone which would then be responsible for associated skeletal muscle insulin resistance. Determination of concentrations of circulating testosterone levels are, however necessary to verify this statement.

The increased [^{3}H] deoxy-glucose counts found in the urine for the OB/IR control and both test groups following the glucose clearance experiment (fig. 4.37) is unusual as the glucose should only be in the urine when the blood glucose levels are higher than the Tm value, which was not the case here. Even though this is an extremely sensitive method of determining glucose levels there should not be any significant differences between the groups. An explanation for this increased urinary glucose may be an increase in circulating inflammatory cytokines augmented by the OB/IR diet. These inflammatory cytokines normally increase the permeability of capillaries and therefore may affect the glomerular filtration within the kidneys and in so doing allow more glucose to be excreted in the urine in relation to the lean control group.

An investigation into the metabolic effects brought about by the OB/IR diet, used in this study, was undertaken by Nkabinde (2004). The study showed that the diet brought about hyperinsulanemia after 6 weeks followed by a significant reduction in circulating serum insulin levels after 12 weeks. This reduction was found to be attributed to a significant reduction in functional β-cells as determined through pancreatic immuno-cytochemistry

studies. The increase in gluconeogenesis and β-oxidation imply that the rats in the present study were shifting towards full blown type II diabetes. As already discussed, the insulin resistant phase is characterized by suppressed β-oxidation leading to an increase in intracellular fatty acyl-CoAs which augments insulin resistance and insulin secretion. The increased β-oxidation found for the OB/IR group will allow for a reduction in intracellular fatty acyl-CoAs leading to a decrease in insulin secretion. It is important to note that this decrease in intracellular fatty acyl-CoAs does not alleviate insulin resistance. Increased plasma triglycerides and free fatty acids, linked to adipocyte dysfunction, directly inhibit glucose transport, GLUT4 concentration, glucose phosphorylation, insulin stimulated tyrosine phosphorylation of IRS-1, the association of the p85 subunit of PI-3-kinase with IRS-1, the activation of phosphoinositol-3-kinase and glycogen synthase (Tippett and Neet, 1982; Dresner *et al*., 1999; Thompson and Cooney, 2000; Kruszynska *et al*., 2002; Kashyap *et al*., 2002).

Metformin was chosen as a positive control for this experiment as it has proven itself for decades as an effective hypoglycaemic agent in the treatment of type II diabetes brought about by insulin resistance. Although the early steps which mediate its antidiabetic action remain unclear it is still prescribed to patients suffering from type II diabetes in an attempt to bring about a normal lifestyle for these individuals.

Certain aspects of the blood glucose lowering characteristics, brought about by metformin, have been identified over the many years of its use; in particular its ability to inhibit intestinal glucose uptake, decrease gluconeogenesis and increase hepatic glycogen synthesis (Jackson *et al*., 1987; Mithieux *et al*., 2002). The inhibition of the enzymatic activity of complex I of the respiratory chain, by metformin, has been uncovered as the mechanism which brings about its accelerated rate of glucose uptake. Complex I impairment of cellular respiration immediately reduces the ATP/ADP, ATP/AMP and phosphocreatine to creatine ratios, *in vivo*, thereby causing an activation of AMP activated protein kinases, which in turn stimulates glucose transport, glycolysis and glycogenesis on the short term and alleviates hyperglycaemia and insulin resistance in the long term. The principle behind this mechanism of action is the same as that found during

muscle contractions associated with prolonged exercise training, which would also result in an overall decrease in the ATP/ADP ratios. Thiazolidone drugs were also found to significantly inhibit cellular respiration through promoting an increase in circulating adiponectin, and are thought to alleviate hyperglycaemia in this way (Young *et al*., 1996; Hardie and Hawley, 2001; Musi *et al*., 2002; Hayashi *et al*., 2000; Mu *et al*., 2001; Zhou *et al*., 2001; Dean and Ruderman, 2002; Hawley *et al*., 2002).

Metformin has been shown to significantly reduce body weight in obese human subjects and Zucker rats by Paolisso and colleges (1998). However, no significant fluctuations in weight were evident throughout the present study for the metformin treated group (refer to fig. 4.29). The weight loss associated with metformin treatment in obese subjects is thought to be associated with a decrease in food intake brought about by enhanced insulin sensitivity. This observation came about when chronic intracerebroventricular administration of insulin in different animals led to a dose-dependent reduction in food intake. Fierdman (1995) hypothesized that metformin affects food intake by improving energy (ATP) production within the body. In other words a decline in ATP production in obese individuals brought about by decreased glycolysis and increased gluconeogenesis, resulting from impaired glucose uptake, acts as a metabolic stimulus that triggers feeding (Paolisso *et al*., 1998). This theory contradicts the findings that metformin reduces ATP levels by suppressing the respiratory chain through inhibition of complex I (Young *et al*., 1996; Hayashi *et al*., 2000; Hardie and Hawley, 2001; Mu *et al*., 2001; Zhou *et al*., 2001; Hawley *et al*., 2002; Dean and Ruderman, 2002; Musi *et al*., 2002). Since the rats for this study were not obese, no significant decrease in rat weight was expected for the metformin treated group. All the rats received the same amount of food throughout the experiment and were not overfed at any time.

Suzuki *et al*., (2002) found evidence contradicting Paolisso and colleagues (1998), insofar as metformin treatment significantly increased body weight in obese Wistar rats in comparison to both obese and lean controls, even though food intake was slightly, but insignificantly, suppressed relative to the obese control group. Suzuki *et al*., (2002) found no weight difference between liver, mesenteric or inguinal adipose tissues between the

different groups. A slight but insignificant increase in brown adipose tissue was evident, but no explanation was attempted, by the authors, for the weight gain found following metformin treatment.

A significant increase in epididymal fat weight was found for the metformin treated group, in the present study (2.3 ± 0.12%; $p < 0.001$), compared to both the OB/IR (1.4 ± 0.3%) and lean control group (1.0 ± 0.17%) (fig. 4.38). This increase in epididymal fat weight would not cause a significant increase in body weight since it makes up such a small percentage of the total body weight. The reason for the increased weight of the epididymal fat pads, for the metformin group, is presently unknown.

No fluctuation in the basal metabolic rate was found, following metformin treatment, when compared to either of the control groups (fig. 4.32), nor was it expected. Metformin treatment is not known to significantly alter the basal metabolic rate, even in obese individuals. A study undertaken by Paolisso *et al*., (1998) found metformin treatment to cause no fluctuations in basal metabolic rate in obese subjects, thereby confirming the results obtained in the present study.

The hyperinsulinaemia associated with metformin treatment, in the present study (fig. 4.3.6), is disturbing at first sight, being significantly elevated relative to the OB/IR control group. However, as already mentioned the OB/IR control rats are expected to be moving into full blown type II diabetes which is associated with β-cell apoptosis and a subsequent decrease in the production and secretion of insulin. The elevated serum insulin levels, resulting from metformin treatment relative to the OB/IR group, could thus result from the medication not allowing the pathogenesis of full blown type II diabetes to progress as it normally would, through the apoptosis of β-cells. Previous studies have shown serum insulin levels to remain unchanged (hyperinsulanaemic) in obese subjects following metformin therapy (Jackson *et al*., 1987; Paollisso *et al*., 1988; Davidson and Peters, 1997; Suzuki *et al*., 2002). It has been well documented that metformin does not increase insulin secretion (Karam *et al*., 1978) and as it is unable to reduce hyperinsulinaemia. The reason for this is due to metformin being unable to significantly

decrease plasma free fatty acids in obese subjects (Jackson *et al*., 1987; Paollisso *et al*., 1988; Davidson and Peters, 1997; Suzuki *et al*., 2002). As already discussed, increased intracellular acyl-CoAs resulting from high fat feeding eventually leads to an increase in insulin secretion, a consequence of β-cell dysfunction (Newgard and McGarry, 1995; Matschinsky, 1996; Shimabukuro *et al*., 1998; McGarry, 2002). As already mentioned, the increased β-oxidation and gluconeogenesis, associated with the OB/IR group, imply that these rats are shifting towards full blown type II diabetes. The increased β-oxidation, associated with the OB/IR group, will alleviate the accumulation of intracellular fatty acyl-CoAs and in doing so cause a reduction in insulin secretion. The metformin, however, causes a significant reduction in enzymes involved in β-oxidation, thereby not allowing for the removal of intracellular acyl-CoAs which may be the reason for the significantly higher serum insulin levels for this group in comparison to the OB/IR control group. The increased hepatic TNFα levels associated with the OB/IR control group (refer to table 4.6.5.), was only slightly and insignificantly decreased by metformin treatment; OB/IR: 0.156 ± 0.011% IOD versus Metformin: 0.13 ± 0.016% IOD (results not shown). Although only hepatic TNFα levels were measured, the results suggest that the total concentration of TNFα may be increased or decreased. As already mentioned, increased TNFα levels have been associated with increased cellular insulin resistance (Gual *et al*., 2005). Increased TNFα levels have also been shown to promote β-cell dysfunction, increasing insulin production and secretion. The specific reason as to why the serum insulin levels were higher for the metformin group in comparison to the OB/IR control group is unknown and needs further investigation.

The hepatic insulin resistance, brought about by the OB/IR diet, marked by the increase in gluconeogenic enzymes, enzymes involved in β-oxidation and a decrease in glycogen content are all factors which are reversed following metformin treatment; this implies alleviation in hepatic insulin resistance. An increase in the active form of glyceraldehyde-3-phosphate dehydrogenase (table 4.6.2) was found following metformin treatment, relative to the OB/IR diet. This enzyme catalyzes the first step in the pay-off phase of glycolysis (Nelson and Cox, 2000), which implies an increase in the glycolytic flux. The increase in active hepatic aldolase B would imply that this enzyme is active for the

forward (glycolytic) reaction rather than the reverse (glyconeogenic) reaction, if the body is to avoid futile cycling. The decreased activity of the gluconeogenic enzyme, glucose-6-phosphatase (fig. 4.40), is another indication that this pathway is suppressed. The reduction in the activity of 3-hydroxyacyl-CoA dehydrogenase and levels of 2,4-dienoyl CoA reductase, relative to the OB/IR control, is reason to assume a decrease in β-oxidation. As already stated, β-oxidation is the source of ATP necessary to drive gluconeogenesis, however if insulin resistance is eliminated there is no reason for β-oxidation to take place.

The reduction in hepatic cytochrome c oxidase, subunit Va, is one of the hypoglycaemic mechanisms associated with metformin treatment. Subunit Va of cytochrome c oxidase contains the heme-a chain and forms the terminal oxidase in the mitochondrial electron transport system located in the inner mitochondrial membrane. A decrease in this protein implies a decrease in oxidative phosphorylation and cellular respiration, a relatively new hypoglycaemic trait discovered for metformin. As already mentioned, Brunmair *et al*., (2004), found metformin to significantly inhibit complex I of the respiratory chain, a trait which is believed to contribute to its antidiabetic properties. The inhibition in the enzymatic activity of complex I impairs mitochondrial function and cellular respiration leading to anaerobic glycolysis and lactate accumulation, often associated with metformin treatment (lactic acidosis). Zou *et al*., (2004) demonstrated that inhibition of the respiratory chain complex I not only leads to a decrease in ATP synthesis but also leads to the release of O_2^- and reactive nitrogen species ($ONOO^-$) from the respiratory chain. The $ONOO^-$ activates c-Src which in turn activates PI-3-kinase and PDK-1 to promote the activation of AMP-activated protein kinase (AMPK) through unknown proteins. AMPK is known to decrease hepatic glucose production, promote glucose uptake in skeletal muscle, increase lipogenesis and promote triglyceride and cholesterol synthesis (Zou *et al*., 2004). A reduction in complex IV will still impair cellular respiration and promote PI-3-kinase activation through an increased $ONOO^-$ concentration. This may be the reason for the significant increase in 2-Cys peroxiredoxin, Hbp23 concentration following metformin treatment. This enzyme is expressed under

conditions of stress brought about by reactive O_2 and reactive N_2 species (Hirotsu *et al*., 1999).

The reason that the insulin receptor β-subunit concentration, for the muscle samples, is not increased relative to the OB/IR control, following metformin treatment (fig. 4.43), is believed to be due to the maintained hyperinsulinaemia (fig. 4.34) which promotes down regulation of the receptor. Despite this, metformin treatment accelerated glucose clearance (fig. 4.35) and significantly increased the [^{3}H] deoxyglucose concentration in the muscle (fig. 4.36a). Metformin treatment has been reported to increase or fail to alter the density and binding affinity of insulin receptors from normoglycaemic and diabetic individuals (Davidson and Peters, 1997). Although tyrosine phosphorylation of the β-subunit was not determined, for the present study, it is suspected that metformin does not increase insulin sensitivity but rather accelerates glucose clearance through post receptor mechanisms. The increase in IRS-1 and IRS-2 concentrations, relative to the OB/IR diet, may indicate a mechanism through which metformin is directly or indirectly increasing the concentration of the IRS proteins. The IRS-1 protein is only slightly and insignificantly increased, relative to the OB/IR group, reasons for this may lie in the unaltered TNFα concentration mentioned earlier. An increase in circulating TNFα leads to a decrease in the expression of IRS-1 and GLUT4 (Bjornholm and Zierath, 2005). The slight decrease in TNFα levels (shown previously) does not seem to be sufficient to significantly increase the concentrations of both IRS-I and GLUT4 and must therefore be a direct or indirect action of metformin. Activation through tyrosine phosphorylation or inactivation through serine phosphorylation was not determined for the IRS-1 or IRS-2 proteins and the increased concentrations of these proteins may not promote GLUT4 translocation if they are phosphorylated at a serine residue. Further investigations need to confirm this, although Brunmair *et al*., (2004) and Zou *et al*., (2004) implied that metformin promotes glucose uptake into the muscle independently of IRS-1 and IRS-2 activation. The subsequent activation of the PI-3-kinase, resulting from the inhibition of respiratory complex I, may be a result of the increased concentration of the p85 subunit and protein kinase B associated with the metformin treatment. The increase in PIP3

concentration is of course a result of the increased PI-3-kinase activity suggested by Brunmair *et al*., (2004) and Zou *et al*., (2004).

Metformin treatment was shown to significantly increase the activity of the 17-β-hydroxysteroid dehydrogenase, type IV (table 4.6.2), enzyme relative to the OB/IR control group. The function of this enzyme has already been discussed in some detail, as have the potential consequences associated with its action. Metformin has been known to increase insulin sensitivity, allowing androgen levels to fall i.e. total testosterone, free testosterone and androstenedione, and has been used successfully in the treatment in polycystic ovary syndrome. However, it is unclear how much of the action of metformin is due to a direct improvement in peripheral insulin sensitivity and how much occurs indirectly through a consequent improvement in hyperandrogenaemia (Livingstone and Collison, 2002). Since *S. frutescens* was able to promote insulin sensitivity without affecting the activity of 17-β-hydroxysteroid dehydrogenase, implicates metformin's ability in controlling circulating testosterone levels through 17-β-hydroxysteroid dehydrogenase activity. Further studies are however necessary to confirm this.

The overactive citrin carrier protein (aspartate / glutamate shuttle), for the OB/IR group in the liver, is significantly reduced following metformin treatment (refer to table 4.6.2.), allowing for a relative decrease in the shuttling of aspartate and glutamate between the cytosol and the mitochondrial matrix (refer to fig. 5.1), this reduction is however, not lower than that found for the lean control group (results not shown). The mitochondrial malate dehydrogenase activity is returned to within the normal range, as a result of metformin treatment. This enzyme is responsible for converting malate (which is transported from the cytosol into the mitochondria via the malate / oxoglutarate shuttle) into oxaloacetate. The increase in mitochondrial malate dehydrogenase indicates an increase in the malate / oxoglutarate shuttle's activity, which may be due to an increase in glycolysis. The glutamate oxaloacetate transaminase 2 activity is also increased as a result of metformin treatment, relative to the OB/IR control group; again this is not higher than that found for the lean control (results not shown). This enzyme's activity

was reduced for the OB/IR group relative to the lean control, allowing for less oxaloacetate to be converted into aspartate.

The increased activity of ornithine transcarbamoylase (table 4.6.2) in the liver, for the metformin group, is unexpected since the above mentioned proteins suggest that the medication suppresses the urea cycle. An increase in ornithine transcarbamoylase may imply an increase in ornithine / citrulline shuttling between the mitochondria and the cytosol, leading to an increased concentration of cytosolic citrulline. Nakata *et al*., (2003) showed that an increased concentration of cytosolic citrulline in β-cells lead to a significant increase in insulin secretion. They found that the metabolism of physiologic concentrations of citrulline by the citrulline-argininosuccinate-arginine cycle leads to nitric oxide production and resultant potentiation of glucose-induced insulin release, in which a Ca^{2+}-mediated pathway could be involved. Although no β-cell proteomics were performed for the present study, the implied increased concentration of hepatic cytosolic citrulline may also occur within the β-cell, this would augment insulin secretion which could also explain the increased serum insulin levels documented in the present study (fig. 4.34). Further investigations are required to confirm this.

The significant reduction in intestinal glucose uptake (figs. 4.41 and 4.42) is a common hypoglycaemic property associated with metformin treatment (Stumvoll *et al*., 1995). The significant reduction in muscle glycogen content, for the metformin group relative to the OB/IR control (fig. 4.39), may imply an increase in muscle glycogen phosphorylase activity and a subsequent decrease in muscle glycogen synthase. This is however only speculation and further investigation into glycogen synthase and phosphorylase activities is needed for clarification. The increased concentrations of anti-oxidant enzymes such as catalase may be another anti-diabetic mechanism associated with metformin treatment. A significant reduction in catalase activity is associated within diabetic subjects and is thought to augment β-cell and cardiomyocyte dysfunction (Ye *et al*., 2004).

The inability of metformin to decrease plasma free fatty acids and triglycerides (Jackson *et al*., 1987; Paollisso *et al*., 1988; Davidson and Peters, 1997; Suzuki *et al*., 2002) is a

definite disadvantage of this drug. As has already been discussed the build up of intracellular fatty acyl-CoAs is the culprit which augments insulin resistance leading to the development of the metabolic syndrome. The hyperinsulinaemia may be a result of the elevated plasma free fatty acids, however, muscle and liver insulin resistance seems to be reversed and glucose clearance is definitely accelerated in comparison to the OB/IR control group (fig. 4.35). The mechanism of glucose uptake into the liver and muscle tissue involves post receptor mechanisms, involving inhibition of the respiratory complex I-AMPK activation and finally PI-3-kinase activation, which eventually results in GLUT4 translocation. Although IRS-1 (not significantly increased) and IRS-2 (significantly increased) protein concentrations were increased relative to the OB/IR group, their phosphorylation status remains to be determined. Even if the IRS-1 and IRS-2 proteins are inactivated through serine phosphorylation AMPK activation is sufficient to promote muscle glucose clearance (through GLUT4 translocation), inhibit hepatic glucose production, triglyceride synthesis and lipogenesis (Zou *et al*., 2004). Since metformin does not promote a significant increase in β-oxidation, a possible fate of intracellular fatty acids in muscle and liver is their transportation and storage in white adipose tissue. This may be the reason for the significant increase in epididymal fat pads (fig. 4.38), this is however purely speculative and needs further investigation. The increased weight of the fat pads may not be a result of increased adipocyte proliferation as there was no significant reduction in TNFα, which is a result of PPARγ antagonists (decreasing adipocyte hypertrophy by increasing their differentiation).

Metformin is an effective antidiabetic agent which has brought about a relatively normal lifestyle for many individuals suffering from type II diabetes. Over the past years the introduction of alternative anti-diabetic drugs such as sulfonylureas, and more recently, PPARγ antagonists have not necessarily overshadowed metformin, but instead have opened up a new avenue of research. Numerous clinical trials have recently emerged in which various combinations of these drugs are being tested in order to bring about the most effective response. As all these drugs have individual metabolic pathways in which they bring about hypoglycaemia, they also all have their individual side effects. By combining these drugs it is hoped to increase the efficacy of their antidiabetic potential

while at the same time canceling out each others side effects. It seems we still have a long way to go considering that we are still learning about alternative metabolic effects for one of the oldest drugs in the diabetes trade, namely metformin.

The *S. frutescens* extract was effective in alleviating hyperinsulinaemia (fig. 4.34) associated with insulin resistance, while maintaining normoglycaemic levels (fig. 4.33), and significantly reduced hyperglycaemia brought about by loss of β-cell function, associated with STZ treatment (fig. 4.51). The fact that the extract is able to alleviate both type I and type II diabetic complications and that it is able to compete with insulin for receptor binding (fig. 4.56) suggests that it may itself be mimicking the action of insulin. Although the extract was able to increase GLUT4 translocation, independent of insulin binding, the statistical significance of the results could not be varified for reasons already discussed (fig. 4.57b). The GLUT4 translocation is not enough evidence to suggest that the extract is mimicking the action of insulin through binding to the receptor and initiating a response. GLUT4 translocation may be a result of complex post receptor activation mechanisms augmented by the extract. Although the mimicking of insulin by the *S. frutescens* extract cannot be ruled out at this stage, insulin independent receptor β-subunit tyrosine phosphorylation by the extract would serve to confirm such a role for the extract.

Despite a reduced basal metabolic rate (fig. 4.32) no significant weight gain was found for the *S. frutescens* group in comparison to the OB/IR control or metformin group (figs. 4.32 & 4.33). Anecdotal evidence from doctors and health care workers has implicated *S. frutescens* in promoting appetite and weight gain for patients who were underweight due to AIDS related complications (Chaffy and Stokes, 2002). The weight gain implicated by Chaffy and Stokes (2002) is undoubtedly in response to an increased appetite; however the rats in the present study all received the same amount of food daily. The increased weight of the epididymal fat pads (fig. 4.38) did not have any effect on the body weight of the *S. frutescens* group. The reason for the increase in epididymal adipose tissue weight may be an increase in white adipose tissue proliferation, a potential hypoglycaemic trigger, which will be discussed in more detail at a later stage.

The alleviation of hyperinsulinaemia, brought about by the OB/IR diet, may be due to the reduction in TNFα following *S. frutescens* treatment (table 4.6.7). An increase in the activity of enzymes involved in β-oxidation may also play a role in alleviating β-cell dysfunction through the removal of the intracellular fatty acyl-CoAs. 3-Hydroxyacyl-CoA dehydrogenase, binary complex (with NADH and estradiol) was found to be elevated, while 2,4-dienoyl CoA reductase 1 was found to be reduced following *S. frutescens* treatment in comparison to the OB/IR diet. The concentrations of 3-hydroxyacyl-CoA dehydrogenase, binary complex (with NADH and estradiol) and both the active and inactive forms of 3-hydroxyacyl-Coa dehydrogenase were found to be significantly elevated by *S. frutescens* in comparison to the lean control. These results may imply a possible increase in total β-oxidation, resulting from *S. frutescens* treatment, which would reduce intracellular levels of fatty acyl-CoAs. A significant increase in catalase activity following *S. frutescens* treatment (table 4.6.3) also promotes alleviation in the metabolic syndrome by decreasing reactive oxygen species which may cause inflammation (Ye *et al*., 2004). Fernandes *et al*., (2004) found that a hot water extract of *S. frutescens* possess significant reactive oxygen species scavenging properties in cell free and in stimulated neutrophil systems. It seems that the extract is able to scavenge for reactive oxygen species while activating natural scavengers in the body; this may be why this plant has been earmarked in the fight against cancer (Tai *et al*., 2004; Chinkwo *et al*., 2005).

The decrease in hepatic glucose production resulting from *S. frutescens* treatment is evident in the significant reduction in the activities and concentrations of certain gluconeogenic enzymes. *S. frutescens* significantly reduced the three rate limiting enzymes of gluconeogenesis: pyruvate carboxylase, fructose-1,6-bisphosphatase (table 4.6.7) and glucose-6-phosphatase (fig. 4.40), implying an increase in glycolytic flux as indicated by the increase in glyceraldehyde-3-phosphate dehydrogenase and aldolase B (table 4.6.3). The extract was even able to increase the levels of enzymes, relative to the lean control group, responsible for the first and second steps of the pay off phase in glycolysis, namely: the active form of D-glyceraldehyde-3-phosphate dehydrogenase and phosphoglycerate kinase 1 (table 4.6.4). The fact that the extract is able to significantly

increase the glycolytic flux in an obese / insulin resistant model beyond that of a lean control displays the positive effects it has on glucose metabolism. This gives us a clue into the potential this plant has on reversing the effects associated with the metabolic syndrome.

The relative increase in activity and concentration of transketolase (table 4.6.3) implies an increase in the nonoxidative pentose phosphate pathway resulting in an increase in NADPH production. This would imply an increase in fatty acid synthesis, which may be a result of increased insulin sensitivity brought about by *S. frutescens* treatment.

S. frutescens was able to accelerate glucose clearance (fig. 4.35) relative to that of the OB/IR group, this is an indication of the reversal of insulin resistance and the metabolic syndrome. The increased [^{3}H] deoxyglucose counts in the muscle (fig. 4.36a) implies an increase in the PI-3-kinase pathway which is either directly or indirectly influenced by the extract. The ability of the extract to alleviate the hyperinsulinaemia instilled by the OB/IR diet (fig. 4.34) did not have any effect on the, previously down regulated, insulin receptor β-subunit (fig. 4.43). The low concentration of the receptor may be due to the extract initiating an insulin mediated response by binding to it at extremely low concentrations; again this is speculative and needs further investigation. The concentrations of both IRS-1 (fig. 4.44) and IRS-2 (fig. 4.45) were significantly increased in the muscle for the *S. frutescens* treated group, relative to the OB/IR control group. Reasons for these increases and that of GLUT4 (fig. 4.50) and protein kinase B (fig. 4.49), may be due to a decrease in circulating free fatty acids, associated with high fat feeding. A measurement of plasma fatty acid concentrations is necessary to confirm this statement. The phosphorylation states of IRS-1 and IRS-2 need to be determined to establish whether the extract was promoting glucose clearance through directly binding to the insulin receptor or whether it was eliciting a response by activating proteins situated further downstream in the cascade. The increase in inositol-1,4,5-triphosphate receptor (fig. 4.48), relative to the OB/IR group, is a result of the increased p85 subunit (fig. 4.46), and implies an increase in the catalytic subunit of the PI-3-kinase protein.

The high [^{3}H] deoxyglucose associated with the epididymal fat pads (fig. 4.36a) may give a clue into the hypoglycaemic properties of the extract. This increase in glucose uptake may be due to an increase in the mitotic activities of the white adipocytes, which may result in the enlarged epididymal fat pads associated with *S. frutescens* treatment (fig. 4.38). The *S. frutescens* extract may be acting as a PPARγ ligand, resulting in the inhibition of mature adipocyte hypertrophy through an increase in adipocyte proliferation. PPARγ is a ligand-activated transcription factor and a member of the nuclear hormone receptor superfamily that functions as a heterodimer with a retinoid X receptor (RXR). Adipocyte hypertrophy, which converts small adipocytes into larger ones, results in the production and secretion of adipokines, *i.e.* resistin, angiotensinogen, plasminogen activator inhibitor-1, TNFα, interleukins and leptin, all of which promote insulin resistance and augment the metabolic syndrome (Bays *et al*., 2005; Tsuchida *et al*., 2005). In other words the fat cell becomes dysfunctional. Reversal of adipocyte hypertrophy, by PPARγ ligand, slows the production and secretion of these factors promoting insulin resistance (adipocytokines), and promotes the secretion of adiponectin (refer to fig. 5.2) (Bays *et al*., 2005).

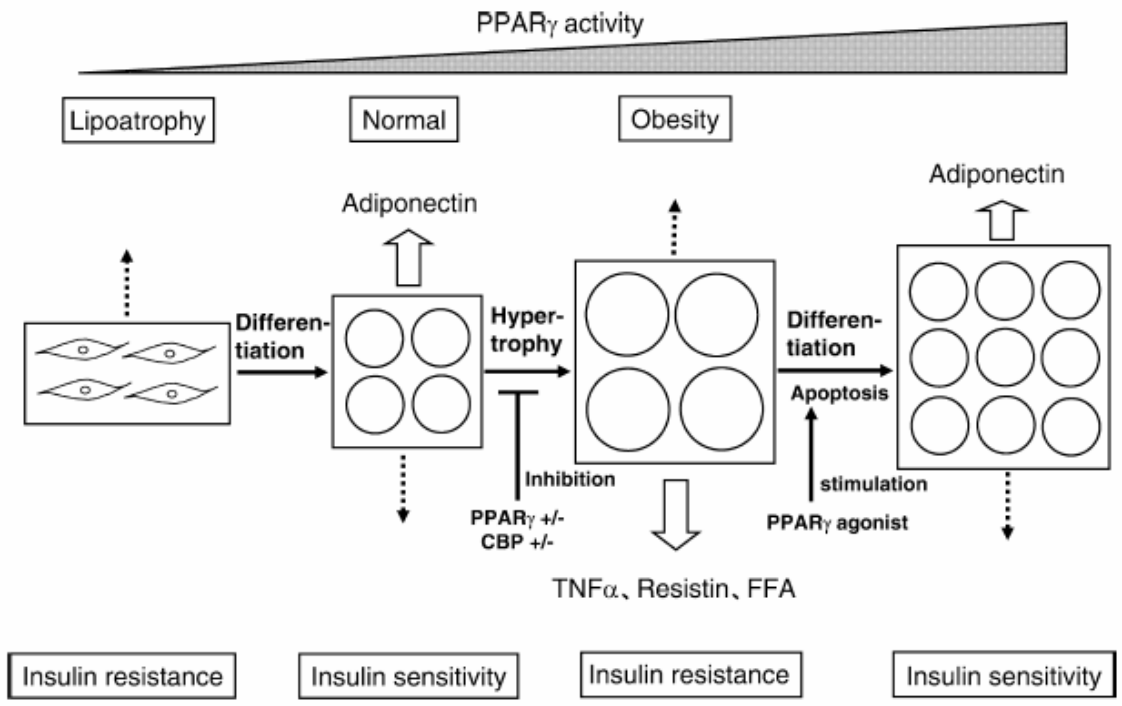

Figure 5.2: Mechanisms by which PPARγ regulate insulin sensitivity (Tsuchida *et al*., 2005)

Adiponectin is expressed only in adipocytes and is secreted into circulation to promote insulin sensitivity in peripheral tissues (refer to fig. 5.3) (Bays *et al*., 2005).

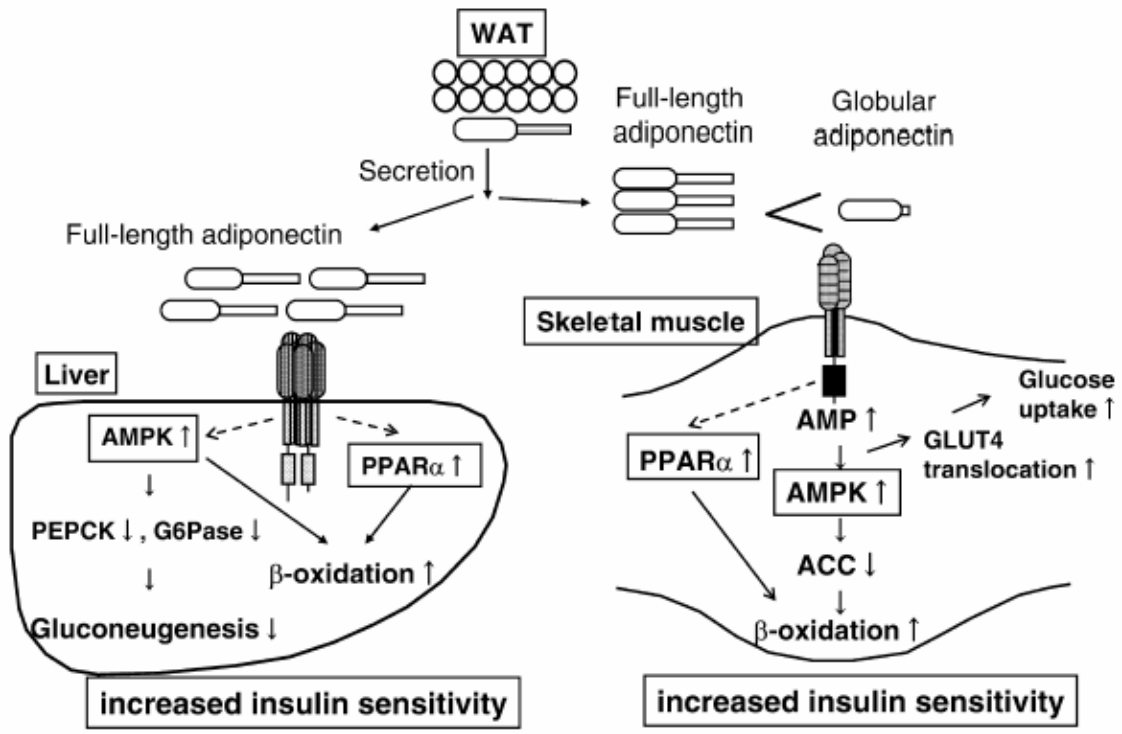

Figure 5.3: Mechanisms by which PPARγ promote hepatic and muscle insulin sensitivity (Tsuchida *et al*., 2005)
Key: AMPK – AMP Activated Protein Kinase, ACC – Acetyl CoA Carboxylase

The increased glucose uptake into the muscle and the epididymal fat pads (fig. 4.36a), the increased weight of the fat pads (fig. 4.38), the decrease in TNFα (table 4.6.7), the increased β-oxidation and the accelerated rate of glucose clearance (fig. 4.35) all seem to imply that the *S. frutescens* extract may contain a ligand for PPARγ. This, however, needs further investigation for confirmation. The significant increase in apoptosis-inducing factor (table 4.6.3), relative to the OB/IR control, may indicate another attribute associated with PPARγ agonists. Thiazolidinediones are also known to increase apoptosis of adipocytes, thereby decreasing adipocyte hypertrophy and plasma fatty acids (Tsuchida *et al*., 2005). Apoptotic cell death is a physiological mechanism that eliminates unwanted cells by triggering their intrinsic suicide program (Kerr *et al*., 1972; Chinkwo *et al*., 2005). This process is characterized by morphological changes such as membrane blebbing, cell shrinkage, protein fragmentation, chromatin condensation and DNA

degradation followed by rapid engulfment of cell debris by neighbouring cells (Christop, 2003; Chinkwo *et al*., 2005). Chinkwo *et al*., (2005) showed that *S. frutescens* promoted apoptosis in three different cell lines; CHO, Caski and Jurkat T lymphoma cells through flip-flop translocation of phosphatidyl serine, a cellular phospholipid membrane.

The relatively low glycogen concentration found in both the liver and the muscle, for the extract treated group in comparison to both the lean and OB/IR controls (fig. 4.39), is puzzling as insulin sensitivity is expected to promote glycogen synthesis. At this stage the effect of the extract on glycogen synthase and glycogen phosphorylase is unknown and needs to be investigated. The glycogen concentrations for the STZ treated group is, however, elevated in both the muscle and the liver following extract treatment (fig. 4.53). The increase in glycogen content for this study may be a direct result of the extract but is more likely due to the increased serum insulin (fig. 4.52) associated with extract treatment. Results obtained from the OB/IR study do not implicate the extract in promoting insulin secretion (fig. 4.34). The increased serum insulin levels, following extract treatment, in the STZ rats may be due to the extract promoting β-cell proliferation and differentiation. Fernandez-Alvarez *et al*., (2004) demonstrated that the anti-diabetic property of sodium tungstate was mediated through pancreatic regeneration, in STZ treated rats. The results suggested that sodium tungstate may have increased the phosphorylation of PDX-1, a pancreatic transcription factor involved in pancreas development and neogenesis.

The citrin carrier protein (aspartate / glutamate shuttle), found to be up regulated in the OB/IR control group, was significantly reduced following *S. frutescens* treatment (table 4.6.3). As already discussed this protein is responsible for shuttling aspartate and glutamate between the cytosol and the mitochondrial matrix. The reduced citrin activity would result in a decrease in mitochondrial glutamate, which is the reason for the low concentration of mitochondrial glutamate dehydrogenase found. *S. frutescens* treatment also reduced the concentrations of carbamoyl-phosphate synthetase-1 and ornithine transcarbamylase. Glutamate dehydrogenase is involved in the deamination of glutamate, carbamoyl-phosphate synthetase-1 detoxifies the resulting NH_4^+ and ornithine

transcarbamylase incorporates this product into the urea cycle. The low concentration of these proteins implies a decrease in total deamination for the *S. frutescens* group, suggesting a decrease in protein degradation, which is a common source of substrates for the citric acid cycle during times of starvation or metabolic disturbances such as diabetes. The decrease in protein degradation is coupled with an increase in protein synthesis through the significant elevation of both the translation elongation factor-1-α-1-like-14 and the translation elongation factor-1-α-1, relative to the OB/IR group.

Citrin was also found to be significantly reduced by *S. frutescens* treatment in comparison to the lean control group (table 4.6.4), while both ornithine transcarbamylase (table 4.6.4) and carbamoyl-phosphate synthetase-1 (table 4.6.8) were significantly increased. This result implies that glutamine, from extrahepatic tissues, is entering the mitochondria to undergo deamination, upon which the resulting NH_4^+ would enter the urea cycle. Glutamine is a major transport form of ammonia, it is a non-toxic neutral compound that can pass through cell membranes with ease, whereas glutamate, which bears a net negative charge, cannot (Nelson and Cox, 2000). A potential increase in glutamine would imply an accelerated rate of amino acid degradation occurring in the extrahepatic tissues, relative to the lean control group. This is however speculative as there was no change in concentration or activity of glutaminase evident. Glutaminase is a mitochondrial enzyme which converts glutamine into glutamate and NH_4^+ (Nelson and Cox, 2000).

The increase in the arginosuccinate synthetase levels (table 4.6.3) for the *S. frutescens* treated group, relative to the OB/IR control, is unexpected since there seems to be a reduction in the deamination-urea cycle process. Arginosuccinate synthetase is responsible for converting cytosolic citrulline and aspartate into arginosuccinate, which is then lyased by arginosuccinate lyase to form arginine, which enters the urea cycle, and fumurate, which enters the citric acid cycle (Nelson and Cox, 2000). However if this enzyme's activity is also increased in the β-cells then it would lead to a decrease in cytosolic citrulline, meaning a decrease in insulin secretion via the citrulline-argininosuccinate-arginine cycle proposed by Nakata *et al*., (2003).

The significant decrease in intestinal glucose uptake associated with *S. frutescens* treatment displays another hypoglycaemic trait of the extract (figs. 4.41 & 4.42). The extract seemed to be more effective in inhibiting intestinal glucose uptake than the positive control metformin. Inhibition of glucose uptake has long since been known as a mechanism for reducing blood glucose levels for metformin. *S. frutescens* has shown significant inhibition of Na^+K^+ ATPase activity in the jejunum (fig. 4.54). A decrease in the Na^+K^+ ATPase activity implies less cytosolic Na^+ is being pumped out of the cell in exchange for extracellular K^+ (refer to fig. 5.4). This results in a relatively high concentration of cytosolic Na^+, leading to a decrease in the concentration gradient for extracellular Na^+. The decreased concentration gradient allows less Na^+ to sneak back into the cell through a passive transport system on the intestinal luminal side of the brush border. As this is the only mode of entry for ingested glucose, a decrease in this transport system severely hinders intestinal glucose uptake (Tortora and Grabowski, 2003). The length of the villus may also affect intestinal glucose uptake.

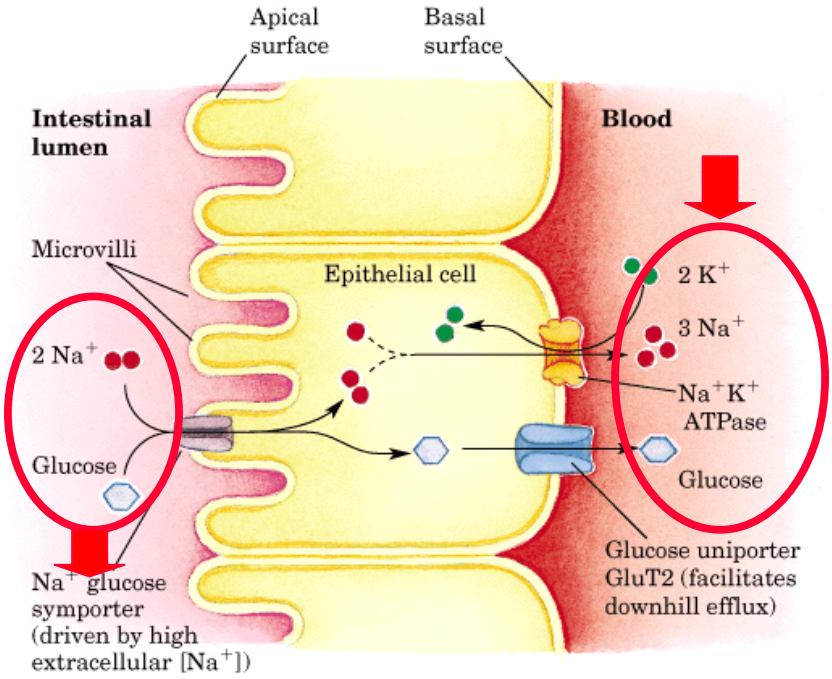

Figure 5.4: Intestinal glucose uptake facilitated by secondary active transport (Mizuma et al., 1997).

S. frutescens seems effective in alleviating insulin resistance brought about by high fat feeding. Although some of its hypoglycaemic properties have been uncovered (such as the inhibition of intestinal glucose uptake), the exact mechanism by which it reverses insulin resistance (fig. 4.52) while accelerating glucose clearance (figs. 4.35 and 4.51) is

still speculative. The present study has indicated that *S. frutescens* is an effective antidiabetic tool for both type I and type II diabetes and their associated complications. The results obtained from the present work has raised several questions and opened up new avenues for future research.

Further clarification on the mechanism of action of the extract is to be pursued in future studies, such as whether *S. frutescens* does mimic the action of insulin (as suggested by its ability to bind to the insulin receptor) or whether it affects proteins situated further down the cascade to initiate GLUT4 translocation. The active compound also needs to be isolated, probably by using high performance liquid chromatography, and screening of potential candidates for accelerated glucose uptake in normal and insulin resistant induced cell lines. Cell lines to be used for such a screening study could include C_2C_{12} (a mouse muscle cell line) and 3T3-L1 (fat cell line). Reversal of serine phosphorylation on IRS-1 and IRS-2 by the extract, could be determined in an insulin resistant liver cell line, assuming that *S. frutescens* does indeed reverse IRS serine phosphorylation as is presently expected. To determine if *S. frutescens* has any effect in promoting β-cell differentiation, in the presence of STZ, INS-1 cells can be incubated with the extract and viable cells can be compared to control cells. It could, however, be more effective to determine the number of β-cells in a STZ rat model treated with *S. frutescens* extract and compare that to the numbers in an untreated STZ control group.

Once the active compound/s has been identified their efficacy can be measured using an OB/IR rat model and the results compared with those obtained from the present study. It may also be necessary to determine which proteins are affected in the muscle and adipose tissue by using 2-D electrophoresis. A 2-D electrophoretic profile of serum proteins may also prove useful in determining which hormones and cytokines are affected by both the high fat diet and by the *S. frutescens* treatment. The effect of *S. frutescens* extract on the expression of PPARγ is presently being investigated by a colleague using quantitative RT-PCR. This procedure will allow for the PPARγ mRNA to be quantified in the liver, muscle and adipose tissue of the OB/IR rats which were used for this study.

APPENDIX I

A1. Quantification of Insulin Degrading Enzyme

A1.1. Liver-6 week sacrifice:

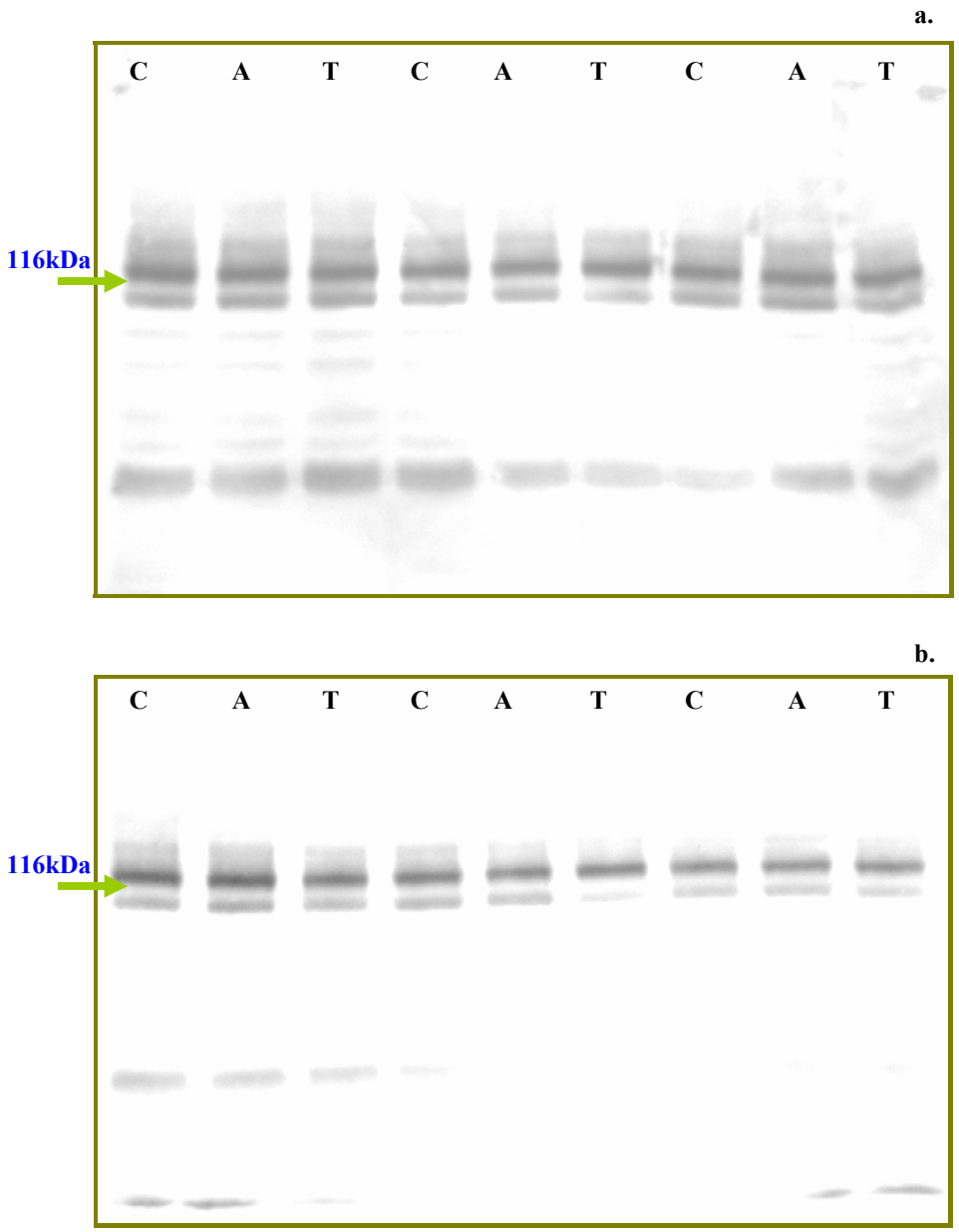

Figure A1 a & b: Liver samples after 6 weeks treatment. ECL hyperfilm after 5 minutes exposure to - rabbit IgG, peroxidase secondary antibody (1:2000) bound to rabbit anti-insulin degrading enzyme primary antibody (1:4000). Each lane contains 50 µg total protein loaded on 7.5% SDS gel, followed by a 2 hour semi-dry transfer and an overnight block in 5% BSA. Two blots were necessary to fit all the samples in, hence figures a and b.
Key: C - control, A – amitriptyline, T - trimipramine

A1.2. Muscle-6 week sacrifice:

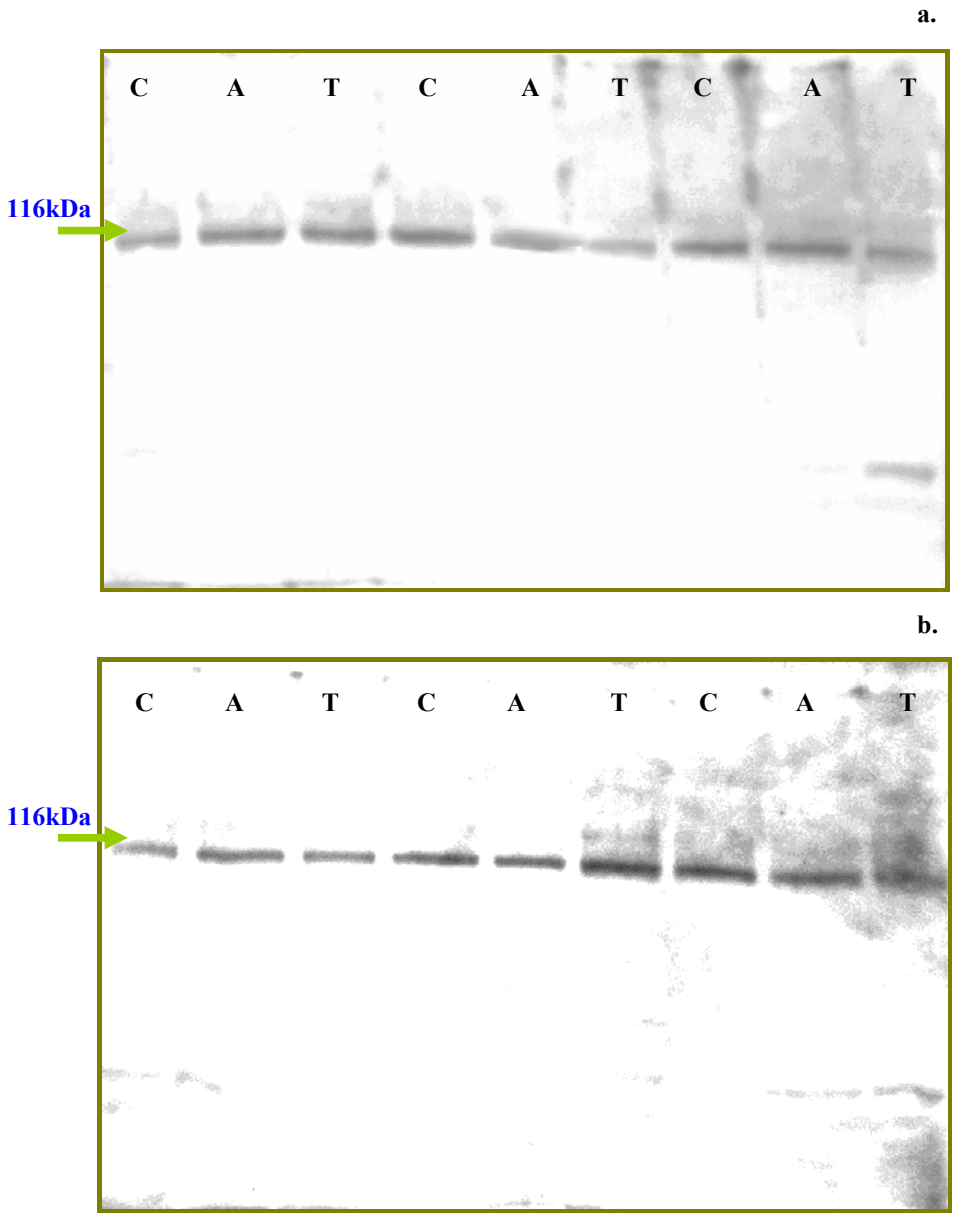

Figure A2 a & b: Muscle samples after 6 weeks treatment. ECL hyperfilm after 5 minutes exposure to anti-rabbit IgG, peroxidase secondary antibody (1:2000) bound to rabbit anti-insulin degrading enzyme primary antibody (1:4000). Each lane contains 50 µg total protein loaded on 7.5% SDS gel, followed by a 2 hour semi-dry transfer and an overnight block in 5% BSA. Two blots were necessary to fit all the samples in, hence figures a and b.
Key: C - control, A – amitriptyline, T – trimipramine

A2. Diabetic Study Muscle Protein Separation

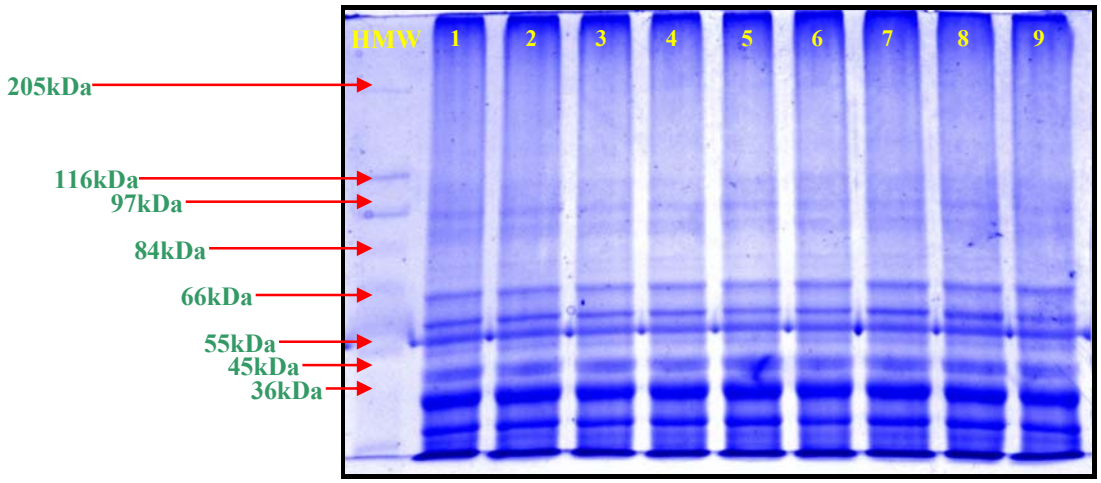

Figure A3: Muscle protein extracts used for Western blots. Twenty microgram total protein separated on 7.5% SDS polyacrylamide gel, followed by coomasie blue staining.
Key: HMW - High Molecular Weight marker, 1→9 – Muscle protein extract

A3. Western Blots From Diabetes Study

A3.1. Muscle Insulin Receptor β Subunit Quantification

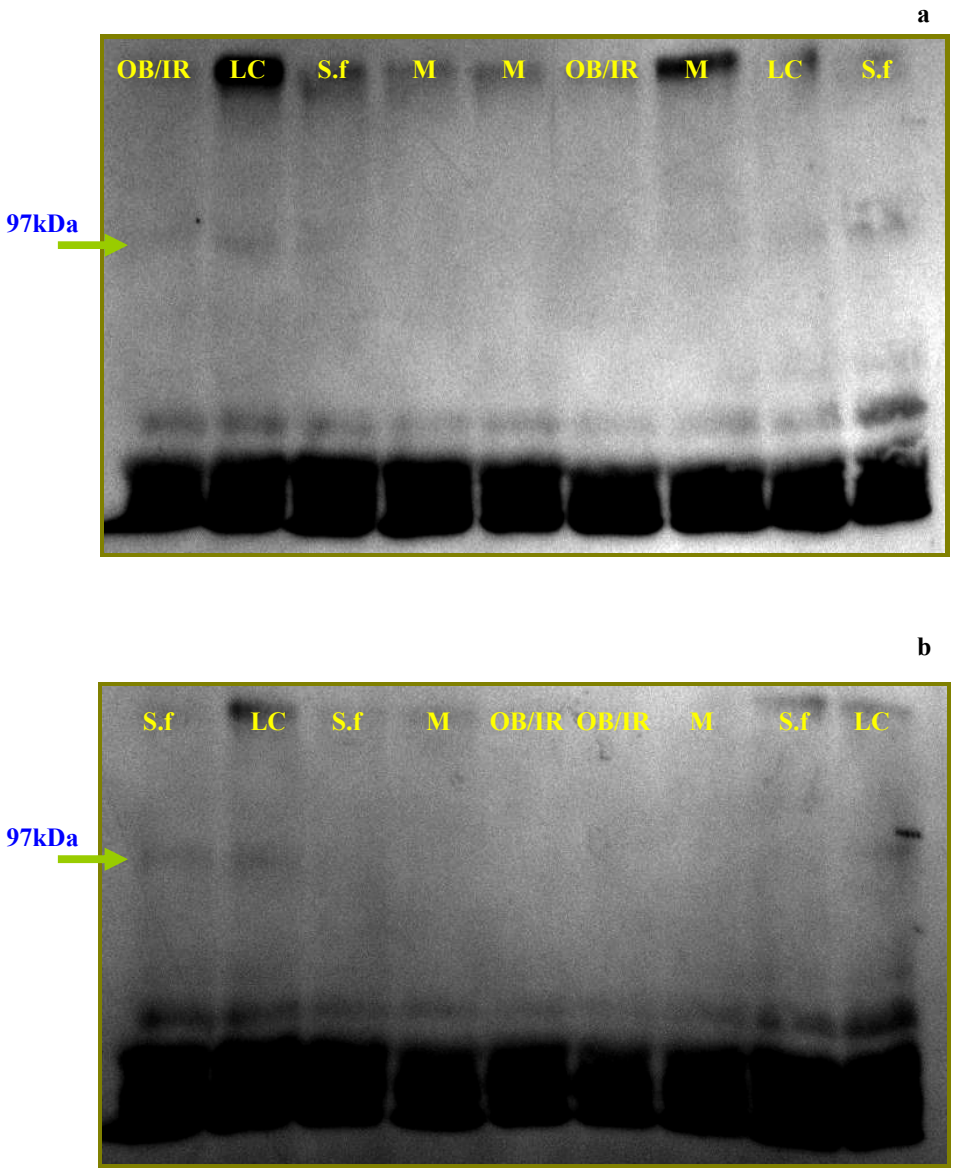

Figure A4 a & b: ECL hyperfilm after 5 minutes exposure to anti-rabbit IgG, peroxidase secondary antibody (1:2000) bound to rabbit anti-p-tyrosine phosphorylated insulin receptor-β subunit primary antibody (1:1000). Each lane contains 50 µg total protein loaded on 7.5% SDS gel, followed by a 2 hour semi-dry transfer and an overnight block in 5% BSA. Two blots were necessary to fit all the samples in, hence figures a and b.
Key: OB/IR - obese/insulin resistant, LC - lean control, M - metformin and S.f - *S. frutescens*.

A3.2. Muscle Insulin Receptor Substrate-1 (IRS-1) Quantification

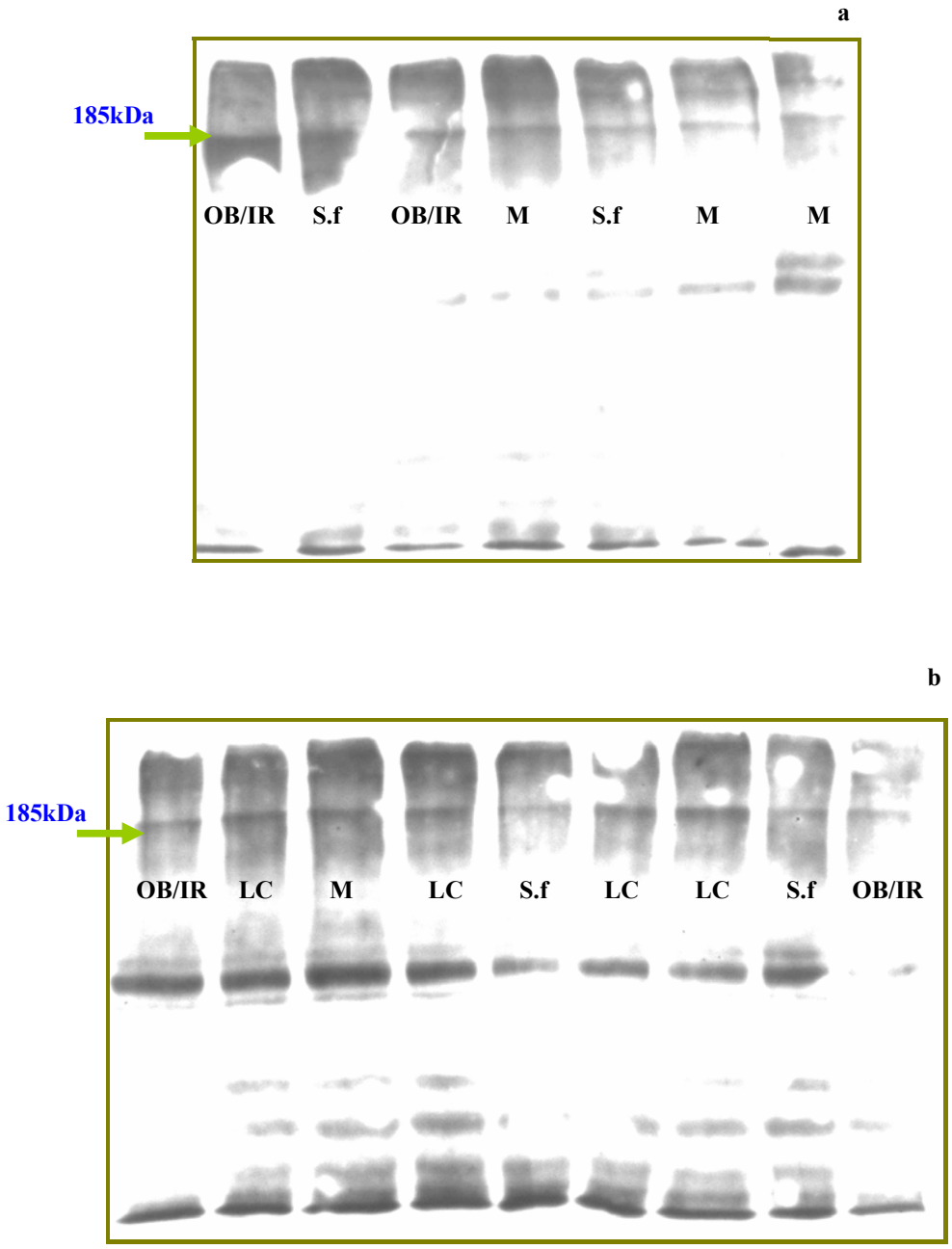

Figure A5 a & b: ECL hyperfilm after 5 minutes exposure to anti-rabbit IgG, peroxidase secondary antibody (1:2000) bound to rabbit anti-IRS-1 primary antibody (1:1000). Each lane contains 100 µg total protein loaded on 7.5% SDS gel, followed by a 2 hour semi-dry transfer and an overnight block in 5% BSA. Two blots were necessary to fit all the samples in, hence figures a and b.
Key: OB/IR - obese/insulin resistant, LC - lean control, M - metformin and S.f - *S. frutescens*.

A3.3. Muscle Insulin Receptor Substrate-2 (IRS-2) Quantification

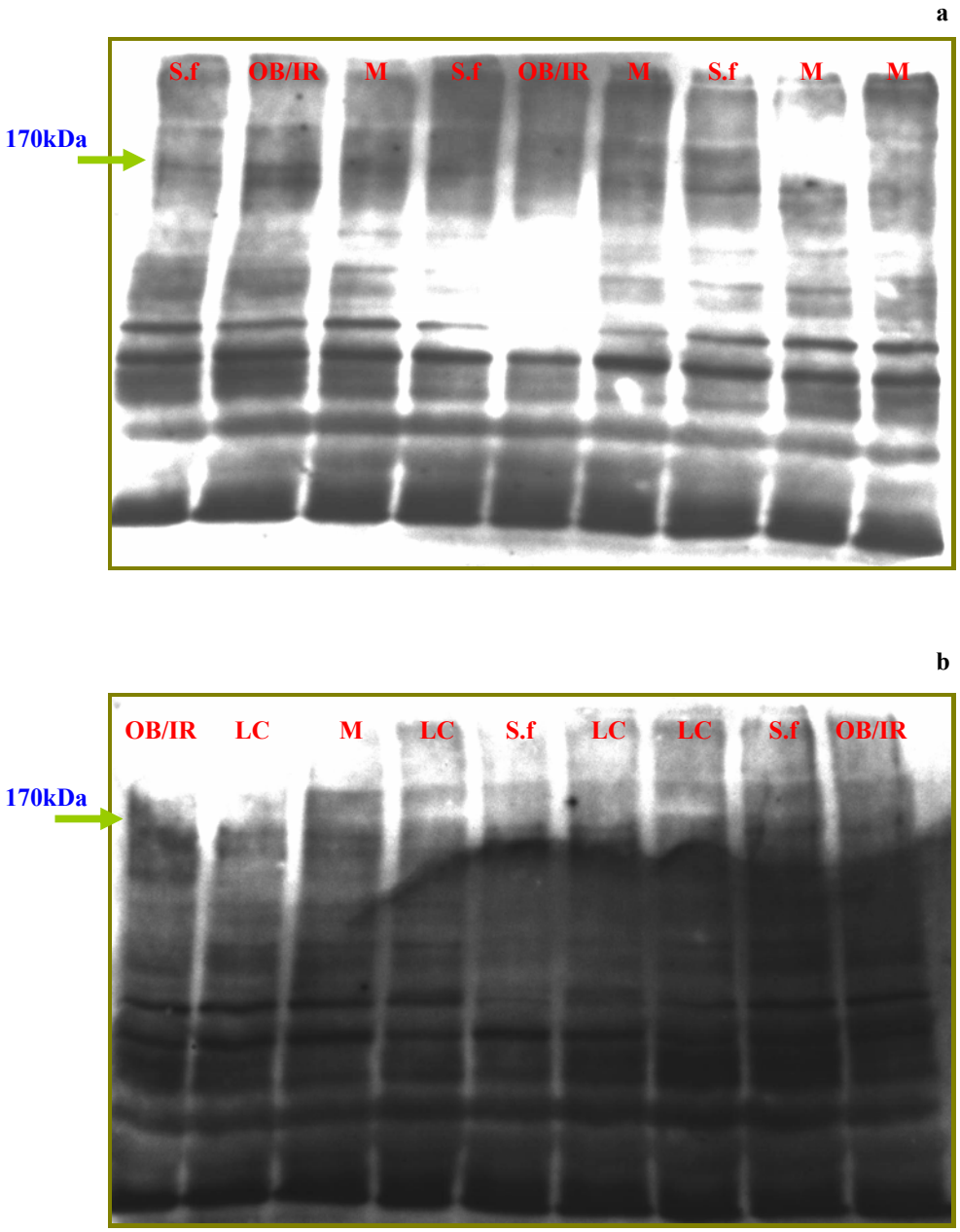

Figure A6 a & b: ECL hyperfilm after 5 minutes exposure to anti-rabbit IgG, peroxidase secondary antibody (1:2000) bound to rabbit anti-IRS-2 primary antibody (1:1000). Each lane contains 100 µg total protein loaded on 7.5% SDS gel, followed by a 2 hour semi-dry transfer and an overnight block in 5% BSA. Two blots were necessary to fit all the samples in, hence figures a and b.
Key: OB/IR - obese/insulin resistant, LC - lean control, M - metformin and S.f - *S. frutescens*.

A3.4. Muscle PI-3-Kinase, p85 Subunit Quantification

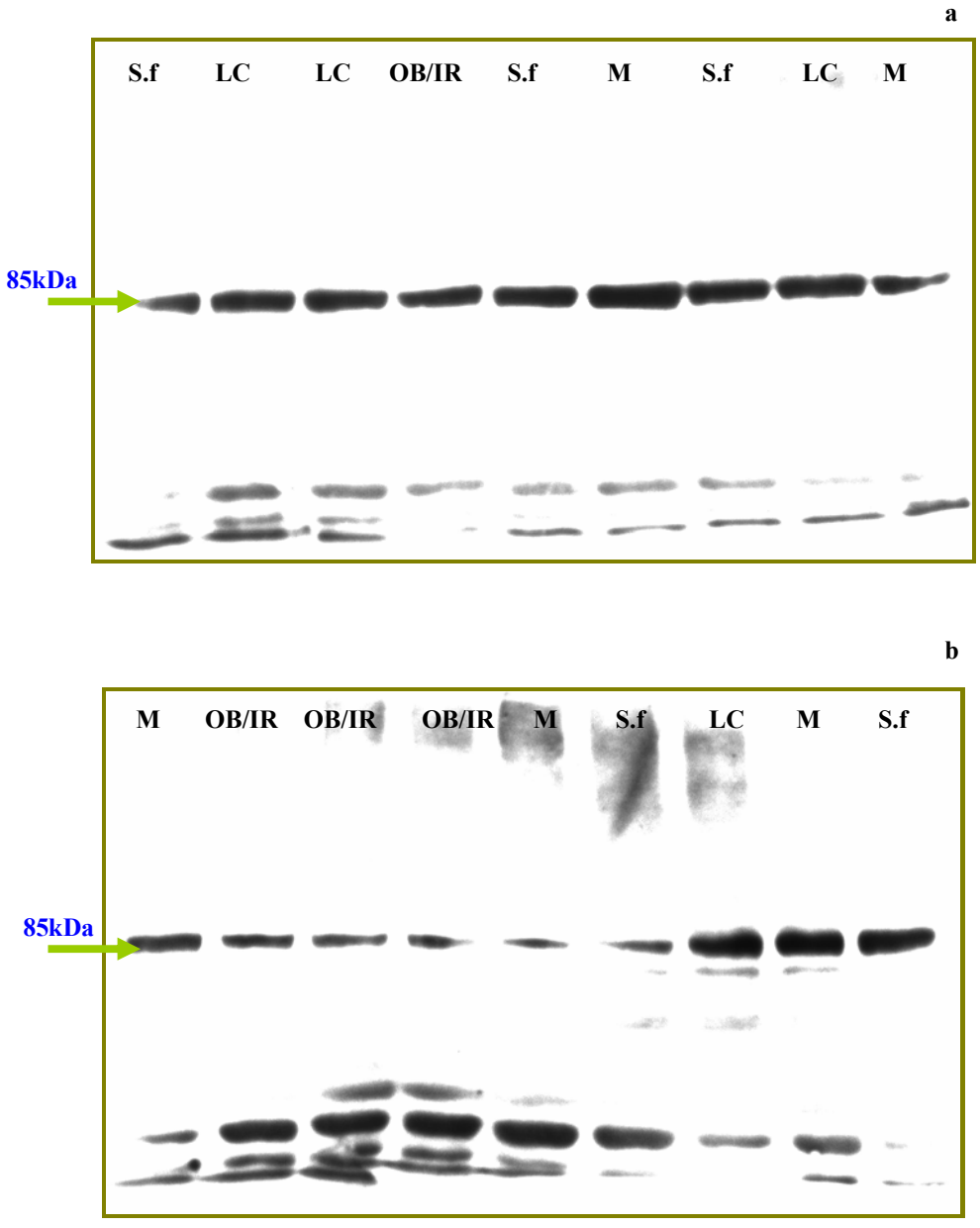

Figure A7 a & b: ECL hyperfilm after 5 minutes exposure to anti-rabbit IgG, peroxidase secondary antibody (1:2000) bound to rabbit anti-PI-3-kinase, p85 residue primary antibody (1:2000). Each lane contains 100 µg total protein loaded on 7.5% SDS gel, followed by a 2 hour semi-dry transfer and an overnight block in 5% BSA. Two blots were necessary to fit all the samples in, hence figures a and b.
Key: OB/IR - obese/insulin resistant, LC - lean control, M - metformin and S.f - *S. frutescens*.

A3.5. Muscle p38 Phosphorylated MAPK Residue Quantification

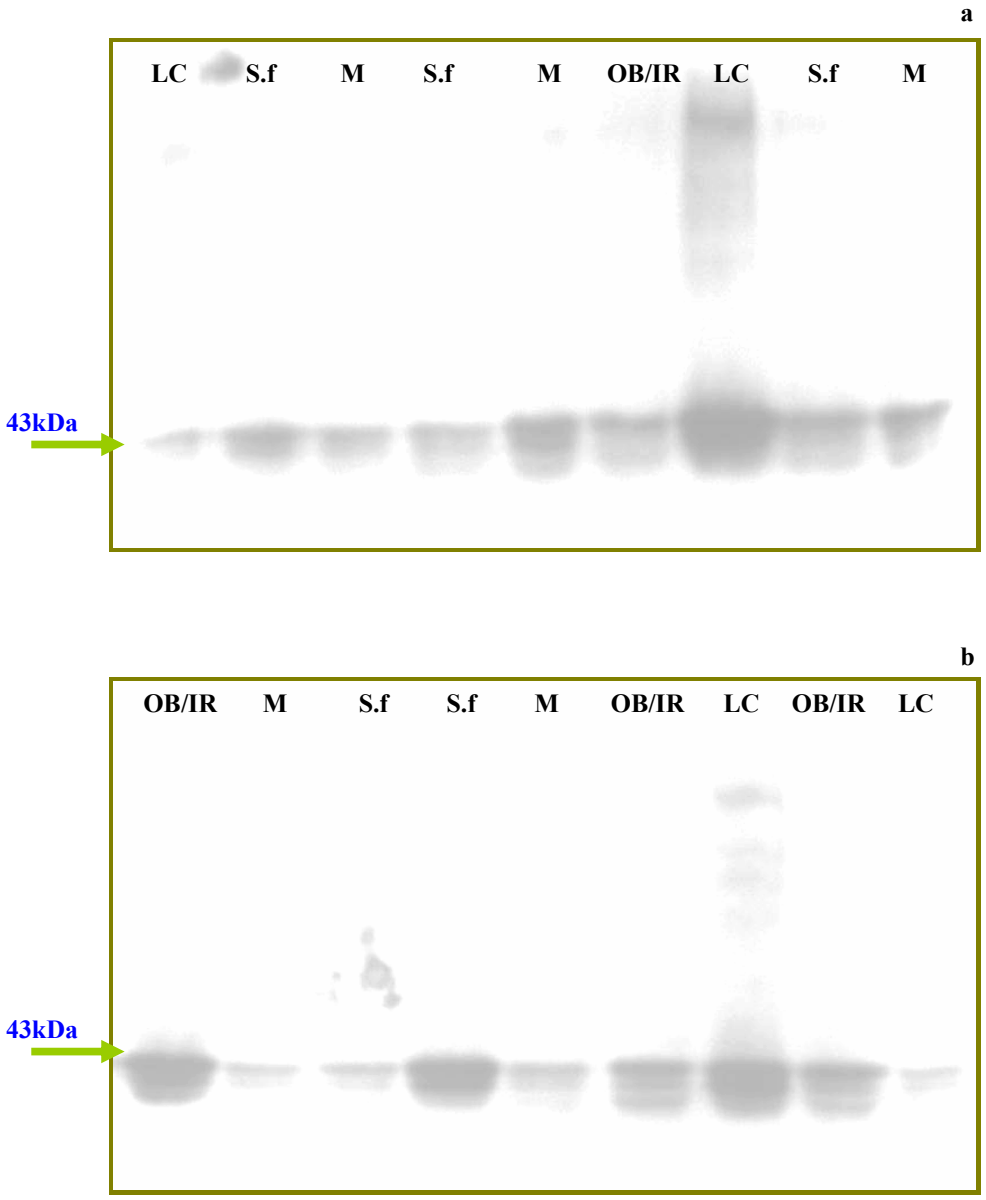

Figure A8 a & b: ECL hyperfilm after 5 minutes exposure to anti-rabbit IgG, peroxidase secondary antibody (1:2000) bound to rabbit anti-p38 phosphorylated residue primary antibody (1:2000). Each lane contains 100 µg total protein loaded on 7.5% SDS gel, followed by a 2 hour semi-dry transfer and an overnight block in 5% BSA. Two blots were necessary to fit all the samples in, hence figures a and b.
Key: OB/IR - obese/insulin resistant, LC - lean control, M - metformin and S.f - *S. frutescens*.

A3.6. Muscle Inositol 1,4,5-Triphosphate Receptor Quantification

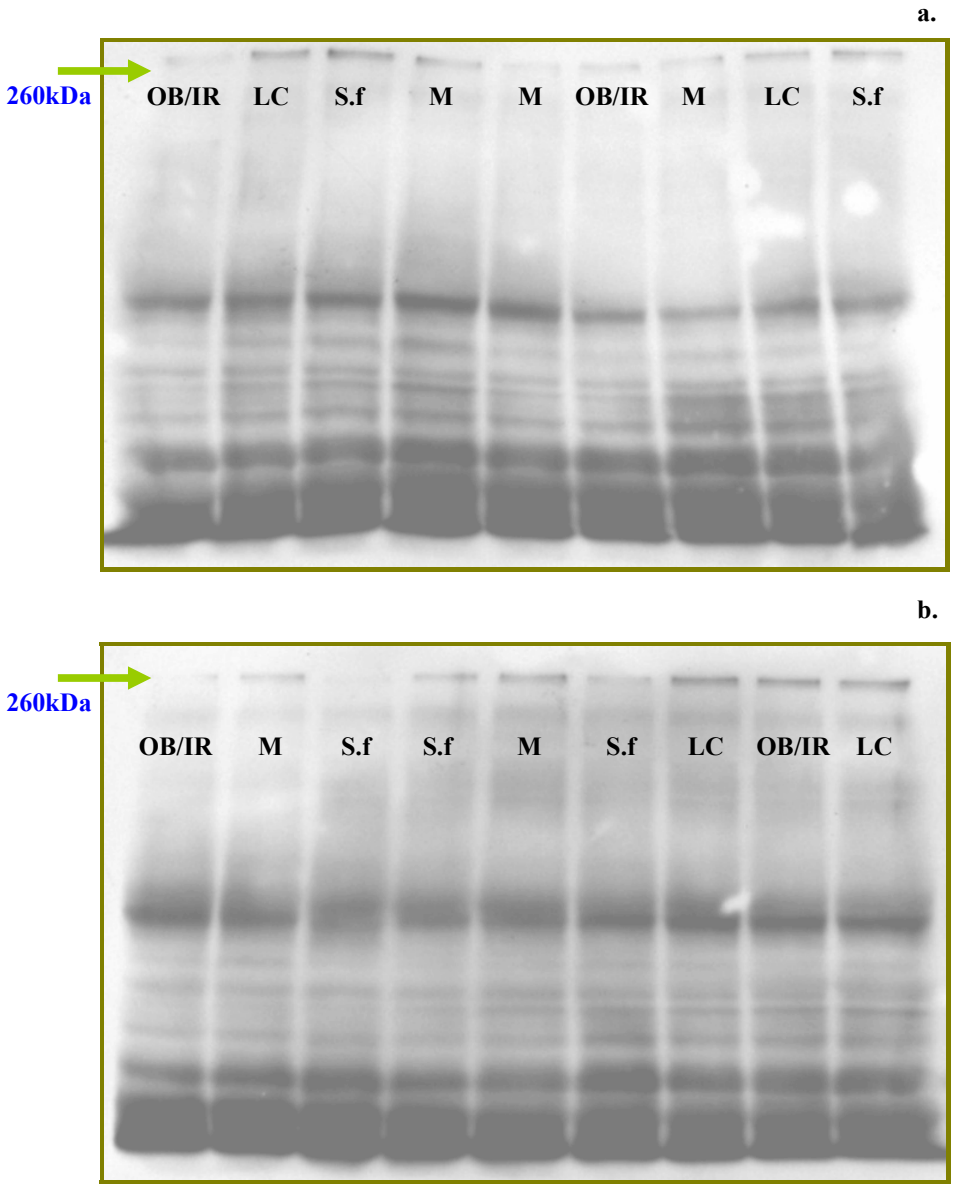

Figure A9 a & b: ECL hyperfilm after 5 minutes exposure to anti-rabbit IgG, peroxidase secondary antibody (1:2000) bound to rabbit anti-inositol 1,4,5 triphosphate receptor primary antibody (1:100). Each lane contains 100 µg total protein loaded on 7.5% SDS gel, followed by a 2 hour semi-dry transfer and an overnight block in 5% BSA. Two blots were necessary to fit all the samples in, hence figures a and b.
Key: OB/IR - obese/insulin resistant, LC - lean control, M - metformin and S.f - *S. frutescens*

A3.7. Muscle Protein Kinase B Quantification

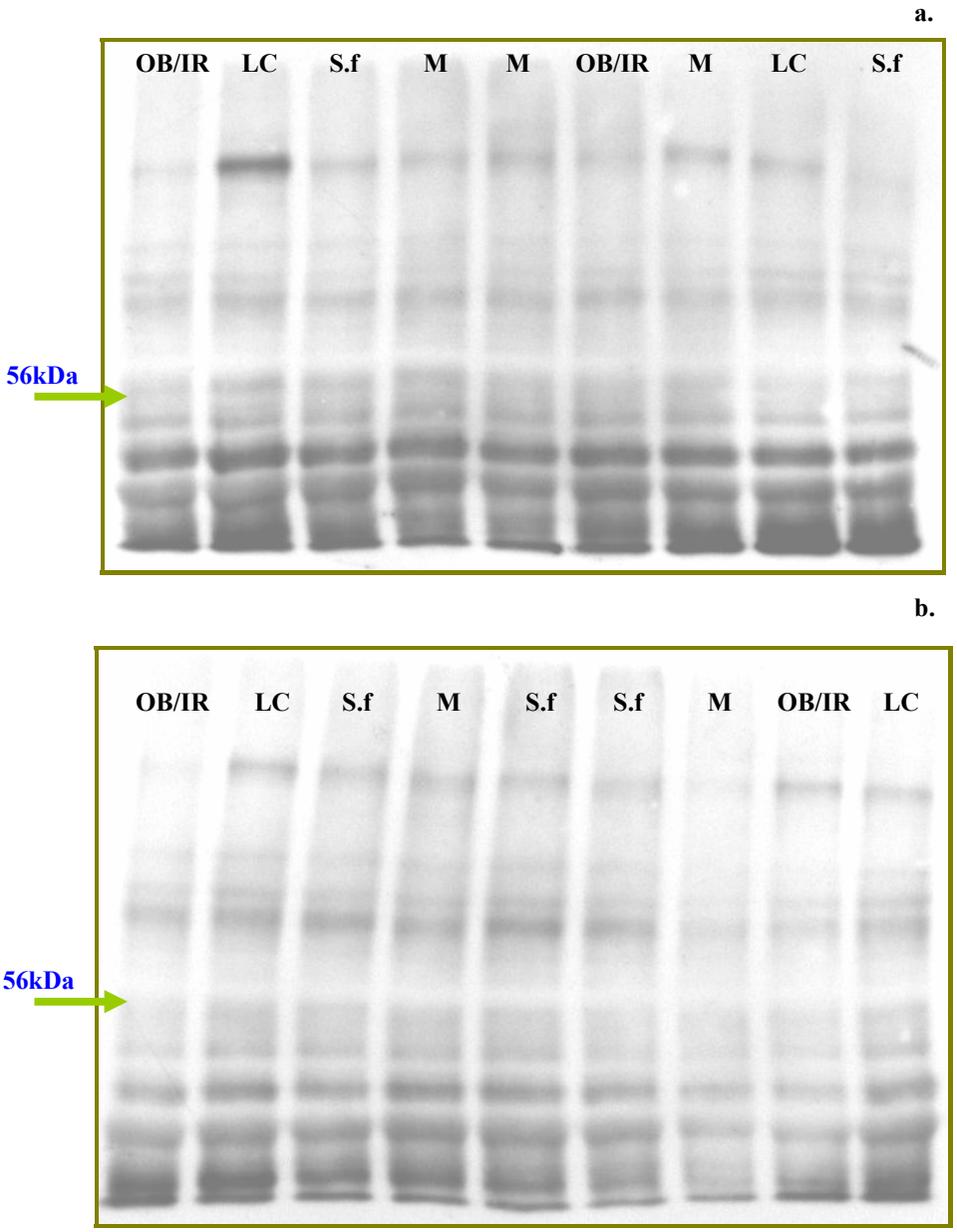

Figure A10 a & b: ECL hyperfilm after 5 minutes exposure to anti-rabbit IgG, peroxidase secondary antibody (1:2000) bound to rabbit anti-protein kinase B primary antibody (1:4000). Each lane contains 50 µg total protein loaded on 7.5% SDS gel, followed by a 2 hour semi-dry transfer and an overnight block in 5% BSA. Two blots were necessary to fit all the samples in, hence figures a and b.
Key: OB/IR - obese/insulin resistant, LC - lean control, M - metformin and S.f - *S. frutescens*.

A3.8. Muscle GLUT4 Quantification

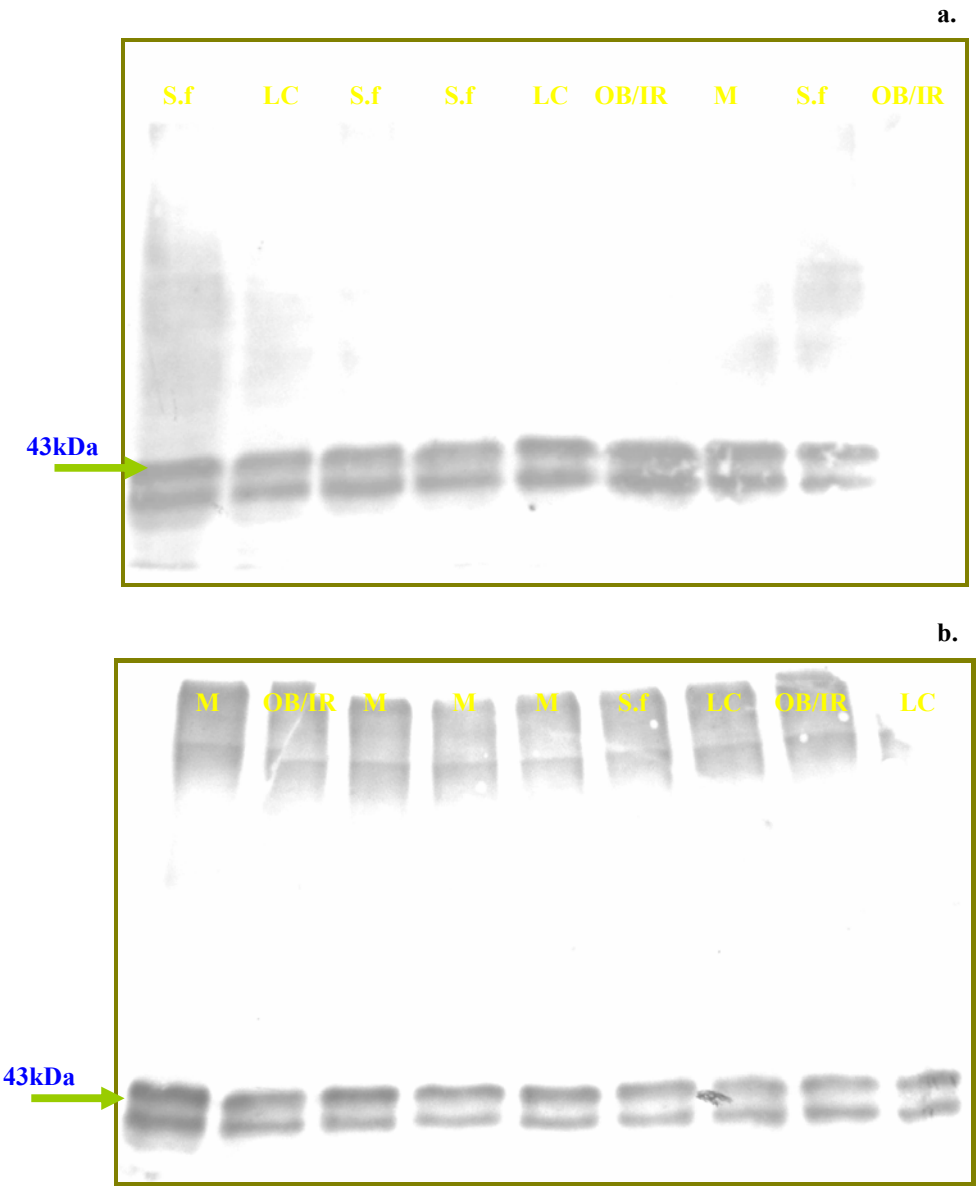

Figure A11 a & b: ECL hyperfilm after 5 minutes exposure to anti-rabbit IgG, peroxidase secondary antibody (1:2000) bound to rabbit anti-GLUT4 primary antibody (1:4000). Each lane contains 50 µg total protein loaded on 7.5% SDS gel, followed by a 2 hour semi-dry transfer and an overnight block in 5% BSA. Two blots were necessary to fit all the samples in, hence figures a and b.
Key: OB/IR - obese/insulin resistant, LC - lean control, M - metformin and S.f - *S. frutescens*.

REFERENCES

- Akiyama TE, Meinke PT, Berger JP 2005 PPAR ligands: potential therapies for metabolic syndrome, *Current Diabetes* Reports **5**:45–52
- Aleyassine H and Lee SH 1972 Inhibition of insulin release by substrates and inhibitors of monoamine oxidase, *Am J Physiol* **222**:565–569
- Andreasson K, Galuska D, Thorne T, Sonnenfeld T, Wallberg-Henriksson H 1991 Decreased insulin-stimulated 3-O-methylglucose transport in *in vitro* incubated muscle strips from type II diabetic subjects, *Acta Physiol Scan* **142**:255-260
- Ansseau M, von Frenckell R, Mertens C, de Wilde J, Botte L, Devoitille JM, Evrard JL, Nayer AD, Darimont P, Dejaiffe G, Mirel J, Meurice E, Parent M, Couzinier JP, Demarez JP, Serre C 1989 Controlled comparison of two doses of milnacipran and amitriptyline in major depressive inpatients, *Psycopharmacology* **98**:163-168
- Araki E, Lipes MA, Patti ME, Bruning JC, Haag B, 3rd, Johnson RS, Kahn CR 1994 Alternative pathway of insulin signalling in mice with targeted disruption of the IRS-1 gene, *Nature* **372**:186-190
- Aspinwall CA, Lakey JRT, Kennedy RT 1998 Insulin stimulated insulin secretion in single pancreatic beta cells, *The American Society for Biochemistry and Molecular Biology*, New York
- Babenko AP, Gonzalez G, Bryan J 1999 Two regions of sulfonylurea receptor specify the spontaneous bursting and ATP inhibition of K_{ATP} channel isoforms, *J Biol Chem* **274**:11587-11592
- Bak JF, Moller N, Schmitz O, Saaek A, Pedersen O 1992 *In vivo* insulin action and muscle glycogen synthase activity in type 2 (non insulin dependent) diabetes mellitus: effects of diet treatment, *Diabetologia* **35**:777-794
- Baron AD, Schaeffer L, Shragg P, Kolterman OG 1987 Role of hyperglucagonemia in maintenance of increased rates of hepatic glucose output in type II diabetics, *Diabetes* **36**:274-283
- Barrow GI and Feltham RKA 1995 Cowan and Steel's manual for the identification of medical bacteria third edition, Cambridge University Press Great Britain
- Bargis-Surgey P, Lavergne JP, Gonzalo P, Vard C, Filhol-Cochet O, Reboud JP 1999 Interaction of elongation factor eEF-2 with ribosomal proteins, *Eur J Biochem* **262**: 606-611
- Barthel A, Schmoll D, Kruger KD, Bahrenberg G, Walther R, Roth RA, Joost HG 2001 Differential regulation of endogenous glucose-6-phosphatase and phosphoenolpyruvate carboxykinase gene expression by the forkhead transcription factor FKHR in H4IIE-hepatoma cells, *Biochem Biophys Res Commun* **285**:897-902
- Bates SH, Jones RB, Bailey CJ 2000 Insulin-like effect of pinitol, *Br J Pharmacol***130**(8):1944-1948
- Baukrowitz T and Fakler B 2000 K_{ATP} channels; linker between phospholipid metabolism and excitability, *Biochem Pharmacol* **60**:735-740
- Bays H, Mandarino L, DeFronzo R 2004 Mechanisms of endocrine disease, *J Endocrinology and Metabolism* **89**(2):463-478
- Becker J 1974 Depression: theory and research second edition, V.H. Winston and Sons, New York:235-242
- Beintema JJ and Campagne RN 1987 Molecular evolution of rodents, *Mol Biol Evol* **4**(1):10-18
- Bellacosa A, Testa JR, Staal SP, Tsichlis PN 1991 A retroviral oncogene, Akt, encoding a serine-threonine kinase containing an SH2-like region, *Science* **254**(5029):274-277
- Benediktsson R, Yau JL, Low S, Brett LP, Cooke BE, Edwards CR, Seckl JR 1992 11 beta-hydroxysteroid dehydrogenase in the rat ovary: high expression in the oocyte, *Journal of Endocrinology* **135**(1):53-58
- Benn JJ and Sonksen PH 1993 *Diabetes,* Medicine International**21**:7
- Bentley GA, Dodson EJ, Dodson GG, Hodgkin DC, Mercola DA 1976 Structural rearrangements in insulin: a comparison of 2 and 4 zinc insulin structures, *Nature***261**:166-168
- Benzi L, Trischitta E, Ciccarone AM, Cecchetti P, Brunetti A, Cai F, Vigneri R, Navalesi R 1988 Metformin improves the reduced insulin internilisation and intracellular processing in obese diabetic patients but not in subjects with simple obesity, *Diabetologia* **31**:469A

- Berken GH, Weinstein DO, Stern WC 1984 Weight gain: A side effect of tricyclic antidepressants *J Affect Disord* **7**:133-138
- Bernstein JG 1987 Induction of obesity by psychotropic drugs Ann *N Y Acad Sci* **499**:203-15
- Bjornholm M and Zierath JR 2005 Insulin signal transduction in human skeletal muscle: identifying the defects in Type II diabetes, *Biochemi* **33**:354-357
- Blundell T, Dodson G, Hodgkin D, Mercola D 1972 Insulin: the structure in the crystal and its reflection in chemistry and biology, *Adv Protein Chem* **26**:279-402
- Boden G 1999 Free fatty acids, insulin resistance, and type 2 diabetes mellitus, *Proc Assoc Am Physicians* **111**:241-248
- Boden G, Chen X, Ruiz J, White JV, Rossetti L 1994 Mechanisms of fatty acid-induced inhibition of glucose uptake, *J Clin Invest* **93**:2438-46
- Boesch JS, Lee L, Lindahl RG 1996 Constitutive expression of class 3 aldehyde dehydrogenase in cultured rat corneal epithelium, *J Biol Chem* **271**(9):5150–5157
- Browner MF, Nakano K, Bang AG, Fleffenzk RJ 1989 Human muscle glycogen synthase with DNA sequence: anegatively charged protein with ansymmetric charge distribution, *Proc Natl Acad Sci USA* **86**:1443-1447
- Brunmair B, Staniek K, Gras F, Scharf N, Althaym A,1 Clara R, Roden M, Gnaiger E, Nohl H, Waldhausl W, Furnsinn C 2004 Thiazolidinediones, like metformin, inhibit respiratory complex I: A common mechanism contributing to their antidiabetic actions?, *Diabetes* **53**:1052-1059
- Burant, CF, Flink, S, Depaoli, AM, Chen, J, Lee, W, Hediger, MA, Buse, JB, and Chang, EB 1994 Small intestine hexose transport in experimental diabetes, *J Clin Invest* **93**:578-585
- Cahill CM, Tzivion G, Nasrin N, Ogg S, Dore J, Ruvkun G, Alexander-Bridges M 2001 Phosphatidylinositol 3-kinase signaling inhibits DAF-16 DNA binding and function via 14-3-3-dependent and 14-3-3-independent pathways, *J Biol Chem* **276**:13402-13410
- Cao QP, Geiger R, Langner D, Geisen K 1986 Biological activity *in vivo* of insulin analogues modified in the N-terminal region of the B-chain, *Biol Chem Hoppe Seyler* **367**(2):135-140
- Caro JF, Ittoop O, Pories WJ, Meelheim D, Flickinger EG, Thomas F, Jenquin M, Silverman JF, Khazanie PG, Sinha MK 1986 Studies on the mechanism of insulin resistance in the liver from humans with non-insulin-dependent diabetes Insulin action and binding in isolated hepatocytes, insulin receptor structure, and kinase activity, *J Clin Invest* **78**:249-58
- Caro JF, Sinha MK, Raju SM, Ittoop O, Pories WJ, Flickinger EG, Meelheim D, Dohm GL 1987 Insulin receptor kinase in human skeletal muscle from obese subjects with and without non-insulin dependent diabetes, *J Clin Invest* **79**:1330-1337
- Case CC, Jones PH, Nelson K, O'Brian Smith E, Ballantyne CM 2002 Impact of weight loss on the metabolic syndrome, *Diabetes, Obesity and Metabolism* **4**:407-414
- CDC/NCHS 2004 Respective health examination surveys, Centers for Disease Control and Prevention/National Center for Health Statistics, http://wwwcdcgov/nchs/
- Chadwick WA 2003 Observed metabolic changes in male Wistar rats after treatment with an antidepressant implied in undesirable weight gain, or *Sutherlandia frutescens* for type II diabetes, *Bsc (Hons) project report submitted in the Department of Biochemistry and Microbiology,* University of Port Elizabeth
- Chaffy N and Stokes T 2002 Aids herbal therapy, *Trends in Plant Science* **7**:57
- Chambliss, KL, Gray RGF, Rylance G, Pollitt RJ, Gibson KM 2000 Molecular characterization of methylmalonate semialdehyde dehydrogenase deficiency, *J Inherit Metab Dis* **23**:497-504
- Chavez JA, Knotts TA, Wang LP, Lit G, Dobrowsky RT, Florant GL, Summers SA 2003 A role for ceramide, but not diacylglycerol, in the antagonism of insulin signal transduction by saturated fatty acids, *J Biol Chem* **278**:10297-10303
- Cheatham B, Vlahos CJ, Cheatham L, Wang L, Blenis J, Kahn CR 1994 Phosphatidylinositol 3-kinase activation is required for insulin stimulation of pp70 S6 kinase, DNA synthesis, and glucose transporter translocation, *Mol Cell Biol* **14**:4902-4911
- Cheeseman CI and Maenz DD 1989 Rapid regulation of D-glucose transport in basolateral membrane of rat jejunum, *Am J Physiol* **256**:G878-G883

- Chiang SH, Baumann CA, Kanzaki M, Thurmond DC, Watson RT, Neudauer CL, Macara IG, Pessin JE, Saltiel AR 2001 Insulin-stimulated GLUT4 translocation requires the CAP-dependent activation of TC10, *Nature* **410**:944-948
- Chinkwo KA 2005 *Sutherlandia frutescens* Extracts can induce apoptosis in cultured carcinoma cells, *J Ethnopharm* **98**:163-170
- Christop B 2003 The Bcl-2 protein family: Sensors check point for life or death decision, *Molecular Immunology* **39**:615–647
- Clark F, Molero JC, James D E 2000 Release of insulin receptor substrate proteins from an intracellular complex coincides with the development of insulin resistance, *J Biol Chem* **275**:3819-3826
- Clarke JF, Young PW, Yonezawa K, Kasuga M, Holman GD 1994 Inhibition of the translocation of GLUT1 and GLUT4 in 3T3-L1 cells by the phosphatidylinositol 3-kinase inhibitor, wortmannin, *Biochem J* **300**:631-635
- Clement K 1999 Leptin and the genetics of obesity, *acta. Paediatr. Suppl* **428**:51-57
- Cline GW, Petersen KF, Krssak M, Shen J, Hundal RS, Trajanoski Z, Inzucchi S, Dresner A, Rothman DL, Shulman GI 1999 Impaired glucose transport as a cause of decreased insulin stimulated muscle glycogen synthesis in type 2 diabetes *N Engl J Med* **341**:240-246
- Coffer PJ and Woodgett JR 1991 *Eur J Biochem* **201**:475
- Colowick SP 1973 The hexokinases In Boyer PD (ed) The enzymes, vol 9 New York: Academic Press, pp 1-48
- Comi RJ, Grunberger G, Gorden P 1987 Relationship of insulin binding and insulin-stimulated tyrosine kinase activity is altered in type II diabetes, *J Clin Invest* **79**: 453-462
- Cook RJ and Wagner RC 1984 Glycine N-methyltransferase is a folate binding protein of rat liver cytosol (S-adenosylmethionine/one-carbon metabolism/methylation), *Proc NatI Acad Sci* **81**:3631-3634
- Cooper B and Gerlis, L 1997 A consumer's guide to precription medcines, Ted Smart, Great Britain
- Corvi MM, Soltys CM, Berthiaume LG 2001 Regulation of mitochondrial carbamoyl-phosphate synthetase 1 activity by active aite fatty acylation, *J Biol Chem* **276**(49): 45704–45712
- Cosmatos S, Cheng K, Okada Y, Katsoyannis PG 1978 *J Biol Chem* **253**:6586-6590
- Cusi K, Maezono K, Osman A, Pendergrass M, Patti ME, Pratipanawatr T, DeFronzo RA, Kahn CR, Mandarino LJ 2000 Insulin resistance differentially affects the PI 3-kinase and MAP kinase-mediated signaling in human muscle, *J Clin Invest* **105**:311-320
- Cutfield JF, Cutfield SM, Dodson EJ, Dodson GG, Reynolds CD, Vallely D 1981 In structural studies on molecules of bBiological interest (Dodson, G G, Glusker, J, & Sayre, D, Ed) pp 527-546, Oxford University Press
- Cutler D 1989 Deferoxamine therapy in high-ferritin diabetes, *Diabetes* **38**:1207-1210
- Czech MP and Corvera S 1999 Signaling mechanisms that regulate glucose transport, *J Biol Chem* **274**:1865-1868
- Dallman MF, Strack AM, Akana SF, Bradbury MJ, Hanson ES, Scribner KA, Smith M 1993 critical role of glucocorticoids with insulin in daily energy flow,*Front Neuroendocrinol* **14:**303–347
- Davani B, Khan A, Hult M, Mårtensson E, Okret S, Efendic S, Jornvall H, Oppermann UCT 2000 Type 1 11β-hydroxysteroid dehydrogenase mediates glucocorticoid activation and insulin release in pancreatic islets, *J Biol Chem* **275**:34841-34844
- Davidson MB and Peters AL 1997 An overview of metformin in the treatment of type II diabetes mellitus, *Am J Med* **102**:99-110
- Davis MD, Parniak MA, Kaufman S, Kempner E 1997 The role of pPhenylalanine in structure–function relationships of phenylalanine hydroxylase revealed by radiation target analysis, *Proc Natl Acad Sci* **94**: 491-495
- Davis A, Christtiansen M, Horowitz JF, Klein S, Hellerstein MK, Ostlund RE 2000 Effect of pinitol treatment on iInsulin action in subjects with insulin resistance, *Diabetes Care* **23**:1000-1005

- Davison KK and Birch LL 2001 Childhood overweight: A contextual model and recommendations for future research, *Obesity Reviews* **2**(3):159-171
- Dean DJ and Ruderman NB 2002 Role of AMP kinase and malonyl CoA in exercise-stimulated skeletal muscle metabolism and insulin action In *Muscle Metabolism* Zierath JR, Wallberg-Henriksson H, Eds New York, Taylor & Francis
- Debnam ES, Smith MW, Sharp PA, Srai SK, Turvey A, Keable S J 1995 The effects of streptozotocin diabetes on sodium-glucose transporter (SGLT1) expression and function in rat jejunal and ileal villus-attached enterocytes, *Eur J Physiol* **430**:151-159
- De Fea K and Roth RA 1997 Modulation of insulin receptor substrate-1 tyrosine phosphorylation and function by mitogen-activated protein kinase, *J Biol Chem* **272**:31400-6
- De Fea K and Roth RA 1997 Protein kinase C modulation of insulin receptor substrate-1 tyrosine phosphorylation requires serine 612, *Biochemistry* **36**:12939-12947
- De Mars R, Le Van S. L, Trend B.L, Russell BL 1976 Abnormal ornithine carbamoyltransferase in mice having the sparse-fur mutation, *PNAS* **73**(5): 1693-1697
- DeFronzo RA, Goodman AM and the Multicellular Metformin Study Group 1995 Efficacy of metformin in patients with non-insulin dependent diabetes mellitus, *N Engl J Med* **333**:541-549
- DeFronzo RA and Mandarino LJ 2003 Pathogenesis of type II diabetes mellitus, Endotext.org your endocrine source, www.endotext.org.
- Deshmukh R and Franco K 2003 Managing weight gain as a side effect of antidepressant therapy, *Cleveland Clinical Journal of Medicine* **70**:614-623
- Dieuaide-Noubhani M, Asselberghs S, Mannaerts GP & Van Veldehoven PP 1997*a* Evidence that multifunctional protein 2, and not multifunctional protein 1, is involved in the peroxisomal-oxidation of pristanic acid, *Biochemical Journal* **325** 367–373
- Dieuaide-Noubhani M, Novikov D, Vanderkerckhove J, Veldhoven PPV & Mannaerts GP 1997*b* Identification and characterization of the 2-enoyl-CoA hydratases involved in peroxisomal, oxidation in rat liver, *Biochemical Journal* **321**:253–259
- Doluisio JT, Billups NF, Dittert LW, Sugita ET, Swintosky JV 1969 Drug absorption: an *in situ* rat gut technique yielding realistic absorption rates, *J Pharm Sci* **58**:1196-1200
- Dresner A, Laurent D, Marcucci M, Griffin ME, Dufour S, Cline SW, Slezak LA, Andersen DK, Hundal RS, Rothman DL, Pertersen KF, Shulman GI 1999 Effects of free fatty acids on glucose transport and IRS-1 associated phosphatidylinositol 3-kinase activity, *J Clin Invest* **103**:253-259
- Duckworth WC 1979 Insulin degradation by liver cell membranes, *Endocrine Rev* **104**:1758-1764
- Duckworth WC 1988 Insulin degradation: Mechanisms, products, and significance, *Endocrine Rev* **9**(3):319-344
- Duckworth WC, Peavy DE, Hamel FG 1997 Two pathways for insulin metabolism in adipocytes, *Biochem Biophys Acta* **1358**:163-171
- Duckworth WC 1997 Tumor necrosis factor and insulin resistance: Specificity of sequence accounts of inhibition of insulin action, *J Lab Clin Med* **130**(2):139-146.
- Duckworth WC, Bennet RG, Hamel FG 1998 Insulin degradation: Progress and potential, *Endocrine Rev* **19**(5):608-624
- Ducluzeau PH, Perretti N, Laville M, Andreelli F, Vega N, Riou JP, Vidal H 2001 Regulation by insulin of gene expression in human skeletal muscle and adipose tissue Evidence for specific defects in type 2 diabetes, *Diabetes* **50**:1134-1142
- Duggirala R, Blangero J, Alamsy L, Arya R, Dyer TD, Williams KL, Leach RJ, O'Connell P, Stern MP 2001 A major locus for fasting insulin concentrations and insulin resistance on chromosome 6q with strong pleiotropic effects on obesity-related phenotypes in nondiabetic mexican americans, http://www/query.fcgi?cmd=Retrieve&db=PubMed
- Dullo AG and Miller DS 1987 Thermogenic drugs and the treatment of obesity: sympathetic stimulants in animal models, *Br J Nutr* **52**:179-196
- Dunaif A, Xia J, Book CB, Schenker E, Tang Z, 1995 Excessive insulin receptor serine phosphorylation in cultured fibroblasts and in skeletal muscle. A potential mechanism for insulin resistance in the polycystic ovary syndrome, *J Clin Invest* **96**:801-810
- Dyer O 2002 First cases of type II diabetes found in white UK teenagers, *Br Med J* **324**:506

- Eaton WW, Armenian H, Gallo J 1996 Depression and risk for onset of type II diabetes, *Diabetes Care* **19**:1097–1102
- Echwald SM, Bjorbaek C, Hansen T, Clausen JO, Vestergaard H, Zierath JR, Printz RL, Granner DK, Pedersen O 1995 Identification of four amino acid substitutions in hexokinase II and studies of relationships to NIDDM, glucose effectiveness, and insulin sensitivity, *Diabetes* **44**:347-353
- Eckman EA and Eckman CB 2005 β-degrading enzymes: Modulators of alzheimer's disease pathogenesis and targets for therapeutic intervention, *Biochem Soc Trans* **33**:1101–1105
- Ellis L, Morgan DO, Clauser E, Roth RA, Rutter WJ 1987 A membrane-anchored cytoplasmic domain of the human insulin receptor mediates a constitutively elevated insulin-independent uptake of 2-deoxyglucose, *Mol Endocrinol* **1**:15-24
- Esser MJ, Chase T, Allen GV, Sawynok J 2003 Chronic administration of amitriptyline and caffeine in a rat model of neuropathic pain: multiple interactions, *European Journal of Pharmacology* **430**:211-218
- Evans JL and Rushakoff RJ 2002 Oral pharmacological agents for type II diabetes: Sulfonylureas, meglitinides, metformin, thiazolidinediones, α-glucosidase inhibitors and emerging approaches, Endotext.org your endocrine source, www.endotext.org.
- Fan LQ, Cattley RC, Corton JC 1998 Tissue-specific induction of 17-hydroxysteroid dehydrogenase type IV by peroxisome proliferator chemicals is dependent on the peroxisome proliferator-activated receptor, *Journal of Endocrinology* **158:** 237–246
- Fanghanel G, Sanchez-Reyes L, Trujillo C, Sotres D, Espinosa-Campos J 1996 Metformin's effects on glucose and lipid metabolism in patients with secondary failure to sulfonylureas, *Am Diabetes Ass* Alexandria **19**:1185-1193
- Farese RV 2001 Insulin-sensitive phospholipid signaling systems and glucose transport update II, *Exp Biol Med*(Maywood) **226**:283-95
- Fava M 2000 Weight gain and antidepressants, *J clin Psychiatry* **11**:37-41
- Feinstein R, Kanety H, Papa MZ, Lunenfeld B, Karasik A 1993 Tumor necrosis factor-α suppresses insulin-induced tyrosine phosphorylation of insulin receptor and its substrates, *J Biol Chem* **268**:26055-26058
- Feldman JM 1976 Inhibition of pancreatic islet monoamine oxidase by adrenergic antagonists and ethanol, *Endocrine Res Comm* **2**:503–520
- Feldman H and Rodbard D 1971 "Mathematical theory of radioimmunoassays", in: WD Odell and Doughaday, WH (Ed), Principles of competative protein binding assays Philadelphia: JB Leppincott Company; pp 138-203
- Fernandes AC, Cromarty AD, Albrecht C, van Rensburg CEJ 2004 The antioxidant potential of *Sutherlandia frutescens*, *J Ethnopharm* **95**:1–5
- Fernandez-Alvarez J, Barbera A, Nadal B, Barcelo-Batllori S, Piquer S, Claret M, Guinovart JJ, Gomis R 2004 Stable and functional regeneration of pancreatic β-Cell population in nSTZ-rats treated with tungstate, *Diabetalogia* **47**:470-477
- Fernstorm MH and Kupfer DJ 1988 Antidepressant-induced weight gain: A comparison study of four medications, *Psychiatry Res* **3**:265-271
- Ferri C, Bellini C, Desideri G, Di Francesco L, Baldoncini R, Santucci A 1995 Plasma endothelin-1 levels in obese hypertensive and normotensive men, *Diabetes* **44**(4):431–436
- Fierdman MI 1995 Control of energy intake by energy metabolism, *Am J Clin Nutr* **62**:1096S-1100S
- Fisher L, Chesla CA, Mullan JT, Skaff MM, Kanter RA 2001 Contributors to depression in latino and European-American patients with type 2 diabetes, *Diabetes* Care **24**:1751–1757
- Flatt PR 1992 Nutrient regulation of insulin secretion, Portland Press Research Monograph
- Flatt JP 1995 Use and storage of carbohydrate and fat *Am J Clin Nutr* 61, *Suppl* **4**:952S–959S
- Freedman BD, Lee EJ, Park Y, Jameson JL 2005 A dominant negative peroxisome proliferators activated receptor-in mouse exhibits features of the metabolic syndrome, JBC Papers in Press
- Freidenberg GR, Henry RR, Klein HH, Reichart DR, Olefsky JM 1987 Decreased kinase activity of insulin receptors from adipocytes of non-insulin-dependent diabetic studies, *J Clin Invest* **79**:240-250

- Freidenberg GR, Reichart D, Olefsky JM, Henry RR 1988 Reversibility of defective adipocyte insulin receptor kinase activity in non-insulin dependent diabetes mellitus. Effect of weight loss, *J Clin Invest* **82**:1398-1406
- Fruebis J, Tsao TS, Javorschi S, Ebbets-Reed D, Erickson MR, Yen FT, Bihain BE, Lodish HF 2001 Proteolytic cleavage product of 30-kDa adipocyte complement-related protein increases fatty acid oxidation in muscle and causes weight loss in mice, *Proc Natl Acad Sci U S A* **98**:2005-10
- Fujishiro M, Gotoh Y, Katagiri H, Sakoda H, Ogihara T, Anai M, Onishi Y, Ono H, Funaki M, Inukai K, Fukushima Y, Kikuchi M, Okai Y, Asano T 2001 MKK6/3 and p38 MAPK Pathway activation is not necessary for insulin-induced glucose uptake but regulates glucose transporter expression, *J Biol Chem* **276**(23):19800-19806
- Gallo JJ 1999 Tricyclic antidepressants versus selevtive serotonin reuptake inhibitors, *Am Med Ass* **8**(4):1-7
- Ganong F 1993 Review of medical physiology sixteenth edition, Prentice-Hall International Inc
- Garland EJ, Remick RA, Zis AP 1988 Weight gain with antidepressants and lithium *J Clin Pharmacol* **8**:323-330
- Garvey WT 1998 Insulin action and insulin resistance: diseases involving defects in insulin receptors, signal transduction, and the glucose transport effector system, *Am J Med* **105**:331-345
- Gehringer MM, Downing TG, Graz CJM 1998 Microbiology practical manual 201, Biochemistry and Microbiology Department, University of Port Elizabeth
- Geiger R, Geisen K, Summ HD, Langner D 1975 Hoppe-Seyler's *Z Physiol Chem* **356**:1635-1649
- Geiger R, Geisen K, Regitz G, Summ HD, Langner D 1980 Insulin analogoues with substitution of A1-glycine by D-amino acids and omega-amino acids, *Hoppe-Seyler Z Physiol Chem* **361**:563–570
- Geiger R, Geisen K, Summ HD 1982 Exchange of A1-glycine in bovine insulin with L- and D-tryptophan, *Hoppe-Seyler Z Physiol Chem* **363**:1231–1239
- Gericke N 2001 Diabetes and *Sutherlandia, Sutherlandia* Dot Org, http://wwwsutherlandiaorg/diabeteshtml
- Gibbon CJ 2000 South African medicines formulary, INCE Cape, Woodstock, Cape Town
- Giblin JP, Leaney JL, Tinker A 1999 The molecular assembly of ATP-sensitive potassium channels, *J Biol Chem* **274**:22652-22659
- Gibson DM and Harris RA 2002 Metabolic regulation in mammals, Taylor and Francis Group, New York
- Goodnick PJ 2001 Use of antidepressants in treatment of comorbid diabetes mellitus and depression as well as in diabetic neuropathy, **:** *Annals of Clinical Psychiatry* **13**(1):31-41
- Goodwin GW, Rougraff PM, Davis FJ, Harris RA 1989 Purification and characterization of methylmalonate-semialdehyde dehydrogenase from rat liver, *The American Society for Biochemistry and Molecular Biology* **264**(25):14965-14971
- Gottfries CG 1981 Influence of depression and antidepressants on weight, *Acta Psychiatrica* **290**:353-356
- Gram LF 1983 Antidepressants: Receptors, pharmacokinetics and clinical effects, In Burrows GD, Norman TR, Davies B, Drugs in psychiatry: Antidepressants volume I, Elsevier Science Publishers, Amsterdam, New York, Oxford
- Greco AV, Mingrone G, Capristo E 1995 Effects of dexfen- fluramine on free fatty acid turnover and oxidation in obese patients with type 2 diabetes mellitus *Metabolism*, **442** (Suppl 2):57–61
- Griest JH and Griest TH 1979 Antidepressant Treatment-The Essentials, The Williams and Wilkins Company, New York
- Gual P, Marchand-Brustel Y, Tanti JF 2005 Positive and negative regulation of insulin signaling through IRS-1 phosphorylation, *Biochimie* **87**:99–109
- Guo S, Rena G, Cichy S, He X, Cohen P, Unterman T 1999 Phosphorylation of serine 256 by protein kinase B disrupts transactivation by FKHR and mediates effects of insulin on insulin-like growth factor-binding protein-1 promoter activity through a conserved insulin response sequence, *J Biol Chem* **274**:17184-92

- Haffner S, Karhapaa P, Mykkanen L, Lansko M 1993 Insulin resistance, body fat distribution and sex hormones in men, *Diabetes* **43**:212-219
- Hakanson R, Lundquist I, Rerup C 1967 On the hyperglycaemic effect of dopa and dopamine, *Eur J Pharmacol* **1**:114–119
- Hanely AG, Harris SB, Gittelsohn J, Wolever TS, Saksvig B, Zinman B 2000 Overweight among children and adolescents in a native canadian community: Prevalence and associated factors, *Am J Clin Nutr* **71**(3):693-700
- Hardie DG and Hawley SA 2001 AMP-activated protein kinase: the energy charge hypothesis revisited, *Bioassays* **23**:1112–1119
- Harnett SM, Oosthuizen V, van de Venter M 2005 Anti-HIV Activities of organic and aqueous extracts of *Sutherlandia frutescens* and *Lobostemon trigonus*, *J Ethnopharm* **96**:113-119
- Hawley SA, Gadalla AE, Olsen GS, Hardie DG 2002 The antidiabetic drug metformin activates the AMP-activated protein kinase cascade via an adenine nucleotide-independent mechanism, *Diabetes* **51**:2420–2425
- Hayashi T, Hirshman MF, Fujii N, Habinowski SA, Witters LA, Goodyear LJ 2000 Metabolic stress and altered glucose transport: activation of AMPactivated protein kinase as a unifying coupling mechanism, *Diabetes* **49**:527–531
- Heil SG, Lievers KJA, Boers GH, Verhoef P, den Heijer M, Trijbels FJM, Blom HJ 2000 Betaine-homocysteine methyltransferase (BHMT): Genomic sequencing and relevance to hyperhomocysteinemia and vascular disease in humans, *Molecular Genetics and Metabolism* **71**: 511–519
- Hering B 2005 Islet Transplants, *Islet Technologies*
- Hermann LS, Schersten B, Bitzin PO, Kjellstrom T, Lindgarde F, Melander A 1994 Therapeutic comparison of metformin and sulfonylurea, alone and in various combinations, *Am Diabetes Ass, Diabetes Care, Alexandria* **17**:1100-1109
- Hernandez-Sanchez C, Ito Y, Ferrer J, Reitman M, LeReith D 1999 Characterization of the mouse sulfonylurea receptor 1 promoter and it's regulation, *J Biol Chem* **274**:18261-18270
- Hieble JP, Nichols AJ, Langer SZ, Ruffolo RR 1995 Pharmacology of the sympathetic nervous system, in PJ Munson principles of pharmacology, Chapman and Hall, New York
- Hinze-Selch D, Schuld A, Kraus T, Kuhn M, Uhr M, Haack M, Pollmacher T 2000 Effects of antidepressants on weight gain and on the plasma levels of leptin, TNF-alpha and soluble TNF receptors: A longitudinal study in patients treated with amitriptyline or paroxetine, *Neuropsychopharmacology* **23**:13-19
- Hirotsu S, AbeY, Okada K, Nagahara N, Hori H, Nishino T, Hakoshima T 1999 Crystal structure of a multifunctional 2-cys pPeroxiredoxin heme-binding protein 23 kDa/proliferation-associated gene product, *PNAS* **96** (22): 12333-12338
- Hitman GA, Hawrammi K, McCarthy MI, Viswanathan M, Snehalatha C, Ramachandran A, Tuomilehto J, Tumilehto-Wolf E, Nissenen A, Pedersen O 1995 Insulin receptor substrate-1 gene mutations in NIDDM: implication for the study of polygenic disease, *Diabetologia* **38**:481-486
- Hojlund K, Wrzesinski K, Mose Larsen P, Fey SJ, Roepstroff P, Handberg A, Dela F, Vinten J, McCormack JG, Reynet C, Nielsen HB 2003 Proteome analysis reveals phosphorylation of ATP synthase β-subunit in human skeletal muscle and proteins with potentila roles in type 2 diabetes, *J Biol Chem* **278**(12):10436-10442
- Holden HM and Banaszakg LJ 1983 L-3-hydroxyacyl coenzyme A aehydrogenase, *Journal of Biological Chemistry* **258**(4):2383-2389
- Holister LE 1995 Antidepressant agents, In Katzung BG (Ed) Basic and clinical pharmacology. Appleton and Lang, Connecticut USA:448-459
- Holmang A and Bjorntorp P 1992 The Effects of testosterone on insulin sensitivity in male rats, *Acta Physiol Scand* **146**:505-510
- Hotamisligil GS 1999 The role of TNFalpha and TNF receptors in obesity and insulin resistance, *J Int Med* **245**:(6)621–625
- Hotamisligil GS, Peraldi P, Budavari A, Ellis R, White MF, Spiegelman BM 1996 IRS-1-mediated inhibition of insulin receptor tyrosine kinase activity in TNF-α and obesity-induced insulin resistance, *Science* **271**:665-668

- Hsueh WA and Law RE 1999 Insulin signaling in the arterial wall, *Am J Cardiol* **84**:21J-24J
- Hubbard SR 1997 Crystal structure of the activated insulin receptor tyrosine kinase in complex with peptide substrate and ATP analog, *Embo J* **16**:5572-81
- Hubbard SR, Wei L, Ellis L, Hendrickson WA 1994 Crystal structure of the tyrosine kinase domain of the human insulin receptor, *Nature* **372**:746-754
- Hurr NA 1996 The effect of aerobic exercise on the adipose tissue of subjects using antidepressant medication, M.Sc Dissertation, University of Port Elizabeth
- Imai Y, Philippe N, Accili D, Taylor SI 1997 Expression of variant forms of insulin receptor substrate-1 identified in patients with noninsulin dependent diabetes mellitus, *J Clin Endocrinol Metab* **82**:4201-4207
- Isacsson V and Wettermark G 1974 Chemiluminescence in analytical chemistry, *Anal Chim Acta* **68**:339-362
- Isomoto S, Kondo C, Yamada M, Matsumoto S, Higashiguchi O, Horio Y, Matsuzawa Y, Kurachi Y 1996 A novel sulfonylurea receptor forms with BIR (Kir62) a smooth muscle type ATP-sensitive K^+ channel, *The American Society for Biochemistry and Molecular Biology* **271**:24321-24324
- Jackson RA, Hawa MI, Jaspan JB, Sim BM, Disilvo L, Featherbe D and Kurtz AB 1987 Mechanism of metformin action in non-insulin dependent diabetes, *Am Diabetes Ass* New York **36**:632-640
- JAMA 2004 Overweight and obesity — Statistics, *J Am Med Ass* **291**:2847-50
- James WP 1995 A public health approach to the problem of obesity, *Int J Obes Relat Metab Disord* **19**(Suppl 3):S37-S45
- Janke J, Engeli S, Gorzelniak K, Luft FC, Sharma AM 2002 Resistin gene expression in human adipocytes is not related to insulin resistance, *Obes Res* **10**:1-5
- Jiang G and Zhang BB 2005 Modulation of insulin signaling by insulin sensitizers, *Biochemical Society Transactions* **33**(2):358-361
- Johnson AB, Webster JM, Sum CF 1993 The impact of metformin therapy on hepatic glucose production and skeletal muscle glycogen synthase activity in overweight type II diabetic patients, *Metabolism* **42**:1217-1222
- Jones PF, Jakubowicz T, Pitossi FJ, Maurer F, Hemmings BA 1991 Molecular cloning and identification of a serine/threonine protein kinase of the second-messenger subfamily, *Natl Acad Sci*USA **88**:4171
- Kahn BB, Flier JS 2000 Obesity and insulin resistance, *J Clin Invest* **106**:473-481
- Kanai F, Ito K, Todaka M, Hayashi H, Kamohara S, Ishii K, Okada T, Hazeki O, Ui M, Ebina Y 1993 Insulin-stimulated GLUT4 translocation is relevant to the phosphorylation of IRS-1 and the activity of PI3-kinase, *Biochem Biophys Res Commun* **195**:762-768
- Karam JH, Martin SB, Forsham PH 1978 Antidiabetic drugs after the university group diabetes program, *Annu Rev Pharmacol* **15**:351-366
- Kashyap S, Belfort R, Finlayson J, Barrentine A, Mandarino L, DeFronzo RA, Cusi K 2002 A chronic physiologic increase in FFA in healthy subjects causes insulin signaling defects similar to those of insulin-resistant nondiabetic subjects with strong family history of T2DM, *Diabetes* **51**(Suppl 2):A24
- Kasuga M, Karlsson FA, Kahn CR 1982 Insulin stimulates the phosphorylation of the 95,000-dalton subunit of its own receptor, *Science* **215**:185-187
- Kawakami N, Takatsuka N, Shimizu H 1999 Depressive symptoms and occurrence of type 2 diabetes among Japanese men, *Diabetes Care* **22**(7):1071–1076
- Katz EB, Stenbit AE, Hatton K, DePinho R, Charron MJ 1995 Cardiac and adipose tissue abnormalities but not diabetes in mice deficient in GLUT4, *Nature* **377**:151-155
- Kellerer M, Kroder G, Tippmer S, Berti L, Kiehn L, Mosthaf L, Haring H 1994 Troglitazone prevents glucose-induced insulin resistance of insulin receptor in rat-1 fibroblasts, *Diabetes* **43**:447-453
- Kelley D, Mokan M, Mandarino L 1992 Intracellular defects in glucose metabolism in obese patients with noninsulin-dependent diabetes mellitus, *Diabetes* **41**:698-706

- Kelley DE and Mandarino LJ 2000 Fuel selection in human skeletal muscle in insulin resistance, *Diabetes* **49**:677-683
- Kerr JFR, Wyllie AH, Currie AR, 1972 Apoptosis: A basic biological phenomenon with wide-ranging implication in tissue kinetics, *British Journal of Cancer* **26**:239–257
- Kido Y, Burks DJ, Withers D, Bruning JC, Kahn CR, White MF, Accili D 2000 Tissue-specific insulin resistance in mice with mutations in the insulin receptor, IRS-1, and IRS-2, *J Clin* Invest **105**:199-205
- Klein HH, Vestergaard H, Kotzke G, Pedersen O 1995 Elevation of serum insulin concentration during euglycaemic hyperinsulinemic clamp studies leads to similar activation of insulin receptor kinase in skeletal muscle of subjects with and without NIDDM, *Diabetes* **344**:1310-1317
- Klip A and Leiter LA 1990 Cellular mechanism of action of metformin, *American Diabetes Association, Diabetes Care, Alexandria* **13**:696-704
- Kobayashi M, Ohgaku S, Iwasaki M, Maegawa H, Shigeta Y, Inouye K 1982 Characterization of [LeuB-24]- and [LeuB-25]-insulin analogues receptor binding and biological activity, *Biochem J* **206**(3):597-603
- Konrad RJ, Mikolaenko I, Tolar JF, Liua K, Kudlowa JE 2001 The potential mechanism of the diabetogenic action of streptozotocin: inhibition of pancreatic β-cell O-GlcNAc-selective N-acetyl-b-D-glucosaminidase, *Biochem J* **356**:31-41
- Krook A, Bjornholm M, Galuska D, Jiang XJ, Fahlman R, Myers MG, Wallberg-Henriksson H, Zierath JR 2000 Characterization of signal transduction and glucose transport in skeletal muscle from type 2 diabetic patients, *Diabetes* **49**:284-292
- Kruszynska YT, Mulford MI, Baloga J, Yu JG, Olefsky JM 1998 Regulation of skeletal muscle hexokinase II by insulin in nondiabetic and NIDDM subjects, *Diabetes* **47**:1107-1113
- Kruszynska YT, Worrall DS, Ofrecio J, Frias JP, Macareg G, Olefsky JM 2002 Fatty acid-induced insulin resistance: decreased muscle P13K activiation but unchanged Akt phosphorylation, *J Clin Endocrinol Metab* **87**:226-234
- Kumar N and Dey CS 2002 Gliclazide increases insulin receptor tyrosine phosphorylation but not p38 phosphorylation in insulin-resistant skeletal muscle cells, *J Exp Biol* **205**:3739–3746
- Kulisz A, Chen N, Chandel NS, Shao Z, Schumacker PT 2002 Mitochondrial ROS initiate phosphorylation of p38 MAP kinase during hypoxia in cardiomyocytes, *Am J Physiol Lung Cell Mol Physiol* **282**:L1324–L1329
- Kundua JK, Mossandab KS, Naa HK, Surha YJ 2005 Inhibitory effects of the extracts of *Sutherlandia frutescens* (L) R Br and *Harpagophytum procumbens* DC on phorbol ester-induced COX-2 expression in mouse Skin: AP-1 and CREB as potential upstream targets, *Cancer Letters* **218**:21–31
- Kusari J, Verma US, Buse JB, Henry RR, Olefsky JM 1991 Analysis of the gene sequences of the insulin receptor and the insulin-sensitive glucose transporter (GLUT4) in patients with common-type non-insulin-dependent diabetes mellitus, *J Clin Invest* **88**:1323-1330
- Kwok J and Mitchelson 1981 Depression and antidepressants, *Aus J Pharmacy* 383-397
- Kwok SCM, Steiner DF, Rubenstein AH, Tager HS 1983 Identification of a point mutation in the human insulin gene, *Diabetes* **32**: 872-875
- Laakso M, Malkki M, Kekalainen P, Kuusito J, Deeb SS 1995 Polymorphisms of the human hexokinase II gene: lack of association with NIDDM and insulin resistance, *Diabetologia* **38**:617-622
- Lawrie LC, Dundas SR, Curran S, Murray GI 2004 Liver fatty acid binding protein expression in colorectal neoplasia, *British Journal of Cancer* **90**:1955-1960
- Leenders F, Adamski J, Husen B, Thole HH, Jungblut PW 1994 Molecular cloning and amino acid sequence of the porcine 17-estradiol dehydrogenase, *European Journal of Biochemistry* **222** 221–227
- Lehto M, Huang X, Davis EM, Le Beau MM, Laurila E, Eriksson KF, Bell GI, Groop L 1995 Human hexokinase II gene: exon-intron organization, mutation screening in NIDDM, and its relationship to muscle hexokinase activity, *Diabetologia* **38**:1466-1474
- Lekas MC, Fisher SJ, El-Bahrani B 1999 Glucose uptake during centrally induced stress is insulin independent and enhanced by adrenergic blockade, J *Appl Physiol* **87**(2):722–731

- Livingstone C and Collison M 2002 Sex steroids and insulin resistance, *Clinical Science* **102**:151–166
- Liu, K, Paterson, A J, Chin, E and Kudlow, J E 2000 Glucose stimulates protein modification by O-linked GlcNAc in pancreatic β-cells: linkage of O-linked GlcNAc to β-cell death *Proc Natl Acad Sci USA* **97**:2820-2825
- Lochhead PA, Coghlan M, Rice SQ, Sutherland C 2001 Inhibition of GSK-3 selectively reduces glucose-6-phosphatase and phosphatase and phosphoenolypyruvate carboxykinase gene expression, *Diabetes* **50**:937-946
- Lonnqvist F, Nordfors L, Schalling M 1999 Leptin and its potential role in human obesity, *J Int Med* **245**:643-652
- Lord JM, White SI, Baily CJ, Atkins TW, Fletcher RF, Taylor KG 1983 Effect of metformin on insulin receptor binding and glycaemic control in type II diabetes, *Br Med Ass* London **286**:830-831
- Luo RZ, Beniac DR, Fernandes A, Yip CC, Ottensmeyer FP 1999 Quaternary structure of the insulin-insulin receptor complex, *Science* **285**:1077-80
- MaCsween RNM and Whaley K 1992 Muir's textbook of pathology, Thirteenth edition, London Melbourne Auckland
- Madsen KL, Ariano D, Fedorak RN 1996 Insulin downregulates diabetic-enhanced intestinal glucose transport rapidly in ileum and slowly in jejunum, *J Physiol Pharmacol* **74**:1294-1301
- Magnuson MA, Andreone IL, Printz RL, Koch S, Granner DK 1989 The glucokinase gene: structure and regulation by insulin, *Proc Natl Acad Sci USA* **86**: 4838-4842
- Magnusson I, Rothman DL, Katz LD, Schulman RG, Schulman GI 1992 Increased rate of gluconeogenesis in type II diabetes mellitus A ^{13}C nuclear magnetic resonance study, *J Clin Invest* **90**:1323-1327
- Makino S, Baker RA, Smith MA, Gold PW 2000 Differential regulation of neuropeptide Y mRNA expression in the arcuate nucleus and locus coeruleus by stress and antidepressants *J Neuroendocrinology* **12**:387–395
- Mallisa RJ, Polanda BW, Chatterjeeb TK, Fisherb RA, Darmawana S, Honzatkoa RB, Thomasa JA 2000 Crystal structure of S-glutathiolated carbonic anhydrase III, *FEBS* **482**:237-241
- Mandarino LJ, Madar Z, Kolterman OG, Bell JM, Olefsky JM 1986 Adipocyte glycogen synthase and pyruvate dehydrogenase in obese and type II diabetic patients, *Am J Physiol* **251**:E489-E496
- Mandarino LJ, Printz RL, Cusi KA, Kinchington P, O'Doherty RM, Osawa H, Sewell C, Consoli A, Granner DK, DeFronzo RA 1995 Regulation of hexokinase II and glycogen synthase mRNA, protein, and activity in human muscle, *Am J Physiol* **269**:E701-E708
- Marshall VD and Sokatch JR 1972 Regulation of valine catabolism in *Pseudomonas putida*, *J bact* **110**:1073-1081
- Matschinsky FM 1996 Banting lecture 1995: A lesson in metabolic regulation inspired by the glucokinase glucose sensor paradigm, *Diabetes* **45**:223-241
- Matsuda M, DeFronzo RA, Consoli A, Bressler P, Del Prato S 2002 Dose response curve relating plasma glucagons to hepatic glucose production and glucose disposal in type 2 diabetes mellitus, *Metabolism* **51**:1111-1119
- Matthaei S, Stumvoll M, Keller M, Huring H 2000 Pathophysiology and pharmacological treatment of insulin resistance, *Endo Rev* **21**(6):585-618
- Maurizio F 2000 Weight gain and antidepressants *J Clin Psychiatry* **61**:37-41
- McEvoy RC and Hegre OD 1979 Syngeneic transplantation of fetal rat pancreas III Effect of insulin treatment on the growth and differentiation of the pancreatic implants after reversal of diabetes, *Diabetes* **28**:141-146
- McGarry JD 1992 What if Minkowski had been ageusic? An alternative angle on diabetes, *Science* **258**:766-770
- McGarry JD 2002 Banting Lecture 2001: Dysregulation of fatty acid metabolism in the etiology of type 2 diabetes, *Diabetes* **51**:7-18
- McTernan CL, McTernan PG, Harte AL, Levick PL, Barnett AH, Kumar S 2002 Resistin, central obesity, and type 2 diabetes, *Lancet* **359**:46-7

- McVie-Wylie AJ, Lamson DR, Chen YT 2001 Molecular cloning of a novel member of the GLUT family of transporters, slc2a10 (glut10), localized on chromosome 20q13.1: A candidate gene for NIDDM susceptibility, *Genomics* **72**(1):113-117
- Medical Research Council and National Research Foundation of South Africa 2002 A toxicity study of *Sutherlandia* leaf powder (*Sutherlandia microphylla*) consumption Final Report 2002
- Merrick WC 1992 Mechanism and regulation of eukaryotic, *Microbiology reviews* **56**(2):291-315
- Michalak M, Mariani P, Opas M. 1998 Calreticulin, a multifunctional Ca^{2+} binding chaperone of the endoplasmic reticulum, *Cell Biol Biochim Biol Cell* **76**(5):779-785
- Miki T, Nagashima K, Seino S 1999 The structure and function of the ATP-sensitive potassium channel in insulin secreting pancreatic beta cells, *J Mol Endocrin* **22**:113-123
- MIMS 2000 Medical speciality, Volume 40 No. 12
- Minassian C, Tarpin S, Mithieux G 1998 Role of glucose-6-phosphatase, glucokinase and glucose-6-phosphate in liver insulin resistance and its correction by metformin, *Biochem Pharacol* **55**:1213-1219
- Minokoshi Y, Kim YB, Peroni OD, Fryer LG, Muller C, Carling D, Kahn BB 2002 Leptin stimulates fatty-acid oxidation by activating AMP-activated protein kinase, *Nature* **415**:339-343
- Mithieux G, Guignot L, Bordet JC, Wiernsperger N 2002 Intrahepatic mechanisms underlying the effect of metformin in decreasing basal glucose production in rats fed a high-fat diet, *Diabetes* **51**:139-143
- Miyazaki Y, Pipek R, Mandarino LJ, DeFronzo RA 2003 Tumor necrosis factor and insulin resistance in obese type 2 diabetic patients, *International Journal of Obesity* **27**: 88-94
- Mizuma T, Koyanagi A, Awazu S 1997 Intestinal transport and metabolism of analgesi dipeptide, kyotrophin: Rate-limiting factor in intestinal absorption of peptide as a drug, *Biochimica Biophysica Acta* **1335**:111-119
- Mohammad A, Sharma V, McNeill JH 2002 Vanadium increases GLUT4 in diabetic rat skeletal muscle, *Molecular and Cellular Biochemistry* **233**:139-143
- Molina JM, Ciaraldi TP, Brady D, Olefsky JM 1989 Decreased activation rate of insulin-mediated glucose transport in adipocytes from obese and NIDDM subjects, *Diabetes* **38**:991-995
- Moller DE, Yakota A, Flier JS 1989 Normal insulin receptor cDNA sequence in Pima Indians with non-insulin-dependent diabetes mellitus, *Diabetes* **38**:1496-1500
- Monder C 1991 Corticosteroids, receptors, and the organ-specific functions of 1 1/3-hydroxysteroid dehydrogenase, *FASEBJ* **5**:3047-3054
- Montgomery R, Conway TW, Spector AA, Chappell D 1996 Biochemistry a case oriented approach, Sixth Edition, Mosby, Boston
- Mooradian AD, Failla M, Hoogwerf B, Maryniuk M, Wylie-Rosett J 1994 Selected vitamins and minerals in diabetes mellitus, *Diabetes Care* **17**:464-479
- Morgan CR and Lazarow A 1963 Immunoassay of insulin: Two antibody system plasma insulin levels in normal, subdiabetic and diabetic rats *Diabetes* **12**:115-126
- Moshe D 1998 A biosynthetic study of the genus *Sutherlandia* BrR (*Fabacea, Galegeae*), MSc dissertation submitted to the botany department, faculty of natural sciences, Rand Afrikaans University
- Motsenbocker MA 1968 *Biolum Chemilum***2**:89-95
- Mu J, Brozinick JT, Valladares O, Bucan M, Birnbaum MJ 2001 A role for AMP-activated protein kinase in contraction- and hypoxia-regulated glucose transport in skeletal muscle, *Mol Cell* **7**:1085–1094
- Müller F 2002 *Sutherlandia*: A useful African herb in medical practice, *The South African Journal of Natural Medicine* **8**:69 & 94
- Musi N, Hirshman MF, Nygren J, Svanfeldt M, Bavenholm P, Rooyackers O, Zhou G, Williamson JM, Ljunqvist O, Efendic S, Moller DE, Thorell A, Goodyear LJ 2002 Metformin increases AMP-activated protein kinase activity in skeletal muscle of subjects with type 2 diabetes, *Diabetes* **51**:2074–2081
- Mykkanen L, Zaccaro DJ, Hales CN, Festa A, Haffner SM 1999 The relation of proinsulin and insulin with newly diagnosed type II diabetes: The insulin resistance atherosclerosis study, *Diabetology* **42**(9):1060-1066

- Nagaev I and Smith U 2001 Insulin resistance and type 2 diabetes are not related to resistin expression in human fat cells or skeletal muscle, *Biochem Biophys Res Commun* **285**:561-4
- Nakae J, Park BC, Accili D 1999 Insulin stimulates phosphorylation of the forkhead transcription factor FKHR on serine 253 through a Wortmannin-sensitive pathway, *J Biol Chem* **274**:15982-5
- Nakata, Masanori, Yada, Toshihiko 2003 Nitric oxide-mediated insulin secretion in response to citrulline in islet [beta]-cells, *Pancreas* **27**(3):209-213
- Nakagawa SH and Tager HS 1986 Role of the phenylalanine B25 side chain in directing insulin interaction with its receptor Steric and conformational effects, *J Biol Chem* **261**(16):7332–7341
- Nakagawa SH and Tager HS 1989 Perturbation of insulin-receptor interactions by intramolecular hormone cross-linking analysis of relative movement among residues A1, B1, and B29, *J Biol Chem* **264**(1):272–279
- Nakra BR, Rutland P, Verma S, Gaind R 1977 Amitriptyline and weight gain: a biochemical and endocrinological study *Curr Med Res Opin* **8**:602-6
- Nanjo K, Sanke T, Miyano M, Okai K, Sowa R, Kondo M, Nishimura S, Iwo K, Miyamura K, Given BD, Chan SJ, Tager HS, Steiner DF, Rubenstein AH 1986 Diabetes due to secretion of a structurally abnormal insulin (insulin Wakayama). Clinical and functional characteristics of [LeuA3] insulin, *J Clin Invest* **77**:514-519
- NCBI data base (ProFound, FindPept and FindMod programs) www.proteomics.com
- Nelson DL and Cox MM 2000 Lehninger principles of biochemistry, third edition,Worth Publishers
- Newgard CB and McGarry JD 1995 Metabolic coupling factors in pancreatic B cell signal transduction*Annu Rev Biochem* **64**:689-719
- Newsholme EA and Leech AR 1994 Biochemistry for the medical sciences, John Wiley and Sons, New York
- Nisbet JC, Sturtevant JM, Prins JB 2004 Metformin and serious side effects, *MJA* **180**:53-54
- Nissim I, Horyn O, Daikhin Y, Nissim I, Lazarow A, Yudkoff M 2002 Regulation of urea synthesis by agmatine in the perfused liver: Studies with 15N, *Am J Physiol Endocrinol Metab* **283**: E1123–E1134
- Nkabinde L 2004 The establishment of a rat model of dietary induced obesity and insulin resistance *MSc Thesis Submitted in the Department of Science and Agriculture*, University of Zululand
- Nobrega JN and Coscina DV 1987 Effects of chronic amitriptyline and desipramine on food intake and body weight in rats, *Pharmacol Biochem Behav* **1**:105-112
- Nosadini R, Avogaro A, Trevisan R, Valerio A, Tessari P, Duner E, Tiengo A, Velussi M, Crepaldi G 1987 Effect of metformin on insulin-stimulated glucose turnover and insulin binding to receptors in type II diabetes, *Diabetes Care* **10**:62-67
- Nowak TJ and Handford AG 1999 Essentials of pathophysiology, McGraw-Hill, Boston
- Obermaier-Kusser B, White MF, Pongratz DE, Su Z, Ermel B, Muhlbacher C, Haring HU 1989 A defective intramolecular autoactivation cascade may cause the reduced kinase activity of the skeletal muscle insulin receptor from patients with non-insulin-dependent diabetes mellitus, *J Biol Chem* **264**:9497-9503
- Oda M, Satta Y, Takenaka O, Takahata N 2002 Loss of urate oxidase activity in hominoids and its evolutionary implications, *Mol Biol Evol* **19**(5):640–653
- Ohta N, Burke GT, Katsoyannis PG 1988 *J Protein Chem***7**:55-65
- Ohura T, Kobayashi K, Abukawa D, Tazawa Y, Aikawa J, Sakamoto O, Saheki T, Iinuma K. 2003 A novel inborn error of metabolism detected by elevated methionine and/or galactose in newborn screening: Neonatal intrahepatic cholestasis caused by citrin deficiency, *Eur J Pediatr* **162**: 317–322
- Okada T, Sakuma L, Fukui Y, Hazeki O, Ui M 1994 Blockage of chemotactic peptide-induced stimulation of neutrophils by wortmannin as a result of selective inhibition of phosphatidylinositol 3-kinase, *J Biol Chem* **269**:3563-3567
- Okamura F, Tashiro A, Utsumi A, Imai T, Suchi T, Hongo M 1999 Insulin resistance in patients with depression and its changes in the clinical course of depression: Areport on three cases using the minimal model analysis, *Internal Med* **38**(3):257–260

- Okuno A, Tamemoto H, Tobe K 1998 Troglitazone increases the number of small adipocytes without the change of white adipocyte tissue mass in obese Zucker rats, *J Clin Invest* **101**:1354-1361
- Olefsky JM 1976 Decreased insulin binding to adipocytes and circulating monocytes from obese subjects, *J Clin Invest* **57**:1165-1172
- Ostlund RE and Sherman WR 1998 Pinitol and derivatives thereof for the treatment of metabolic disorders, Washington University, United States Patent
- Ottensmeyer FP, Beniac DR, Luo RZ, Yip CC 2000 Mechanism of transmembrane signaling: insulin binding and the insulin receptor, *Biochemistry* **39**:12103-12112
- Overweight and Obesity — Statistics 2004, www.cdcgov/nchs/data/hus/hus04trend.pdf
- Paolisso G, Amato L, Eccellente R, Gambardella A, Tagliamonte MR, Varricchio G, Carella C, Giugliano D and D'Onofrio F 1998 Effect of metformin on food intake in obese subjects, *Euro J Clin Invest* **28**:441-446
- Park Y and Eisenbarth G.S, Genetic susceptibility factors of type I diabetes in Asians 2001 *Diabets Metab Res Rev* **17**(1):2-11
- Parker A, Meyer J, Lewitzky S, Rennich JS, Chan G, Thomas JD, Orho-Melander M, Lehtovirta M, Forsblom C, Hyrkko A, Carlsson M, Lindgren C and Groop LC 2001 A gene conferring susceptibility to type II diabetes in conjunction with obesity is located on chromosome 18p11, http://www/query.fcgi?cmd=Retrieve&db=PubMed
- Parrizas M, Maestro MA, Fernandez S, Ferrer J 2000 HNF-alpha as a beta cell specific transcriptional regulator, islets in eilat 2000, a combined islet basic science and transplantation meeting
- Pendergrass M, Fazioni E, Saccomani MP, Collins D, Bonadonna R, Gulli G 1995 *In vivo* glucose transport and phosphorylation in skeletal muscle is impaired in insulin resistant, normal glucose tolerant offspring of two NIDDM parents, *Diabetes* **44**(suppl 1):197A
- Pi-Sunyer 1998 Clinical guidelines on the identification, evaluation and treatment of overweight and obesity in adults, National institute of health publication, United States of America, http://wwwnhlbinihgov/guidelines/obesity/ob_homehtm
- Pittman I, Philipson LH, Steiner DF 2004 Secretion, structure and structure-activity relationships, Endotext.org your endocrine source, www.endotext.org.
- Plummer DT 1987 An introduction to practical biochemistry, third edition, McGraw-Hill Book Company, United Kingdom
- Powers AC, Solomon SS and Duckworth WC 1980 Insulin degradation by mononuclear cells, *Diabetes* **29**:27-32
- Pratley RE, Thompson DB, Prochazka M, Baier L, Mott D, Ravussin E, Sakul H, Ehm MG, Burns DK, Foroud T, Garvey WT, Hanson RL, Knowler WC, Bennett PH, Bogardus C 1998 An autosomal genomic scan for loci linked to prediabetic phenotypes in Pima Indians, *J Clin Invest* **101**:1757-1764
- Printz RL, Koch S, Potter LR, O'Doherty RM, Tiesinga JJ, Moritz S, Granner DK 1993 Hexokinase II mRNA and gene structure, regulation by insulin, and evolution, *J Biol Chem* **268**:5209-5219
- Prentice AM and Jebb SA 2001 Beyond body mass index, *Obesity Reviews* **2**(3):141-147
- Pullen RA, Lindsay DG, Wood SP, Tickle IJ, Blundell TL, Wollmer A, Krail G, Brandenburg D, Zahn H, Gliemann J, Gammeltoft S 1976 Receptor binding region of insulin, *Nature* **259**:369-373
- Raab-Graham KF, Cirilo LJ, Boettcher AA, Radeke CM, Vandenberg CA 1999 Membrane topology of the amino-terminal region of the sulfonylurea receptor, *J Biol Chem* **274**:29122-29129
- Rabinovitch A, Quigley C, Russell T, Patel Y, Mintz DH 1982 Insulin and multiplication stimulating activity (an insulin-like growth factor) stimulate islet β-cell replication in neonatal rat pancreatic monolayer cultures, *Diabetes* **31**:160-164
- Randle PJ, Garland PB, Hales CN, Newsholme EA 1963 The glucose fatty acid cycle: its role in insulin sensitivity and the metabolic disturbances of diabetes mellitus, *Lancet* **1**:785-789
- Ranford JC, Coates ARM, Henderson B 2000 Chaperonins are cell-signalling proteins: The unfolding biology of molecular chaperones, *Cambridge University Press* **1462-3994**: 1-17

- Rang HP and Dale MM 1991 Pharmacology, second edition, Churchill Livingstone, London
- Ransford CP 1982 A role for amines in the antidepressant effect of exercise, *Medicine and Science in Sport and Exercise* **14 (1)**:1-10
- Reaven GM, Hollenbeck C, Jeng CY, Wu MS, Chen YD 1998 Measurement of plasma glucose, free fatty acid, lactate, and insulin for 24 h in patients with NIDDM, *Diabetes* **37**:1020-1024
- Reddi AS and Jyothirmayi GN 1992 Effect of chronic metformin treatment on hepatic and muscle glycogen metabolism in KK Mice, *Boichem Med Metab Biol* **47**:124-132
- Reginato MJ and Lazar MA 1999 Mechanisms by which thiazolidinediones enhance insulin action, *Trends in Endocrinology and Metabolism*, Medical Center, Philadelphia **10**:9-13
- Remick RA, Campos PE, Misri S, Miles JE, Van Wyck Fleet J 1982 A comparison of the safety and efficacy of bupropion HCL and amitriptyline hcl in depressed outpatients *Prog Neuropsychopharmacol Biol Psychiatry* **4**(6):523-7
- Rena G, Prescott AR, Guo S, Cohen P, Unterman TG 2001 Roles of the forkhead in rhabdomyosarcoma (FKHR) phosphorylation sites in regulating 14-3-3 binding, transactivation and nuclear targeting, *Biochem J* **354**:605-612
- Ribon V, Printen JA, Hoffman NG, Kay BK, Saltiel AR 1998 A novel, multifuntional c-Cbl binding protein in insulin receptor signaling in 3T3-L1 adipocytes, *Mol Cell Biol* **18**:872-879
- Ricco A, Del Prato S, Vigili de Kreutzenburg S, Tiengo A 1991 Glucose and lipid metabolism in non-insulin dependent diabetes effect of metformin, *Diabetes Metab* **17**:180-184
- Rigler SK, Webb MJ, Redford L, Brown EF, Zhou J, Wallace D, 2001 Weight outcomes among antidepressant users in nursing facilities, *J Am Geriatrics Society* **49**(1):49-55
- Rissanen J, Markkanen A, Karkkainen P, Pihlajamaki J, Kekalainen P, Mykkanen L, Kuusisito J, Karhapaa P, Niskanen L, Laakso M 2000 Sulfonylurea receptor 1 gene variants are associated with gestational diabetes and type II diabetes but not with altered secretion of insulin, *Diabetes Care* **23**(1):70-73
- RodenM, Krssak M, Stingl H, Gruber S, Hofer A, Furnsinn C, Moser E, Waldhausl W 1999 Rapid impairment of skeletal muscle glucose transport/phosphorylation by free fatty acids in humans, *Diabetes* **48**:358-364
- Roesch K, Hynds PJ, Varga R, Tranebjaerg L, Koehler KM 2004 The calcium-binding aspartate/glutamate carriers, citrin and aralar1, are new substrates for the DDP1/TIMM8a–TIMM13 complex, *Human Molecular Genetics* **13**(18):2101–2111
- Rogers PA, Fisher RA, Harris H 1975 An electrophoretic study of the distribution and properties of human hexokinases, *Biochem Genet* **13**:857-866
- Roos M D, Wen X, Kaihong S, Clark J A, Xiaoyong Y, Chin E, Paterson A J, Kudlow J E 1998 Streptozotocin, an analog of N-acetylglucosamine, blocks the removal of O-GlcNAc from intracellular proteins, *Proc Assoc Am Physicians* **110**:1-11
- Rosen OM, Herrera R, Olowe Y, Petruzzelli M, Cobb MH 1983 Phosphorylation activates the insulin receptor tyrosine protein kinase, *Proc Natl Acad Sci USA* **80**:3237-3240
- Rosewell DF and White EH 1978 Methods in enzymology, Academic press, New York, pp 409-423
- Rossetti L, Defronzo RA, Gherzi R, Stein P, Andraghetti G, Falzetti G, Klein-Robbennaar E, Cordera R 1990 Insulin receptor tyrosine kinase activity and *in vivo* insulin action in diabetic rats, *Metabolism* **39**:425–435
- Rothman DL, Shulman RG, Shulman GI 1992 31P nuclear magnetic resonance measurements of muscle glucose-6-phosphate Evidence for reduced insulin-dependent muscle glucose transport or phosphorylation activity in non-insulin-dependent diabetes mellitus, *J Clin Invest* **89**:1069-1075
- Saidu Y 2004 Physicochemical features of rhodanese: A review, *African Journal of Biotechnology* **3**(4):370-374
- Ryan EA, Pick ME, Marceau C 2001 Use of alternative medicines in diabetes mellitus, *Diabetes UK, Diabetic Medicine* **18**:242-245
- Savage DB, Sewter CP, Klenk ES, Segal DG, Vidal-Puig A, Considine RV, O'Rahilly S 2001 Resistin / Fizz3 expression in relation to obesity and peroxisome proliferator-activated receptor-gamma action in humans, *Diabetes***50**:2199-202

- Schalin-Jantti C, Harkonen M, Groop LC 1992 Impaired activation of glycogen synthase in people at increased risk for developing NIDDM, *Diabetes* **41**:598-604
- Scheimann AO, Durham SK, Suwanichkul A, Snuggs MB, Powell DR 2001 Role of three FKHR phosphorylation sites in insulin inhibition of FKHR action in hepatocytes, *Horm Metab Res* **33**:631-638
- Schmitz-Peiffer C, Craig DL, Biden TJ 1999 Ceramide generation is sufficient toa ccount for the inhibition of the insulin-stimulated PKB pathway in C_2C_{12} skeletal muscle cells pretreated with palmitate, *J Biol Chem* **274**:24202-24210
- Scholz TD, Koppenhafer SL, Teneyck CL, Schutte BC 1998 Ontogeny of malate-aspartate shuttle capacity and gene expression in cardiac mitochondria, *Am J Physiol* **274**:C780-C788
- Schwartz GP, Katsoyannis PG 1978 *Biochemistry* **17**:4550-4556
- Seier J, Matsabisa M, Lochner A 2002 A toxicity study of *Sutherlandia* leaf powder consumption, MRC and NRF
- Servier Initial Training Course 2001 Diabetes background, the Servier medical supply company
- Sfakianos MK, Wilson L, Sakalian M, Falany CN, Barnes S 2002 Conserved residues in the putative catalytic triad of human bile acid coenzyme A: Amino acid *N*-acyltransferase, *Journal of Biological Chemistry* **277**(49):47270-47275
- Shaw DM 1984 Handbook of affective disorders, The Boots Company PLC
- Shepard RM and Henquin JC 1995 The role of metabolism, cytoplasmic Ca^{2+}, and pH-regulating exchangers in glucose-induced rise of cytoplasmic pH in normal mouse pancreatic islets, *The American Society for Biochemistry and Molecular Biology* **270**:7915-7921
- Shepherd PR and Kahn BB 1999 Glucose transporters and insulin action implications for insulin resistance and diabetes mellitus, *N Engl J Med* **341**:248-257
- Shepherd PR, Withers DJ, Siddle K 1998 Phosphoinositide 3-kinase: the key switch mechanism in insulin signalling, *Biochem J* **333**:471-490
- Shimabukuro M, Zhoa YT, Levi M, Unger RH 1998 Fatty acid induced B cell apoptosis, *Proc Natl Acad Sci USA* **95**:2498-2502
- Shimomura I, Hammer RE, Ikemoto S, Brown MS, Goldstein JL 1999 Leptin reverses insulin resistance and diabetes mellitus in mice with congenital lipodystrophy, *Nature* **401**:73-76
- Shoelson S, Fickova M, Haneda M, Hanum A, Musso G, Kaiser ET, Rubenstein AH, Tager HS 1983 *Proc Natl Acad Sci USA* **80**:7390-7394
- Shoelson S, Haneda M, Blix P, Nanjo A, Sanke T, Inouye K, Steiner DF, Rubenstein AH, Tager HS 1983 *Nature* **302**:540-543
- Sinasac DS, Moriyama M, Jalil MA, Begum L, Li MX, Iijima M, Horiuchi M, Robinson BH, Kobayashi K, Saheki T, Tsui LC 2004 *Slc25a13*-knockout mice harbor metabolic deficits but fail to display hallmarks of adult-onset type II citrullinemia, *Mol Cell Biol* **24**(2):527–536
- Slobin LI and Carpenter FH 1963 *Biochemistry* **2**:16-22
- Solomon SS, Mishra SK, Palazzolo MR, Postlethwaite AE, Seyer JM 1997 Identification of specific sites in the TNF-alpha molecule promoting insulin resistance in H-411E cells, *J Lab Clin Med* **130**(2):114-120.
- Spiegelman BM and Flier JS 2001 Obesity and the regulation of energy balance, *Cell* **104**:531-43
- Stanley B and Leibowitz S 1985 Neuropeptide Y injected in the paraventricular hypothalamus: a powerful stimulant of feeding behavior *Proc Natl Acad Sci* USA **82**:3940–3943
- Stephens JM, Lee J, Pilch PF 1997 Tumor necrosis factor-alpha-induced insulin resistance in 3T3-L1 adipocytes is accompanied by a loss of insulin receptor substrate-1 and GLUT4 expression without a loss of insulin receptor-mediated signal transduction, *J Biol Chem* **272**:971-6
- Storlien LH, Higson FM, Gleeson RM, Smythe GA, Atrens DM 1985 Effects of chronic lithium, amitriptyline and mianserin on glucoregulation, corticosterone and energy balance in the rat, *Pharmacol Biochem Behav* **1**:119-25
- Stummvoll M, Nurjhan N, Perriello G, Dailey G, Gerich JE 1995 Metabolic effects of metformin in non obese insulin-dependent diabetes mellitus, *N Eng J Med* **333**:550-554
- Suzuki M, Odaka H, Suzuki N, Sugiyama Y and Ikeda H 2002 Effects of combined pioglitazone and metformin on diabetes and obesity in Wistar fatty rats, *Clinical and Experimental Pharmacology and Physiology* **29**:269-274

- Tai J, Cheung S, Chan E, Hasman D 2004 *In vitro* studies of *Sutherlandia frutescens* on human tumor cell lines, *J Ethnopharm* **93**:9-19
- Tamamori A, Okano Y, Ozaki H, Fujimoto A, Kajiwara M, Fukuda K, Kobayashi K, Saheki T, Tagami Y, Yamano T 2002 Neonatal intrahepatic cholestasis caused by citrin deficiency: severe hepatic dysfunction in an infant requiring liver transplantation, *Eur-J-Pediatr* **161**(11):609-13
- Tamemoto H, Tobe K, Yamauchi T, Terauchi Y, Kaburagi Y, Kadowaki T 1997 Insulin resistance syndrome in mice deficient in insulin receptor substrate-1, *Ann N Y Acad Sci* **827**:85-93
- Tamemoto H, Kadowaki T, Tobe K, Yagi T, Sakura H, Hayakawa T, Terauchi Y, Ueki K, Kaburagi Y, Satoh S 1994 Insulin resistance and growth retardation in mice lacking insulin receptor substrate-1, *Nature* **372**:182-6
- Tan RS 1999 Dose of tricyclic antidepressants in elderly patients, *Am. Med. Society* **281**(20):39-45
- Tang ED, Nunez G, Barr FG, Guan KL 1999 Negative regulation of the forkhead transcription factor FKHR by Akt, *J Biol Chem* **274**:16741-16746
- Taniguchi CM, Ueki K, Kahn CR 2005 Complementary roles of IRS-1 and IRS-2 in the hepatic regulation of metabolism, *J Clin Invest* **10**:1-10
- Taylor SI 1992 Lilly lecture: molecular mechanisms of insulin resistance, lessons from patients with mutations in the insulin-receptor gene, *Diabetes* **41**:1473-1490
- Telakowski-Hopkins CA, Rothkopf GS, Pickett CB 1986 Structural analysis of a rat liver glutathione S-transferase Ya gene (gene structure/promoter/heteroduplex analysis/primer extension), *Proc. Nati. Acad. Sci* **83**:9393-9397
- Thameem F, Wolford JK, Bogardus C, Prochazka M 2001 Analysis of PBX1 as a candidate gene for type II diabetes mellitus in Pima indians, *Biochem Biophys Acta* **1518**(1-2):215-220
- Thomas PR, ed 1995 Weighing the options criteria for evaluating weight management programs Washington, DC: National Academy Press
- Thompson AL and Cooney GJ 2000 Acyl-CoA inhibition of hexokinase in rat and human skeletal muscle is a potential mechanism of lipid-induced insulin resistance, *Diabetes* **49**:1761-1764
- Thorell JI and Lanner A 1973 Influence of heparin-plasma, EDTA-plasma and serum on the determination of insulin with three different radioimmunoassays *Scand J Clin Lab Invest* **31**:187-190
- Tiikkainen M, Hakkinen AM, Korsheninnikova E Nyman T, Makimattila S, Yki-Jarvinen H 2004 Effects of rosiglitazone and metformin on liver fat content, hepatic insulin resistance, insulin clearance, and gene expression in adipose tissue in patients with type 2 diabetes, *Diabetes* **53**:2169-2176
- Tippett PS and Neet KE 1982 An allosteric model for the inhibition of glucokinase by long chain acyl Coenzyme A, *J Biol Chem* **257**:14846-14852
- Tomizawa M, Kumar A, Perrot V, Nakae J, Accili D, Rechler MM, Kumaro A 2000 Insulin inhibits the activation of transcription by a C-terminal fragment of the forkhead transcription factor FKHR A mechanism for insulin inhibition of insulin-like growth factor-binding protein-1 transcription, *J Biol Chem* **275**:7289-7295
- Tortora GJ and Grabowski SR 2003 Principles of anatomy and physiology, Harper Collins College Publishers, New York
- Tremblay A 2004 Dietary fat and body weight set point, *Nutrition* Reviews **62**(7): S75–S77
- Trichitta V, Brunetti A, Chiavetta A, Benzi L, Papa V, Vigneri R 1989 Defects in insulin-receptor internalization and processing in monocytes of obese subjects and obese NIDDM patients, *Diabetes* **38**:1579-1584
- Tsuchida A, Yamauchi T, Kadowaki T 2005 Nuclear receptors as targets for drug development: Molecular mechanisms for regulation of obesity and insulin resistance by peroxisome proliferator-activated receptor , CREB-binding protein, and adiponectin, *J Pharmacol Sci* **97**:164 – 170
- Ueda K, Inagaki N, Seino S 1997 MgADP antagonism to Mg^{2+}-independent ATP binding of the sulfonylurea receptor SUR1, *The American Society for Biochemistry and Molecular Biology* **272**:22983-22986

- Ueki K, Yamamoto-Honda R, Kaburagi Y, Yamauchi T, Tobe K, Burgering BM, Coffer PJ, Komuro I, Akanuma Y, Yazaki Y, Kadowaki T 1998 Potential role of protein kinase B in insulin-induced glucose transport, glycogen synthesis, and protein synthesis, *J Biol Chem* **273**:5315-5322
- Uhde I, Toman A, Gross I, Schwanstecher C, Schwanstecher M 1999 Identification of the potassium channel opener site on sulfonylurea receptors, *J Biol Chem* **274**:28079-28082
- Utriainen T, Lovisatti S, Mäkimattila S, Bertoldo A, Weintraub S, DeFronzo R, Cobelli C, Yki-Järvinen H 2000 Direct measurement of the lumped constant for 2-deoxy-[1-^{14}C]glucose *in vivo* in human skeletal muscle, *Am J Physiol Endocrinol Metab* **279**: E228-E233
- van Wyk BE, van Oudtshoorn B, Gericke N 1997 Medicinal plants of South Africa, Briza Publications
- Vass A 2002 Obesity causes 30 000 deaths a year, *BMJ* **324**:192
- Verspohl EJ and Ammon HPT 1980 Evidence for presence of insulin receptors in rat islets of langerhans, *J Clin Inuest* **65**:1230 -1237
- Vestergaard H, Bjocbaek C, Andersen PH, Bak JF, Pedersen O 1991 Impaired expression of glycogen synthase mRNA in skeletal muscle of NIDDM patients, *Diabetes* **40**:1740-1745
- Vestergaard H, Bjorbaek C, Hansen T, Larsen FS, Granner DK, Pedersen O 1995 Impaired activity and gene expression of hexokinase II in muscle from non-insulin dependent diabetes mellitus patients, *J Clin Invest* **96**:2639-2645
- Vigneri R and Goldfine ID 1987 Role of metformin in treatment of diabetes mellitus, *Diabetes Care* **10**:118-122
- Vogt C, Ardehali H, Iozzo P, Yki-Jarvinen H, Koval J, Maezono K, Pendergrass M, Printz R, Granner D, DeFronzo R, Mandarino L 2000 Regulation of hexokinase II expression in human skeletal muscle *in vivo*, *Metabolism* **49**:814-818
- Walker P 2000 HepG2 cells used as an *in vitro* model in the effects of tricyclic antidepressants associated with weight gain. Bsc (Hons) project report submitted in the Department of Biochemistry and Microbiology, University of Port Elizabeth
- Walter RM, Uriu-Hare JY, Lewis Olin K, Oster MH, Anawalt BD, Critchfield JW 1991 Copper, zinc, manganese, and magnesium status and complications of diabetes mellitus, *Diabetes Care* **14**:1050-1056
- Westgard JO 1981 A multi-rule shewart chart for quality control in clinical chemistry *Clin Chem* **27**:493-501
- Wieneke HJ, Danho W, Bullesbach EE, Gatter HG, Zahn H 1983 *Hoppe-Seyler's Z Physiol Chem* **364**:537-550
- Willey KA, Molyneaux LM,Yue DK 1994 Obese patients with type 2 diabetes poorly controlled by insulin and metformin: Effects of adjunctive dexfenfluramine therapy on glycaemic control, *Diabet Med* **11**:701–704
- Williams SR 1997 Nutrition and diet therapy, eighth edition, Mosby, London
- Wilson G 2005 Optimistion of an *in vitro* model for anti-diabetic screening, *MSc project report submitted in the Department of Biochemistry and Microbiology,* Nelson Mandela Metroplolitan University
- Withers DJ, Gutierrez JS, Towery H, Burks DJ, Ren JM, Previs S, Zhang Y, Bernal D, Pons S, Shulman GI, Bonner-Weir S, White MF 1998 Disruption of IRS-2 causes type 2 diabetes in mice, *Nature* **391**:900-904
- White MF and Yenush L 1998 The IRS-signaling system: A network of docking proteins that mediate insulin and cytokine action, *Curr Top Microbiol Immunol* **228**:179-208
- Whitehead TP, Kricka LJ, Carter TJ, Thorpe GH 1979 Analytical luminescence: Its potential in the clinical laboratory, *Clin Chem* **25**:1531-1546
- Wijekoon EP, Skinner C, Brosnan ME, Brosnan JT 2004 Amino acid metabolism in the Zucker diabetic fatty rat: Effects of insulin resistance and of type 2 diabetes**,** *Can J Physiol Pharmacol/Rev can physiol pharmaco l***82**(7):506-514
- Wititsuwannakul D and Kim K 1977 Mechanism of palmityl Coenzyme A inhibition of liver glycogen synthase, *J Biol Chem* **252**:7812-7817

- Wollmer A, Rannefeld B, Johansen BR, Hejnaes KR, Balschmidt P, Hansen FB 1987 Phenol-promoted structural transformation of insulin in solution, *Biol Chem Hoppe-Seyler* **368**:903-911
- Xiangwei W, Leeo CC, Muzny DM, Caskey CT 1989 Urate oxidase: Primary structure and evolutionary implications (sequence comparison/copper binding/protein modification/nonsense mutations in humans), *Proc Nati Acad Sci* **86**:9412-9416
- Yamauchi T, Kamon J, Waki H, Terauchi Y, Kubota N, Hara K, Mori Y, Ide T, Murakami K, Tsuboyama-Kasaoka N, Ezaki O, Akanuma Y, Gavrilova O, Vinson C, Reitman ML, Kagechika H, Shudo K, Yoda M, Nakano Y, Tobe K, Nagai R, Kimura S, Tomita M, Froguel P, Kadowaki T 2001 The fat-derived hormone adiponectin reverses insulin resistance associated with both lipoatrophy and obesity, *Nat Med* **7**:941-6
- Ye G, Metreveli NS, Donthi RV, Xia S, Xu M, Carlson EC, Epstein PN 2004 Catalase protects cardiomyocyte function in models of type 1 and type 2 diabetes, *Am Diab Ass* **382**:43–47
- Yeagley D, Guo S, Unterman T, Quinn PG 2001 Gene- and activation-specific mechanisms for insulin inhibition of basal and glucocorticoid-induced insulin-like growth factor binding protein-1 and phosphoenolpyruvate carboxykinase transcription Roles of forkhead and insulin response sequences, *J Biol Chem* **276**:33705-10
- Yeo EJ and Wagner C 1993 Tissue Distribution of glycine N-methyltransferase, a major folate-binding protein of liver, *Proc Natl Acad Sci* **91**:210-214
- Young M, Radda G, Leighton B 1996 Activation of glycogen phosphorylase and glycogenolysis in rat skeletal muscle by AICAR: an activator of AMPactivated protein kinase, *FEBS Lett* **382**:43–47
- Yu KT and Czech MP 1984 Tyrosine phosphorylation of the insulin receptor β- subunit activates the receptor-associated tyrosine kinase activity, *J Biol Chem* **259**:5277-86
- Zderic TW, Davidson CJ, Schenk S, Byerley LO, Coyle EF 2004 High-fat diet elevates resting intramuscular triglyceride concentration and whole body lipolysis during exercise, *Am J Physiol Endocrinol Metab* **286**:E217–E225
- Zhou B and Zhang ZY 2002 The Activity of the extracellular signal-regulated kinase 2 is regulated by differential phosphorylation in the activation Loop, *J Biol Chem* **277**:13889-13899
- Zhang B, Berger J, Hu E, Szalkowski D, White-Carrington S, Spiegelman BM, Moller DE 1996 Negative regulation of peroxisome proliferator-activated receptor-gamma gene expression contributes to the antiadipogenic effects of tumor necrosis factor-alpha, *Mol Endocrinol* **10**:1457-66
- Zhou G, Myers R, Li Y, Chen Y, Shen X, Fenyk-Melody J, Wu M, Ventre J, Doebber T, Fujii N, Musi N, Hirshman MF, Goodyear LJ, Moller DE 2001 Role AMP-activated protein kinase in mechanism of metformin action, *J Clin Invest* **108**:1167–1174
- Zierath JR, He L, Guma A, Odegoard Wahlstrom E, Klip A, Wallenberg-Henriksson H 1996 Insulin action on glucose transport and plasma membrane GLUT4 content in skeletal muscle from patients with NIDDM, *Diabetologia* **39**:1180-1189
- Zou MH, Kirkpatrick SS, Davis BJ, Nelson JS, Wiles WG, Schlattner U, Neumann D, Brownlee M, Freeman MB, Goldman MH 2004 Activation of the AMP-activated Protein Kinase by the Anti-diabetic Drug Metformin *in vivo*, *J Biol Chem* **279**(42):43940–43951